



UNIVERSITAT DE
BARCELONA

Universal diagnostic platforms based on oligonucleotide codified nanoparticles and DNA microarray devices

Marta Broto Avilés

ADVERTIMENT. La consulta d'aquesta tesi queda condicionada a l'acceptació de les següents condicions d'ús: La difusió d'aquesta tesi per mitjà del servei TDX (www.tdx.cat) i a través del Dipòsit Digital de la UB (diposit.ub.edu) ha estat autoritzada pels titulars dels drets de propietat intel·lectual únicament per a usos privats emmarcats en activitats d'investigació i docència. No s'autoritza la seva reproducció amb finalitats de lucre ni la seva difusió i posada a disposició des d'un lloc aliè al servei TDX ni al Dipòsit Digital de la UB. No s'autoritza la presentació del seu contingut en una finestra o marc aliè a TDX o al Dipòsit Digital de la UB (framing). Aquesta reserva de drets afecta tant al resum de presentació de la tesi com als seus continguts. En la utilització o cita de parts de la tesi és obligat indicar el nom de la persona autora.

ADVERTENCIA. La consulta de esta tesis queda condicionada a la aceptación de las siguientes condiciones de uso: La difusión de esta tesis por medio del servicio TDR (www.tdx.cat) y a través del Repositorio Digital de la UB (diposit.ub.edu) ha sido autorizada por los titulares de los derechos de propiedad intelectual únicamente para usos privados enmarcados en actividades de investigación y docencia. No se autoriza su reproducción con finalidades de lucro ni su difusión y puesta a disposición desde un sitio ajeno al servicio TDR o al Repositorio Digital de la UB. No se autoriza la presentación de su contenido en una ventana o marco ajeno a TDR o al Repositorio Digital de la UB (framing). Esta reserva de derechos afecta tanto al resumen de presentación de la tesis como a sus contenidos. En la utilización o cita de partes de la tesis es obligado indicar el nombre de la persona autora.

WARNING. On having consulted this thesis you're accepting the following use conditions: Spreading this thesis by the TDX (www.tdx.cat) service and by the UB Digital Repository (diposit.ub.edu) has been authorized by the titular of the intellectual property rights only for private uses placed in investigation and teaching activities. Reproduction with lucrative aims is not authorized nor its spreading and availability from a site foreign to the TDX service or to the UB Digital Repository. Introducing its content in a window or frame foreign to the TDX service or to the UB Digital Repository is not authorized (framing). Those rights affect to the presentation summary of the thesis as well as to its contents. In the using or citation of parts of the thesis it's obliged to indicate the name of the author.



UNIVERSITAT DE
BARCELONA



*Universitat de Barcelona, Facultat de Química,
Departament de Química Orgànica*

Consejo Superior de Investigaciones Científicas



*Institut de Química Avançada
de Catalunya*



*Nanobiotechnology for
Diagnostics group*



*Centro de Investigación Biomédica en
Red en Bioingeniería, Biomateriales y
Nanomedicina*

Universal diagnostic platforms based on oligonucleotide codified nanoparticles and DNA microarray devices

Memòria per optar al grau de Doctor per la Universitat de Barcelona
presentada per:

Marta Broto Avilés

Barcelona, maig de 2017

Universitat de Barcelona

Facultat de Química – Departament de Química Orgànica

Programa de doctorat de Química Orgànica

**Universal diagnostic platforms based on oligonucleotide
codified nanoparticles and DNA microarray devices**

Memòria per optar al grau de Doctor per la Universitat de Barcelona
presentada per:

Marta Broto Avilés

Directors:

Prof. M^a Pilar Marco Colás

Professora d'Investigació
Dept. de Nanotecnologia
Química y Biomolecular
Nb4D group, IQAC-CSIC

Dr. Roger Galve Bosch

Investigador
Dept. de Nanotecnologia
Química y Biomolecular
Nb4D group, IQAC-CSIC

Tutor:

Prof. Jordi Robles Brau

Professor titular
Departament de Química Orgànica
Facultat de Química
Universitat de Barcelona

AGRAÏMENTS

Per arribar fins aquí he recorregut un llarg camí i m'agradaria agrair-lo les persones que m'han acompanyat.

Des dels inicis, que el Lalo em va introduir a la ciència que no m'hi he pogut desenganxar. A mesura que anava avançant el Xavi i la Rosa em van donar una segona empenta. Xavi, això que em deies que acabaria fent el doctorat i jo no ho veia clar, ara veig que tenies raó. La vostra influència va marcar sens dubte la meva carrera professional.

Més endavant a la carrera, moltes gràcies a tots el professors que em van inspirar, sobretot al Jordi Robles per el meu primer tastet en investigació. Edu, crec que sense tu les llargues hores de classe i laboratori no haguessin sigut tant entretingudes. Tot i que et feies una mica pesadet, m'encanta quan recordem aquells moments que ens van fer riure tant. I el viatge a Dublín, 'Oh my Goodness', quin fred vam passar. I Carlos, em sap molt greu que no hagi pogut funcionar però aquests sis anys no els podré oblidar mai. Hem evolucionat moltíssim plegats, potser el futur ens tornarà a ajuntar.

Després ja va arribar el Nb4D, per on començar? A síntesi de 'grumetilla' amb el Dani i la Montse, on vaig aprendre realment a fer síntesi. Gràcies per els moments de Rock FM i el 'os voy a dar una patada'. Realment vaig estar molt a gust amb vosaltres. Més endavant a ELISA, on la Glòria, la Gonzalins, la Carme i l'Alex em van rebre amb braços oberts. Carme, ja saps que segueixo els teus passos, i Alex, compartint taula, ja sé que xerro una mica massa, però estic segura que també t'anava bé distreure't una mica. Preparat per la defensa que tinc un bon plegat de fotografies! I Gonzalins, sempre disposada a donar-me una abraçada quan més ho necessito. I van arribar la Laura, el Joanet i l'Ana. Aquesta etapa va ser curta però intensa, i ho demostra la gran amistat que ens ha unit. A vegades trobo a faltar una ombra darrera meu esperant per audiència. I Ana, ja sabem que això només ha sigut l'inici, que el camí que ens queda per recórrer espero que ens mantingui unides. Aquí constarà per primer cop *Branchis*. I per últim la Rita, sens dubte sense la teva contribució aquesta tesi no hagués pogut arribar tant lluny, inspireu molta confiança i tranquil·litat, m'ha agradat moltíssim créixer professionalment al teu costat. I la resta del laboratori amb qui hem

compartit esmorzars, dinar, berenars, pastissos i demés, moltes gràcies per fer-me sentir com part de una gran família.

I no podem oblidar la Pilar, moltes gràcies per aquesta gran oportunitat de treballar al Nb4D, no han sigut uns anys fàcils però quan ha calgut has estat allà per ajudar-me. I Roger, aquest gran professor, mentor, director i amic. No només he crescut professionalment al teu costat, el que m'has aportat va molt més enllà. Mai tindrè paraules suficients per agrair el que has fet per mi.

Also, I want to acknowledge my research stay to Samir, thanks for the opportunity. My officemates in Santa Barbara: Tyler, Bugra and Izzy, you welcomed me, helped me and entertained me with good typing skills. Vinu, Andrés and Anusha, that San Diego trip was *amazing*, I don't recall laughing that much in a long time. Doug for welcoming me in your place. And of course, my dear Debra, preparing Jell-O and Debring were awesome. Also to everyone in lab and Elings, it was an unforgettable experience.

I que seria la tesi sense la vida social per poder mantenir-se psicològicament sa? Lena i Nerea, encara que sempre estem amunt i avall, sempre ens tenim per emergències. Espero que tard o d'hora ens tornem a trobar. Ann, Alba i Marga, gràcies per fer que tots els problemes semblin la tonteria més gran del mon i fer-me riure d'ells. Heu sigut un gran suport en aquesta etapa.

I per últim, la família, Rosa i Lluís, que hagués sigut sense vosaltres, que ho heu donat tot i més. Des que vaig començar aquest camí només heu tingut paraules de suport i ajuda, tapers i viatges en cotxe a Barcelona. Moltes gràcies per el vostre amor. Aquí recullo la feina feta en els projectes del papa i la mama, després de molt patiment han acabat funcionant tots dos. I sens dubte, el més gran agraïment d'aquesta tesi és per la Marieta, moltíssimes gràcies per haver-me esperat. Sempre et portaré al cor, al costat del Jordi.

Marta.

TABLE OF CONTENTS

1	CONTEXT SCENARIO, OBJECTIVES AND STRUCTURE	1
1.1	Research project	2
1.2	Objectives and scientific strategy.....	3
1.3	Thesis structure	4
1.4	Author and research group	6
1.4.1	Publications and patents.....	6
1.4.2	Conferences.....	7
1.4.3	Grants and awards	8
2	INTRODUCTION TO PERSONALIZED MEDICINE AND MULTIPLEXED ASSAYS	9
2.1	Current bioanalytical multiplexed techniques.....	11
2.2	New approaches for disease diagnosis.....	13
2.2.1	Pathogenic diseases	13
2.2.2	Disease biomarker panel.....	14
2.2.3	Therapeutic monitoring	15
3	ANTIBODY PRODUCTION AND VALIDATION	17
3.1	Chapter objective.....	18
3.2	Introduction.....	19
3.2.1	Chemotherapy	19
3.2.2	TDM of cytostatic agents.....	20
3.2.2.1	5-Fluorouracil and tegafur.....	21
3.2.2.2	Cyclophosphamide	24
3.3	Results and discussion	27

3.3.1 Establishment of an immunochemical assay for 5-fluorouracil.....	27
3.3.1.1 Hapten design.....	27
3.3.1.2 Antibody production	30
3.3.1.3 Establishment of the immunochemical assay	31
3.3.1.4 Evaluation of highly heterologous competitors	37
3.3.2 Establishment of an immunochemical assay for tegafur	39
3.3.3 Establishment of an immunochemical assay for cyclophosphamide	40
3.3.3.1 Hapten design.....	40
3.3.3.2 Antibody production	42
3.3.3.3 Establishment of the immunochemical assay	43
3.4 Related publications	45
3.4.1 Publication I: Bioanalytical Methods For Cytostatic Therapeutic Drug Monitoring and Occupational Exposure Assessment.....	45
3.4.2 Publication II: High throughput immunoassay for the therapeutic drug monitoring of tegafur.....	65
3.5 Chapter contributions	78
3.6 Materials and methods	78
3.6.1 Synthesis.	78
3.6.2 Immunochemistry.....	81
4 MONOPLEXED BIOBARCODE ASSAY DEVELOPMENT	85
4.1 Chapter objectives	86
4.2 Introduction.....	87
4.2.1 Coding oligonucleotides	87
4.2.2 Biobarcode	88
4.2.3 Proof of concept, Cardiovascular diseases	91
4.2.3.1 Acenocoumarol (ACL)	91
4.2.3.2 C-reactive protein (CRP)	92

4.3	Results and discussion	93
4.3.1	DNA microarray	94
4.3.2	Magnetic particles functionalization and characterization	96
4.3.3	Encoded probes functionalization and characterization	96
4.3.3.1	Gold nanoparticles functionalization and characterization	96
4.3.3.1.1	<i>Hapten conjugation.....</i>	<i>98</i>
4.3.3.1.2	<i>AuNPs synthesis</i>	<i>99</i>
4.3.3.1.3	<i>AuNPs biofunctionalization and oligonucleotide release</i>	<i>100</i>
4.3.3.1.4	<i>eAuP validation</i>	<i>100</i>
4.3.3.2	Polystyrene microparticles functionalization and characterization	103
4.3.4	Establishment of a NP-based biobarcode assay for acenocoumarol ...	104
4.3.5	Establishment of a NP-based biobarcode assay for C-reactive protein	104
4.4	Related publications	105
4.4.1	Publication III: Biobarcode Assay for the Oral Anticoagulant Acenocoumarol	105
4.4.2	Publication IV: Sandwich NP-based Biobarcode Assay for quantification C-reactive Protein in Plasma Samples	136
4.5	Chapter contributions	168
4.6	Materials and methods	168
4.6.1	Immunochemistry.....	168
5	MULTIPLEXED AND MULTIMODAL BIOBARCODE ASSAY DEVELOPMENT	171
5.1	Chapter objective.....	172
5.2	Introduction.....	173
5.2.1	Spatially localized multiplexed platforms	173
5.2.2	Labeled multiplexed platforms.....	174
5.2.3	Multiplexed biobarcode	175

5.3	Results and discussion	176
5.3.1	Assay design	177
5.3.2	Assay development.....	179
5.4	Related publications	180
5.4.1	Publication V: A Multiplexed and Multimodal Biobarcode, simultaneous tailored detection of small molecules and proteins	180
5.5	Chapter contributions	198
6	CONCLUSIONS.....	199
7	RESUM	203
7.1	Objectius	204
7.2	Introducció	205
7.2.1	Tècniques bioanalítiques multiplexades	206
7.2.1.1	Biobarcode	207
7.3	Resultats i discussió	209
7.3.1	Producció i validació d'anticossos.....	209
7.3.1.1	5-fluorouracil i tegafur	209
7.3.1.2	Ciclofosfamida	212
7.3.2	Desenvolupament d'un biobarcode monoplexat	214
7.3.3	Desenvolupament d'un biobarcode multiplexat	219
7.4	Conclusions.....	221
8	ANNEX. NANOCARRIER SYSTEM FOR 5-FLUOROURACIL DRUG DELIVERY	223
8.1	Chapter objective.....	224
8.2	Introduction.....	225

8.2.1 Liposomes.....	226
8.2.2 Liposomes for 5FU encapsulation	227
8.3 Results and discussion	227
8.3.1 Nanocarrier design.....	228
8.3.2 Synthesis of the drug conjugate	229
8.3.3 Drug encapsulation and particle characterization	230
8.3.4 Targeted functionalization	232
8.3.5 In vitro studies	233
8.4 Related publications	235
8.5 Conclusions.....	235
8.6 Materials and methods.....	236
9 BIBLIOGRAPHY.....	241
10 ACRONYMS, ABBREVIATIONS AND TABLES	249
10.1 Acronyms and abbreviations.....	250
10.2 Table of figures	254
10.3 Table of tables	259

1 CONTEXT SCENARIO, OBJECTIVES AND STRUCTURE

1.1 RESEARCH PROJECT

The present doctoral thesis has been carried out in the framework of two different research projects:

1. **Development of occupational exposure monitoring systems.** In collaboration with CETEMMSA Technological Center (part of the EURECAT Technology Center of Catalonia).

In this project, the main objective was the development of a monitoring device to control occupational exposure to cytostatic drugs in hospitals. These devices could be personalized monitoring tools based on an immunosensor printed on a flexible material incorporated over textile fibers or paper, that would respond with an optic or electrochemical signal after specific interaction with those cytostatics.

2. **OligoCODEs project. Universal diagnostic platforms based on oligonucleotide codified nanoparticles and DNA microarray sensor devices.** MINECO, Dirección General de Investigación Científica y Técnica, Subdirección General de Proyectos de I+D. MAT2011-29335-C03-01. MAT2012-38573-C02-01.

The fundamental of the OligoCODEs approach is the capability to translate any type of biomolecular interaction into a PCR-less DNA amplification process that is finally detected on a DNA-microarray biosensor platform. With the proposed approach, nucleic acids, proteins, peptides or small organic molecules biomarkers could be detected using the same chip and sensor technology, independently from the different chemical nature of the biomarker targets. The technology and tools developed are based on the use of oligonucleotide codified biohybrid nanoparticles, biofunctionalized magnetic particles and DNA microarrays on electrochemical sensor transducers. As a proof-of-concept, the project has focused on the detection of cancer and cardiovascular biomarkers.

Specific tasks addressed in this thesis concern the development of multiplexed assays for two problematic scenarios: the therapeutic drug monitoring (TDM) of cytostatic drugs and cardiovascular disease (CDV) diagnosis.

- The first one, focused on personalized medicine due to highly recommended therapeutic drug monitoring of chemotherapeutic agents was addressed by the production of specific bioreceptors for the drugs. Most used cytostatics were selected including 5-fluorouracil; tegafur, main 5-fluorouracil prodrug; and cyclophosphamide. We focused on the production of polyclonal antibodies for specific detection of these drugs and the development of an enzyme linked immunosorbent assay (ELISA) for antibody validation.
- In the second scenario, CVDs diagnosis was addressed based on the development of a biobarcode platform. First, establishing protocols for components preparation, and then applying established protocols for detection of small molecules and proteins related to CVDs, to, finally, combine them in a multiplexed assay.

Finally, preliminary studies addressed to develop a nanocarrier system for 5-fluorouracil drug delivery were performed within the frame of a collaboration with the Mitragotri's group in University of California Santa Barbara (USA). The investigation was made during a 4-month pre-doctoral stage in such institute under the supervision of Dr. Samir Mitragotri and thanks to the FPI stage grant. The goal of the research stage was to complete the scientific training by applying the knowledge and technology generated to other fields of interest.

1.2 OBJECTIVES AND SCIENTIFIC STRATEGY

The main objective of this thesis has been demonstrating the universality of the biobarcode approach by showing that biomarkers of different chemical nature, at distinct concentration ranges, can be analyzed with the same DNA-platform. To accomplish this aim, the following secondary objectives were addressed:

1. Establishing a procedure for the preparation of biofunctional nanoparticles on a reproducible manner. For this purpose, antibodies or antigens, and specific oligonucleotide sequences for each biomarker target have been covalently attached to the nanoparticles on a particular ratio.

2. Performing studies addressed to achieve the release of the oligonucleotides used as codes on the distinct biohybrid nanoparticles, in order to accomplish the maximum efficiency.
3. Assessing the possibility to modulate the signal amplification by varying the charge of oligonucleotides on the biofunctional nanoparticles.
4. Development and evaluation of the biobarcode assay for each of the biomarker targets addressed, this will involve the use of immunoreagents produced for proteins and small molecules. For this objective it will be crucial to take into consideration the clinical requirements regarding performance and detectability to be achieved.
5. Assessing the possibility to develop a multiplexed assay by combining the distinct biofunctional nanoparticles produced and characterized with the objective to determine simultaneously different biomarker targets on a single run.

1.3 THESIS STRUCTURE

The structure of the present thesis, including the content of each chapter is shown in figure 1. Chapters are organized according the logic evolution of a bioanalytical technique development. Chapter 3 addressed the production of antibodies for cytostatic drugs, nevertheless, as commented in section 1.1, in this project we could not reach following stages of the bioanalytical technique development, for this reason both chapter 4 and 5 only address the problematic related to cardiovascular diseases.

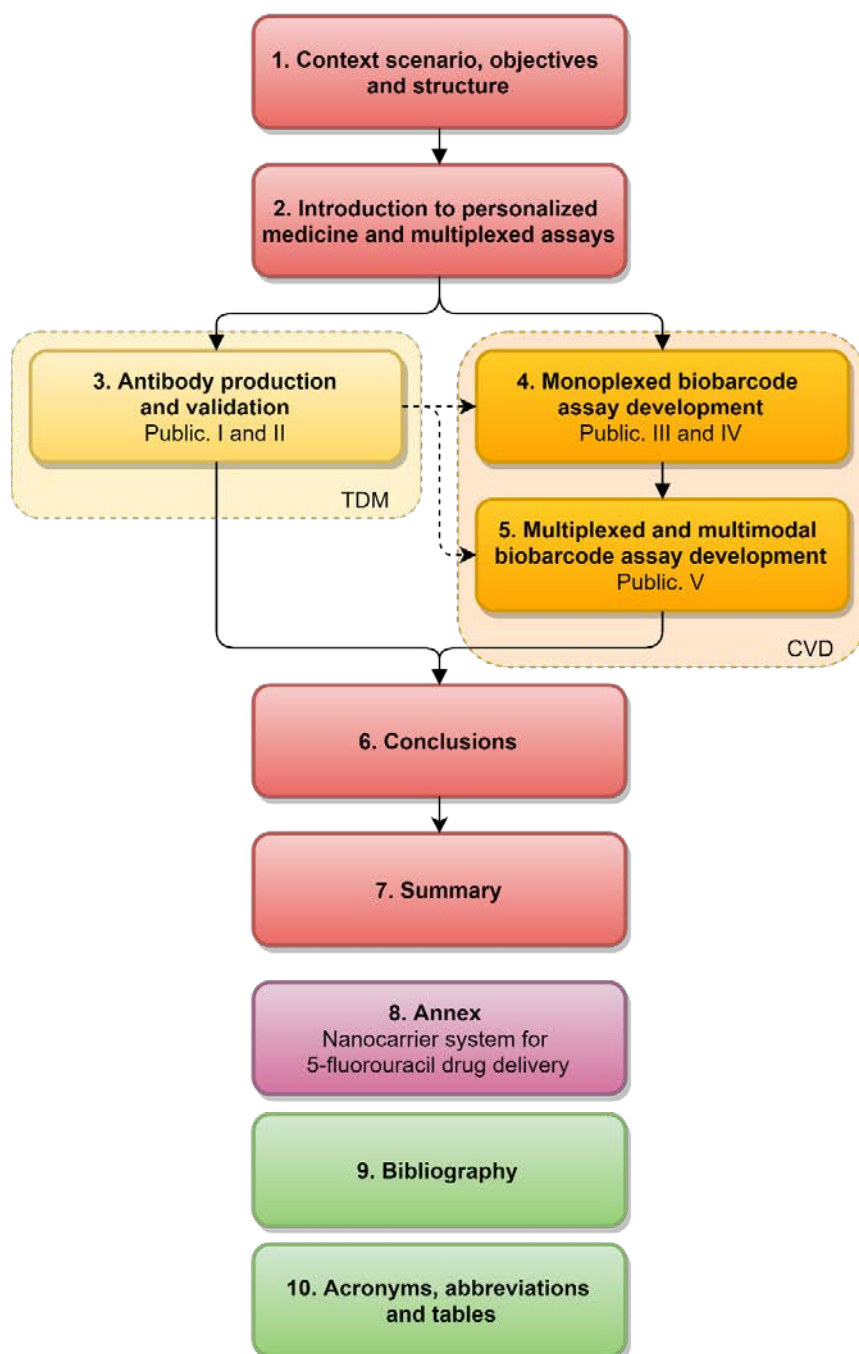


Figure 1.1 The structure of this thesis related to the different chapters and the parts included in each one. Dotted line corresponds to the work that could not be undertaken.

1.4 AUTHOR AND RESEARCH GROUP

The PhD student and author of this thesis, Marta Broto, had a Chemistry degree from the University of Barcelona (2011). Then she did a MSc of Advanced Chemistry specialized in Organic Chemistry (2013) with a scholarship awarded by Centro de Investigación Biomédica en Red en Bioingeniería, Biomateriales y Nanomedicina (CIBER-BBN). In this stage, she started working as a master student in the research group Nb4D (Nanobiotechnology for Diagnostic). Afterwards, in 2014, she started her PhD studies, this time with a FPI scholarship.

Nb4D belongs to Spanish Research Council (CSIC) and it is homed in the Advanced Chemistry Institute of Catalonia (IQAC). The group is also part of the Research Center of web biomedical research in bioengineering, biomaterials and nanomedicine (CIBER-BBN), an initiative of the Carlos III Health Institute (ISCIII), focused on improving excellence research in health and biomedicine. The Nanobiotechnology for Diagnostics Group, headed by M^a Pilar Marco, is based on the development of novel molecular diagnostic tools to provide alternatives to the actual limitations existing in several fields but particularly in the clinical and food safety areas.

1.4.1 PUBLICATIONS AND PATENTS

Broto, M., R. McCabe, R. Galve and M. P. Marco "A Multiplexed and Multimodal Biobarcode, simultaneously tailored detection of small molecules and proteins." Submitted.

Broto, M., R. Galve and M. P. Marco "Sandwich NP-based Biobarcode Assay for quantification C-reactive Protein in Plasma Samples." Submitted.

Broto, M., J. P. Salvador, R. Galve and M.-P. Marco "Biobarcode Assay for the Oral Anticoagulant Acenocoumarol." Submitted.

Broto, M., R. McCabe, R. Galve and M. P. Marco (2017) "High throughput immunoassay for the therapeutic drug monitoring of tegafur." Analyst **142**: 2404-2410

Broto, M., R. Galve and M. P. Marco (2017) "Bioanalytical Methods For Cytostatic Therapeutic Drug Monitoring and Occupational Exposure Assessment." Trends in Analytical Chemistry **93**: 152-170.

S. Mitragotri, K. M. Camacho, S. Menegatti, M. Broto "Drug formulations for cancer treatment". Patent in preparation, UC Case No. 2016-246 (2).

Broto, M., S. Matas, R. Babington, M. P. Marco and R. Galve (2015). "Immunochemical detection of penicillins by using biohybrid magnetic particles." Food Control **51(0)**: 381-389.

Valera, E., R. Babington, M. Broto, S. Petanas, R. Galve and M.-P. Marco (2013). Chapter 7 - Application of Bioassays/Biosensors for the Analysis of Pharmaceuticals in Environmental Samples. Comprehensive Analytical Chemistry. D. B. Mira Petrovic and P. Sandra, Elsevier. **Volume 62**: 195-229.

1.4.2 CONFERENCES

Marta Broto, J. Pablo Salvador, Roger Galve and M.-Pilar Marco. "NP-based biobarcode assay for small molecules detection by indirect competitive format" (Poster). 5th International Conference on Bio-sensing Technology (2017-Riva del Garda, Italy)

Marta Broto, J. Pablo Salvador, Roger Galve and M.-Pilar Marco. "Competitive biobarcode assay for detection of small analytes" (Presentation). VIII Workshop CBN'16. (2016-Barcelona, Spain)

Sonia Matas, Marta Broto, Ruth Babington, M.-Pilar Marco, Roger Galve. "Immunochemical detection of total penicillins by using biohybrid magnetic particles" (Poster). EuroResidue VIII. (2016-Egmond aan Zee, The Netherlands)

Marta Broto, J. Pablo Salvador, Roger Galve and M.-Pilar Marco. "Competitive biobarcode assay for detection of small analytes" (Poster). 11th Workshop on Biosensors & Bioanalytical Microtechniques in Environmental, Food & Clinical Analysis (2015-Regensburg, Germany)

Sonia Matas, Marta Broto, M.-Pilar Marco, Roger Galve. "Development of an immunoassay for the detection of penicillin hypersensitivity" (Poster). VI

workshop on analytical nanoscience and nanotechnology (2013-Alcalá de Henares, Spain)

1.4.3 GRANTS AND AWARDS

- 2016 Best oral presentation, VIII Workshop CBN'16
- 2016 Grant for research stages in other public or private R&D centers, Ministry of Economy, Industry and Competitiveness of the Spanish government (EEBB-I-16-10608)
- 2015 Poster prize awarded for excellent presentation, 11th Workshop on Biosensors & Bioanalytical Microtechniques in Environmental, Food & Clinical Analysis
- 2013 Fellowship for predoctoral contract of PhD candidates (FPI), Ministry of Economy, Industry and Competitiveness of the Spanish government. (BES-2013-062819)
- 2011 Grant for researchers training of CIBER-BBN, CIBER-BBN
- 2011 Scholarship for department collaboration, University of Barcelona

2 INTRODUCTION TO PERSONALIZED MEDICINE AND MULTIPLEXED ASSAYS

In vitro diagnostics (IVDs) are tests that can detect diseases, conditions, or infections. Some tests are used in laboratory or other health professional settings and other tests are for consumers to use at home¹. Although there are several techniques used in IVDs, including chromatographic techniques and PCR (polymerase chain reaction), those could be time consuming, require qualified personnel and are expensive. Only some bioanalytical techniques have the properties of being reliable, low-cost, sensitive, fast, portable, less invasive and easy-to-use. Furthermore, they usually are suitable for the screening of many samples. These techniques, use a recognition element of biological nature, and can be separated in three major groups:

- **Bioassay** is a tool for the determination of a biological activity, or for the quantification of a target analyte based on his activity, using recognition elements such as bacteria, cells or tissues. This recognition event is mainly determined by physical or indirect measurement methods.
- **Biochemical assay** is an assay where the biorecognition element is a defined biomolecule such as an enzyme, an oligonucleotide, a protein or an antibody which interacts with the target under stoichiometric conditions.
- **Biosensor** is a self-contained device, consisting of a biological recognition element in direct contact with a transduction element, which converts the biological recognition event into a useable output signal.

Lately, personalized medicine has become a striking feature in the diagnostic field. It has generated the need for development of new technologies and refinement of the existing ones, to improve the clinical outcome and the quality of life of patients. Recent advances in genomics and proteomics studies have been a driving force toward the development of fast, automatized, high-throughput, multiplexed diagnostic techniques that will be essential for personalized medicine.

2.1 CURRENT BIOANALYTICAL MULTIPLEXED TECHNIQUES

A multiplex assay is a type of assay that simultaneously measures multiple analytes in a single run/cycle of the assay. Analytical separation techniques like high-performance liquid chromatography, capillary electrophoresis and liquid or gas chromatography have been extensively used as multiplexed assays for TDM and biomarker detection. Nevertheless, they lack of fast, economical and high-throughput and require appropriate sample treatment. Bioanalytical techniques combined with nanotechnology have widely spread in the recent years, and are the perfect tool to address the problematic stated before of detection of multiple analytes. It is though that they will be able to revolutionize personalized medicine such as pregnancy tests and glucose tests did years ago.

Multiplexed techniques must cope with some challenges. First, target compounds can be presented in a wide range of concentrations. For instance, plasma protein concentrations range from mg/mL (serum albumins) down to few pg/mL (interleukins), which differ in nine orders of magnitude. Second, detection of compounds of different chemical nature (proteins, small drugs and miRNAs²) are emerging as disease biomarkers claiming for multimodal platforms.

Many attempts have been done for multiplexed analysis by using immunochemical techniques, easily and readily miniaturized by employing nanostructured surface sensors or micro and nanoparticles. For example, several strategies have been used for multiplexed protein detection such as surface plasmon resonance (SPR), flow cytometry, ELISA (which has been multiplexed with fluorescent detection labels), protein microarrays, lab-on-a-chip devices³ and lateral flow systems⁴. Alternatively, quantitative polymerase chain reaction (qPCR) and DNA-microarray have been widely used for multiplexed DNA detection⁵. A vital aspect for multiplexing is the capacity to discriminate between different analytes. Various kinds of assay platforms have been introduced such as spatial localization or multiple labels⁶. They will be deeply discussen in chapter 5. Each developed analytical technique shows different strengths and weaknesses and they should be considered depending their specific needs.

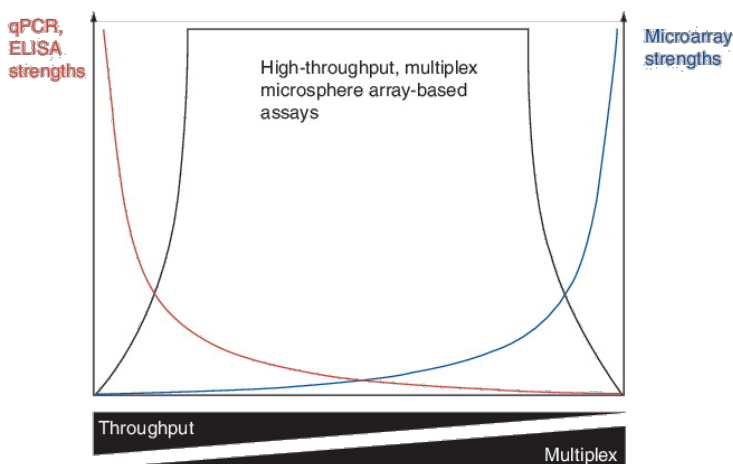


Figure 2.1 Performance parameters for a detection platform. The gold standard technique is actually a compromise between the multiplex level and platforms that are capable of high throughput analysis.⁵

Anyway, there is still a lack of outstanding, robust and affordable analytical platform that is set to become the gold standard for personalized medicine. While immunoassays provide the throughput analysis of multiple samples at the same time, microarrays provide the detection of multiple compounds (Figure 2.1). In this thesis, we propose the biobarcode as this gold standard technique. This technique not only is suitable for multiplex and throughput detection but it could also confer multimodality. Biobarcode has recently emerged as a new bioanalytical technique with proven excellent capabilities such as analysis of biomarkers of different chemical nature⁷⁻⁹; analysis of different biomarkers^{10, 11}; and also high sensitivity, reaching concentrations as low as zM ¹². Biobarcode characteristics will be presented in detail in section 4.2.2.

Nevertheless, incorporation of these technologies to routine clinics should face the challenge of operational and quality control issues like immobilization strategies, crossreactivity and availability of standardized reagents, robust automation and operational costs. Furthermore, appropriate algorithms and directives for data management should also be implemented¹³.

2.2 NEW APPROACHES FOR DISEASE DIAGNOSIS

In clinical laboratories, the need for multiplexed techniques, detection of multiple compounds at the same time, arises from three fundamental problematics: pathogenic disease identification, biomarker's panel for disease evaluation and therapeutic monitoring¹⁴.

- First, rapid test to identify causative agents of a disease are crucial for patient survival.
- Secondly, biomarker panels are emerging for diseases in which one only biomarker is not enough for the correct stratification of the disease risk.
- Finally, therapeutic monitoring can be divided in two subgroups: drug monitoring or response monitoring. The first is the evaluation of a drug concentration of a biological sample, the second is the evaluation of a biomarker concentration to evaluate the effect of the treatment, both strategies combined could become the key for individualized disease treatment and stage evaluation.

Thus, multiplexed techniques are useful for disease screening, disease stratification and disease treatment. They are a profitable technology for improving diagnostic efficiency, enhancing the diagnostic precision for specific diseases and reducing diagnostic costs.

Even though disease biomarker's panel and therapeutic monitoring have only been addressed, these three problematics will be described below.

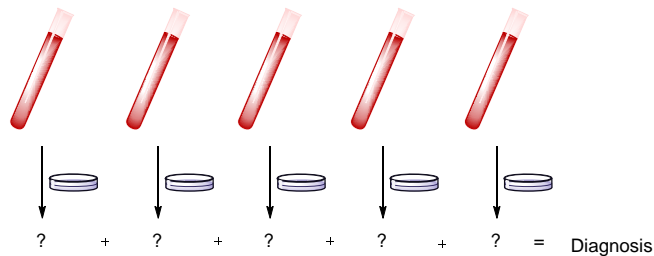
2.2.1 PATHOGENIC DISEASES

Pathogenic evaluation in an advanced stage is of importance since even trace amounts of biological agents can produce serious results. Furthermore, there has been a growing interest in pathogen identification due to the considerable increased threat of infectious diseases for the public¹⁵.

Classically, commonly used microbiological identification methods have been time consuming and required expensive equipment, therefore there is a need for

fast diagnostic methods. Furthermore, clinicians face infection diagnosis with a 'rule out' process. It is based on subsequent analysis for different pathogens, each analysis being time consuming, while patient is treated with broad-spectrum drugs. Nevertheless, multiplexed assays could benefit patient treatment with the 'rule in' approach, in only one assay multiple pathogens could be screened⁵.

Rule out



Rule in

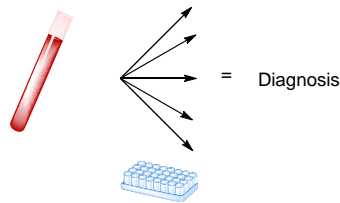


Figure 2.2 Diagram showing 'rule out' and 'rule in' approaches for pathogenic disease diagnostic. Multiplexed assays based on 'rule in' approach could boost pathogen identification⁵

2.2.2 DISEASE BIOMARKER PANEL

Biomarkers are key players in building fundamental science, supporting early diagnosis of diseases and following their progression, improving efficacy and safety of treatments, optimizing patient selection and adapting dosing of drugs and helping decide which therapy is most appropriate.

Despite the widespread use of some biomarkers, like PSA for prostate cancer diagnosis, a lot of diseases have also been reported in which a sole biomarker is not enough for an accurate diagnosis. Some examples are Alzheimer's disease¹⁶, cardiovascular diseases^{17, 18} or colorectal¹⁹ and breast²⁰ cancer. As a result, the traditional approach of evaluating a single biomarker has not been able to

contribute substantially to the risk stratification of the individual patients. Therefore, understanding the relationship between various biomarkers could become a profitable approach to enhance risk assessment. Another reason for inconvenient use of a single biomarker is that false positives and negatives would be minimized when detecting a panel biomarker, reducing patient risk²¹.

2.2.3 THERAPEUTIC MONITORING

The pharmacokinetic monitoring of a drug is called therapeutic drug monitoring (TDM). It has been stated that some drugs should be subjected to pharmacokinetic monitoring when it presents a narrow therapeutic window, no suitable parameter is available to evaluate the clinical efficacy, present a high interindividual variability, and it's applied in long-term-therapy schedules. The last and striking requirement for TDM is the need of a reliable analytical method for its quantification. In addition, there is a growth in popularity to tailor treatment based on the specific pharmacokinetics of a patient which can be affected by a number of factors including age, weight and diet.

Drug monitoring of a therapy is helpful in intensive care situations (i.e., aminoglycosides antibiotic, vancomycin, caffeine in neonatal apnea), but is mostly known for chronic therapy such as immunosuppressant, anti-arrhythmic, and many anti-epileptic drugs. In these cases, drug monitoring helps to evaluate the onset response and adjust the dose²². Furthermore, TDM is an exceptional tool to better understand why patients do not respond satisfactorily to a particular dose.

Alternatively, there is a growing interest of drug discovery complemented by the possibility to test response biomarkers, called therapeutic response monitoring (TRM, Figure 2.3), which would also lead to an increased efficacy and reduced side-effects²³. Biomarkers have the potential to expedite drug development, increase patient safety, and optimize clinical response²⁴, thus, following of patients remission and confirming treatment efficiency²⁵. Biomarkers used in drug discovery are either disease-related or efficacy-related biomarkers. The former is mechanistically linked to the disease, its progression and susceptibility, while the latter aim to determine if a drug hits the desired target, and if this binding leads to successful modulation of the pathway. Although this challenging

area has been first focused on drug development and clinical trials, there still remains a recent concern in the discovery of reliable response markers that could be measured in biological samples without harsh sample treatment.

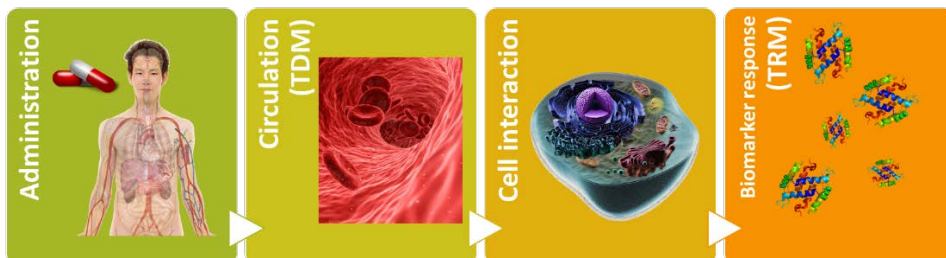


Figure 2.3 Scheme representing the path of a therapeutic drug in the human body. Analysis of the circulating drug concentration is performed in biofluids, which is referred to as therapeutic drug monitoring. The interaction of the therapeutic drug with the targeted cells can lead to morphological responses or to changes in the levels of biomarkers or metabolites, and TRM can be applied.

The majority of the literature has focused on TDM, leaving TRM in a negligible place. Therapeutic response monitoring techniques are still at an early stage of development, but are very promising for improving in the years to come. Opportunities, therefore, reside in the development of novel bioanalytical techniques for both TDM and TRM²⁵. As McKeating *et al.* discussed in their review an example that combined TDM of fungal infection and TRM of beta-glucans, indicators of the disease could be used to provide accurate and reproducible results to monitor a variety of disease states. In contrast, TRM in cancer treatment is proposed to generate specific patterns that might permit the generation of response algorithms that empirically eliminate the need for drug determination. But, first, advances in this field require the identification of the correlation between drug concentration, toxicity and response biomarkers²⁶.

3 ANTIBODY PRODUCTION AND VALIDATION

3.1 CHAPTER OBJECTIVE

This chapter (Figure 3.1) aimed to produce bioreceptors, antibodies, for cytostatic drugs and validate them via development of an immunoassay. 5-fluorouracil and cyclophosphamide were selected since both drugs are widely used for the treatment of cancer and have been suggested that TDM could improve clinical outcome and reduce toxicity. Although the final objective was implementing this newly produced bioreceptors in a multiplexed platform, it was not addressed due to difficulties found during validation of the antibodies.

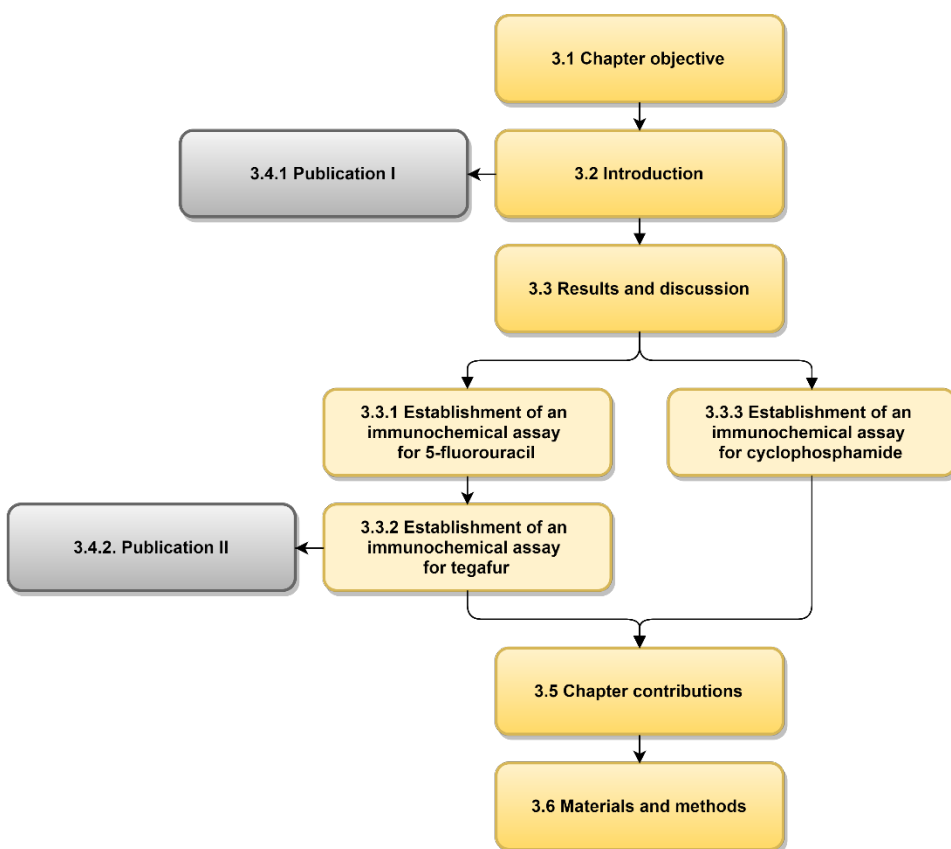


Figure 3.1 Structure of chapter 3 related to the different sections

3.2 INTRODUCTION

Cancer is the second cause of death worldwide and the global burden is expected to grow to 21.7 million new cases and 13 million deaths by 2030²⁷. Cancer is caused by an uncontrolled division of abnormal cells in a part of the body. Possible cancer treatment include surgery, radiation, hormonal therapy, chemotherapy, targeted therapy and immunotherapy and it is chosen depending on the type, location, grade of the cancer and person's health.

3.2.1 CHEMOTHERAPY

Chemotherapy is a popular treatment of cancer. Cytostatic drugs have been designed to keep neoplastic cells from dividing. Cancer cells tend to divide more rapidly than normal cells and, therefore, they are more likely to die from the treatment. Cytostatics drugs are classified as antimetabolites, DNA-interactive agents and antitubulin agents (Figure 3.2):

- Antimetabolites resemble cellular metabolites such as folic acid, purine and pyrimidine nucleotide bases, interfering with DNA precursors and cellular metabolism, examples of this group include 5-fluorouracil, capecitabine, gemcitabine and methotrexate.
- DNA-interactive agents enclose different compounds that interact directly with cellular DNA avoiding its replication, main examples are platinum agents like cisplatin or carboplatin, alkylating agents as cyclophosphamide or an intercalating agents as doxorubicin.
- Finally, antitubulin agents interfere with the formation of mitotic spindle, arresting the mitosis process, this group includes docetaxel and vincristine.

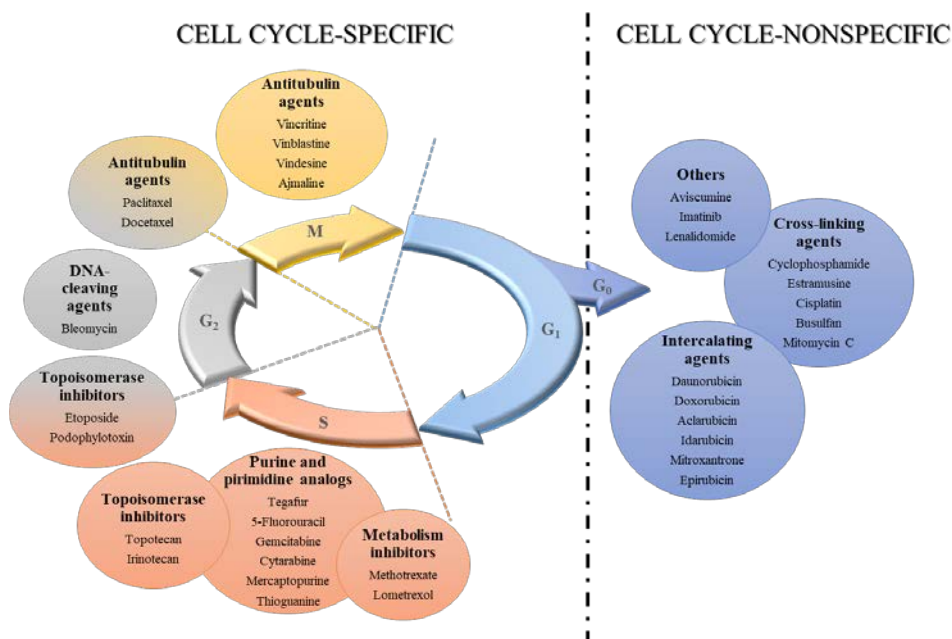


Figure 3.2 List of cytostatic drugs grouped by family. Colors indicate the cell-cycle stage in which each family acts (G₀, resting; G₁, growth or gap 1; S, DNA synthesis; G₂, growth or gap 2; M, mitosis)

3.2.2 TDM OF CYTOSTATIC AGENTS

The majority of anticancer drugs are cytotoxic in nature, and have limited specificity, consequently, the optimal dose for a given patient is very narrow. Thus, cytostatic agents fulfil requirements to be monitored (see section 2.2.3). In addition, TDM is a must for successful cancer treatment due to the high rate of patients being exposed outside the therapeutic window. Phase III trials sometimes fail due to low efficacy as a result of underdosing²⁸ or life-threatening side effects as a result of overdosing.

Despite the problematic stated above, TDM is only routinely applied to methotrexate²⁹. Main reasons for its low actual application are related to fundamental practical and scientific challenges^{26, 28, 30, 31}.

1. Lack of established exposure-response relationship. Arising from pharmacokinetics and pharmacodynamics variability, a single dose may

result in a range of exposures, and a single exposure may result in a range of responses.

2. Several widely used anticancer agents are pro-drugs and require in vivo activation. This activation can occur intracellularly avoiding TDM approaches.
3. Frequent use of multidrug treatments in established regimens combined with additional agents to manage side effects. Pharmacokinetic - pharmacodynamics relationships are more difficult to model for drug combinations.
4. Highly applied intravenous administration present a drastic decrease in concentration. Furthermore, some drugs tend to bound to proteins difficulting its detection.
5. Therapeutic drug monitoring cost and its prospective validation has also been stated as a limitation. Even though, accurate treatment could also lead to reduced treatment costs.

Hence, due to the challenge we are facing, necessary analytical equipment and expertise should be developed as a step towards TDM implementation. These analytical techniques should have a broad linear range since drug concentration can vary from μM to nM over only a few hours. More information about bioanalytical techniques for TDM of cytostatic drugs can be found in section 3.4.1.

3.2.2.1 5-Fluorouracil and tegafur

5-fluorouracil (5FU), first described in 1950s, belongs to the antimetabolite family. It's a fluorinated uracil analog that works into uracil biosynthetic processes: inhibits thymidylate synthase and incorporates its active forms into RNA and DNA (Figure 3.3). The main mechanism of 5FU activation is conversion to fluorouridine monophosphate (FUMP) by orotate phosphoribosyltransferase or fluorodeoxyuridine monophosphate (FdUMP) by thymidine phosphorylase and thymidine kinase. Dihydropyrimidine dehydrogenase (DPD)-mediated conversion of 5FU to dihydrofluorouracil (DHFU) is the rate-limiting step of 5FU catabolism in normal and tumor cells. Up to 80% of administered 5FU is broken down by DPD in the liver.

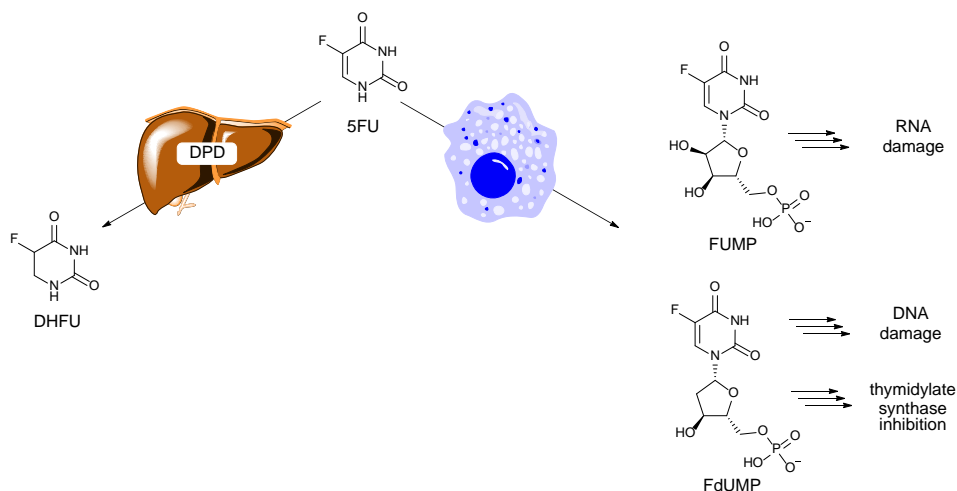


Figure 3.3 Metabolic pathway of 5-fluorouracil. DHFU, dihydrofluorouracil; DPD, dihydropyrimidine dehydrogenase, 5FU, fluorouracil; FUMP, fluorouridine monophosphate; FdUMP, fluorodeoxyuridine monophosphate.

However, different polymorphisms have been described for the gene which encodes DPD enzyme, the 5FU main detoxification route. DPD deficiency could result in 5FU accumulation and, consequently, in an increase of the toxicity. Oral derivatives have been employed to overcome this toxicity. These prodrugs have been designed as orally administered drugs reporting prolonged 5FU exposure and lower peak concentrations. What is more, they provide pharmacoeconomic advantages by reducing administration costs and toxicity related hospitalizations³². Tegafur (FT, ftorafur) is a established prodrug oxidized to 5FU by two catabolic routes: oxidation by cytochrome P450 (CYP2A6) enzyme in liver microsomes or by thymidine phosphorylase in the liver cytosol.

5FU is the most widely used cytostatic drug³³ and is considered by far the most active antineoplastic agent. Both 5FU and FT are administered for colorectal, breast, and head and neck cancers, among others. Significant side effects related to these compounds are bone marrow depression and gastrointestinal toxicity. They are often given in combination with other cytostatic agents to alter its bioavailability and toxicity and improve its clinical outcome³⁴.

TDM of 5FU, as for most cytostatic agents, faces the lack of clear correlation between the drug dose and the drug effect. Nonetheless, a recent study claims that the intensity of the drug effect is related to plasma levels of the drug,

proposing plasma levels of 5FU as the key for TDM³⁵. Nowadays, 5FU dosing is based on body surface area calculations that presents a wide range of interpatient variation³⁶. Thus, plasma concentration studies have been confirmed by the validation in more than one trial with results of improved therapeutic index³⁷. Due to its short elimination half-live, adjustment of the dose is tailored to the elimination capacity of the individual patient and is performed either during the administration or the next cycle of treatment³¹. Concerning TRM, molecular biomarkers that predict tumor sensitivity to 5FU have been identified, including mRNA and protein expression levels of thymidylate synthase³⁸.

Analytical methods for 5FU and FT have traditionally implied chromatographic methods. An extensive analysis of these methods was published by Nussbaumer *et al.*³⁹. However, these methods have the limitation of needing sample pretreatment and not being fast, economical and high-throughput systems. Despite the high quantity of chromatographic methods developed for this purpose, seldom bioanalytical techniques have been described (Table 3.1).

Table 3.1 Bioanalytical techniques for 5FU and FT detection

Compound	Assay Type	Matrix	LOD	Miscellaneous	Ref
5FU	Nanoparticle immunoassay	Plasma	400 nM	Commercially available (My5FU™, Saladax biomedical)	40, 41
	ECL ^a	Plasma	40 nM	mAb ^c conjugated to a ruthenium chelate	42, 43
	Biosensor	Pharmaceutical formulation	2.4 μM	DNA glassy carbon electrode	44
	Biosensor	Pharmaceutical formulation & urine	20 nM	Chitosan stabilized gold particles on multiwall carbon nanotube modified electrode	45
FT	cELISA ^b	Urine	3.1 μM	pAb ^d	46

a) ECL, electroluminescence assay. b) cELISA, competitive enzyme linked immunosorbent assay. c) mAb, monoclonal antibody. d) pAb, polyclonal antibody.

In the case of FT, only one immunoassay has been developed for its quantification in urine samples⁴⁶. Although detectability was in the range of some regimes used, high crossreactivity with 5-fluorouridine was found preventing its use in plasma samples. Further work has addressed 5FU problematic. Salamone *et al.* raised monoclonal antibodies⁴⁷ and implemented

them in a homogeneous nanoparticle immunoassay obtaining a detectability of $0.4 \mu\text{M}$ ^{40, 41}. This assay is commercialized as My5FU™ by Saladax biomedical. Simultaneously, an electroluminescence assay was also developed based on monoclonal antibodies conjugated to a ruthenium chelate^{42, 43} by Wellstat Diagnostics LLC. A LOD of an order of magnitude lower than My5FU™ was reported but slight crossreactivity with tegafur was observed. Finally, chitosan stabilized gold particles on multiwall carbon nanotube modified electrode improved its LOD down to 20 nM ⁴⁵. However, this assay was only applied in urine samples and pharmaceutical formulations.

3.2.2.2 Cyclophosphamide

Cyclophosphamide (CP) is also a cytostatic drug that belongs to the alkylating agent family, it is a nitrogen mustard and its mechanism of action is based on inter- and intra-strand DNA crosslink. After intravenous or oral administration (Figure 3.4), cyclophosphamide is rapidly distributed in the body, but it is inactive by itself. In the liver, 75-80% of the drug is enzymatically activated⁴⁸ and converted to 4-hydroxycyclophosphamide (4OHCP), which stays in equilibrium with aldophosphamide (aldoCP). 4OHCP and aldoCP readily cross the cell membranes by passive diffusion. In cells with high levels of aldehyde dehydrogenase 1 (ALDH) (for example, hematopoietic stem cells), aldophosphamide is irreversibly converted to carboxyphosphamide (CXCP). In the absence of a high concentration of aldehyde dehydrogenase (for example, lymphocytes), aldophosphamide spontaneously liberates phosphoramidate mustard and acrolein. Phosphoramidate mustard is a bifunctional DNA alkylating molecule and forms interstrand DNA crosslinks, primarily at the guanine sites, producing cell death. Carboxyphosphamide does not decompose to phosphoramidate mustard and therefore lacks alkylating and cytotoxic activity. CP detoxification route involves aldehyde dehydrogenase, consequently, cells with high concentration of this enzyme will be relatively resistant to it.

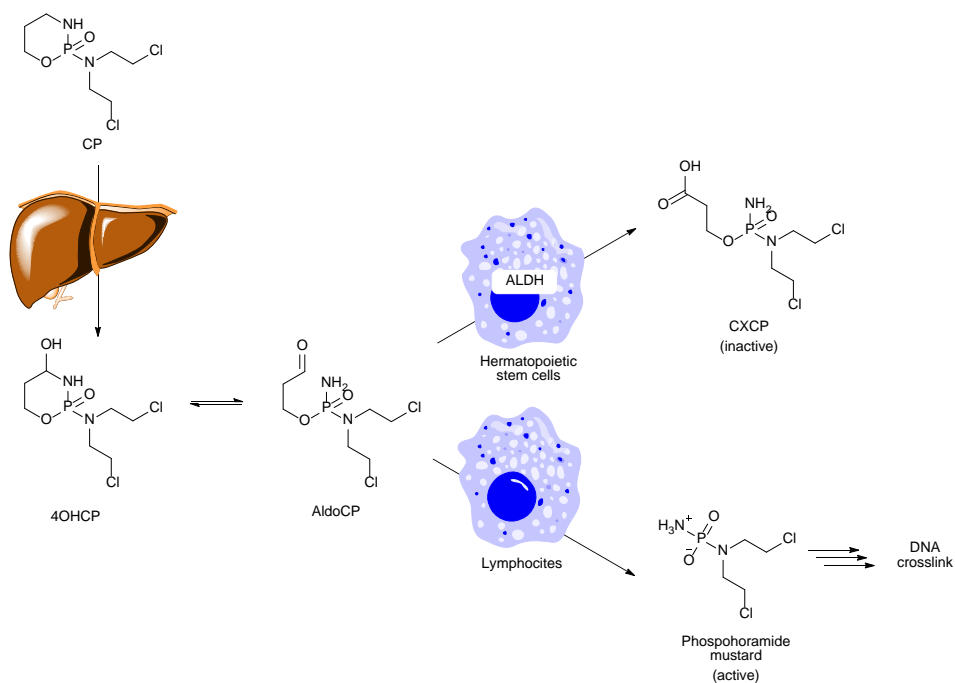


Figure 3.4 Metabolic pathway of cyclophosphamide. CP, cyclophosphamide; 4OHCP, 4-hydroxycyclophosphamide; AldoCP, aldophosphamide; ALDH, aldehyde dehydrogenase 1; CXCP, carboxyphosphamide.

CP is one of the most successful anticancer agents after 60 years of its clinical trials as chemotherapeutic agent⁴⁹. The lack of cell-cycle selectivity has promoted its use in clinical oncology as a single-dose therapy⁵⁰. Hence, its principal risk arises from its accumulation due to this high dose regime. It is used for the treatment of a broad range of cancers as bronchus, breast, ovary and lymphoid and pediatric malignancies, as well as, bone marrow transplantation and different autoimmune conditions. Toxic effects related to this drug are bone marrow suppression, cardiac and gonadal toxicity, hemorrhagic cystitis and carcinogenesis.

Despite the extended use of cyclophosphamide, there is insufficient work concerning TDM. In contrast to 5-fluorouracil, that several studies have focused on pharmacokinetic and pharmacodynamics variability of the drug and how TDM can improve clinical outcome, less publications have addressed this problematic for CP. Cyclophosphamide metabolites role in the efficacy and toxicity is unclear, nevertheless, relationship between exposure and toxicity has been proposed⁴⁹,

⁵⁰. In addition, variations on pharmacokinetics have also been discussed aiming to improve the therapeutic index⁴⁸.

Since 2001, several chromatographic methods for cyclophosphamide quantification in biological samples have demonstrated good quantitative performance in terms of sensitivity and selectivity, obtaining LOQ in the nM range³⁹. Recently a LC-MS/MS method has been also reported with a LOQ in the pM range for urine samples⁵¹.

Table 3.2 Bioanalytical techniques for CP detection

Compound	Assay Type	Matrix	LOD	Miscellaneous	Ref
CP	Bioassay	Biological fluids	-	Walker-256	52
	Bioassay	Tissue	38 $\mu\text{mol/Kg}$	Chinese Hamster V79 cell line	53
	cELISA ^a	-	0.1 μM	pAb ^b , only for active metabolites	54
	Biosensor	Serum	12 μM	P450 Multiwalled carbon nanotube	55

a) cELISA, competitive enzyme linked immunosorbent assay. b) pAb, polyclonal antibody.

Nevertheless, seldom bioanalytical assays have been reported for cyclophosphamide (Table 3.2). At first, two bioassays^{52, 53} were developed for clinical trials pharmacokinetic studies but did not reach further application. Only one patented immunoassay has been developed for TDM⁵⁴. Polyclonal antibodies produced were only selective for an active metabolite and not for the main drug. Consequently this immunoassay has not reached the market. Finally, a biosensor for cyclophosphamide quantification has been developed and challenged with human serum samples⁵⁵. A carbon nanotube electrode was able to enhance sensitivity reaching LOD of 12 μM , within the therapeutic range for certain regimes. Furthermore, this last assay was also able to quantify multi-panel drugs including benzphetamine, dextromethorphan, naproxen and flurbiprofen, nevertheless, not all compounds reached required detectability.

3.3 RESULTS AND DISCUSSION

This chapter describes hapten design and antibody production for 5-fluorouracil and cyclophosphamide. Antibody validation problematic found with 5FU is discussed to finally propose the development of an immunoassay for tegafur.

3.3.1 ESTABLISHMENT OF AN IMMUNOCHEMICAL ASSAY FOR 5-FLUOROURACIL

3.3.1.1 Hapten design

Small molecules are not immunogenic by itself since they are quickly degraded and excreted. In order to produce antibodies against these molecules, they have to be coupled to a higher molecular weight carrier to produce an immunogenic response (Figure 3.5).

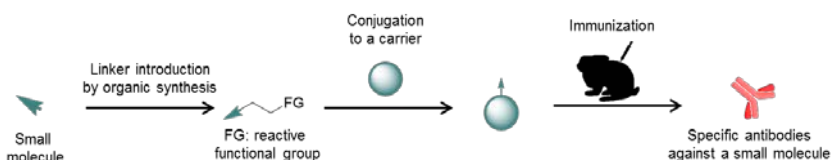


Figure 3.5 Scheme showing the procedure required for the production of antibodies against small molecules.

Firstly, a hapten should be designed. A hapten is a small molecule with similar physico-chemical properties to the analyte, in which a linker is introduced for the coupling to the carrier protein. The conjugation to the highly immunogenic protein is done through its reactive groups of proteins such as amines or carboxylic acids.

In our case, alkyl chain of the hapten was designed with a terminal acid group, which could be easily activated for the subsequent reaction with the amino groups of the protein. This conjugate is called immunogen, which is then injected into New Zealand female Rabbits for the production of polyclonal antibodies. Within this scope, three haptens were designed for antibody production against 5FU (Figure 3.6).

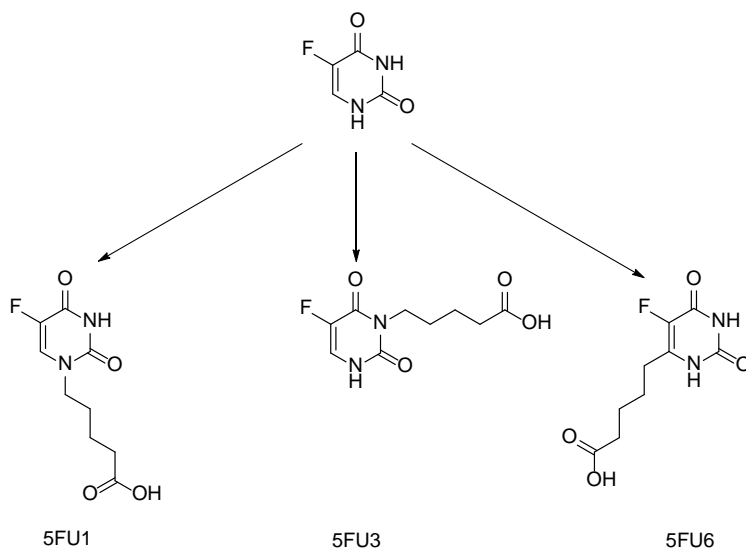


Figure 3.6 Structure of 5FU and design of 5FU haptens.

Haptens were designed with the linkers at position 1, 3 and 6 of the aromatic ring. Within this design, antibodies produced against 5FU3 and 5FU6 haptens could be selective for the free drug. Otherwise, the ones produced against 5FU1 could be selective for 5FU metabolites or prodrugs^{46, 47} since they also have alkyl chains at position 1. The procedures of hapten synthesis are reported in section 3.4. Haptens with linker at position 1 and 3 were already reported by Salamone *et al.*⁴⁷ and Wellstat diagnostics⁴³. Thus, our main contribution has been the synthesis of 5FU6, which could become the ideal hapten for 5FU detection since it has all the heteroatoms exposed.

Basically, 5FU1 and 5FU3 synthesis were done taking advantage of the nucleophilic amines. Methylbromovalerate was introduced aided by base treatment for amine deprotonation. Some bases were tried, KOH⁵⁶ or NaH⁵⁷, like reported in the literature without successful results. Desired products were obtained with trimethylamine treatment in DMF⁵⁸ reporting a yield of 12 % for methyl 5-(5-fluoro-2,4-dioxo-3H-pyrimidin-1-yl)pentanoate, and 5 % of methyl 5-(5-fluoro-2,4-dioxo-1H-pyrimidin-3-yl)pentanoate. Final deprotection of the acid groups to obtain 5FU1 and 5FU3 was done with base treatment.

On the other hand, the synthesis of 5FU6 was designed using a brominated resin⁵⁹. The first step was the synthesis of the α -fluoro- β -ketoester. This system

was used for cycling with urea, which was previously attached to the resin. Finally, the ester was hydrolyzed and released to obtain the desired hapten (Figure 3.7).

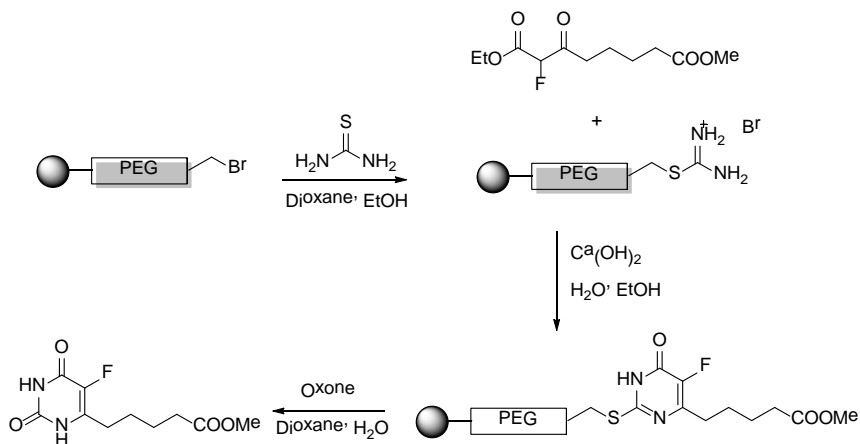


Figure 3.7 Synthesis of 5FU6 proposal

Synthesis of the fluoroketoester by reaction of ethyl fluoroacetate and methyl adipoyl chloride⁶⁰ was successfully accomplished with a yield of 35%, after a separation step by column chromatography. Nevertheless, the formation of the ring via solid phase synthesis reported a really low yield (2%). Briefly, the synthesis in solid phase is based in three steps that could not be fully characterized (Figure 3.8).

Hence, other strategies for ring formation were evaluated. First, the same reaction in solution was tried. This reaction was also carried in ethanol aided by calcium hydroxide as a base at reflux conditions⁶¹. Unfortunately, this approach did not yield the desired product. Finally, a solvent-free microwave assisted method⁶² was evaluated and optimized providing the best results until now. This strategy reported a 10% yield after column purification. Final deprotection of the acid was also done with base treatment with high yield to obtain 5FU6.

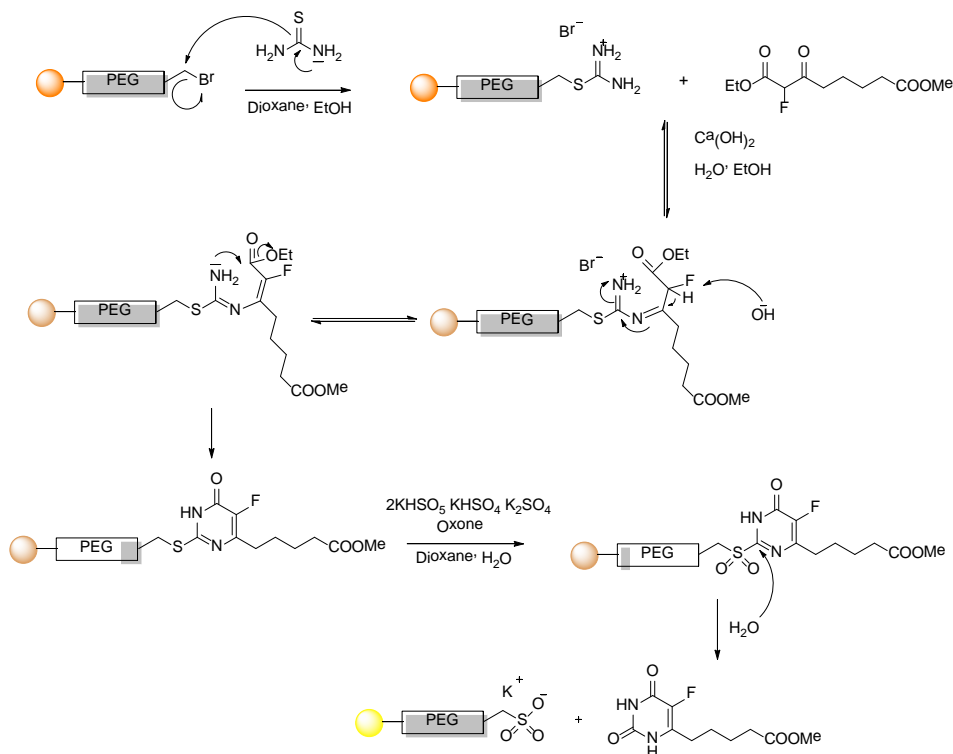


Figure 3.8 Mechanism of solid phase synthesis of uridine rings

3.3.1.2 Antibody production

Having the haptens synthesized, immunogens were prepared covalently conjugating the haptens with Horseshoe Crab Hemocyanin (HCH) via carbodiimide/N-hydroxysuccinimide strategy. The conjugation yield evaluation was performed by MALDI-TOF-MS and can be found in Table 3.3. Due to HCH high molecular mass, bovine serum albumin (BSA) had to be prepared as a reference.

Table 3.3 Hapten densities of produced immunogens for 5FU detection

Immunogen	# of residues (of BSA reference)
5FU1-HCH	19
5FU3-HCH	19
5FU6-HCH	14

Each conjugate was used for immunizing three New Zealand female rabbits (5FU1-HCH were named 337-338-339, 5FU3-HCH were named 340-341-342 and

5FU6-HCH were named 326-327-328). Antisera titer were evaluated along time with a non-competitive ELISA, measuring the absorbance related to the binding of serial dilutions of each antiserum with their corresponding hapten-BSA conjugates. The results are shown in Figure 3.9. Good antibody titer for all haptens were reported. After first immunization, specific antibodies were produced in all cases. Both protocols for immunogen production and immunization can be found in section 3.4.

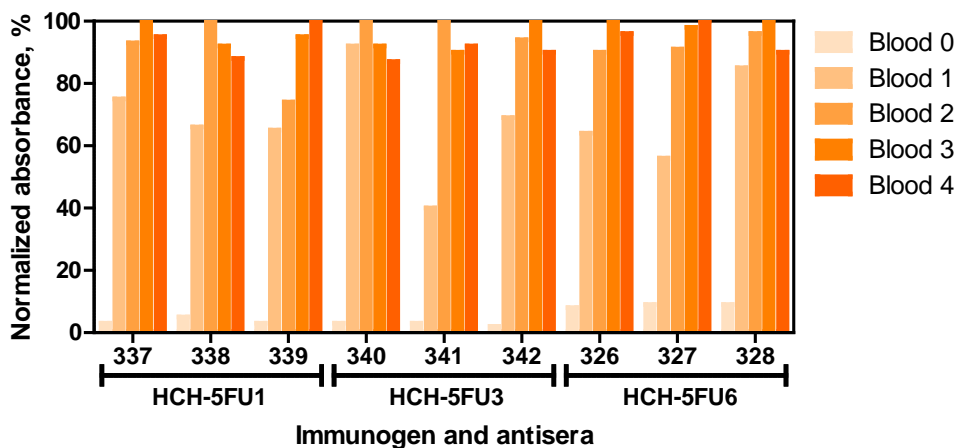


Figure 3.9 Antibody titer to evaluate the response of the antisera produced by non-competitive ELISA. Antigen had a concentration of 1 $\mu\text{g}/\text{mL}$, antisera had a concentration of 1/256000 for As337-342 and 1/64000 for As326-328.

3.3.1.3 Establishment of the immunochemical assay

Immunoassays are based on the principle that antibodies recognize its analytes specifically. There are different kinds of ELISA depending on the weight of the target analyte. High molecular weight analytes are detected with sandwich ELISA, while, low molecular weight molecules can't be detected directly and a competitor (Ag, a hapten conjugated with a protein) is required. This type of assay is called a competitive ELISA.

Competitive assays can be direct, when the competitor is labeled with the enzyme that catalyze a colorimetric reaction. Or indirect, when a secondary labeled antibody is required. This secondary antibody is specific for the constant

fraction of the first antibody. The assay used in this project was the indirect format (Figure 3.10).

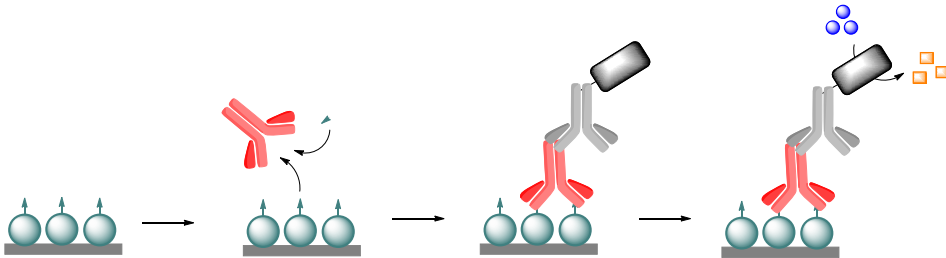
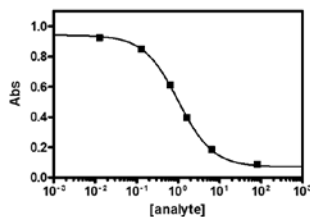


Figure 3.10 Indirect competitive assay. First, the competitor is adsorbed on the well; then, both competitor and analyte compete for the binding site of the antibody; after that a secondary labeled antibody is added and finally, a substrate allows the colorimetric reaction.

Usually, these assays are done in microtiter well plates where, in a sequence of steps, different reagents are added and then washed with the help of a detergent (tween 20) used for avoiding non-specific interactions.

In competitive assays the concentration of the analyte is indirectly proportional to the colorimetric detection (see Figure 3.11). The representation of the logarithm of analyte concentration in front of the measured signal (absorbance) gives the typical inhibition curve (sigmoidal shape). This curve, fitted to a 4 parameters equation, will give the features of the assay.



$$f(x) = A_{max} \frac{(A_{min} - A_{max})}{\left(1 - \left(\frac{x}{IC_{50}}\right)^{Hillslope}\right)}$$

Figure 3.11 Inhibition curve of the competitive ELISA and its fitted equation. IC_{50} : half maximal inhibitory concentration, A_{max} : maximum absorbance, A_{min} : minimum absorbance, Hillslope: slope of the linear part of the curve.

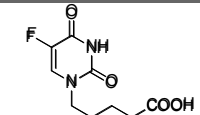
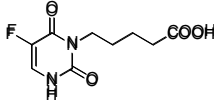
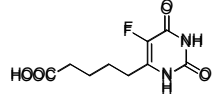
First of all, a set of competitor haptens were produced. The strategy used was also the carbodiimide/N-hydroxysuccinimide chemistry. Nevertheless, a different carbodiimide was used to avoid linker recognition. In this case, proteins used

were albumin from bovine serum (BSA), conalbumin from chicken egg white (CONA) and albumin from chicken egg white (OVA) and an aminopolysaccharide, aminodextran (AD). They were chosen since they provide different carrier conformations and availability of lysine groups. Densities are listed in Table 3.4. OVA and AD could not be analyzed by MALDI-TOF-MS and were further evaluated by checkerboard titration assays.

Table 3.4 Hapten densities of produced competitors for 5FU detection

Hapten	# of residues of BSA conjugates	# of residues of CONA conjugates
5FU1	29	26
5FU3	30	25
5FU6	21	17

Table 3.5 Summary of hapten structure, antisera obtained from the immunized rabbits with hapten-HCH and the competitors prepared for 5-fluorouracil

Hapten name	Structure of the hapten	Antisera	Antigens/Competitors
5FU1		As337, As338, As339 from immunized rabbits against 5FU1-HCH conjugate	5FU1-BSA, 5FU1-CONA, 5FU1-OVA, 5FU1-AD
5FU3		As340, As341, As342 from immunized rabbits against 5FU3-HCH conjugate	5FU3-BSA, 5FU3-CONA, 5FU3-OVA, 5FU3-AD
5FU6		As326, As327, As328 from immunized rabbits against 5FU6-HCH conjugate	5FU6-BSA, 5FU6-CONA, 5FU6-OVA, 5FU6-AD

Appropriate concentrations of the competitor and antisera were established for all the combinations of Ag-As (Table 3.5). Surprisingly, any combination showed an IC_{50} lower than 10 μ M, even though antibodies had been produced against three different haptens. There was a very good recognition of the competitors but they did not recognize the analyte (5FU). An explanation could be that the antibodies are more affine for the antigens than for the analyte (Figure 3.12).

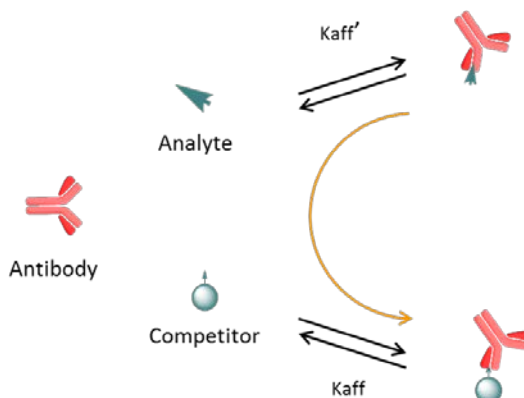


Figure 3.12 Affinity constants of the antibody for the analyte and for the competitor. There is no inhibition of the interaction with the competitor because the affinity constant with the analyte ($K_{aff'}$) is smaller than with the competitor (K_{aff}).

Since it was not clear why there was no inhibition with the presence of 5FU, several hypotheses were proposed. This work was partly carried out by Rita McCabe:

1. The problem could arise due to a low interaction of the target analyte. 5FU has different tautomeric forms⁶³ and could form dimers⁶⁴ or base pairs preventing its detection by the antibodies. Proposed strategies had focused on trying to favour affinity of the antibodies for the analyte.
 - a. Physico-chemical parameters like tween 20 concentration, divalent ions presence or pH were evaluated to elucidate if any of them could affect the biorecognition. Tween 20 could be forming micelles with the drug and avoiding its interaction with antibodies, addition of calcium in the buffer could prevent dimer formation⁶⁵ and pH could affect 5-fluorouracil tautomerism⁶⁶ and also deprotonate the drug⁶⁶.
 - b. Preparation of 5FU stock in different solvents like DMSO, PBS or NaOH 1N were also assessed.
 - c. Addition of organic solvents like EtOH, DMSO or ACN was evaluated, trying to increase 5FU solubility.

None of the previous strategies reported an improvement of the detectability.
2. The problem could arise from hapten conjugation and antibody production. The hypothesis were focused on evaluating if any mistake was produced during antibody production.

- a. Haptens could have been degraded after production. Haptens were well characterized via NMR, IR and UV-Vis and compared against the free drug obtaining similar results in all cases (Figure 3.13). UV spectra of haptens show two bands corresponding to keto and enol form of the fluorouracil ring⁶⁷, while no significant conclusions resulted from IR comparison. In addition, there was no hapten degradation.

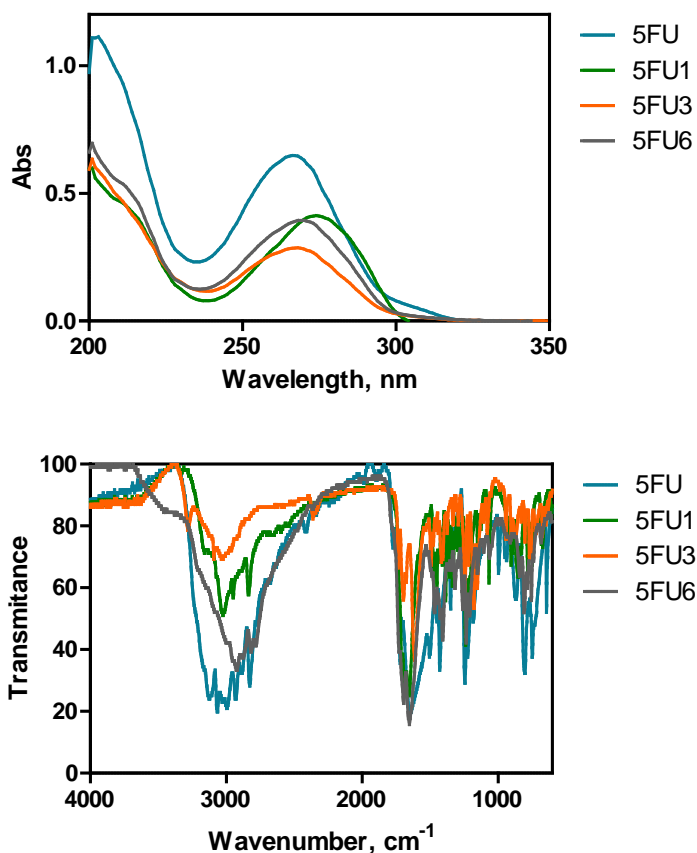


Figure 3.13 UV-Vis and IR spectra of 5FU and the three haptens

- b. Hapten design could have changed the localized charges of the atoms involved in the recognition, producing antibodies not suitable for 5FU detection. Analysis of punctual charges of all atoms, jointly with pKa values of amino groups, were evaluated and compared with free 5FU. Marvin Sketch software was used

for the theoretic calculations. The results, listed in Table 3.6, showed no significant difference between haptens and the drug.

Table 3.6 Comparison of the punctual charge and pKa of 5FU and the haptens

Atom	5FU	5FU1	5FU3	5FU6
1	-0.08	-0.09	-0.09	-0.10
1'	0.21	-	0.20	0.20
2	0.20	0.18	0.18	0.18
2'	-0.38	-0.35	-0.35	-0.35
3	-0.11	-0.10	-0.10	-0.11
3'	0.19	0.19	-	0.19
4	0.21	0.19	0.19	0.19
4'	-0.46	-0.42	-0.42	-0.42
5	0.09	0.10	0.10	0.09
5'	-0.13	-0.13	-0.13	-0.13
6	0.15	0.13	0.12	0.14
6'	0.10	0.10	0.10	-
pKa NH 1	12.02	-	9.41	12.14
pKa NH 3	7.76	8.04	-	8.04

- c. After activation of the carboxylic groups of the hapten, an interreaction could have been produced with the nitrogen leading to the formation of a hapten dimer or polymer. To prove this hypothesis wrong, ^{19}F NMR of the activated haptens was done reporting the presence of only two products, the unreacted hapten and its activated form.

Having discarded all possible solutions, crossreactivity with parent compounds was tested trying to evaluate why antibodies were not recognizing the desired compound. One antibody for each immunogen was selected and tested against the CONA conjugates of the three haptens. All combinations were spiked with 5FU-related compounds such as 5-bromouracil (5BrU), 1,3-dimethyl-5-fluorouracil (5FDMU), FT, uridine (Urd), 5-fluoro-2'-deoxyuridine (5FdUrd), 5-bromo-2'-deoxyuridine (5BrdUrd) and thymine (T). All compounds were spiked at 1 μM and its signal inhibition was compared to a blank. An example of the results can be found in Figure 3.14.

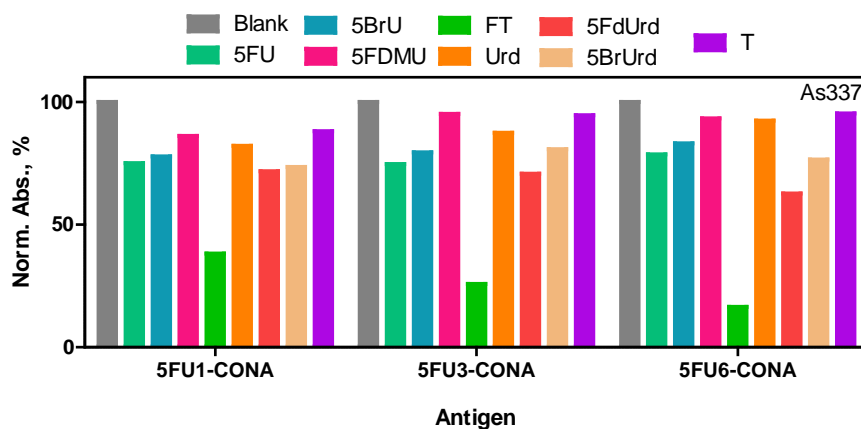


Figure 3.14 Cross-reactivity of the antibodies with 7 related compounds of 5FU: the drug and a control at 1 μ M (Antigen had a concentration of 0.03, 0.05 and 0.125 μ g/mL respectively for each conjugate, antisera (As337) had a concentration of 1/256000, 1/256000 and 1/4000 respectively for each conjugate). The data was normalized and the maximal absorbance, the blank control, was given a 100% of signal. The rest of absorbance inhibitions were calculated based upon the control's signal.

It was observed that antibody As337 showed inhibition for tegafur, a 5-fluorouracil prodrug that presents an alkyl chain in position one of the aromatic ring, as the immunogen used to produce it (5FU1-HCH). Consequently, a tegafur immunoassay was developed and has been described in section 3.3.2.

3.3.1.4 Evaluation of highly heterologous competitors

In a last attempt to develop an immunoassay for 5FU detection, we proposed the preparation of competitors with higher heterology comparing with the analyte. These competitors could have lower affinity for the antibodies and favour the formation of the analyte-antibody complex. Within this purpose, four commercially available heterologous haptens were selected: 5-Bromo-2,4-dioxo-3,4-dihydropyrimidin-1(2H)-yl)acetic acid (5BrU1), 3-(2,4-Dioxo-3,4-dihydropyrimidin-1(2H)-yl)propanoic acid (U1), 1-methyl-L-4,5-dihydroorotic acid (3MeDHU6) and 1,3-Dimethyl-2,6-dioxo-1,2,3,6-tetrahydropyrimidine-4-carboxylic acid (1,3MeU6) (Figure 3.15). There are two haptens with the linker at position 1, and two haptens with the linker at position 6 of the aromatic ring.

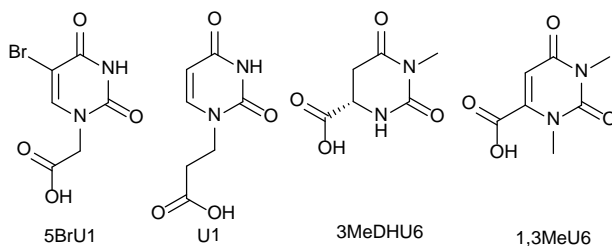
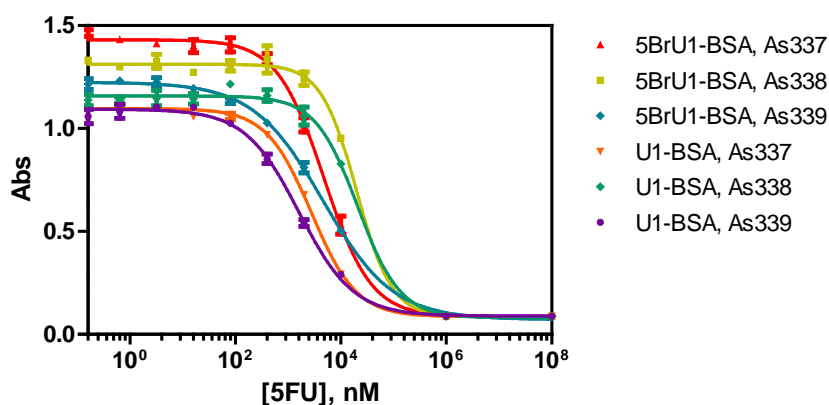


Figure 3.15 Structure of highly heterologous competitors

Haptens were conjugated to BSA as carrier protein and evaluated with MALDI-TOF-MS. Reported hapten density was 6, 6, 7 and 3 for each hapten respectively. Then, all antisera and newly prepared haptens were tested in an inhibition assay in which the analyte, 5FU, was also added at a concentration of 10 μM to evaluate possible inhibition. Results showed that new competitors were only recognized mainly by the antisera produced against the immunogen with the linker at the same position. Briefly, 5BrU1-BSA and U1-BSA were only recognized by As337, 338 and 339 (produced against 5FU1-HCH), and 3MeDHU6-BSA and 1,3MeU6-BSA were only recognized by As326, 327 and 328 (produced against 5FU6-HCH). Antisera produced against 5FU3-HCH was not able to recognize any of these new competitors. Some inhibition was observed with the combination of antisera 5FU1-HCH and the competitors with the linker at position 1. Thus, 2D assays were done with all the combinations to optimize immunoreagent concentrations, and different inhibition curves were obtained (Figure 3.16).

Although these calibration curves were not optimized by means of physico-chemical parameters, promising results were obtained with the combination of U1-BSA and As339. This combination reported an IC_{50} around 1.6 μM and an IC_{90} of 100 nM, which is four times lower than the immunoassay marketed by Saladax biomedical⁴⁰, and close to the ones produced by Wellstat Diagnostics⁴².



Parameters	5BrU1-BSA, As337	5BrU1-BSA, As338	5BrU1-BSA, As339	U1-BSA, As337	U1-BSA, As338	U1-BSA, As339
[Ag], $\mu\text{g/mL}$	0,1	0,1	0,1	0,25	0,25	0,25
[As], dilution	1/128000	1/64000	1/64000	1/32000	1/128000	1/16000
A_{\min}	0,08504	0,08455	0,06755	0,08570	0,07969	0,08882
A_{\max}	1,431	1,312	1,225	1,097	1,158	1,094
Hillslope	-0,9729	-1,293	-0,6483	-1,016	-1,074	-0,8438
IC_{50} , nM	4777	19756	4667	2745	21023	1622
R^2	0,997	0,995	0,998	0,998	0,993	0,996

Figure 3.16 Calibration curve parameters of competitors with linker in position 1 versus antisera produced against HCH-5FU1.

As a conclusion, further optimization studies changing physico-chemical parameters should be undertaken.

3.3.2 ESTABLISHMENT OF AN IMMUNOCHEMICAL ASSAY FOR TEGAFUR

As explained in section 3.3.1, tegafur was the only compound that inhibited the interaction of antibodies raised against 5-fluorouracil and its competitors. Thus, an immunoassay for this drug was optimized. Best results were obtained with the combination As337 and 5FU6-CONA, showing an IC_{50} of 35.6 nM and a LOD of 2.7 nM were reported. Immunoassay was also challenged with plasma samples with successful results. This study was also carried out with the help of Rita McCabe, that run the optimization of the physicochemical parameters and preliminary studies of the matrix effect of serum samples. A detailed explanation

of all the work concerning this section can be found in the related publication (section 3.4.1).

3.3.3 ESTABLISHMENT OF AN IMMUNOCHEMICAL ASSAY FOR CYCLOPHOSPHAMIDE

A detailed description of all procedures related to this experimental part can be found in section 3.6.

3.3.3.1 Hapten design

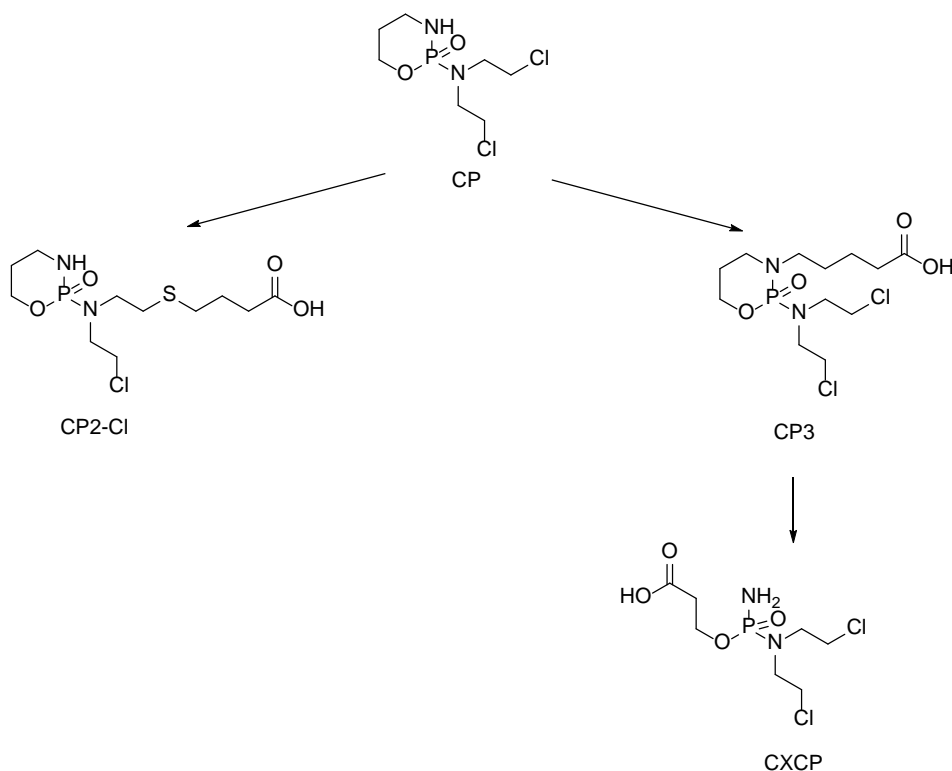


Figure 3.17 Structure of CP hapten design.

In the case of cyclophosphamide, three haptens were proposed (Figure 3.17). The hapten CP2-Cl was designed with the spacer arm in substitution of a chlorine,

trying to expose the cyclophosphamide moiety. While hapten CP3 was designed with the linker attached to the nitrogen of the ring, trying to expose the mustard moiety. The last one could be suitable for several CP metabolites⁵⁴ (AldoCP or CXCP). The hapten CXCP (commercially available) was also used to raise antibodies against the mustard moiety.

In order to synthesize CP2-Cl, the introduction of the alkyl chain was carried via a nucleophilic attack of the chlorine group. Our first approach was the introduction of methyl mercaptopropionate to CP with subsequent hydrolysis of the ester. The main drawback of this strategy was that phosphoramidate is not stable under basic conditions once the ester had to be hydrolyzed. For this reason, the benzyl group was selected because of its deprotection under catalytic hydrogenation. Consequently, our second approach (Figure 3.18) was the protection of dithiobutyric acid with the benzyl group, then the addition of the alkyl chain to the cyclophosphamide, and finally the deprotection of the acid by the mild conditions.

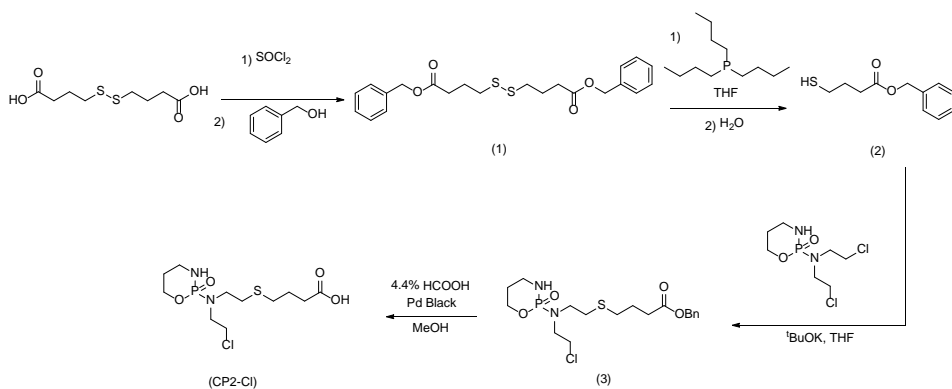


Figure 3.18 Synthesis design of CP2-Cl hapten

The formation of the benzyl ester was done in a two-step reaction, activating the dithiobutyric acid with thionyl chloride and subsequent adding benzyl alcohol, achieving a reaction yield of 87%. Initially, the reduction of the disulfide bond was tried with NaBH₄ which resulted in the hydrolysis of the benzyl group. We changed the strategy using phosphines⁶⁸, a procedure previously reported in our group. Di(*n*-butyl)phenylphosphine polystyrene (DBPP) resin and tritertbutylphosphine were tried. Unfortunately, both phosphines reported low yields suggesting that a less steric hindrance reagent would provide better results. For that reason, tributylphosphine was used obtaining the desired

product with 97% yield. At that point, the spacer arm was introduced to the cyclophosphamide using potassium tertbutoxide, a non-nucleophile base to avoid transesterification, and product was purified by column chromatography obtaining a 13% yield. Finally, catalytic transfer hydrogenation with formic acid and Pd black⁶⁹, reported a yield of 97%.

Concerning CP3 hapten synthesis (Figure 3.19), the same strategy introducing a benzyl protected spacer arm was used. In this case, the spacer was functionalized with a terminal halide group as a leaving group, trying to react with the amino of the cyclophosphamide. Nevertheless, different strategies reported in the literature⁷⁰ were tested without successful results.

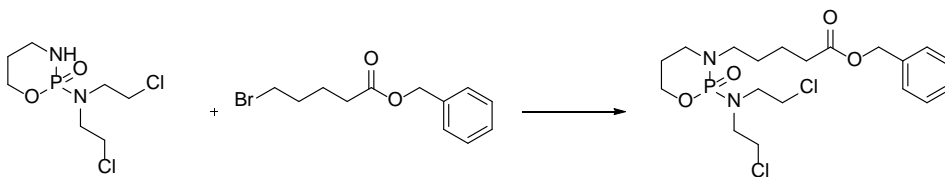


Figure 3.19 Synthesis of CP3 benzyl ester

3.3.3.2 Antibody production

Immunogens were prepared covalently conjugating the haptens (CP2-Cl and CXCP) to Horseshoe Crab Hemocyanin (HCH) via carbodiimide/N-hydroxysuccinimide strategy, the same strategy used for 5FU immunogens. The conjugation yield is shown in Table 3.7.

Table 3.7 Hapten densities of produced immunogens for CP detection

Immunogen	# of residues (of BSA reference)
CP2-Cl-HCH	15
CXCP-HCH	10

Each conjugate was used for immunizing three New Zealand female rabbits (CP2-Cl-HCH were named 343, 344 and 345; CXCP-HCH were named 346, 347 and 348). Antisera titer was evaluated along time with a non-competitive ELISA with their corresponding hapten-BSA conjugate. The results are shown in Figure 3.20. Good antibody titer for all haptens were reported. Along the immunization, a reduction of the antibody titer signal was observed. Sometimes, the immunological system of the host animal increase the antibody specificity instead of antibody avidity.

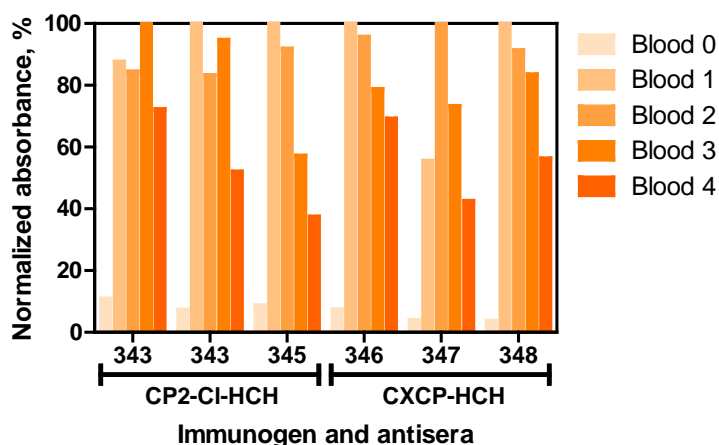


Figure 3.20 Antibody titer to evaluate the response of the antisera produced. Antigen had a concentration of 1 µg/mL, antisera had a concentration of 1/256000.

3.3.3.3 Establishment of the immunochemical assay

This task was achieved with the help of Rita McCabe. First of all, a set of competitors were produced following the same strategy described for 5FU competitors. Haptens were conjugated to three carrier proteins (BSA, CONA, OVA) and an aminopolysaccharide (AD). Densities are listed in Table 3.8.

Table 3.8 Hapten densities of produced competitors for CP detection

Immunogen	# of residues of BSA conjugates	# of residues of CONA conjugates
CP2-Cl	4	15
CXCP	7	10

Table 3.9 Summary of hapten structure, antisera obtained from the immunized rabbits with hapten-HCH and the competitors prepared for cyclophosphamide

Hapten name	Structure of the hapten	Antisera	Antigens/Competitors
CP2-Cl		As343, As344, As345, from immunized rabbits against CP2-Cl-HCH conjugate	CP2-Cl-BSA, CP2-Cl-CONA, CP2-Cl-OVA, CP2-Cl-AD
CXCP		As346, As347, As348, from immunized rabbits against CXCP-HCH conjugate	CXCP-BSA, CXCP-CONA, CXCP-OVA, CXCP-AD

Appropriate concentrations of the competitors and antisera were established for all the combinations (Table 3.9) using 2D titration assays. Calibration curves were assayed with combinations of six antisera against 8 competitors. The best IC_{50} was obtained with the combination of CXCP-BSA and As343.

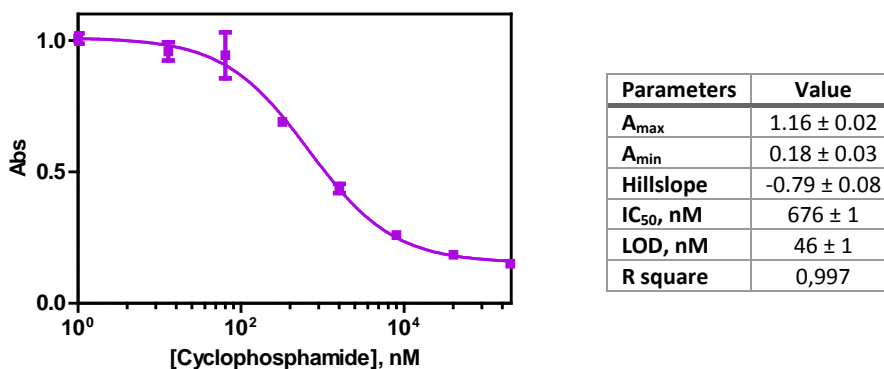


Figure 3.21 Calibration curve parameters of CXCP-BSA versus As343. Ag, CXCP-BSA, had a concentration of 0.0625 $\mu\text{g}/\text{mL}$ and As, As343, of 1/8000. Data has been extracted from the four-parameter equation used to fit the standard curves. Data shows the average and standard deviation of the parameters of the assay using three replicates for each concentration of CP measured.

Calibration curve (Figure 3.21) reported an IC_{50} of 676 nM and a limit of detection of 46 nM. Assay features are promising since other reported immunoassays have high crossreactivity with metabolites and a higher LOD^{54, 71}. Future work should address the optimization of the physico-chemical parameters of the assay and also its implementation to human samples, which ranges from 10 to 1 μM in high dose regime⁵⁰, higher than our LOD.

3.4 RELATED PUBLICATIONS

3.4.1 PUBLICATION I: BIOANALYTICAL METHODS FOR CYTOSTATIC THERAPEUTIC DRUG MONITORING AND OCCUPATIONAL EXPOSURE ASSESSMENT

Bioanalytical Methods For Cytostatic Therapeutic Drug Monitoring and Occupational Exposure Assessment

Marta Broto, Roger Galve and M.-Pilar Marco

Trends in Analytical Chemistry **2017**, 93, 152-170.

This publication is a review of current bioanalytical techniques developed for cytostatic compounds quantification trying to focus on therapeutic drug monitoring and occupational exposure assessment. First, TDM and occupational exposure requirements and legislation are deeply discussed and analyzed. Then bioanalytical techniques are reviewed grouped by cytostatic families focusing in main problems found in its development.



Bioanalytical methods for cytostatic therapeutic drug monitoring and occupational exposure assessment



Marta Broto ^{a, b}, Roger Galve ^{a, b, *}, M.-Pilar Marco ^{a, b}

^a Nanobiotechnology for Diagnostics (Nb4D), Department of Chemical and Biomolecular Nanotechnology (NOB), Institute for Advanced Chemistry of Catalonia (IQAC) of the Spanish Council for Scientific Research (CSIC), Jordi Girona 18-26, 08034 Barcelona, Spain

^b CIBER de Bioingeniería, Biomateriales y Nanomedicina (CIBER-BBN), Jordi Girona 18-26, 08034 Barcelona, Spain

ARTICLE INFO

Article history:

Available online 31 May 2017

Keywords:

Cancer
Cytostatic
Chemotherapy
Therapeutic drug monitoring (TDM)
Occupational exposure
Bioanalytical method
Immunoassay
Biosensor
Bioassay

ABSTRACT

Chemotherapy is the use of chemical substances to treat cancer. However, traditional chemotherapeutic agents do not show sufficient specificity for the cancer cells, which means that also healthy cells are strongly affected by these treatments. In parallel, manufacturers and health-care workers are continuously exposed to these cytostatic drugs through the usual procedures. Thus, there is a need to control the real internal dose received by this sector. Bioanalytical techniques may show great potential as tools for establishing a more personalized treatment procedure since therapeutic drug monitoring (TDM) could support clinicians on making and establishing decisions adapted to each patient. Similarly, these bioanalytical procedures may be implemented on those occupational sectors in which risk for exposure to these hazardous drugs exists. In this review, we present the overall situation in that respect and provide information of the bioanalytical techniques reported up to date for the most important cytostatic families.

© 2017 Elsevier B.V. All rights reserved.

1. Introduction

Cancer, also known as a malignant tumor or malignant neoplasm, is a broad group of diseases involving unregulated cell growth. Cells divide and grow uncontrollably forming tumors that may invade nearby parts of the body. In addition, tumor cells may also spread to more distant parts of the body through the lymphatic system or bloodstream causing the metastasis of the cancer. There are over 200 different known cancers that affect humans and in 2012 it was estimated 14.1 million new cancer cases [1]. Lung and prostate cancers are the leading cause of new cases among men, followed by colorectal, stomach and liver cancers. Moreover, lung cancer has the highest mortality rate followed by liver and stomach cancers. Breast cancer is the leading cause for women, followed by colorectal, cervix and lung cancers. In addition, the risk of cancer worldwide before 75 years can approach 35% (over 1 in 3) in some countries of North America, Europe and Australia. Treatment of

cancer is chosen depending on the type, location and grade of the cancer, as well as, person's health and wishes. Treatments include surgery, radiotherapy, chemotherapy and immunotherapy.

Chemotherapy is the most usual treatment approach. One or more anti-cancer drugs, also known as cytostatic or antineoplastic agents, are used as part of a standardized regimen to kill cancer cells to reduce or remove the disease. Except for those cytostatic agents that more selectively block extracellular growth signals (i.e. hormonal therapy or receptor tyrosine kinases), many anticancer drugs are non-specific intracellular poisons that act inhibiting cell division (mitosis), for which reasons are cytotoxic and have a wide range of side-effects, mainly in tissues with fast-dividing cells (blood cells, cells lining the mouths, stomach, etc.). Toxicity can be observed immediately after administration, weeks or even years later. Thus, cytostatic drugs affect the immunosystem, often paralyzing the bone marrow and leading to a decrease of white and blood cells and also platelets. Gastrointestinal effects (nausea, vomits, anorexia, etc.) or hair loss, are also quite common. However, a bunch of other more important undesirable side effects may occur such as secondary acute leukemia, infertility, teratogenicity, neuropathies, cardiopathies, etc.

Setting up the right dose to obtain the desired effect while minimizing those toxic effects can be difficult. If the dose is too low,

* Corresponding author. Nanobiotechnology for Diagnostics (Nb4D), Department of Chemical and Biomolecular Nanotechnology (NOB), Institute for Advanced Chemistry of Catalonia (IQAC) of the Spanish Council for Scientific Research (CSIC), Jordi Girona 18-26, 08034 Barcelona, Spain. Fax: +34 932045904.
E-mail address: roger.galve@iqac.csic.es (R. Galve).

<http://dx.doi.org/10.1016/j.trac.2017.05.005>

0165-9936/© 2017 Elsevier B.V. All rights reserved.

it will be ineffective against the tumor, whereas, at excessive doses, the toxicity (side-effects) will be intolerable for the patient. When chemotherapy was introduced, the BSA (body surface area) formula was adopted as the official standard for chemotherapy dosing due to a lack of a better option. However, nowadays, the validity of this method has been questioned since the formula only takes into account the individual's weight and height. Drug absorption and clearance are influenced by multiple factors, including age, gender, metabolism, disease state, organ function, drug-to-drug interactions, genetics, and obesity, which has a major impact on the actual concentration of the drug in the patient's bloodstream. As a result, there is high variability in the systemic chemotherapy drug concentration among patients dosed by BSA, and this variability has been demonstrated to be more than 10-fold for many drugs [2]. In other words, if two patients receive the same dose of a given drug based on BSA, the concentration of that drug in the bloodstream of one patient may be 10 times higher or lower compared to that of the other patient [3]. This variability is typical with many chemotherapy drugs dosed by BSA. The result of this pharmacokinetic variability among patients is that many patients do not receive the right dose to achieve optimal treatment effectiveness with minimized toxic side effects. Some patients are overdosed while others are underdosed. In fact, several clinical studies have demonstrated that when chemotherapy dosing is individualized to achieve optimal systemic drug exposure, treatment outcomes are improved and toxic side effects are reduced [4].

On the other hand, workers may be exposed to these drugs during manufacturing, transport and distribution or during use in health or home care settings or due to waste disposal. About more than 6 million workers are estimated to be exposed to hazardous drugs, including pharmacist, nurses, physicians, operating room personnel, etc. Numerous studies demonstrate the higher urine mutagenicity or chromosomal aberrations between nurses and pharmacist handling antineoplastic drugs [5], while some others have associated this occupational activity to acute health effects (hair loss, hypersensitivity, etc.) and adverse reproductive outcomes (infertility, congenital malformations, etc.) [6]. Occupational exposure assessment may prevent the appearance of such adverse effects while reducing the health risks of the workers.

A variety of analytical methods have been reported for the analyses of cytostatic drugs in body fluids and used to assess internal worker exposure. Thus, several studies report the appearance of drug markers in the urine of health-care workers [7]. In the same way, therapeutic drug monitoring (TDM) plasmatic levels of the cytostatic drugs may assist clinicians on performing a more personalized medicine. Most of the methods reported are based on HPLC-MS or GC-MS. However, bioanalytical methods based on the use of biomolecular receptors have proven to be excellent analytical techniques for routine monitoring of a variety of biochemical targets including small organic molecules such as the cytostatic drugs. Hence, this review pretends to provide an overview of the state-of-the-art regarding the use of bioanalytical techniques used for the detection of chemotherapeutic agents in body fluids, making emphasis on their potential for as TDM and occupational exposure assessment.

2. Chemotherapy and cytostatics

Anticancer drugs have been used since 1940s, when nitrogen mustards and antifolate drugs were first applied to cancer treatment [8]. These drugs have been designed for specific cancer-related targets. According to its mechanism of action, they can be grouped in those that are related to interrupting processes or inhibiting substances necessary for cellular replication, processes that occur at higher rates in cancer cells, avoiding all growth and

multiplication of them. Different cytostatic drugs show different properties and modes of action. To understand how cytostatic works, it is important to know the life cycle of the cells. Many different signaling pathways control the phases of the cell cycle, including cell growth, DNA replication, distribution of the duplicated chromosomes to daughter cells, and cell division. Cancer cells have lost their inner clock and, as a result, they multiply rapidly, do not mature properly and often become immortal. Most molecular components of the different cytostatic groups can only affect those phases of the cell cycle that involve cell division. Depending on their specific mechanism of action, cytostatic drugs have the ability to prevent the growth and proliferation of cells. Therefore, these compounds are classified (Fig. 1) as antimetabolites, agents that resemble cellular metabolites such as folic acid, purine and pyrimidine nucleotide bases, interfering with DNA precursors and cellular metabolism; DNA-interactive agents that interact directly with cellular DNA avoiding its replication, and include alkylating, cross-linking and intercalating agents, topoisomerase inhibitors and DNA-cleaving agents; finally, antitubulin agents that interfere with the formation of mitotic spindle, arresting the mitosis process.

3. Therapeutic drug monitoring (TDM) of cytostatic drugs

Therapeutic Drug Monitoring (TDM) was first introduced in 1970s as an activity focused on the measurement and interpretation of drug concentration in biological fluids with the aim to achieve the maximum efficiency while reducing the toxicity achieving a more individualized patient care. Essentially, a drug should be subject to TDM when it shows a narrow therapeutic window (Fig. 2), a high interindividual variability regarding drug response, a clear link between the drug concentration and its therapeutic and toxic effects, and also when it has an optimum analytical method to quantify its concentrations.

Nowadays, TDM is not routinely used for chemotherapy agents. There are several reasons, but one major drawback is the lack of established therapeutic concentration ranges. Each cytostatic has a different concentration-effect relationship and a different metabolism for each individual. Depending on the age, general health status, genetic profile, and other medications that can be administered at the same time, each individual will absorb, metabolize and eliminate drugs in a different rate. For example, patients with dihydropyrimidine dehydrogenase deficiency do not metabolize correctly 5-fluorouracil accumulating the drug and increasing toxicity [9]. In addition, the frequent use of multidrug treatments which can overlap therapeutic and toxic effects, and the use of prodrugs also difficult the establishment of an appropriate dosing [10]. Another drawback is the establishment of appropriate analytical methods, not only for monitoring the drug itself but also for the main active metabolites, as the administered dose is not always predictive of an individual's drug exposure level [11].

Traditionally TDM has only been used as a research tool on clinical studies. Notwithstanding, TDM clearly has the potential to improve the clinical use of chemotherapy agents [12]. As mentioned in the introduction, it has been proved that TDM used to individually adjust the dose for each patient can improve the clinical outcomes in different types of cancer. Between the potential benefits we may include minimizing under and overdosing, diagnosing toxicity, detecting drug interactions and adjusting dose in high-risk patients [10]. Furthermore, TDM is an exceptional tool that can lead to understand why patients do not respond satisfactorily to a particular dose [13]. However, developing TDM analytical methods is complex and requires the collaboration of all the professionals involved in cancer treatment.

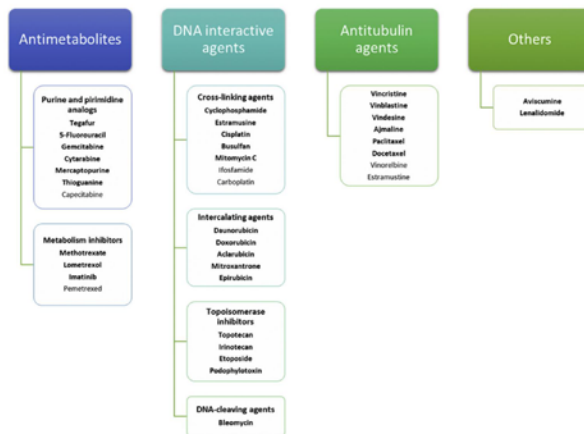


Fig. 1. Scheme showing the most important cytostatic drugs organized by families and types. Compounds that are not in bold have not been discussed in the review.

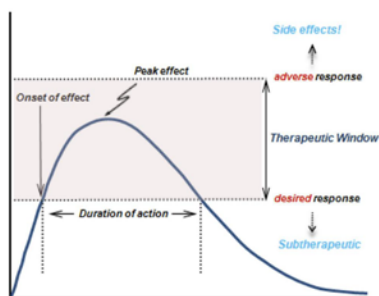


Fig. 2. Representation of plasma drug concentration versus time and indicating the therapeutic range. TDM should be used to ensure personalized protocols in which the plasmatic levels of the cytostatic drugs remain in all cases within this range.

3.1. Guidelines for TDM cytostatic drugs

The most convenient source of drug-level data for therapy is the analytical determination of the levels of the active drug in blood (plasma or serum) [14]. Factors that affect blood drug levels, and that consequently should be taken into account on TDM, are drug pharmacokinetics and pharmacodynamics, as well as the sampling time and the testing methodology. Pharmacokinetics is the striking feature of variability between age, physiology, additional diseases, drug to drug interactions and environmental issues that widely affect ADMET (Absorption, Distribution, Metabolism, Excretion and Toxicity). Pharmacodynamics variability arises from biochemical and physiological effects of drugs in the body that is directly related

to the drug action mechanism. Otherwise, sampling time should be determined for an efficient TDM since drug concentration can vary over the duration of the therapy and it's crucial to achieve a steady state, when drug intake and elimination reach equilibrium. Furthermore, the availability of a testing methodology will ensure access to reliable and robust data to interpret the results and to establish the corresponding therapeutic routine for each patient. Additional considerations for TDM would be the analysis of the therapeutic–toxicity relationship. Also many therapeutic drug metabolites are the active forms and account for therapeutic and toxic effects. The metabolites are often the selected targets on TDM. Apart from that, developed analytical methods should be aware of the requirement for sample treatment. Cytostatic might be present in their protein bound form, requiring for efficient treatments to free the drug, and their chemical nature sometimes make them unstable to light, pH or insoluble, requiring for fast detection methods or specialized treatment. Secondly, it is important that physicians have time to evaluate the result before the patient is scheduled to receive the next dose, usually standard dosing schedules are applied instead of building individual treatments. TDM may allow improving therapeutic efficiency by developing personalized dosing schedules.

The “National Health Service of England” (NHS) in collaboration with the “National Institute for Health and Care Excellence” (NICE) included some antineoplastic compounds in the list of drugs to be monitored in adults in primary care. No other official guidelines have been published regarding TDM of cytostatic drugs. Alternatively, the association “International Association of Therapeutic Drug Monitoring and Clinical Toxicology” (IATDMCT) [15], whose main aim is to improve therapeutic management of patients and the practice of medicine worldwide, has published a couple of guidelines for TDM of 5-fluorouracil and imatinib. This association created in 2015 an Oncology committee with the aim of promoting awareness of TDM needs, stimulating studies and developing consensus guidelines. Otherwise, some articles have been published with reference to guidelines for monitoring [16,17].

4. Occupational exposure to cytostatic drugs

Occupational exposure occurs during the performance of job duties and may pose a risk to the worker. A great number of health-care workers, including nurses, pharmacists, physicians, etc. are potentially exposed to a variety of hazardous drugs in the workplace. Between them, cytostatic agents have been identified as genotoxic substances, and occupational exposure to these drugs consequently raises concerns regarding possible toxic effects on healthcare professionals chronically exposed to these substances.

Cytostatic drugs are indispensable medications in many hospitals, dispensaries, medical practices or outpatient facilities. The number of preparations and applications in Europe is continuously rising because the demographic development and expanded therapeutic possibilities. Health-care working became in contact with these drugs at different points (delivery, preparation of infusions, transport of the infusions, preparation of syringes, plastic bags, administration of the drug, handling of the patient and their body fluids, etc.). Thus, surface contamination by antineoplastic agents in hospital wards has been widely reported [18]. Results confirm that surface contamination is widespread in either preparation or patient areas. Detectable amounts have not only been found in outer surface of vials and safety cabinets but in the floor, on the corridor adjacent to the patient area and close to the chairs for administering drug solution. It has been suggested that contamination of these surfaces might arise from poor handling practices or inadequate cleaning. Furthermore, several studies demonstrate evidence reporting traces of cytostatics in the urine of hospital staff [19]. Otherwise, some also claim that current good practice based on specialized pharmacy units and specially trained nursing staff has reduced the concentration of drugs in biological samples of healthcare workers to undetectable levels [20].

4.1. Biological monitoring (or biomonitoring)

In addition to assess environmental contamination, *biological monitoring* could allow demonstrating whether exposure is associated with significant drug uptake and/or measurable biological effects. It usually implies the repeated measurement of certain exposure-related (bio)chemical markers in biological samples of the workers. Any biomarker proposed should comply with basic criteria such as i) showing a clear correlation with the exposure, ii) the concentration in the sample taken should show correlation with the effect in the target tissue where the hazard exerts its toxic activity, iii) it should allow monitoring the effect of protective measures; iv) variability due to individual response or other factors should be characterized and v) the type of sample used should be minimally invasive and easy to obtain. In addition of measuring parent compounds or their metabolites, alternative strategies address the development of biomarkers based on biological effect or susceptibility [21].

4.2. Regulations and legislation regarding occupational exposure assessment of cytostatic drugs

Both, US and the EU, are investing efforts on reducing risks at work, including those associated to the exposure to hazardous chemicals. In the US, the National Institute for Occupational Safety and Health (NIOSH) is responsible for conducting research and making recommendations for the prevention of such work-related risks. The Occupational Safety and Health Administration (OSHA) is an agency of the US Department of Labor whose mission is to assure safe and healthful working conditions and is responsible for issuing all the necessary workplace health and safety regulations. OSHA has set guidelines and legislation addressed to protect workers

(access to hazard information, use of protective equipment, etc.) and requirements to employers to ensure workplaces free of recognized hazards. In this context, OSHA has set limits on hazardous chemical exposure, known as Permissible Exposure Limits (PEL). OSHA PELs are legal limits in the US for exposure of an employee to a chemical substance, usually on a time-weighted average (TWA) or average exposure over a specific period that usually correspond to the 8 h workday. Nowadays, the OSHA annotated Z-tables contain additionally the California Division of OSHA (Cal/OSHA) PELs, the NIOSH Recommended Exposure Limits (RELs) and the Threshold Limit Values (TLVs[®]) of the American Conference of Governmental Industrial Hygienists (ACGIH[®]).

The Cal/OSHA has the most extensive list of PELs in the US and these are enforced in the workplaces only under its jurisdiction, however provide additional information on acceptable levels of chemicals in the workplace. Although without legislative intent, NIOSH publishes its recommendations in publicly available sources such as the NIOSH Pocket Guide to Chemical Hazards, Criteria Documents, Current Intelligence Bulletins, Alerts, Special Hazard Reviews, Occupational Hazard Assessments, and Technical Guidelines. Thus a NIOSH alert for *Preventing Occupational Exposure to Antineoplastic and Other Hazardous Drugs* was published in 2004, and updated in 2010, 2012 and 2014 [22] which in its Appendix A contains a list of drugs that were deemed to be hazardous and require special handling. According to a Federal Register Notice [23], 33 drugs in addition to 3 drugs with manufacturer's warnings were determined to have one or more characteristics of a hazardous drug. The list of proposed additions can be found at www.regulations.gov, and it contains as cytostatic drugs several new tyrosine kinase inhibitors. Finally, the ACGIH[®], aiming at advancing on occupational and environmental health issues, publishes every year updated editions of their TLVs[®]. The TLVs[®] refer to airborne concentrations of chemical substances and represent conditions under which it is believed that nearly all workers may be repeatedly exposed, day after day, over a working lifetime, without adverse health effects. In respect to biological monitoring exposure, the ACGIH[®] publishes also every year updated books with information related to Biological Exposure Index (BEI[®]) which do not have either a legal character but provide guidance values for assessing concentrations of biomarkers of exposure in biological fluids such as blood or urine [24]. Thus, BEIs represent the levels of determinants that are most likely to be observed in specimens collected from health workers who have been exposed to chemicals in the same extent as workers with inhalation exposure at the TLV[®].

The European Union has also intended to regulate this field and to provide a legal frame to protect workers from the exposure to chemical hazards at their workplaces. The Scientific Committee on Occupational Exposure Limit Values (SCOEL) was set up in 1995 with the mandate to advise the European Commission on occupational exposure limits for chemicals in the workplace. Nowadays the SCOEL is regulated by the Commission Decision 2014/113/EU, which aligns its functioning with the Commission's rules on expert groups. The European Agency for Safety and Health at Work (EU-OSHA) also contributes to the actual European Commission Strategic Framework for Safety and Health at work 2014–2020 and previous ones, whose objective is to coordinate occupational health and safety policies in the EU. The SCOEL prepares scientific recommendations for the Commission which are used to underpin regulatory proposals on occupational Exposure Limit Values (OELVs) for chemicals in the workplace. OELV means the limit of the time-weighted average of the concentration of a chemical agent in the air within the breathing zone of a worker in relation to a specified reference period. Member States should keep workers' and employers' organizations informed of the OELVs set at a Community level. For any chemical for which an OELV is

established at a Community level, Member States should establish a national occupational exposure limit value, taking into account the Community limit value, determining its nature in accordance with national legislation and practice.

This type of legislation was first introduced by the Council Directive 80/1107/EEC, as amended by Council Directive 88/642/EEC, on the protection of workers from the risks related to exposure to chemical, physical and biological agents at work. The Directive sets out the principles for assessing and preventing risks at work from the use of chemical agents and includes the legal framework for *indicative* OELVs (IELVs) and *binding* OELV (BOELVs). The Directive 98/24/EC on the protection of the health and safety of workers from the risks related to chemical agents at work laid down the minimum requirements in this respect establishing OELVs for certain chemicals. This directive also sets health surveillance (HS) and employers' obligations to determine, assess and prevent risks arising from hazardous chemical agents. A key feature of the directive was the setting of exposure limits, which was subsequently updated by Commission Directives 2000/39/EC, 2006/15/EC and 2009/161/EU, placing also the obligation to the member states to implement these directives in their current legislation. The lists of recommended OELs are being regularly updated according to the SCOEL suggestions, being the last SCOEL update is from June 2014, but up to now cytostatic agents are still under evaluation and no official OELs have been established.

The EU also establishes the Biological Limit Values (BLV) as reference values for the evaluation of potential health risks in the practice of occupational health. They are established by SCOEL based on currently available scientific data. The BLVs define maximum levels of substances in humans, their metabolite, or indicator of effect e.g. in blood, urine or breath. For many substances, the data are too limited to support a biological monitoring method, or a metabolite or indicator cannot be defined. Furthermore, they have launched the web www.roadmaponcarnogens.eu, its main aim is to share good practices between companies and organizations.

Cytostatic/cytotoxic drugs are between the most important chemical risks identified between the health-care professionals. Despite that, and of the effort made by those agencies trying to provide guidelines to protect health-care workers using antineoplastic agents, currently, no NIOSH RELs, OSHA PELs, ACGIH TLVs® and BEIs® or EC OELVs and BLVs have been established yet for cytostatics. The main reason for it relies on the lack of sufficient scientific information to set up appropriate biomarkers and on the complexity of the actual analytical procedures to analyze them in the environment and in biological fluids, and consequently on the lack of information to correlate the environmental and biological values with the risk of the health-care workers to suffer adverse effects.

Some pharmaceutical manufacturers have developed risk-based occupational exposure limits to be used in their own manufacturing settings, and this information may be found available in some cases. Other guidelines have been published by the International Agency for Research on Cancer (IARC) [25] in France, who has evaluated and classified several antineoplastic drugs as human carcinogens (Group 1) and, of course, the European Medicines Agency (EMA) [26], who published in July 2012 a pharmacovigilance legislation that had significant implications for applicants and holders of EU marketing authorizations, as well as for patients and healthcare professional regulators.

5. Analytical methods for cytostatic drugs quantification

The *analytical method* is critical for the validity/reliability of a biomarker for either TDM or occupational exposure. Accuracy,

precision, reproducibility, recovery, sensitivity and specificity influence the consistency of the results in relation to the reference values concerned. Moreover, several factors may affect the quality of the samples and the measurement of biomarkers: type of the matrix, point in time of collection, containers and preservatives and other additives used to stabilize the sample, storage temperature and transport time.

Biomonitoring occupational exposure and TDM can be performed in many kinds of *sample matrices*. The appropriate matrix depends on the biomarker selected (exposure, effect or susceptibility), on the type of chemical (parent compound, metabolite, etc.) and its properties (hydrophobicity/hydrophilicity, stability, etc.). For routine purposes, *urine* is the most accepted matrix since it can be obtained under regular bases in a noninvasive manner. Concentration in urine reflects the mean plasma levels of the substance since the last urination. The concentration is adjusted as a function of the creatinine concentration (between 0.3 and 3 g L⁻¹). *Blood* is also used for biomonitoring exposure, particular for inorganic substances or organic chemicals that are poorly metabolized. For regular assessment it is desirable to have analytical methods with high detectability in order to reduce the sample volume needed. *Exhaled air* is also a noninvasive sample that has been used to measure volatile chemicals. Finally, *hair* has become a relevant sample matrix which could be used for TDM but for biomonitoring occupational exposure is not advisable since it can be contaminated by the environment. Other proposed samples which have been much more rarely used have been saliva, sweat, feces, semen or several tissues.

An adequate *sampling strategy* (the timing and the frequency of sample collection) is crucial for effective biomonitoring and TDM programs. Sampling strategy requires knowledge about the biomarker half-life. In the different matrices biomarkers have different half-lives. Even a single biomarker may have different half-lives on different time scales (i.e. a rapid drop of the concentration within days at the beginning of the exposure), followed by a slow decrease in years. For the case of occupational exposure, substances with long half-life, during continuous exposure, concentration may end up reaching a certain value that remains stable (equilibrium) and reflects long-term intake. In such a case, the timing of sample collection during a working day or even working week is not important. However, enough time must be left to reach equilibrium (e.g. lead, cadmium). When the half-life is short (a few hours – a day) the concentration varies remarkably during the working day or week, thus timing of sampling is essential. Such a concentration reflects exposure over a short time and may not be representative of average long-term exposure. A meaningful picture of the average exposure may be obtained only from several samples.

Nowadays, only chromatographic methods are being used for the detection of cytostatic drugs in body fluids. We highly recommend the review published by Nussbaumer et al. [27] regarding chromatographic methods applied on the cytostatic quantification. This review could be very useful when comparing chromatographic techniques with the bioanalytical techniques compiled in this manuscript. However, sensitivity of chromatographic methods is often not enough, usually requires sample preparation or clean-up steps as solid phase extraction, and are not suitable when a huge number of samples have to be analyzed. Furthermore, they are time consuming, more expensive and require qualified personnel. Occupational exposure assessment requires high-throughput screening (HTS) methods in order to be able to process high number of samples and also short time of analysis. All these features are also advantageous for therapeutic drug monitoring in hospitals, considering the undesirable secondary effects associated to cytostatic drugs. Point-of-care (PoC) methods could also provide

advantages for the case of certain occupational sectors avoiding the need to send samples to a central laboratory and providing the possibility to obtain exposure data in a real time. Bioanalytical methods, based on the use of bioreceptors to selectively bind the desired target substances can fulfill these requirements in many applications besides other advantages such as reliability, low-cost, short analysis times and no need for sample treatment. Features such as affinity and specificity are inherent to many biomolecules used as receptors in these types of assays. Moreover, bioanalytical methods can be established in a great variety of analytical configurations, from sensing units in automated devices, to HTS methods or PoC devices. In general, seldom reviews have been published concerning detection of cytostatics by bioanalytical methods including laboratory methods and rapid tests. With this scenario, the present review aims at providing an overview or the state-of-the-art regarding the availability of bioanalytical techniques for cytostatic drugs and their potential use on TDM and OEM.

6. Bioanalytical assays for cytostatic drugs

Although frequently it may be found that the terms biosensor, biochemical assay and bioassay are used indistinctly in different reports, we discriminate clearly between each of these bioanalytical techniques. The criteria used in this review will be according to the definitions that appear in the Text Box 1. It is not the aim of this paper to provide details on the different bioanalytical principles or configurations for which the reader is addressed to many other reviews and papers in which this information can be found extensively described [28].

During the last years a significant number of publications have demonstrated the potential of bioanalytical methods. Fig. 3 shows the scientific articles, patents and commercialized products published concerning bioassays, biochemical assays and biosensors for cytostatic detection. Around 140 scientific articles have been published since the early 70s, being the biochemical the most frequently reported technique. Moreover, the interest for the potential impact of biosensors may have also contributed to an increment in the number of publications.

In this review, we analyze the current situation on the most important cytostatic drug groups. A summary of some of the relevant analytical features of the bioanalytical methods reported for antimetabolites, DNA-interactive agents, antitubulin agents and

other cytostatic compounds is presented in Tables 1–3, respectively (for the corresponding chemical structures, see Fig. 4). It's worth noting that methotrexate and paclitaxel are the most studied antineoplastics accounting for around 30% of the publications. Regarding the type of biological samples addressed, blood has been the most investigated one, and could be directly related to TDM. Also urine has been used as biological sample (see Fig. 5), which could be suitable for both TDM and OEM due to its non-invasive characteristics. Despite the amount of assays developed for blood samples, few of them have been applied for an extensive TDM study, and none of them, even in urine samples have been used for OEM. It is also remarkable the number of assays developed exclusively to analyze pharmaceutical formulation or plant extracts, in this case with the aim of seeking new therapeutic targets structurally related to known parent drugs.

Usefulness of listed bioanalytical techniques should be discussed within detection sensitivity. In the case of TDM, due to high inter- and intra-patient variability, it is difficult to establish a certain concentration range. Also, the drug concentration is dependent on the regime or drug combinations used in the treatment. Thus, a specific range for every patient should be characterized depending on its pharmacokinetics along time. Furthermore, the relationship of drug vs toxicity is not clear in most of the compounds, which is why this technology is also required. Concerning OEM, analysis of samples of healthcare workers should be as low as possible to be able to detect even traces of these compounds.

6.1. Purine and pyrimidine analogs

6.1.1. 5-Fluorouracil and Tegafur

5-Fluorouracil (5-FU) is considered by far the most active anti-neoplastic agent and is the most widely used chemotherapeutic agent worldwide. It has been used for more than 50 years to treat colorectal, breast, aerodigestive tract, head and neck cancers. Significant side effects have been related to this compound such as bone marrow depression and gastrointestinal toxicity. Furthermore, high pharmacokinetic variability interpatient and inpatient has been proved resulting in an inadequate dosage [9]. Barely rapid techniques have been developed to monitor this compound although it has been used for many years. Originally, 5-FU monitoring was based on the detection of its main prodrug, tegafur. In 1999, Nagayama built a competitive enzyme linked immunosorbent assay (cELISA) that was able to detect tegafur in urine samples within an LOD of 3 μM [29]. Later on, Broto et al. developed another cELISA with an LOD of 2.7 nM in plasma samples, low crossreactivity was obtained with main metabolites and 5-FU [30]. Nevertheless, there is no clear evidence that tegafur concentration in urine may have a direct relationship with the 5-FU toxicity. In 2006, Salamone et al. raised monoclonal antibodies against 5-FU conjugates. They described two cELISA for plasma samples obtaining different crossreactivities against its main prodrug Tegafur (0.5 and 200%) and low crossreactivities with other pyrimidines [31]. This difference of crossreactivities arises from the use of two different immunogens; one of them was synthesized introducing the linker in the nitrogen N1 of the uracil ring reporting a higher crossreactivity with Tegafur, while the other immunogen was prepared with the linker in position N3, reporting lower crossreactivity with the prodrug. Same authors developed a homogeneous nanoparticle immunoassay [32] based on a turbidimetric method using an Olympus AU400 clinical analyzer capable of analyzing samples within 10 min obtaining an LOD of 0.4 μM . This Personalized Chemotherapy Management (PCM) kit is commercialized as My5FU by Saladax Biomedical Inc. Simultaneously, Wellstat Diagnostics LLC developed a PoC diagnostic system based on specific monoclonal antibodies conjugated with a

Text box 1

Distinct bioanalytical techniques can be classified as:

- **Bioassay** is a tool for the determination of a biological activity, or for the quantification of a target analyte based on his activity, using recognition elements such as bacteria, cells or tissues. This recognition event is mainly determined by physical or indirect measurement methods.
- **Biochemical assay** is an assay where the biorecognition element is a defined biomolecule such as an enzyme, an oligonucleotide, a protein or an antibody which interacts with the target under stoichiometric conditions.
- **Biosensor** is a self-contained device, consisting of a biological recognition element in direct contact with a transduction element, which converts the biological recognition event into a useable output signal. Biosensors can be classified according to either the method of signal transduction or to the biorecognition principle.

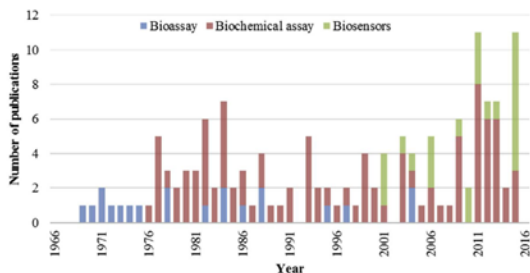


Fig. 3. Publication profile from 1966 to 2016 of bioanalytical methods for cytostatics. Publications are organized according to the type of bioanalytical method (data has been extracted from the publications listed in Tables 1–3).

Table 1
Bioanalytical methods for antimetabolites.

Family	Compound	Assay type	Matrix	LOD	Miscellaneous	Ref	
Purine and pyrimidine analogs	Tegafur	eELISA ^a	Urine	3.1 μM	pAb ^b	[29]	
		eELISA	Plasma	2.7 nM	pAb	[30]	
	5-Fluorouracil	Nanoparticle immunoassay	Plasma	0.4 μM	Commercially available (My5FU™, Saladax biomedical)	[32]	
		ECL ^b	Plasma	0.04 μM	mAb ^c conjugated to a ruthenium chelate	[33]	
	Biosensor	Pharmaceutical formulation	Pharmaceutical formulation	2.4 μM	DNA glassy carbon electrode	[34]	
		Biosensor	Pharmaceutical formulation & urine	–	20 nM	Chitosan stabilized gold particles on multiwall carbon nanotube modified electrode	[35]
	Gemcitabine	eELISA	–	–	IC ₅₀ : 0.03 μM	mAb, Indirect format	[37]
		RIA ^d	Plasma, serum, urine, cerebrospinal fluid	–	4 nM	pAb	[38]
	Cytarabine	RIA	Plasma	10 nM	pAb	[38]	
			Plasma	0.24 nM	pAb	[38]	
Plasma			0.7 pmol/assay	pAb	[38]		
Plasma			82 nM	pAb	[38]		
Plasma			0.1 pmol/5 × 10 ⁶ cells	pAb	[38]		
Bioassay			Biological fluid	0.4 μM	<i>Streptococcus faecalis</i>	[38]	
Bioassay		Plasma & urine	0.1 μM	<i>Streptococcus faecium</i>	[38]		
Mercaptopurine	Biosensor	Pharmaceutical formulation	2.0 μM	Differential pulse voltammetry, DNA modified carbon electrode	[39]		
	Biosensor	Blood	15 nM	Glassy carbon electrode modified with DNA decorated with graphene oxide	[40]		
Thioguanine	Biosensor	–	–	0.12 μM	dsDNA ^e -modified gold electrode	[42]	
Metabolism inhibitor	Methotrexate	EIA ^d	Plasma	0.01 μM	Competitive format	[43]	
		EIA	Plasma & serum	0.02 μM	Commercially available (ARK™ Methotrexate assay, by ARK diagnostics, Inc.)	[44]	
	EMIT	EMIT ^f	Serum	0.2 μM	Homogeneous enzyme immunoassay	[45]	
		EMIT ^g	Plasma & serum	0.05 μM	Commercially available (Syva ^h -Emit ^h assay, Dade-Behring) on the Syva Solaris ^h System	[46]	
	EMIT	EMIT	Plasma	0.05 μM	Commercially available (Syva ^h -Emit ^h assay, Dade-Behring) on the a Siemens Viva E instrument	[47]	
		FPIA ⁱ	Plasma & serum	0.02 μM	Commercially available (Methotrexate II Abbott TDxFLx ⁱ , Abbott technologies)	[49]	
	LSPR ^j	LSPR ^j	Serum	155 nM	Competitive format with folic acid functionalized AuNPs ^k	[53]	
		SPR ^l	Pharmaceutical formulation	28 nM	1 fM	Coupled to sequential injection analysis	[54]
	Biosensor	Biosensor	Pharmaceutical formulation & urine	8 nM	dsDNA glassy carbon electrode	[55]	
		Lometrexol	PCFIA ^m	Serum	0.2 nM	Antibody labeled polystyrene beads	[56]
Imatinib	Nanoparticle-immunoassay	Plasma	18 nM	Commercially available (MyImatinib™, Saladax biomedical) Bechman Coulter AU480™ analyzer	[57]		

The table includes most important bioanalytical detection methods for each compound. ^aeELISA, competitive enzyme linked immunosorbent assay, ^bECL, electrochemiluminescence assay, ^cRIA, radioimmunoassay, ^dEIA, enzyme immunoassay, ^eEMIT, enzyme multiplied immunoassay technique, ^fFPIA, fluorescence polarization immunoassay, ^gLSPR, localized surface plasmon resonance, ^hSyva, surface plasmon resonance, ⁱPCFIA, particle concentration fluorescence immunoassay, ^jpAb, polyclonal antibody, ^kmAb, monoclonal antibody, ^ldsDNA, double-stranded DNA, ^mAuNPs, gold nanoparticles.

ruthenium chelate. This electrochromic assay (ECL) allowed the analysis of plasma within 15 min with an LOD of 0.04 μM [33], an order of magnitude lower than the assay developed by Saladax Biomedical. In 2015, two biosensors were developed for 5-fluorouracil quantification [34,35] standing on the electrocatalytic oxidation of the drug. Only the second one, developed by Satyanarayana et al. [35], and based on chitosan stabilized gold particles on carbon nanotube composite modified electrodes, obtained an LOD of 20 nM with very short analysis times. Unfortunately, there are no bioanalytical techniques described targeting 5-FU main metabolites, which would be extremely useful in toxicity studies. The main drawback in 5-FU monitoring is that until now a clear correlation between the drug dose and the drug effect has not been found, therefore no reliable biomarker has been established. A recent study claims that the intensity of the drug effect is related to plasma levels of the drug [9], which identifies 5-fluorouracil concentration in plasma as the key for TDM, however it is necessary to obtain additional scientific data to establish the parent compound as biomarker for TDM or biological monitoring. Concerning suitable LOD of bioanalytical techniques for TDM, tegafur can be found from 6.5 to 2 μM in plasma samples within S-1 regime [36]. Thus assay developed by Nagayama does not fulfill plasma requirements. The same regime is used for 5-fluorouracil reaching a concentration from 1.1 to 0.01 μM [36], for which Wellstat PoC and Satyanarayana biosensor would be appropriate.

6.1.2. Gemcitabine

Gemcitabine is used for metastatic non-small cell lung, pancreatic, and bladder cancers. Unfortunately, it has been related with some side effects such as bone marrow suppression and liver and kidney damage. Saladax Biochemical developed as well a eLISA against this cytostatic drug only in buffer conditions, obtaining an IC_{50} of 0.03 μM . The hapten was designed by introducing a spacer arm in the 5' position of the sugar moiety obtaining low crossreactivities with its main metabolites [37]. In order to apply this technology for TDM further evaluation of matrix effect and crossreactivity should be done.

6.1.3. Cytarabine

Cytarabine or cytosine arabinoside inhibits the synthesis of deoxyribonucleic acid. It is mainly used in acute myeloid leukemia and non-Hodgkin lymphoma, and usually it is given in combination with thioguanine and anthracycline (doxorubicin or daunorubicin). El-Subbagh and Al-Badr analyzed and compared the analytical methods, either chromatographic or bioanalytical, used for cytarabine until 2009 [38].

6.1.4. Mercaptopurine

Mercaptopurine is an immunosuppressive drug. It is used to treat leukemia, pediatric non-Hodgkin's lymphoma, polycythemia vera, psoriatic arthritis and inflammatory bowel disease. Serious adverse side-effects are allergic reactions, symptoms of bleeding, etc. A differential pulse voltammetry (DPV) method was described for the quantification of this drug. The assay was based in a DNA-modified carbon paste electrode able to selectively detect the compound. It was only applied in the analysis of pharmaceutical formulations reaching an LOD of 2.0 μM [39]. Recently, many electrochemical biosensors have also been developed, all of them reporting better detectabilities. The biosensor developed by Yan and Li [40] was based on a glassy carbon electrode modified with DNA and decorated with graphene oxide. This assay achieved an LOD of 15 nM, with good recoveries in blood samples, fitting TDM requirements, from 1.6 to 0.16 μM [41].

6.1.5. Thioguanine

Thioguanine is used to treat many types of leukemia, ulcerative colitis and some autoimmune diseases. Symptoms of overdose may include unusual bleeding or bruising, fever, sore throat and signs of infection. A DNA modified electrode was published for the detection of thioguanine using a similar strategy than Zhu et al. applied for mercaptopurine [39]. In this case, a composite film modified gold electrode containing dsDNA was used, obtaining a good sensitivity and an LOD of 0.12 μM . Nevertheless, high cross-reactivities were obtained with epinephrine, noradrenaline and dopamine [42] limiting its applicability for TDM and OEM.

6.2. Metabolism inhibitors

6.2.1. Methotrexate

Methotrexate is a folic acid antagonist. It is indicated for the treatment of leukemia, non-Hodgkin's lymphoma, osteosarcoma, head and neck cancer and other malignancies and severe psoriasis, asthma, rheumatoid arthritis, sarcoidosis and transplantation therapy. However, it also has severe toxicity attributed to its low selectivity and, in addition, it is usually used with high-dose therapy regimens. Methotrexate monitoring at fixed time intervals is crucial since a rescue is administered until methotrexate falls below 0.05 μM . Consequently, analytical methodologies are required for therapeutic drug monitoring in order to detect methotrexate concentrations down to 0.05 μM . For this reason, this is the only cytostatic drug for which guidelines to be routinely monitored have been proposed. Probably methotrexate has been the antineoplastic drug most studied. Different enzyme immunoassays and biosensors have been reported for the last 30 years.

6.2.1.1. EIA. Several enzyme immunoassays (EIA) have been developed for the detection of methotrexate. In 1999, Widemann et al. [43] adapted an EIA to a 96-well microplate format, allowing a high-throughput screening assay of 30 small volume biological samples in 20 min, with an LOD of 0.01 μM and a low percentage of crossreactivity of 4% with one of its main metabolites, the 2,4-diamino-N-methylpteroid acid (DAMPA). Afterwards, ARK Diagnostics developed the ARKTM Methotrexate Assay [44], based on homogeneous enzyme immunoassay for the quantification of methotrexate in human serum or plasma. The assay reaches an LOD of 0.02 μM , with no matrix effect but high crossreactivity with DAMPA (64–100%). Although most assays have very low cross-reactivity with the major metabolite 7-hydroxymethotrexate, DAMPA shows a high crossreactivity in methotrexate assays ranging from 44% to 100%. This is probably caused by the design of the methotrexate-immunogen conjugate that is linked via its acid group to the immunogenic protein, exposing the same epitope than the DAMPA molecule. Consequently, immunoassays main disadvantage is the low specificity for methotrexate.

6.2.1.2. EMIT. Enzyme multiplied immunoassay technique (EMIT) was the first "homogeneous immunoassay" to be widely used commercially, introduced by Syva Company in 1973. It is a common method for qualitatively and quantitatively determines drugs in biological samples. Even though an EMIT assay for methotrexate-albumin conjugate in human plasma was developed by Dade Behring (Liederbach, Germany) with the Syva Solaris[®] System, it did not reach the required limit of detection of 0.05 μM for TDM purposes [45]. Later on, many attempts for the optimization of that assay were done, achieving finally this required limit. Hartung et al. [46] obtained an LOD of 0.05 μM increasing reagent concentrations by 1.5-factor. In 2012, Borgman et al. [47] also changed the assay parameters and the calibration of the EMIT by using Viva E instrument (Siemens), reducing the assay detection limit to 0.05 μM

as well. Therefore, all the performed optimizations obtained an accurate assay ranging from 0.05 to 1.0 μM with low interferences and low crossreactivities.

6.2.1.3. FPIA. Fluorescence polarization immunoassay (FPIA) is a homogeneous immunoassay useful for rapid and accurate detection of antibodies or antigens. The principle of the assay is based on a fluorescent dye attached to the immunoreagent that can be excited by phase-polarized light at the appropriate wavelength. The technique measures the decrease of the rotation rate of small molecules once they are attached to the specific antibody. In 1983, Schmidt et al. [48] developed a FPIA that latter on was commercialized by Abbott Laboratories (Abbott Park, Illinois, USA) as Methotrexate Abbott TDx[®] analyzer system. The assay achieved an LOD of 0.05 μM , without any matrix effect but with high crossreactivity against DAMPA. Finally, the immunoassay was improved and commercialized again as Methotrexate II Abbott TDxFLx[®] [49]. This method is the most used for TDM for its simplicity and sensitivity and is routinely used for pharmacokinetic studies.

The three commercial mentioned methods (EIA, EMIT and FPIA) were compared and discussed in a previous work published by Suh-Lailam et al. [50]. The three assays showed similar LODs around 0.01–0.02 μM , as well as similar CVs and recoveries. Nevertheless, Syva[®] Emit[®] had a narrowed working range than the others. Pharmacokinetics in high dose methotrexate regime ranges from 100 to 0.01 μM , which make commercially available assays sufficient for methotrexate TDM [51]. Nevertheless, in case of pediatric regimes their detectability could be helpful to determine the concentration peak but not the full clearance of the drug since plasma concentration ranges from 1 to 0.001 μM [52].

6.2.1.4. Biosensors. Moreover, Zhao et al. [53] developed a localized surface plasmon resonance (LSPR) biosensor. The biosensor basis developed by Zhao et al. consisted on a competitive binding assay of folic acid functionalized gold nanoparticles to human dihydrofolate reductase enzyme. The features of the assay, including a solid-phase extraction step, showed an LOD of 155 μM in serum, with very low crossreactivities with its main metabolites including DAMPA. Later on, this assay was implemented into a miniaturized multi-channel surface plasmon resonance (SPR) instrument. Transducer was changed to SPR in order to avoid matrix effect and, consequently, sample pre-treatment. An LOD of 28 nM was obtained within only 60s. Electrochemical sensor technology was also proposed for the detection of methotrexate. Then, a sequential injection analysis coupled to an amperometric biosensor was developed to detect concentrations as low as 1 fM of *D*-methotrexate in buffer [54], with high-throughput capability of 34 samples per hour. This assay attempted to detect separately *L*- and *D*-methotrexate in pharmaceutical formulations, using *L*-amino acid oxidase, *L*-glutamate oxidase and horseradish peroxidase at different combinations to finally obtain the best detection capabilities. Moreover, a dsDNA modified glassy carbon electrode was also applied for methotrexate quantification. This modification resulted in a better sensibility compared to bare electrode due to its intercalative and electrostatic binding properties [55]. The assay was applied in pharmaceutical formulations and diluted urine without arduous sample treatment. LOD was in the order of 8 nM. Nevertheless, crossreactivities with other antimetabolites were not evaluated.

6.2.2. Lometrexol

Lometrexol, or 5,10-dideaza-5,6,7,8-tetrahydrofolic acid, is a folate analog, that inhibits glycylamide ribonucleotide

formyltransferase, a crucial enzyme in purine biosynthetic pathway, interfering in the DNA synthesis and stacking cells in the S phase of the cell cycle. It can be used in tumors that are resistant to folate antagonist (methotrexate). In 1991, a competitive particle concentration fluorescence immunoassay (PCFIA) was described for the detection of lometrexol in human serum samples [56]. This assay was performed in a filter-bottomed microtiter plate, where lometrexol conjugated to a fluorescent protein competed with free lometrexol for the binding site of a specific antibody bound to polystyrene particles. This kind of assay allows a faster and automated detection compared to conventional immunoassays. Although samples should be diluted five-fold to avoid filter clogging, the assay showed a 0.2 nM detection limit, good precision and low crossreactivities with other folate analogs or methotrexate. This assay was applied in Phase I clinical studies demonstrating its capability for TDM.

6.2.3. Imatinib

It is a tyrosine-kinase inhibitor used in the treatment of chronic myelogenous leukemia and gastrointestinal stromal tumors. Compared to other cytostatic agents it has a less benign adverse effect profile. Common side effects are similar to other drugs but severe side effects include congestive cardiac failure. Even tough tyrosine-kinase inhibitors are recommended for therapeutic drug monitoring [17] seldom bioanalytical methods have been developed for this purpose. Monoclonal and polyclonal antibodies were raised for imatinib mesylate detection and an immunoassay was developed by Saladax Biomedical [57]. Low crossreactivity with its active metabolite *N*-desmethyl imatinib was obtained. These monoclonal antibodies were conjugated to 200 nm particles for the incorporation into an automated immunoassay using the Bechman Coulter AU480[™] analyzer obtaining a sensitivity of 18 nM. This assay has been commercialized with TDM purposes.

6.3. Cross-linking agents

6.3.1. Cyclophosphamide

Cyclophosphamide is a nitrogen mustard alkylating agent from the oxazophosphorine group. First described in 1958 by Arnold and Bourseaux, this prodrug is widely used as chemotherapeutic agent. Cyclophosphamide is inactive by itself. With the help of cytochrome P-450 oxidase system in the liver, the inactive drug is converted into phosphoramidate mustard and acrolein which are very active compounds. Phosphoramidate crosslinks DNA by adding an alkyl radical to the guanine base of DNA strand. This induces inhibition of DNA replication, leading to cell death. Cyclophosphamide also produces immunosuppressive effects possibly through a cytotoxic effect on lymphocytes. It is used for the treatment of various cancers, including breast, lymphoid and pediatric malignancies and bone marrow transplantation. Severe side effects include bone marrow suppression, hemorrhagic cystitis and stomach ache. Concerning therapeutic drug monitoring only one patented cELISA type assay for the detection of the active metabolites of cyclophosphamide has been developed. Salamone et al. [58] raised antibodies against a protected aldehyde of an active metabolite of cyclophosphamide. The assay showed an LOD of 0.1 μM and low crossreactivities with other compounds of the same family, convenient for TDM which ranges from 10 to 1 μM in high dose regime [59]. In buffer conditions, Carrara et al. [60] developed a multiwalled carbon nanotube P450 biosensor. Carbon nanotubes enhanced the sensitivity and reached detection limits of 12 μM for cyclophosphamide in human serum, allowing the detection of the drug

Table 2
Bioanalytical methods for DNA-interactive agents.

Family	Compound	Assay type	Matrix	LOD	Miscellaneous	Ref
Cross-linking agents	Cyclophosphamide	cELISA ^a	–	0.1 μ M	pAb, only for active metabolites	[58]
		Biosensor	Serum	12 μ M	P450 Multiwalled carbon nanotube	[60]
	Estramustine	RIA ^b	Plasma	11 nM	pAb	[61]
		Bioassay	Plasma	33 μ M	PC-9 cell line, tumor clonogenic assay	
	Cisplatin	Bioassay	Plasma	–	HeLa cell line, tumor clonogenic assay	
		HMDE ^c	Serum	2.5 μ M	Metallothionein modified	[62]
		Fluorescent assay	–	720 nM	G-quadruplex DNA-based	[63]
	Busulfan	cELISA	Plasma	0.3 μ M	Direct assay	[12]
		Immunoassay	Plasma	0.2 μ M	Roche Cobas [®] c111 chemistry analyzer	[65]
	Mitomycin C	EIA ^d	Serum and urine	12 nM	pAb, direct assay	[68]
	7-N-(p-hydroxyphenyl)mitomycin C	EIA	Serum	16 pmol/assay	pAb, direct assay	[69]
	Daunorubicin	RIA	Plasma	–	–	[70]
			Urine	–	–	
	Doxorubicin	cELISA	–	–	mAb ^e	[71]
		ELISA ^a	Biological fluids	1 nM	Commercially available (Adriamycin BioAssay™ ELISA Kit, US Biological Life sciences)	[72]
	Biosensor	–	0.1 nM	DNA-modified nitrocellulose membrane	[77]	
	Biosensor	–	4 pM	DNA multiwalled carbon nanotube modified pencil graphite electrode	[79]	
	Aclarubicin	EIA	Serum	12 pmol/assay	mAb	[119]
	Mitoxantrone	Biosensor	–	80.4 nM	Differential pulse voltammetry, dsDNA carbon paste electrode	[75,76]
	Epirubicin	–	–	50 nM	–	
	Doxorubicin	Biosensor	Pharmaceutical formulation & plasma	0.01 nM	DNA glassy carbon electrode	[78]
	Daunorubicin	–	–	0.1 nM	–	
	Idarubicin	–	–	0.2 nM	–	
Topoisomerase inhibitor	Topotecan	ELISA	Serum & urine	0.2 nM	pAb, direct format	[80]
		Biosensor	–	–	Differential pulse voltammetry, DNA modified pencil graphite electrode	[81]
	Etoposide	ELISA	–	–	pAb, mAb	[82]
		RIA	Plasma	8 nM	pAb	[83]
		RIA	Plasma	0.05 pmol/assay	pAb	[83]
		ELISA	–	10 nM	pAb	[83]
	Etoposide, Teniposide	ELISA	Plasma	0.8 nM	pAb	[83]
		ELISA	Blood & urine	0.07 nM	pAb	[83]
		RIA	Urine	1 nmol/assay	pAb	[83]
		ELISA	Plant extract	0.16 nmol/assay	pAb	[84]
DNA-cleaving agent	Peplomycin	EIA	Blood and urine	0.03 pmol/assay	pAb	[86]
		RIA	Plasma and serum	2 nM	pAb	[85]
	Bleomycin	EIA	Tissue	0.02 pmol/assay	pAb	[87]
		Biosensor	–	100 pM	DNA modified gold electrode, square wave voltammetry	[88]
		Biosensor	–	14 μ M	Impedance spectroscopy, Pencil graphite electrode	[89]
		Exo III-aided DNA recycling amplification	Serum	23 pM	Fluorescence detection	[90]
		Fluorescence quenching	Serum	0.2 nM	Perylene–DNA complex	[91]

The table includes most important bioanalytical detection methods for each compound. ^acELISA, competitive enzyme linked immunosorbent assay, ^bRIA, radioimmunoassay, ^cHMDE, hanging mercury drop electrode, ^dEIA, enzyme immunoassay, ^eELISA, enzyme linked immunosorbent assay, ^fpAb, polyclonal antibody, ^gmAb, monoclonal antibody.

within the therapeutic range. Although the presence of dextromethorphan inhibited the drug detection, the problem was solved using an approximation of Randles-Sevcik equation that accounts for drug interaction.

6.3.2. Estramustine

Estramustine is an antineoplastic drug made as a combination of a nitrogen mustard and the hormone estrogen. This drug is basically used in prostate cancer. Adverse effects include congestive heart failure, stroke, heart attack, pulmonary embolism and thrombophlebitis. In 1978, a radioimmunoassay was developed by Forsgren et al. [61] achieving a LOD of 11 nM for estramustine phosphate. A low crossreactivity with its main metabolites was reported. It was applied for pharmacokinetic studies in animal plasma.

6.3.3. Cisplatin

Cisplatin is an inorganic platinum agent (*cis*-diamminedichloroplatinum) with antineoplastic activity. It forms highly reactive and charged platinum complexes which are susceptible of nucleophilic attack of guanine (G) and cytosine (C) nucleobases, inducing intrastrand and interstrand DNA cross-links, as well as DNA-protein cross-links. These cross-links result in apoptosis and cell growth inhibition. Cisplatin is used to treat sarcomas, carcinomas, lymphomas, bladder cancer, cervical cancer and germ cell tumors. Principal side effects are nephrotoxicity, neurotoxicity and bone marrow suppression. In 2006, Petrova et al. [62] developed an electrochemical biosensor based on metallothionein modified hanging mercury drop electrode (HMDE) for the detection of cisplatin. The assay reached an LOD of 2.5 μ M in human serum. Afterwards, in 2014 Yang et al. [63] reported a G-quadruplex DNA-

based fluorescent assay achieving LODs of 720 nM in buffer, and showing a slight crossreactivity with oxaplatin. However, it was tested in mouse urine samples obtaining good recoveries. Despite the efforts directed towards bioanalytical assay development for cisplatin, they do not reach required detectability, around 3–0.03 μM [64].

6.3.4. Busulfan

Although busulfan is a cell cycle non-specific alkylating agent in the class of alkyl sulfonates, it is not a structural analog of the nitrogen mustards. It has been used in bone marrow transplantation, leukemia and lymphoma. Main side effects include pulmonary fibrosis, hyperpigmentation, seizures and veno occlusive disease. It is commonly administered with cyclophosphamide and fludarabine. In 2009, Courtney et al. [12] raised highly selective monoclonal antibodies against a hapten that was isoelectronic to busulfan. They substituted the two sulfonic groups of the molecule by sulfonamides, a most stable functional group, in order to prepare the immunogen. A direct ELISA was developed achieving an LOD around 0.3 μM , within only 30 min and not showing crossreactivities with its main metabolites (sulfolane, tetrahydrophene and 3-hydroxy-sulfolane). Using the same hapten strategy, Saladax Biomedical Inc. raised monoclonal antibodies as well. These antibodies were conjugated to nanoparticles and were used to develop an assay for the Roche Cobas[®] c111 chemistry analyzer. Within 12 min, an LOD of 0.2 nM was obtained with no crossreactivities with its main metabolites [65] making it useful for TDM, between 10 and 0.6 μM for a certain regime [66], and also for occupational exposure. The main problem of this commercial immunoassay was that busulfan standards were not stable along time in solution. Consequently, authors also patented the use of its isoelectronic form as standard in order to obtain higher stability along time [67].

6.3.5. Mitomycin C

Mitomycin is a natural product isolated from *Streptomyces caespitosus* or *Streptomyces lavendulae*. It is used to treat upper gastro-intestinal cancers, anal cancers, breast cancers and bladder tumors. Side effects include bone-marrow damage, lung fibrosis and renal damage. In 1982, Fujiwara et al. developed an EIA for the detection of mitomycin C in rat serum and urine with a limit of detection of 12 nM [68]. Afterwards, they also developed an EIA for the detection of 7-N-(*p*-hydroxyphenyl)mitomycin C, an analog of the drug with improved properties [69]. Assay crossreactivities were low with other mitomycin analogs and the LOD was 16 pmol per assay tube in human serum.

6.4. Intercalating agents

6.4.1. Anthracycline

Anthracyclines are derived from *Streptomyces peucetius* and their antineoplastic use was settled in the 1960s. They are among the most effective anticancer treatments ever developed and are effective against a good few of cancers. Unfortunately, their efficacy in treating cancer is limited by a cumulative dose-dependent cardiotoxicity, which can cause irreversible heart failure. This antineoplastic class includes doxorubicin, daunorubicin, epirubicin and the anthracycline analog mitoxantrone, among others. The initial attempts of anthracycline detection by bioanalytical techniques were the production of specific antibodies against daunorubicin by Bachur et al. in 1977. They developed a RIA for pharmacokinetic studies [70]. Later on, in 2009 Salamone et al. patented a doxorubicin immunoassay using monoclonal

antibodies [71]. This indirect ELISA was only used in buffer conditions, showing low crossreactivity with its main metabolite, doxorubicin aglycone, since hapten was designed exposing the sugar moiety and placing spacer arm in the hydroxyacetyl moiety. Low crossreactivity with metabolites would facilitate the study of toxicity related to drug presence, boosting TDM establishment. An ELISA kit for the detection of doxorubicin is also commercialized by United States Biological [72]. This commercially available kit, only designed for research use, has an LOD of 1 nM and low crossreactivity with some analogs, providing an adequate method for TDM even for pediatric regimes, ranging from 920 to 18 nM [73].

In 1998 it was developed the first biosensor for anthracycline analysis. Square wave voltammetry (SWV) was used to establish an electrochemical procedure for the evaluation of the mitoxantrone behavior with a DNA modified glassy carbon electrode [74]. Later on, DPV was applied for the detection of mitoxantrone using a DNA modified carbon paste electrode [75]. The biosensor showed an LOD of 80.4 nM and the analysis was made in only 5 min. Nevertheless, authors stated that bare electrode reported a higher response than DNA modified electrode since the intercalating agent involved in bonding the DNA was not available for oxidation. Simultaneously, the same strategy was applied by the same authors for the detection of epirubicin [76], achieving an LOD of 50 nM within 5 min. However, both biosensors were not specific since other intercalating agents could interfere with its oxidation peak potential. Later, in 2006 an amperometric biosensor based on a DNA-modified nitrocellulose membrane was published for the detection of doxorubicin. An LOD of 0.1 nM was obtained with only 40 min of assay [77]. Finally, in 2015 Evtugyn et al. [78] used a DNA-sensor, based on glassy carbon electrode modified with electropolymerized neutral red and polycarboxylated thiacalix[4]arene, for quantification of anthracycline derivatives achieving LODs of 0.05, 0.1 and 0.5 nM for doxorubicin, daunorubicin and idarubicin, respectively. The same electrodes were later functionalized with polyaniline by electropolymerization, extending the pH range of electrochemical activity, and improving LODs to 0.01, 0.1 and 0.2 nM. In 2016, another biosensor for doxorubicin detection was developed by Tai et al. [79] with a slight detection improvement. Assays listed above can be applied to TDM or occupational exposure since they already have required detectability, but as long as crossreactivity with other compounds is low.

6.5. Topoisomerase inhibitors

Topoisomerase inhibitors interfere with the action of topoisomerase enzymes, which control the changes in DNA structure. They are divided into two major groups depending its target enzyme: Topoisomerase I inhibitors include irinotecan and topotecan, and Topoisomerase II include etoposide among others. Most common side effects are myelosuppression, diarrhea and susceptibility to infections. Main applications are for the treatment of colon, ovarian, testicular and lung cancer, lymphoma, sarcoma and leukemia. Irinotecan is mainly used in combination with 5-fluorouracil and leucovorin.

6.5.1. Topoisomerase I inhibitors

There are only two published bioanalytical methods. In 2001, Saita et al. raised polyclonal antibodies against topotecan [80] and developed a direct ELISA for the lactone form of topotecan with an LOD of 0.2 nM. Lactone formation is reversible and pH-dependent, but only the lactone form is the one that inhibits the topoisomerase.

Nevertheless, the assay showed high crossreactivity with SN-38 and camptothecin and low recognition of its carboxylate form and camptothecin-21-isopropylamide, concluding that antibody is specific for the lactone epitope [80]. On the other hand, a DNA modified pencil graphite electrode was used by DPV to quantify irinotecan. Different DNA electrode modifications were studied and optimized [81]. Finally, in 2001 Salamone et al. patented a competitive ELISA assay for irinotecan detection [82] either using polyclonal or monoclonal antibodies.

6.5.2. Topoisomerase II inhibitors

Different analytical and bioanalytical techniques (RIA, ELISA, etc.) have been reported for etoposide which were extensively reviewed by Lee et al. in 1995 [83]. Since then, no other bioanalytical methods have been published, other than an immunoassay for podophyllotoxin, the natural precursor of etoposide and teniposide, which was used for the screening of potential new drugs in plants. The immunoassay reached an LOD of 0.16 nM with high crossreactivity with its synthetic derivatives [84]. Further development of matrix effect would be required for its use in the problematic stated in this review.

6.6. DNA-cleaving agent

6.6.1. Bleomycin

Bleomycin is a complex of glycopeptides produced by *Streptomyces verticillus* and classified as "antitumor antibiotics". These drugs act during multiple phases of the cell cycle and are considered cell-cycle specific. Bleomycin name includes a family of related compounds which its main therapeutical forms are A₂ and B₂. This family is used for the treatment of Hodgkin's lymphoma, squamous cell carcinoma and testicular cancer. Side effects include pulmonary fibrosis and renal and lung toxicity. Many types of assays used in pharmacokinetic studies were developed for bleomycin detection, including microbiological assays, RIA and EIA. Later on, biosensor technology has also been used for its detection. The first specific assay, a RIA, was developed in 1976 by Broughton et al. for bleomycin sulfate [85]. This assay had low crossreactivity against other antineoplastic drugs. In 1981, Fujiwara et al. published an EIA for the detection of the bleomycin analog, pepleomycin [86]. This direct EIA was used in rabbit blood and urine for developing pharmacokinetic studies, obtaining an LOD of 0.03 pmol. Later on, using the same immunoreagents an assay for bleomycin was optimized to reach an LOD of 0.02 pmol [87]. Crossreactivities with different types of bleomycins were variable, from 277% for type B₂ and less than 5% for types A₂, A₂'-b, A₅ and the second generation of bleomycin analogs. This assay was applied to the analysis of rat tissues for pharmacokinetic studies, proving its suitability for TDM. More recently, some advances have been produced concerning bleomycin detection. A DNA electrochemical sensor was developed for the detection of this drug in clinical samples with a high sensitivity of 100 pM [88]. Cross-reactivity with other DNA-cleaving agents was not studied, thus, further studies would be required for TDM or occupational exposure evaluation. Recently, electrochemical impedance spectroscopy has also been used for its detection [89]. The working concentration for optimization studies was settled at 14 μM but no working range or LOD was established. Mitomycin C and cis-platin interfered with the sensor response. On the other hand, since bleomycin induce molecular beacon scission to trigger Exo III assisted DNA recycling and assay was developed based on the detection of the scission agent by fluorescence [90]. An LOD of 0.38 pM was obtained, which is far lower than other methods, showing low

crossreactivity against daunorubicin, mitomycin and dactinomycin. This assay was finally applied to the analysis of human serum with good recoveries which would be a good tool for TDM. Also, in 2015, Kong et al. [91] designed a perylene–DNA complex quencher probe for bleomycin detection via DNA strand scission with low cross-reactivities with other DNA-interactive agents. Although the authors claim that the assay was simple and rapid they could not reach previously reported assay detectabilities. Most described assays would fit TDM samples that can range from 2.8 to 0.7 μM [92].

6.7. Antitubulin agents

6.7.1. Vinca alkaloids

Vinca alkaloids are derived from periwinkle plant *Catharanthus roseus*. Because of the tubulin-binding properties of these agents, they are used either as cytostatic, for leukemia and lymphomas, or immunosuppressive drugs. Vinca alkaloids include vinblastine, vincristine, vindesine, ajmaline and vinorelbine. RIA was the major trend for vinca alkaloid detection. Hence, Teale et al. developed a RIA for the detection of two different vinca alkaloid derivatives in plasma samples. The assay reached an LOD of 3 nM for vinblastine and 5 nM for vincristine, showing low crossreactivity for several cytostatics of other families [93], its characteristics were promising for TDM purposes. Other RIAs for the detection of vinblastine and vincristine were published [94] without improving by far the parameters obtained by Teale. In 1984, Hacker et al. developed a direct ELISA for the detection of vinblastine and vincristine obtaining an LOD of 6 fmol and low crossreactivity with other common cytostatics. However, it was only tested in rat serum [95]. In 1993, Lelievre et al. developed a RIA and EIA for the detection of "S 12363", a Vinca alkaloid derivative with improved properties, using monoclonal antibodies. LOD values of 106 and 42 pM in plasma were obtained respectively for the RIA and the EIA [96] with, however, high cross-reactivity with vindesine, vincristine and vinblastine. Babkina and Ulakhovich [97] developed two ELISAs and an amperometric DNA sensor for the detection of indole-containing alkaloids. Both ELISAs were applied for the detection of ajmaline, achieving LODs of 0.1 and 1.5 μM. The DNA-biosensor was developed for the detection of vincristine, obtaining an LOD of 1.1 μM. The recoveries were studied in serum samples and the results were compared with a reference method obtaining similar values, thus proven adequate for TDM, but with some limitations for real samples ranging from 4.6 to 0.3 μM [98]. In 2012, Nakano et al. developed a direct ELISA for the detection of vindesine with an LOD of 0.03 nM in human serum. The assay reported low cross-reactivity with other vinca alkaloids, with good recoveries and specificities [99] fitting real plasma concentration (from 60 to 1 nM) [100]. Finally, Salamone et al. patented the production of the immunoreagents required for the development of an immunoassay for vincristine detection [101], improving the high crossreactivity showed against other vinca alkaloids and reported in other immunoassays. In conclusion, some assays suitable for TDM requirements have been reported.

6.7.2. Taxanes

Taxanes are diterpens produced by plants of the genus *Taxus*. Taxanes have a unique mechanism of action as inhibitors of mitosis. They block cell cycle progression through centrosomal impairment, induction of abnormal spindles and suppression of spindle microtubule dynamics. Taxane family includes paclitaxel, docetaxel and cabazitaxel. They are used in ovarian, breast, lung

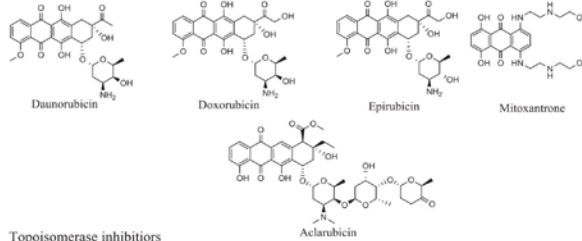
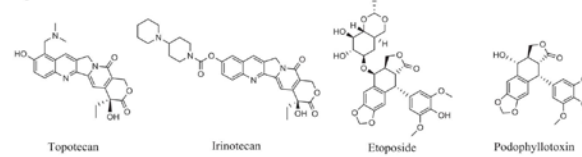
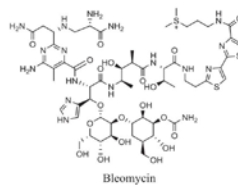
Table 3
Bioanalytical methods for antitubulin agents and other cytostatic compounds.

Family	Compound	Assay type	Matrix	LOD	Miscellaneous	Ref	
Antitubulin agents	Vincristine	ELISA ^a	–	–	mAb ^b	[101]	
	Vincristine	RIA ^b	Plasma	5 nM	pAb ⁱ	[93]	
	Vinblastine	RIA	Biological fluids	3 nM	–	–	
				0.5 nM	pAb	[120]	
				5 nM	–	–	
				6 fmoI	Direct assay	[95]	
	Catharanthine moiety	RIA	Plasma	106 nM	mAb	[96]	
	Ajmaline	EIA ^c	–	42 nM	–	–	
	Ajmaline	ELISA	Serum	0.1 nM	–	[97]	
	Vincristine	Biosensor	Serum	1.5 nM	DNA-modified electrode	[97]	
	Vindesine	ELISA	Serum	1.1 nM	–	–	
	Paclitaxel	Biochemical assay	Serum	0.03 mM	Direct format	[99]	
			Plant extract	0.1 μ M	Tubulin polymer formation	[102]	
			Plant extract	1 nM	pAb	[103]	
			Plant extract & plasma	0.4 nM	pAb, Indirect format	[104]	
			Plasma	0.1 pM	Competitive direct format	[106]	
			Plant extract	2 nM	mAb	[121]	
			Nanoparticle-immunoassay	Serum	13 nM	Commercially available (MyDocetaxel™, Saladax biomedical) Olympus AU400 analyzer	[122]
			FIA ^e	Plasma	8.3 nM	Competitive assay, silanized glass capillary column, tetrakis(4-carboxyphenyl)porphyrin displacement of tubulin	[107]
			Fluorescent bioassay	–	125 nM	–	[108]
		Biosensor	–	10 pM	Enzyme-channeling assay	[109]	
		Biosensor	Pharmaceutical formulation, serum & urine	0.01 nM	DNA-multitwall carbon nanotubes chitosan-modified pencil graphite electrode	[110]	
		Microcantilever immunosensor	Plasma	1 nM	mAb coated gold microcantilever	[111]	
		SERS ^f	–	1 nM	UV assisted nanoprint lithography	[112]	
	Paclitaxel	EIA	Plant extract	0.6 nM	mAb, competitive format	[105]	
	Baccatin III	–	–	1.1 nM	–	–	
	Taxane moiety	–	–	0.6 nM	–	–	
	Docetaxel	Nanoparticle-immunoassay	Plasma	35 nM	Commercially available (MyDocetaxel™, Saladax biomedical) Olympus AU400 analyzer	[113]	
Others	Avicumine	IPCR ^g	Plasma	100 pg/mL	Sandwich format IPCR ^g coupled to PCR-ELISA ^h	[116]	
	Lenalidomide	ELISA	Plasma	IC ₅₀ : 4–42 nM	mAb	[117]	
		ELISA	–	IC ₅₀ : 39 nM	pAb	[118]	

The table includes most important bioanalytical detection methods for each compound. ^aELISA, enzyme linked immunosorbent assay, ^bECL, electrochromic assay, ^cEIA, enzyme immunoassay, ^dFPIA, fluorescence polarization immunoassay, ^eFIA, fluorescent immunoassay, ^fSERS, surface enhanced Raman scattering, ^gIPCR, immuno polymerase chain reaction, ^hmAb, monoclonal antibody, ⁱpAb, polyclonal antibody, ^jPCR, polymerase chain reaction, ^kELISA, enzyme linked oligonucleotide sorbent assay.

and pancreatic cancer. Major side effects include hair loss, muscle and joint pains, diarrhea and others. Beforehand, taxol-dependent formation of tubulin polymers was used for the design of a biochemical assay with a detection capability of 0.1 μ M and applied in preliminary pharmacokinetic studies in rabbits [102]. Furthermore, an ELISA was developed for the detection of paclitaxel in plant tissues [103] and was applied in the screening of potential species producing taxanes. Grothaus et al. also developed an EIA for the detection of taxanes in plant tissues with slightly improved sensitivities [104]. They produced specific monoclonal antibodies against paclitaxel, baccatin III (paclitaxel precursor) and a taxane moiety reaching an LOD in the nM range [105]. In 1997, Suye et al. published the first assay applied in human plasma. It was a receptor protein-based bioassay [106] able to achieve and of 0.1 pM, which is far lower than the therapeutic ranges of this cytostatic drugs. The assay showed low cross-reactivities for the taxane precursors (baccatin III, cephalomanine and 10-deacetyl taxol). Since taxanes are extracted from plants, its bioanalytical detection methods have focused on this application and did not focus on TDM and occupational exposure. The features of these assays are noted in Table 3. The latter FIA assay, published in 2000 by Sheikh et al. [107], was based on the displacement of a rhodamine-labeled paclitaxel that competed for the binding site of specific antibodies inside a silanized glass capillary column. This kind of assay had the advantage of the short analysis times (4 min).

Another sort of assay was described later by Morais et al. [108], in which fluorescence shift was measured when antineoplastic presence displaces tetrakis(4-carboxyphenyl)porphyrin from the binding site of the tubulin complex. Although it allows rapid analysis, the LOD achieved of 125 nM was higher than previous assays in buffer conditions. Moreover, two biosensors were designed for paclitaxel detection. First, used glucose oxidase and tubulin co-immobilized on a graphite carbon electrode for the detection of paclitaxel in an enzyme-receptor channeling amperometric biosensor [109]. This assay showed shorter assay times, nevertheless, the detection capabilities were not further improved. Then, a ds-DNA modified pencil graphite electrode biosensors was designed, it was able to increase the detectability to 0.01 nM [110] using carbon nanotube decorated chitosan-modified electrode. Finally, a quartz crystal microbalance (QCM) [111] and surface-enhanced Raman scattering (SERS) [112] technologies have also been applied for the detection of paclitaxel. Microcantilever gold surface was functionalized with a specific mAb to reach an LOD of 1 nM. On the other hand, in 2006 Salamone et al. patented an immunoassay for the detection of docetaxel [113]. Authors raised monoclonal antibodies against this compound, and conjugated them to nanoparticles, to develop a nanoparticle-based turbidimetric immunoassay. Using an Olympus AU400 analyzer, 400 samples of 2 μ L were able to be measured within only 9 min achieving an LOD of 35 nM. Values

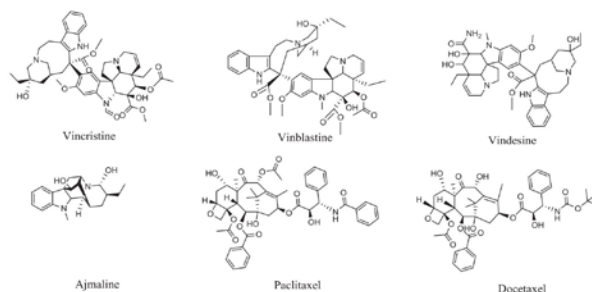
DNA interactive agents**Cross-linking agents****Intercalating agents****Topoisomerase inhibitors****DNA-cleaving agents****Fig. 4.** Continued

drug routinely monitored and there are three commercially available assays for this drug (ARK diagnostics, Dade-Behring and Abbott Laboratories). On the other hand, Saladax Biomedical, Inc. has done a remarkable effort to develop bioanalytical methods concerning therapeutic drug monitoring. Under the name of *MyCare diagnostics tests*, this company has four commercially available assays for 5-fluorouracil, paclitaxel, docetaxel and imatinib, and they claim to have 13 assays in development, most of them related with cytostatics.

Obviously, there is a very important gap related to the monitoring and detection of these drugs. The increasing pressure for a targeted and personalized medicine and evaluation of

occupational exposure are claiming for new low-cost, rapid and reliable bioanalytical techniques, nevertheless, as stated before, seldom bioanalytical assays have reached its final purpose. With this review we intended to provide an overview of the state of the art in this field which could be the base for further developments of bioreceptors showing better features or even transducer principles, that in combination with these bioreceptors may give rise to a new generation of bioanalytical tools able to assist the regulatory agencies on performing the necessary studies for a more personalized medicine and to protect workers from the exposure to cytostatics and other chemical hazards.

Antitubulin agents



Others

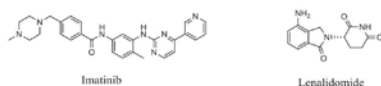


Fig. 4. Continued

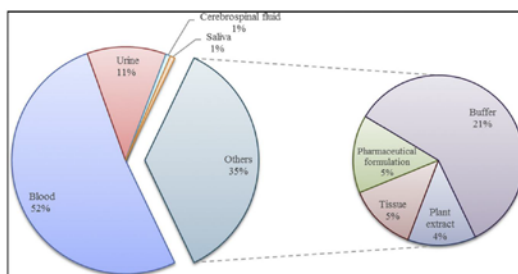


Fig. 5. Overview of sample matrices analyzed for cytostatic drugs expressed in percentage (data has been extracted from the publications listed in Tables 1–3).

Acknowledgments

The Nb4D group (formerly Applied Molecular Receptors group, AMRg) is a consolidated research group (Grup de Recerca) of the Generalitat de Catalunya and has support from the Departament d'Universitats, Recerca i Societat de la Informació de la Generalitat de Catalunya (expedient: 2014 SGR 1484). CIBER-BBN is an initiative funded by the Spanish National Plan for Scientific and Technical Research and Innovation 2013–2016. Iniciativa Ingenio 2010, Consolider Program, CIBER Actions are financed by the Instituto de Salud Carlos III with assistance from the European Regional Development Fund. This work was performed as part of a research contract with CETEMMSA Technological Center (part of the EURE-CAT Technology Center of Catalonia). Marta Broto wishes to thank

the FPI-fellowship (BES-2013-062819) from the Spanish Ministry of Economy and Competitiveness.

References

- [1] American Cancer Society. <http://canceratlas.cancer.org/>, 2016.
- [2] A. Felici, J. Verweij, A. Sparreboom, Dosing strategies for anticancer drugs: the good, the bad and body-surface area, *Eur. J. Cancer* 38 (2002) 1677–1684.
- [3] S.D. Baker, J. Verweij, E.K. Rowinsky, R.C. Donehower, J.H.M. Schellens, L.B. Grochow, A. Sparreboom, Role of body surface area in dosing of investigational anticancer agents in adults, 1991–2001, *J. Natl. Cancer Inst.* 94 (2002) 1883–1888.
- [4] O. Capitain, A. Asevoaia, M. Boisdron-Celle, A.-L. Poirier, A. Morel, E. Gamelin, Individual fluorouracil dose adjustment in FOLFOX based on pharmacokinetic follow-up compared with conventional body-area-surface dosing: a phase II, proof-of-concept study, *Clin. Colorectal Cancer* 11 (2012) 263–267.

- [15] M. Sorsa, D. Anderson, Monitoring of occupational exposure to cytostatic anticancer agents, *Mutat. Res.* 355 (1996) 253–261.
(a) P.J. Sessink, R.P. Bos, Drugs hazardous to healthcare workers. Evaluation of methods for monitoring occupational exposure to cytostatic drugs, *Drug Saf.* 20 (1999) 347–359.
- [16] G. Drankasaris, M. Johnston, S. Poirier, T. Schueller, D. Milliken, E. Green, B. Zanke, Are health care providers who work with cancer drugs at an increased risk for toxic events? A systematic review and meta-analysis of the literature, *J. Oncol. Pharm. Pract.* 11 (2005) 69–78.
(a) B. Valanis, W.M. Vollmer, P. Steele, Occupational exposure to antineoplastic agents: self-reported miscarriages and stillbirths among nurses and pharmacists, *J. Occup. Environ. Med.* 41 (1999) 632–638.
- [17] P.J. Sessink, M.C. Van de Kerckhof, R.B. Anziosi, J. Noordhoek, R.P. Bos, Environmental contamination and assessment of exposure to antineoplastic agents by determination of cyclophosphamide in urine of exposed pharmacy technicians: is skin absorption an important exposure route? *Arch. Environ. Health* 49 (1994) 165–169.
(a) H.J. Mason, S. Blair, C. Sams, K. Jones, S.J. Garfitt, M.J. Cuschieri, P.J. Baxter, Exposure to antineoplastic drugs in two UK hospital pharmacy units, *Ann. Occup. Hyg.* 49 (2005) 603–610.
- [18] B.A. Chabner, T.G. Roberts Jr., Timeline: chemotherapy and the war on cancer, *Nat. Rev. Cancer* 5 (2005) 65–72.
- [19] A.B. van Kallenburg, J.G. Maring, Evaluation of 5-fluorouracil pharmacokinetic models and therapeutic drug monitoring in cancer patients, *Pharmacogenomics* 14 (2013) 799–811.
- [10] B. Gao, S. Yeap, A. Clements, B. Balakrishnar, M. Wong, H. Gurney, Evidence for therapeutic drug monitoring of targeted anticancer therapies, *J. Clin. Oncol.* 30 (2012) 4017–4025.
- [11] E. Elansson, J.D. Lindh, R.E. Malmstrom, O. Beck, M.L. Dahl, Therapeutic drug monitoring for tomorrow, *Eur. J. Clin. Pharmacol.* 69 (Suppl. 1) (2013) 25–32.
- [12] J.B. Courtney, R. Harney, Y. Li, G. Lundell, G.A. McMillin, G. Agarwal, J.M. Juenke, A. Mathew, R. Gonzalez-Espinosa, M. Fleisher, S.J. Salamone, Determination of bupivacaine in human plasma using an ELISA format, *Ther. Drug Monit.* 31 (2009) 489–494.
- [13] P.Y. Muller, M.N. Milton, The determination and interpretation of the therapeutic index in drug development, *Nat. Rev. Drug Discov.* 11 (2012) 751–761.
- [14] G. McMahon, R. O'Connor, Therapeutic drug monitoring in oncology: does it have a future? *Bioanalysis* 1 (2009) 507–511.
- [15] <https://www.jatdmct.org/>
- [16] K.W. Jones, S.R. Patel, A family physician's guide to monitoring methotrexate, *Am. Fam. Physician* 62 (2000) 1607–1612, 1614.
- [17] H. Yu, N. Steeghs, C.M. Nijenhuis, J.H. Schellens, J.H. Beijnen, A.D. Huijtema, Practical guidelines for therapeutic drug monitoring of anticancer tyrosine kinase inhibitors: focus on the pharmacokinetic targets, *Clin. Pharmacokinet.* 53 (2014) 305–325.
- [18] B. Kopp, R. Schieri, D. Nowak, Evaluation of working practices and surface contamination with antineoplastic drugs in outpatient oncology health care settings, *Int. Arch. Occup. Environ. Health* 85 (2013) 47–55.
(a) C. Sottani, B. Porro, M. Imbrani, C. Minola, Occupational exposure to antineoplastic drugs in four Italian health care settings, *Toxicol. Lett.* 213 (2012) 107–115.
- [19] C. Schreiber, K. Radon, A. Pethran, R. Schieri, K. Hauff, C.H. Grimm, K.S. Boes, D. Nowak, Uptake of antineoplastic agents in pharmacy personnel. Part II: study of work-related risk factors, *Int. Arch. Occup. Environ. Health* 76 (2003) 11–16.
(a) C.Y. Hon, G. Astrakianakis, Q. Danyuk, W. Chu, Pilot evaluation of dermal contamination by antineoplastic drugs among hospital pharmacy personnel, *Can. J. Hosp. Pharm.* 64 (2011) 327–332.
- [20] E. Ziegler, H.J. Mason, P.J. Baxter, Occupational exposure to cytotoxic drugs in two UK oncology wards, *Occup. Environ. Med.* 59 (2002) 608–612.
- [21] A. Suspiro, J. Prista, Biomarkers of occupational exposure do anticancer agents: a minireview, *Toxicol. Lett.* 207 (2011) 42–52.
- [22] C. Roussel, J.H. Connor, Chemotherapy: current and emerging issues in safe handling of antineoplastic and other hazardous drugs, *Oncol. Pharm.* 7 (4) (2014) 14–17.
- [23] Department of Health and Human Services, Centers for Disease Control and Prevention, (CDC-2015-0034; NIOSH 233-A) List of antineoplastic and other hazardous drugs in healthcare settings: proposed additions to the NIOSH hazardous Drug List 2016 8 (102) (2015) 30463.
- [24] M.S. Morgan, The biological exposure indices: a key component in protecting workers from toxic chemicals, *Environ. Health Perspect.* 105 (Suppl. 1) (1997) 105–115.
www.jarc.fr/
- [25] www.ema.europa.eu/ema/
- [26] S. Nussbaumer, P. Bonnabry, J.L. Veuthey, S. Fleury-Souverein, Analysis of anticancer drugs: a review, *Talanta* 85 (2011) 2265–2289.
- [27] L.X. Zhao, L. Sun, X.G. Chu, Chemiluminescence immunoassay, *TRAC – Trends Anal. Chem.* 28 (2009) 404–415.
(a) N. Haang, Hiep, J. Park, S. Kang, M. Kim, Surface plasmon resonance: a versatile technique for biosensor applications, *Sensors* 15 (2015) 10481–10510.
(b) A. Nehra, K.P. Singh, Current trends in nanomaterial embedded field effect transistor-based biosensor, *Biosens. Bioelectron.* 74 (2015) 731–743.
(c) V.C. Dicalescu, A.-M. Chiorescu-Paquim, A.M. Oliveira-Brett, Applications of DNA-electrochemical biosensor, *TRAC – Trends Anal. Chem.* 79 (2016) 23–36.
(d) S. Vigneshwar, C.S. Sidhakumari, B. Senthilumar, H. Prakash, Recent advances in biosensor technology for potential applications – an overview, *Front. Bioeng. Biotechnol.* 4 (2016) 111.
(e) B. Derkus, Applying the miniaturization technologies for biosensor design, *Biosens. Bioelectron.* 79 (2016) 901–913.
(f) V. Cristiani-Gaita, M. Thompson, Aptamers, antibody scFv, and antibody Fab' fragments: an overview and comparison of three of the most versatile biosensor biorecognition elements, *Biosens. Bioelectron.* 85 (2016) 32–45.
- [29] I. Nagayama, An Immunological Method for Measuring Tegafur in Urine, Taiho Pharmaceutical Co., Ltd., Japan, 1999, p. 4.
- [30] M. Broto, R. McCabe, R. Galve, M.-P. Marco, High throughput immunoassay for the therapeutic drug monitoring of tegafur, *Analyst* (2017). <http://dx.doi.org/10.1039/C7AN00418D>.
- [31] S. Salamone, J. Courtney, D. Stocker, 5-Fluoro-uracil Immunoassay, 2006 (Google Patents).
- [32] J.H. Beumer, M. Boisdron-Celle, W. Clarke, J.B. Courtney, M.J. Egorin, E. Garnel, R.L. Harney, C. Harumett-Stabler, S. Lepp, Y. Li, G.D. Lundell, G. McMillin, G. Milano, S.J. Salamone, Multicenter evaluation of a novel nanoparticle immunoassay for 5-fluorouracil on the Olympus AU400 analyzer, *Ther. Drug Monit.* 31 (2009) 688–694.
(a) S.J. Salamone, C.N. Benfield, J.B. Courtney, R.L. Harney, D.R. Kozo, Y. Li, G.D. Lundell, Rapid 5-fluorouracil plasma quantification by immunoassay: validation with FOLFOX clinical samples, *J. Clin. Oncol.* 29 (2011) 1.
- [33] P.H.J. White, M. Bonen, M.K. Barnat, R. von Borstel, Point-of-care (POC) diagnostic assay for 5-fluorouracil (5-FU) quantitation to enable dose adjustment and detect dihydropyrimidine dehydrogenase (DPD) deficiency, *J. Clin. Oncol.* (2011) e19562.
(a) P.Q. Hu, X. Huang, B.R.W. Von, Assays, Antibodies, Immogens and Compositions Related to 5-FU, 2013.
- [34] D. Koyuncu Zeybek, B. Demir, B. Zeybek, S. Pekyaydirmci, A sensitive electrochemical DNA biosensor for antineoplastic drug 5-fluorouracil based on glassy carbon electrode modified with poly(bromocresol purple), *Talanta* 144 (2015) 793–800.
- [35] M. Satyanarayana, K.Y. Goud, K.K. Reddy, K.V. Gobi, Biopolymer stabilized nanogold particles on carbon nanotube support as sensing platform for electrochemical detection of 5-fluorouracil in-vitro, *Electrochim. Acta* 178 (2015) 608–616.
- [36] E. Booka, C.K. Imamura, H. Takeuchi, Y. Hamamoto, D. Gomi, T. Mizukami, T. Ichijima, K. Tateishi, T. Takahashi, H. Kawakubo, K. Soejima, N. Boku, Y. Tanigawa, Y. Kitagawa, Development of an S-1 dosage formula based on renal function by a prospective pharmacokinetic study, *Gastric Cancer* 19 (2016) 876–886.
- [37] S.J. Salamone, J.B. Courtney, H. Sard, C. Spedaliere, Gemcitabine Immunoassay, Saladax Biomedical Inc., USA, 2012, p. 18. Cont.-in-part of U.S. Ser. No. 114,218.
- [38] H.J. El-Sulbogh, A.A. Al-Badr, Cytarabine, in: G.B. Harry (Ed.), Profiles of Drug Substances, Excipients and Related Methodology, Academic Press, 2009, pp. 37–113 (Chapter 2).
- [39] J.-J. Zhu, K. Gu, J.-Z. Xu, H.-Y. Chen, DNA modified carbon paste electrode for the detection of 6-mercaptopurine, *Anal. Lett.* 34 (2001) 329–337.
- [40] Z.H. Yan, H. Li, Voltammetric determination of 6-mercaptopurine at Co(III) trisphenanthroline complex and DNA decorated with graphene oxide modified glassy carbon electrode, *Int. J. Electrochem. Sci.* 10 (2015) 8714–8726.
- [41] K.M. Kersten, A.J. Matzger, Improved pharmacokinetics of mercaptopurine afforded by a thermally robust hemihydrate, *Chem. Commun.* 52 (2016) 5281–5284.
- [42] W. Wang, S.-F. Wang, F. Xie, An electrochemical sensor of non-electroactive drug 6-thioguanine based on the dCdNA/AET/Au, *Sensors Actuators B Chem.* 120 (2006) 238–244.
- [43] B.C. Widemann, F.M. Balis, P.C. Adamson, Dihydrofolate reductase enzyme inhibition assay for plasma methotrexate determination using a 96-well microplate reader, *Clin. Chem.* 45 (1999) 223–228.
- [44] K.C. Kasper, A. Orozco, J. Nguyen, K. Chung, B. Moon, J. Valdez, Monitoring methotrexate by ARK immunoassay, *Ther. Drug Monit.* 33 (2011) 547–548.
- [45] M.A. Perce, S.H. Bodourian, Enzyme immunoassay and enzyme inhibition assay of methotrexate, with use of the centrifugal analyzer, *Clin. Chem.* 27 (1981) 380–384.
- [46] G. Hartung, S. Heeger, T. Bertsch, E. Frei, A. Wunder, M. Kränzel, G. Stehle, M. Weigand, H.J. Schrenk, H. Sinn, W. Queisser, Adaptation and clinical evaluation of a homogenous enzyme multiplied immunoassay technique (EMIT) for drug monitoring of a methotrexate–albumin conjugate (MTX-HSA) in humans, *Oncol. Res. Treat.* 23 (2000) 352–357.
- [47] M.P. Borgnani, M.F. Hiemer, A.R. Molinelli, J.C. Ritchie, S.A. Jortani, Improved sensitivity for methotrexate analysis using enzyme multiplied immunoassay technique on the Siemens Viva-E instrument, *Ther. Drug Monit.* 34 (2012) 193–197.
- [48] R.L. Schmidt, H.N. Panas, J.E. Solomon, A fluorescent polarization immunoassay for the quantitation of methotrexate, *Clin. Chem.* 29 (1983) 1274.
- [49] S.L. Jeweland, J. Tyner, D. Nystrom, M. Isa, K.L. Trimpe, Development of the Tdx/TdxFLx methotrexate II assay, *Clin. Chem.* 40 (1994) 1033.
- [50] B. Sub-Lailam, J. Juenke, C. Thompson, L. Wilson, K. Johnson-Davis, Performance characteristics of three assays for the therapeutic drug monitoring of

- methotrexate, in: 13th International Congress of Therapeutic Drug Monitoring & Clinical Toxicology, Salt Lake City, USA, 2013.
- [51] M.S. Roberts, N.S. Selvo, J.K. Roberts, V.M. Daryani, T.S. Owens, K.E. Harstead, A. Gajjar, C.F. Stewart, Determination of methotrexate, 7-hydroxymethotrexate, and 2,4-diamino-N10-methylptericoic acid by LC-MS/MS in plasma and cerebrospinal fluid and application in a pharmacokinetic analysis of high-dose methotrexate, *J. Liq. Chromatogr. Relat. Technol.* 39 (2016) 745–751.
- [52] M. Lucchesi, M. Guidi, C. Fonte, S. Farina, P. Fiorini, C. Favre, M. de Martino, I. Sardi, Pharmacokinetics of high-dose methotrexate in infants aged less than 12 months treated for aggressive brain tumors, *Cancer Chemother. Pharmacol.* 77 (2016) 857–864.
- [53] S.S. Zhao, M.A. Bichelberger, D.V. Colin, R. Robitaille, J.N. Pelletier, J.F. Masson, Monitoring methotrexate in clinical samples from cancer patients during chemotherapy with a LSPR-based competitive sensor, *Analyst* 137 (2012) 4742–4750.
- [54] S.S. Zhao, N. Bukar, J.L. Toulouse, D. Pelechac, R. Robitaille, J.N. Pelletier, J.F. Masson, Miniature multi-channel SPR instrument for methotrexate monitoring in clinical samples, *Biosens. Bioelectron.* 64 (2015) 664–670.
- [55] R.-i. Stefan, R.G. Bokretsson, J.F. van Staden, H.Y. Aboul-Enein, Simultaneous determination of *l*- and *d*-methotrexate using a sequential injection analysis/ amperometric biosensors system, *Biosens. Bioelectron.* 19 (2003) 261–267.
- [56] F. Wang, Y. Wu, J. Liu, B. Ye, DNA Langmuir–Blodgett modified glassy carbon electrode as voltammetric sensor for determination of methotrexate, *Electrochim. Acta* 54 (2009) 1408–1413.
- [57] I.D. Taber, P. O'Brien, R.R. Bowsher, J.R. Sportsman, Competitive particle concentration fluorescence immunoassay for measuring 5,10-dihydroxy-5,6,7,8-tetrahydrofolate acid (Methotrexate) in serum, *Clin. Chem.* 37 (1991) 254–260.
- [58] S.J. Salamone, J.B. Courtney, A. Volkov, Imatinib Immunoassay, Saladax Biomedical Inc., USA, 2011, p. 54 (Chemical Indexing Equivalent to 154: 276021 [US]).
- [59] J.H. Beumer, D. Kozo, R.L. Harney, C.N. Baldasano, J. Jarrah, S.M. Christner, R. Parise, I. Baburina, J.B. Courtney, S.J. Salamone, Automated imatinib immunoassay, *Ther. Drug Monit.* (2014).
- [60] S.J. Salamone, J.B. Courtney, S.J. Salamone, S. Salamone, S. Salamon, D. Stock, New Cytoxin Antibody that Substantially Selectively Binds to Protected Aldehyde Cyclophosphamide Metabolite and Does Not Substantially Cross-react with Cyclophosphamide, Useful for Detecting Active Metabolites of Cyclophosphamide, SALADAX Biomed. Inc. (SALA-Non-standard), pp. 1774331–1774332.
- [61] M.E. de Jonge, A.D. Huitema, S. Rodenhuis, J.H. Beijnen, Clinical pharmacokinetics of cyclophosphamide, *Clin. Pharmacokinet.* 44 (2005) 1135–1164.
- [62] S. Carrara, A. Cavallini, V. Eraklin, G. De Micheli, Multi-panel drugs detection in human serum for personalized therapy, *Biosens. Bioelectron.* 26 (2011) 3914–3919.
- [63] B. Forsgren, P.O. Gurnarsson, S.A. Johansson, R. Kant, Radioimmunoassay of estramustine phosphate in plasma, *Acta Pharm. Suec.* 15 (1978) 200–210.
- [64] J. Petřelová, D. Potesil, J. Zehnalák, B. Sures, V. Adam, L. Trnkova, R. Kizek, Cisplatin electrochemical biosensor, *Electrochim. Acta* 51 (2006) 5169–5173.
- [65] H. Yang, H. Cui, L. Wang, L. Yan, Y. Qian, X.E. Zheng, W. Wei, J. Zhao, A label-free G-quadruplex DNA-based fluorescence method for highly sensitive, direct detection of cisplatin, *Sensors Actuators B Chem.* 202 (2014) 714–720.
- [66] J.R. Eads, J.H. Beumer, L. Negra, J.L. Holleran, S. Stoychev, N.J. Meropol, A pharmacokinetic analysis of cisplatin and 5-fluorouracil in a patient with esophageal cancer on peritoneal dialysis, *Cancer Chemother. Pharmacol.* 77 (2016) 333–338.
- [67] S.J. Salamone, C.N. Benfield, J.B. Courtney, R.L. Harney, D.R. Kozo, Y. Li, G.D. Lundell, L.M. Shaw, J.A.M. Gardiner, A rapid nanoparticle immunoassay to quantitate busulfan in plasma, *Biol. Blood Marrow Transplant.* 15 (2009) 154.
- [68] F.A. de Castro, C. Piana, B.P. Simões, V.L. Lanchote, O. Della Pasqua, Busulfan dosing algorithm and sampling strategy in stem cell transplantation patients, *Br. J. Clin. Pharmacol.* 90 (2015) 619–629.
- [69] S.J. Salamone, J.B. Courtney, Y. Li, Stabilized Standards for Busulfan Immunoassay, Saladax Biomedical Inc., 2012.
- [70] K. Fujiwara, H. Saikusa, M. Yasuno, T. Kitagawa, Enzyme immunoassay for the quantification of mitomycin C using β -galactosidase as a label, *Cancer Res.* 42 (1982) 1487–1491.
- [71] K. Fujiwara, H. Nakamura, T. Kitagawa, N. Nakamura, A. Saito, K. Hara, Development and application of a sensitive enzyme immunoassay for 7-N-(p-hydroxyphenyl)mitomycin C, *Cancer Res.* 44 (1984) 4172–4176.
- [72] N.R. Bachur, C.E. Riggs, M.R. Green, J.J. Langone, H. Vanvunakis, L. Levine, Plasma adriamycin and daunorubicin levels by fluorescence and radioimmunoassay, *Clin. Pharmacol. Ther.* 21 (1977) 76–77.
- [73] S.J. Salamone, J.B. Courtney, S. He, Doxorubicin Immunoassay, Saladax Biomedical Inc., 2009.
- [74] Adriamycin (ADR) BioAssay™ ELISA Kit (Mouse).
- [75] M. Kriščiák, G. Hiempe, S. Völter, N. Andre, M. Džuráček, G. Biogno, W. Kępczyk, M. Borowski, R. Hiemle, A.V. Boddy, J. Boas, Pharmacokinetic and pharmacodynamic study of doxorubicin in children with cancer: results of a "European Pediatric Oncology Off-patents Medicines Consortium" trial, *Cancer Chemother. Pharmacol.* 78 (2016) 1175–1184.
- [76] A.M.O. Brett, T.R.A. Maceo, D. Raimundo, M.H. Marques, S.H.P. Serrano, Voltammetric behaviour of mitoxantrone at a DNA-biosensor, *Biosens. Bioelectron.* 13 (1998) 861–867.
- [77] A. Erdem, M. Ozsoz, Voltammetry of the anticancer drug mitoxantrone and DNA, *Turk. J. Chem.* 25 (2001) 469–475.
- [78] A. Erdem, M. Ozsoz, Interaction of the anticancer drug epirubicin with DNA, *Anal. Chim. Acta* 437 (2001) 107–114.
- [79] S.S. Babkina, Y.N. Moiseyeva, N.A. Ullakhovich, Determination of doxorubicin by means of an amperometric biosensor, *Farmatsiya (Moscow)* (2006) 9–11.
- [80] G. Evtugyn, A. Porfirieva, V. Stepanova, H. Budnikov, Electrochemical biosensors based on native DNA and nanosized mediator for the detection of anthracycline preparations, *Electroanalysis* 27 (2015) 629–637.
- [81] R. Shamagsumova, A. Porfirieva, V. Stepanova, Y. Osin, G. Evtugyn, T. Hianik, Poly(aniline)-DNA based sensor for the detection of anthracycline drugs, *Sensors Actuators B Chem.* 220 (2015) 573–582.
- [82] M. Taei, H. Salavati, F. Hasanpour, A. Shafiq, Biosensor based on ds-DNA-decorated Fe₃O₄/SiO₂-chitosan modified multiwalled carbon nanotubes for biodection of doxorubicin, *IEEE Sens. J.* 16 (2016) 24–31.
- [83] T. Saita, H. Fujito, M. Mori, Determination of topotecan by ELISA, *Biol. Pharm. Bull.* 24 (2001) 321–326.
- [84] S.N. Topkaya, S. Aydinlik, N. Aladag, M. Orsoz, D. Ozkan-Arıksoyul, Different DNA immobilization strategies for the interaction of anticancer drug irinotecan with DNA based on electrochemical DNA biosensors, *Comb. Chem. High Throughput Screen.* 13 (2010) 582–589.
- [85] S.J. Salamone, J.B. Courtney, A. Volkov, H. Zhang, H. Sardi, V. Hegde, Irinotecan Immunoassay, Saladax Biomedical Inc., USA, 2011, p. 54 (Chemical Indexing Equivalent to 155:30702 [US]).
- [86] K.H. Lee, H.K. Wang, Antitumor agents, 165. Current status of bisaniloyl of etoposide and related compounds, *J. Food Drug Anal.* 3 (1995) 209–232.
- [87] K. Yoo, J.R. Porter, Immunoassay of podophylotoxin, *J. Nat. Prod.* 56 (1993) 715–721.
- [88] A. Broughton, J.E. Strong, Radioimmunoassay of bleomycin, *Cancer Res.* 36 (1976) 1418–1421.
- [89] S.T. Crooke, F. Luft, A. Broughton, J. Strong, K. Casson, L. Einhorn, Bleomycin serum pharmacokinetics as determined by a radioimmunoassay and a microbiologic assay in a patient with compromised renal function, *Cancer* 39 (1977) 1430–1434.
- [90] K. Fujiwara, M. Yasuno, T. Kitagawa, Enzyme immunoassay for perylenequin, a new bleomycin analog, *Cancer Res.* 41 (1981) 4121–4126.
- [91] K. Fujiwara, M. Ise, H. Saikusa, H. Nakamura, T. Kitagawa, S. Takahashi, Sensitive enzyme immunoassay for the quantification of bleomycin using beta-galactosidase as a label, *Cancer Treat. Rep.* 67 (1983) 363–369.
- [92] B.C. Yin, D. Wu, B.C. Ye, Sensitive DNA-based electrochemical strategy for trace bleomycin detection, *Anal. Chem.* 82 (2010) 8272–8277.
- [93] A. Erdem, G. Cogur, Impedimetric detection of in situ interaction between anti-cancer drug bleomycin and DNA, *Int. J. Biol. Macromol.* 61 (2013) 295–301.
- [94] F. Gan, J. Lei, H. Ju, Ultrasensitive fluorescence detection of bleomycin via exonuclease III-aided DNA recycling amplification, *Chem. Commun. (Camb.)* 49 (2013) 7561–7563.
- [95] R.-M. Kong, N.-N. Sun, F. Qu, H. Wu, H. Wang, J. You, Sensitive fluorescence "turn-on" detection of bleomycin based on a superquenched perylene-DNA complex, *RSC Adv.* 5 (2015) 86949–86954.
- [96] A. Groselj, M. Krzan, T. Kosjek, M. Bosnjak, G. Sersa, M. Cemazar, Bleomycin pharmacokinetics of bolus bleomycin dose in elderly cancer patients treated with electrochemotherapy, *Cancer Chemother. Pharmacol.* 77 (2016) 939–947.
- [97] J.D. Teale, J.M. Clough, V. Marks, Radioimmunoassay of vincristine and vinorelbine, *Br. J. Clin. Pharmacol.* 4 (1977) 169–172.
- [98] R.J. Owellen, M. Blair, A. Van Tosh, F.C. Hains, Determination of tissue concentrations of vinca alkaloids by radioimmunoassay, *Cancer Treat. Rep.* 65 (1981) 469–475.
- [99] M.P. Hacker, J.R. Dank, W.B. Ershler, Vincristine pharmacokinetics measured by a sensitive enzyme-linked immunosorbent assay, *Cancer Res.* 44 (1984) 478–481.
- [100] E. Lefievre, J. Guillaudoux, H. Gardona, A. Bourguignat, F. Lolicic, P. Solere, C. Lucas, C. Sauveur, Human pharmacokinetics of a new vinca alkaloid 5-12363 with use of a monoclonal antibody-based radioimmunoassay or enzyme-immunoassay, *Cancer Res.* 53 (1993) 3536–3540.
- [101] S.S. Babkina, N.A. Ullakhovich, Determination of pharmaceuticals based on indole alkaloids with amperometric DNA-sensors and enzyme immunoassay test-system, *Anal. Lett.* 44 (2011) 837–849.
- [102] R.W. Sparidans, P. Langendijk, E. Boers, E. van Kan, H.L. Tan, J.H. Beijnen, Liquid chromatographic assay with fluorescence detection to determine ajmaline in serum from patients with suspected brugada syndrome, *J. Chromatogr. B* 878 (2010) 2168–2172.
- [103] Y. Nakano, T. Saita, H. Fujito, Development of a specific and sensitive enzyme-linked immunosorbent assay for vindesine, *Yakugaku Zasshi* 132 (2012) 727–732.
- [104] R.-H. Zhu, H.-D. Li, H.-L. Cai, Z.-P. Jiang, P. Xu, L.-B. Dai, W.-X. Peng, Validated HILIC-MS/MS assay for determination of vindesine in human plasma: application to a population pharmacokinetic study, *J. Pharm. Biomed. Anal.* 96 (2014) 31–36.

- [101] S.J. Salamone, J.B. Courtney, D.J. Cline, Vincristine immunoassay, SaladaX Biomedical Inc., USA, 2012, p. 51 (Chemical Indexing Equivalent to 156:496735 (US)).
- [102] E. Hamel, C.M. Lin, D.G. Johns, Tubulin-dependent biochemical assay for the antineoplastic agent taxol and application to measurement of the drug in serum, *Cancer Treat. Rep.* 66 (1982) 1381–1386.
- [103] M. Jaziri, B.M. Dhallo, M.H. Vanhaelen, R.J. Vanhaelen-Fastre, A. Zhiri, A.G. Becu, J. Homes, Enzyme-linked immunosorbent assay for the detection and the semi-quantitative determination of taxane diterpenoids related to taxol in *Taxus* sp. and tissue cultures, *J. Pharm. Belg.* 46 (1991) 93–99.
- [104] P.G. Grothaus, T.J. Raybould, G.S. Bignami, C.B. Lazo, J.B. Byrnes, An enzyme immunoassay for the determination of taxol and taxanes in *Taxus* sp. tissues and human plasma, *J. Immunol. Methods* 158 (1993) 5–15.
- [105] P.G. Grothaus, G.S. Bignami, S. O'Malley, K.E. Harada, J.B. Byrnes, D.F. Waller, T.J.G. Raybould, M.T. McGuire, B. Alvarado, Taxane-specific monoclonal antibodies: measurement of taxol, baccatin III, and "total taxanes" in *Taxus brevifolia* extracts by enzyme immunoassay, *J. Nat. Prod.* 38 (1995) 1003–1014.
- [106] S. Suye, S. Tandel, A. Mulchandani, A receptor protein-based bioassay for quantitative determination of paclitaxel, *Anal. Chem.* 69 (1997) 3633–3635.
- [107] S.H. Sheikh, B.A. Abela, A. Mulchandani, Development of a fluorescence immunoassay for measurement of paclitaxel in human plasma, *Anal. Biochem.* 283 (2000) 33–38.
- [108] S. Morais, P.C. Pandey, W. Chen, A. Mulchandani, A novel bioassay for screening and quantification of taxanes, *Chem. Commun. (Camb.)* (2003) 1188–1189, <http://dx.doi.org/10.1039/B302112B>.
- [109] S.-i. Suye, D. Nakamoto, T. Hori, F. Sugawara, A. Mulchandani, A tubulin-based quantitative assay for taxol (paclitaxel) with enzyme channeling sensing, *Electroanalysis* 16 (2004) 685–690.
- [110] M. Taeli, F. Hassanpour, H. Salavati, Z. Saadeghi, H. Alvandi, Highly selective electrochemical determination of taxol based on ds-DNA-modified pencil electrode, *Appl. Biochem. Biotechnol.* 176 (2015) 344–358.
- [111] C.G. Xue, H.W. Zhao, S.Q. Wu, T.G. Nan, B.M. Wang, Q.C. Zhang, X.P. Wu, Research on paclitaxel microcantilever immunosensor, *Chin. J. Anal. Chem.* 39 (2011) 863–866.
- [112] M. Cottat, N. Lidgi-Guigui, F. Hamouda, B. Bartelien, D. Venkataraman, R.S. Marks, T.W.J. Steele, M.L. de la Chapelle, Highly sensitive detection of paclitaxel by surface-enhanced Raman scattering, *J. Optics* 17 (2015) 114019.
- [113] S. Salamone, J. Courtney, G. Lundell, Docetaxel immunoassay, 2006 (Google Patents);
(a) S.J. Salamone, H. Zhang, R.L. Harney, G.D. Lundell, D.J. Cline, H. Raiz, Y. Li, J.B. Courtney, Quantification of docetaxel plasma concentrations using a novel nanoparticle-based immunoassay, *J. Clin. Oncol.* 29 (2011) 1;
(b) D.J. Cline, H. Zhang, G.D. Lundell, R.L. Harney, H.K. Riaz, J. Jarrah, Y. Li, M. Miyazaki, J.B. Courtney, I. Baburina, S.J. Salamone, An automated nanoparticle-based homogeneous immunoassay for determining docetaxel concentrations in plasma, *Ther. Drug Monit.* 35 (2013) 803–808.
- [114] Y.W. Lim, B.C. Goh, L.Z. Wang, S.H. Tan, B.Y.S. Chuah, S.E. Lim, P. Iau, S.A. Buhari, C.W. Chan, N.B. Sukri, M.T. Cordero, R. Soo, S.C. Lee, Pharmacokinetics and pharmacodynamics of docetaxel with or without ketoneazole modulation in chemonaive breast cancer patients, *Ann. Oncol.* 21 (2010) 2175–2182;
(a) I.R. Younis, D.J. George, T.J. McManus, H. Hurwitz, P. Creel, A.J. Armstrong, J.J. Yu, K. Bacon, G. Hobbs, C.J. Peer, W.P. Petros, Clinical pharmacology of an atransentan and docetaxel regimen in men with hormone-refractory prostate cancer, *Cancer Chemother. Pharmacol.* 73 (2014) 991–997.
- [115] H. Kenmotsu, Y. Tanigawara, Pharmacokinetics, dynamics and toxicity of docetaxel: why the Japanese dose differs from the Western dose, *Cancer Sci.* 106 (2015) 497–504.
- [116] M. Adler, M. Langer, K. Witthohn, J. Eck, D. Blöhm, C.M. Niemeier, Detection of rViscumin in plasma samples by immuno-PCR, *Biochem. Biophys. Res. Commun.* 300 (2003) 757–763;
(a) M. Adler, M. Langer, K. Witthohn, K. Wilhelm-Ogunbiyi, P. Schoffski, P. Fumoleau, C.M. Niemeier, Adaptation and performance of an immuno-PCR assay for the quantification of Avicumine in patient plasma samples, *J. Pharm. Biomed. Anal.* 39 (2005) 972–982.
- [117] S.J. Salamone, J.B. Courtney, H. Sand, V. Hegde, A. Volkov, Lenalidomide and Thalidomide immunoassays, SaladaX Biomedical Inc., USA, 2011, p. 64 (Chemical Indexing Equivalent to 155:449481 (US)).
- [118] I.A. Darwish, N.Z. Alzoman, R.M. Abuhejal, T.E. El-Samani, Synthesis of hapten and preparation of specific polyclonal antibody with high affinity for lenalidomide, the potent drug for treatment of multiple myeloma, *Chem. Cent. J.* 6 (2012) 125.
- [119] M. Sohda, K. Fujiwara, H. Saikusa, T. Kitagawa, N. Nakamura, K. Hara, H. Tone, Sensitive enzyme immunoassay for the quantification of adacinomycin A using β -D-galactosidase as a label, *Cancer Chemother. Pharmacol.* 14 (1985) 53–58.
- [120] V.S. Sedhi, S.S. Burton, D.V. Jackson, A sensitive radioimmunoassay for vincristine and vinblastine, *Cancer Chemother. Pharmacol.* 4 (1980) 183–187.
- [121] C. Bicampupaia, M. Page, Development of a fluorescence polarization immunoassay (FPIA) for the quantitative determination of paclitaxel, *J. Immunol. Methods* 212 (1998) 1–7.
- [122] D.J. Cline, H. Zhang, G.D. Lundell, R.L. Harney, H.K. Riaz, J. Jarrah, Y. Li, M. Miyazaki, J.B. Courtney, I. Baburina, S.J. Salamone, Development and evaluation of a nanoparticle-based immunoassay for determining paclitaxel concentrations on routine clinical analyzers, *Ther. Drug Monit.* 35 (2013) 809–815.

3.4.2 PUBLICATION II: HIGH THROUGHPUT IMMUNOASSAY FOR THE THERAPEUTIC DRUG MONITORING OF TEGAFUR

High throughput immunoassay for the therapeutic drug monitoring of tegafur

Marta Broto, Rita McCabe, Roger Galve and M.-Pilar Marco

Analyst **2017**, 142, 2404-2410

This publication describes the development of an immunoassay for tegafur quantification in plasma samples. A reproducible and sensitive competitive indirect ELISA reported a LOD of 2.7 nM, lower than real samples requirements, and low crossreactivity with 5FU and other parent compounds. My main contribution to this paper was the preparation of immunoreagents and final tests with plasma samples, Rita McCabe contributed with immunoreagent combination selection and first trials of matrix effect.



Analyst

PAPER

Cite this: *Analyst*, 2017, **142**, 2404

Received 9th March 2017.

Accepted 3rd May 2017

DOI: 10.1039/c7an00418d

rsc.li/analyst

A high throughput immunoassay for the therapeutic drug monitoring of tegafur†

Marta Broto, ^{1b} ^{a,b} Rita McCabe, ^{1b} ^{a,b} Roger Galve ^{1b} ^{*a,b} and M. -Pilar Marco ^{1b} ^{a,b}

Cancer is a group of diseases in which abnormal cells grow and divide without control, with the potential to invade other parts of the body. Chemotherapy is a type of treatment that uses chemical agents to treat cancer. These drugs are toxic and produce undesirable adverse drug reactions due to their narrow therapeutic window and highly variable pharmacokinetics, thus, they need to be monitored to establish personalized treatment to achieve maximal efficiency and reduce drug toxicity. Nowadays, therapeutic drug monitoring (TDM) is not routinely used for chemotherapy agents, however, TDM has the potential to improve the clinical benefit of chemotherapy drugs. Tegafur, a prodrug of 5-fluorouracil (5FU), is one of the main anti-cancer drugs used worldwide. Herein, a reproducible and sensitive indirect competitive ELISA has been developed and validated in plasma samples. The assay reports an IC₅₀ of 35.6 nM, reaching a limit of detection of 2.7 nM. It is highly reproducible and does not show cross-reactivity with any related compound. In summary, this assay provides a sensitive, accurate and high throughput analytical method for tegafur quantification in plasma, which fits TDM requirements.

1. Introduction

Cancer, also known as malignant tumor or malignant neoplasm, includes a broad group of diseases involving unregulated cell growth. It is a leading cause of death worldwide in high-income countries, and the global burden is expected to grow to 21.7 million new cancer cases and 13 million cancer deaths by 2030.¹ The use of anticancer drugs as a part of a standardized regimen, also called chemotherapy, is the most usual cancer treatment. Anticancer drugs, or antineoplastics, were first introduced in the 1940s.² They have been designed for specific cell-division related targets which include interrupting the processes or inhibiting the substances necessary for cellular replication. These drugs are classified depending on their mechanism of action as antimetabolites, DNA-interactive agents and anti-tubulin agents.

The remarkable characteristics of anticancer drugs are that they show: (1) a narrow therapeutic window, (2) no suitable parameter available to evaluate their clinical efficacy, (3) high inter- and intra-individual therapeutic concentration vari-

ability and (4) long-term standardized regimens. All of these properties combined make these drugs suitable for pharmacokinetic monitoring, known as therapeutic drug monitoring (TDM). TDM is based on the measurement and interpretation of drug concentrations in biological fluids. Thus, patients can benefit from individualized care that will achieve maximum efficiency and reduce toxicity. Despite the suitability of chemotherapeutic agents, monitoring has not been routinely used due to the lack of reliable high-throughput analytical techniques. No official guideline has been published regarding TDM of cytostatic drugs. However, some articles have been published concerning guidelines for routine monitoring.^{3,4} The International Association of Therapeutic Drug Monitoring and Clinical Toxicology (IATDMCT) has also presented some unofficial recommendations.⁵ Nevertheless, the only drug with available assays and that is usually monitored is methotrexate⁶ and there is still a lack of legislation and useful techniques for its compliance.⁷

Within the antineoplastics, 5-fluorouracil (5FU) is the most widely administered anticancer drug.⁸ It belongs to the anti-metabolite family, and its action consists in mimicking the uracil nucleobase, avoiding its correct function in cellular processes. However, there is a very subtle difference between the minimal effective dose and the maximal tolerated dose for 5FU. In addition, the drug exhibits marked individual pharmacokinetic variability. Traditionally, 5FU dosing has been determined using body surface area, but there is enough evidence confirming the lack of scientific rationale for this strategy. Nowadays, there is a well-documented relationship between

^aNanotechnology for diagnostics (Nb4D), Department of Chemical and Biomolecular Nanotechnology, Institute for Advanced Chemistry of Catalonia (IQAC) of the Spanish Council for Scientific Research (CSIC), Spain.

E-mail: roger.galve@iqac.csic.es; Fax: +332045904; Tel: +934006100 (Ext. 5117)

^bCIBER de Bioingeniería, Biomateriales y Nanomedicina (CIBER-BBN), Jordi Girona 18-26, 08034 Barcelona, Spain

† Electronic supplementary information (ESI) available. See DOI: 10.1039/c7an00418d

5FU plasma concentration and its biological effects, including toxicity. These toxicities are especially severe in patients with undiagnosed dihydropyrimidine dehydrogenase (DPD) deficiency,⁹ the main enzyme for detoxification of the drug. Oral derivatives or prodrugs have been employed to overcome 5FU toxicity. These derivatives cause prolonged drug exposure and may confer pharmacoeconomic advantages by reducing administration costs and toxicity-related hospitalization.¹⁰ Tegafur (FT) is the most common 5FU prodrug and is usually administered for the treatment of gastrointestinal, colorectal, breast, and head and neck cancers. Tegafur is transformed into 5FU by the enzyme CYP2A6 present in the liver, and is usually administered jointly with uracil, in a regimen called UFT, to inhibit DPD action. Therapeutic drug monitoring (TDM) has been shown to improve the clinical outcome in patients receiving chemotherapy.¹¹ Consequently, it has also been suggested that FT TDM might be useful for individual dose adjustment efficacy maximization and toxicity minimization.¹² Focusing on tegafur pharmacokinetics, its concentration in plasma is in the order of 4 to 40 μM 24 h after administration, reaching a peak 3 h after administration.^{12,13}

Different detection techniques have been developed to detect tegafur, together with 5-fluorouracil and other drugs administered with the former, mainly by HPLC^{14,15} and LC-MS/MS.^{12,16–18} Among them, Rемаud *et al.* obtained the lowest quantification limit, being 31 nM. However, to date there has not been any method that meets the criteria of being fast, economically affordable, without a sample pretreatment needed and capable of a high throughput analysis. In 1999, Nagayama *et al.* developed and patented the only immunoassay available for the detection of tegafur. They achieved an LOD of 3.1 μM ,¹⁹ which is within the tegafur concentration found in plasma. Nevertheless, a high cross-reactivity was observed with 5-fluorouridine, limiting the assay applicability to urine samples, where the cross-reactant is not present.

In the present work, we have focused our efforts on the production of polyclonal antibodies for the specific detection of tegafur. And we have developed a rapid, simple and sensitive ELISA method for its quantification. The accuracy and precision of the immunochemical determination of tegafur in plasma samples have also been evaluated.

2. Materials and methods

2.1 Chemistry

The instrumentation and reagents section is described in the ESI.†

2.1.1. Preparation of the immunizing hapten 5FU1 and competitor haptens 5FU3 and 5FU6. The characterization of the haptens is described in the ESI (section S1†).

Methyl 5-(5-fluoro-2,4-dioxo-3H-pyrimidin-1-yl)pentanoate (1) and methyl 5-(5-fluoro-2,4-dioxo-1H-pyrimidin-3-yl)pentanoate (2). 5FU (1 g, 7.69 mmol) was dissolved in 20 mL of anhydrous

DMF at r.t., and triethylamine (1.6 mL, 11.53 mmol) was added to the solution. The reaction crude product was placed in an ice bath, and after 20 min, methyl bromoacetate (1.11 mL, 7.69 mmol) was added. The reaction was stopped after 5 h. The crude product was evaporated until dryness, dissolved in ethyl acetate and washed three times with saturated NaHCO₃. Organic phases were mixed, dried with MgSO₄, filtered and evaporated under reduced pressure. The liquid obtained was purified by column chromatography with hexane and diethyl ether to finally obtain the methyl esters of 5FU1 (yield 11%, white solid, *R_f* 0.71 in ethyl acetate) and 5FU3 (yield 5%, white solid, *R_f* 0.5 in ethyl acetate).

5-(5-Fluoro-2,4-dioxo-3H-pyrimidin-1-yl)pentanoic acid (5FU1) and 5-(5-fluoro-2,4-dioxo-1H-pyrimidin-3-yl)pentanoic acid (5FU3). The general procedure is as follows. KOH (200 mg, 3.57 mmol) was dissolved in 5 mL of water and the solution was degassed. Ester 1 (427 mg, 1.75 mmol) or ester 2 (112 mg, 0.46 μmol) was added and the reaction was left for 1 h at r.t. The resulting mixture was acidified with HCl to pH 2 and extracted three times with ethyl acetate. The organic phases were mixed, dried with MgSO₄, filtered and evaporated under reduced pressure (yield 85%, white solid).

1-Ethyl-8-methyl-2-fluoro-3-oxooctanedioate (3). NaH 60% (500 mg, 12.9 mmol) was placed under an inert atmosphere and washed 5 times with pentane. Then 15 mL of anhydrous THF were added and heated at 50 °C. Ethyl fluoroacetate (1 mL, 10.3 mmol) was added dropwise. The reaction was left for 30 minutes and then cooled to 0 °C. Methyl adipoyl chloride (1.5 mL, 8.6 mmol) was added and stirred for 3 h at 0 °C. The reaction crude product was evaporated until dryness. It was dissolved in diethyl ether and washed three times with saturated NaHCO₃. The organic phases were mixed, dried with MgSO₄, filtered and evaporated under reduced pressure. The liquid obtained was purified by column chromatography with hexane and diethyl ether to finally obtain 705 mg of the desired product (yield = 33%, colorless liquid, *R_f* 0.29 in diethyl ether:hexane 1:1).

Methyl 5-(5-fluoro-2,4-dioxo-1H,3H-pyrimidin-6-yl)pentanoate (4). Urea (306 mg, 5.1 mmol) and compound 3 (422.1 mg, 1.7 mmol) were placed in a microwave vessel and shaken for 5 min. Then, the reaction was heated at 160 °C for 30 min. The reaction mixture was dissolved in methanol, filtered and evaporated under reduced pressure. The crude product was purified by column chromatography with ethyl acetate and hexane to finally obtain 50.2 mg of the desired product (yield 12%, white solid, *R_f* 0.38 in ethyl acetate).

5-(5-Fluoro-2,4-dioxo-1H,3H-pyrimidin-6-yl)pentanoic acid (5FU6). Compound 4 (50.20 mg, 0.2 mmol) was placed in a 25 mL round-bottomed flask and 3 mL of KOH (1 N) were added. The reaction was left for 1 h at r.t. Then, 50 mL of saturated NaHCO₃ were added, and the aqueous phase was washed three times with 50 mL of ethyl acetate, acidified with HCl conc. to pH 2, and extracted five times with 50 mL of ethyl acetate. The organic phase was dried with MgSO₄, filtered and evaporated under reduced pressure until dryness (yield 84%, pale other solid).

2.2. Immunochemistry

The instruments and general methods section and the description of all of the buffers used can be found in the ESI (section S2†).

2.2.1. Preparation of the immunogen 5FU1-HCH and the coating antigens. Haptens 5FU1, 5FU3 and 5FU6 (10 μmol) were dissolved in 120 μL DMF anhydrous. Then, a solution of 25 μmol of *N,N'*-diisopropylcarbodiimide (DIC), in the case of the immunizing hapten, or 25 μmol of *N,N'*-dicyclohexylcarbodiimide (DCC), in the case of the competitors, in 60 μL DMF, and a solution of *N*-hydroxysuccinimide (25 μmol) in 60 μL DMF were added sequentially. The mixtures were stirred for 2 hours. The suspensions were centrifuged at 10 000 rpm for 10 min. The supernatants were added dropwise to a solution of 10 mg of the proteins in 1.8 mL of borate buffer, hemocyanin from limulus polyphemus hemolymph (HCH) in the case of the immunizing hapten, and albumin from bovine serum (BSA), conalbumin from chicken egg white (CONA), albumin from chicken egg white (OVA) and aminodextran (AD) in the case of the antigens. The reaction mixtures were gently stirred for 2 hours at r.t. Protein conjugates were purified by dialysis against 0.5 mM PBS (4 \times 5 L) and Milli-Q water (1 \times 5 L), and stored at -40 $^{\circ}\text{C}$. Unless otherwise indicated, working aliquots were stored at 4 $^{\circ}\text{C}$ in PBS at 1 mg mL $^{-1}$. The hapten densities of the bioconjugates were estimated by measuring the molecular weight (MW) of the native proteins and the MW of the conjugates by MALDI-TOF-MS. Because HCH cannot be analyzed by MALDI, simultaneously to the immunogen preparation, the hapten was also conjugated to BSA to evaluate the conjugation degree. We assume that this result can be correlated with the hapten density of the immunogen. MALDI spectra were obtained by mixing 2 μL of the freshly prepared matrix (*trans*-3,5-dimethoxy-4-hydroxycinnamic acid, 10 mg mL $^{-1}$ in ACN/H $_2$ O 70 : 30, 0.1% TFA) with 2 μL of a solution of the conjugates or proteins (10 mg mL $^{-1}$ in ACN/H $_2$ O 70 : 30, 0.1% TFA). The hapten densities (δ hapten) were calculated according to the following equation: $[\text{MW}(\text{conjugate}) - \text{MW}(\text{protein})]/\text{MW}(\text{hapten})$.

2.2.2. Polyclonal antisera. The rabbit immunizations included in this study were carried out in the animal facility of the Research and Development Center (CID) of the Spanish Research Council (CSIC) Registration Number: B9900083. All efforts were made to minimize suffering of the animals. The protocol used for the production of antibodies was conducted in accordance with the institutional guidelines under a license from the local government (DAAM 7463) and approved by the Institutional Animal Care and Use Committee at the CID-CSIC. The antisera (As) obtained by immunizing female white New Zealand rabbits with 5FU1-HCH were named As337, As338 and As339. The evolution of the antibody titer was assessed on a non-competitive indirect ELISA, by measuring the binding of serial dilutions of the different antisera to microtiter plates coated with a fixed concentration of 5FU1-BSA (1 mg mL $^{-1}$). After 6 immunizations, the animals were exsanguinated, and the blood was collected in vacutainer tubes provided with a

serum separation gel. Antisera were obtained by centrifugation at 4 $^{\circ}\text{C}$ for 10 min at 10 000 rpm, and stored at -80 $^{\circ}\text{C}$ in the presence of 0.02% NaN $_3$. Unless otherwise indicated, working aliquots were stored at 4 $^{\circ}\text{C}$.

2.2.3. Non-competitive indirect ELISA. The avidity of the antisera (As337-339) with 12 antigens (5FU1-BSA, 5FU1-CONA, 5FU1-OVA, 5FU1-AD, 5FU3-BSA, 5FU3-CONA, 5FU3-OVA, 5FU3-AD, 5FU6-BSA, 5FU6-CONA, 5FU6-OVA, and 5FU6-AD) was evaluated. Two-dimensional titration assays (2D assays) were carried out, based on the measurement of the binding of different concentration of the antigens (1 μg mL $^{-1}$ to 0.5 ng mL $^{-1}$, and zero, 100 μL per well) against serial dilutions of the antisera (1/1000 to 1/512 000, and zero, 100 μL per well). From these experiments, optimum concentrations for coating antigens and antisera dilutions were chosen to generate around 0.7–1 units of absorbance. The general protocol of the assay is well described in the next section.

2.2.4. Competitive indirect ELISA (5FU6-OVA/As337). A microtiter plate was coated with the antigen 5FU6-OVA (0.25 μg mL $^{-1}$ in coating buffer, 100 μL per well), overnight at 4 $^{\circ}\text{C}$ and covered with an adhesive plate sealer. The next day, the plate was washed four times with PBST (300 μL per well), and the solution of tegafur (from 10 to 0 μM in PBST, 50 μL per well) or the samples were added, followed by the solution of antisera As337 (1/7000 for the solution of tegafur and 1/2000 for the samples, in PBST, 50 μL per well). After 30 min at r.t., the plate was washed as before, and a solution of anti-IgG-HRP (1/6000 in PBST, 100 μL per well) was added to the wells and incubated for 30 minutes at r.t. The plate was washed again, and the substrate solution was added (100 μL per well). Color development was stopped after 30 min at r.t. with 4 N H $_2$ SO $_4$ (50 μL per well), and the absorbances were read at 450 nm. The standard curve was fitted to a four-parameter equation according to the following formula: $y = B(A - B)/[1 - (x/C)^D]$, where A is the maximum absorbance, B is the minimum absorbance, C is the concentration producing 50% of the maximal absorbance, and D is the slope at the inflection point of the sigmoid curve. Unless otherwise indicated, the data presented correspond to the average of at least two well replicates.

2.2.5. ELISA evaluation

Physicochemical parameter optimization. The effects of the physicochemical parameters of the media were tested by introducing variations in the initial conditions of the assay. The study included incubation time, competition time, pH, conductivity or ionic strength and tween 20 concentrations.

Specificity studies. The avidity of the antisera As337 against different structurally-related compounds such as 5-fluorouracil, 5-bromouracil, thymine, 5-fluoro-1,3-dimethyluracil, uridine, 5-fluoro-2'-deoxyuridine and 5-bromo-2'-deoxyuridine was evaluated. The standard curves were performed following the protocol described before. The cross-reactivity (CR) values were calculated according to the equation: $\text{IC}_{50} [\text{nM}] (\text{cross-reactant}) \times 100$.

2.2.5. Plasma samples

Matrix effect studies. Non-specific interferences produced by plasma were assessed by preparing a standard curve at

different plasma dilutions in PBST (1:1, 1:2, 1:4, 1:10, 1:25).

Optimization of the antiserum concentration for sample analysis. The As dilution of the competitive ELISA 5FU6-OVA/As337 in plasma samples was tested by increasing the antibody concentration 1, 2 and 3 times. Subsequently, all immunoassays performed were done with a 1/7000 antisera dilution for the calibration curve in PBST and 1/2000 for the plasma samples.

Reproducibility studies. The assays were carried out three times within three different days, and three times within the same day. The main features of the final assay were described as the mean of all the replicates.

Recovery studies. The recovery of tegafur concentration was assessed by spiking blank plasma at 6 different concentrations (from 100 to 6 nM). The sample concentrations were calculated interpolating the results to tegafur standard curves prepared in PBST. The results were fitted to a linear regression curve between the spiked concentrations and the measured ones.

3. Results and discussion

3.1. Preparation of immunoreagents

As mentioned in the introduction, Nagayama *et al.*¹⁹ reported the only immunoassay available to date for the detection of tegafur. The immunizing conjugate was prepared by oxidation of the sugar of 5-fluorouridine prior to the carrier protein coupling. Thus, the antibodies were able to detect tegafur with an IOD of 3.1 μ M, showing high cross-reactivity with 5-fluorouridine. In a similar context, Salamone *et al.*²⁰ and Hu *et al.*²¹ tried to raise antibodies against 5-fluorouracil placing the spacer arm at position 1 of the uracil ring, the former obtaining high cross-reactivity with tegafur. Consequently, taking previous approaches into account, the chemical structure of the immunizing hapten was designed following chemical criteria with the aim to maximize the exposure of the fluorouracil ring, by substitution of the tetrahydrofuryl moiety of position

1 for the spacer arm. The synthesis of the immunizing hapten and the competitors is presented in Fig. 1. Briefly, 5FU was treated with methyl bromoacetate in the presence of Et_3N . After 20 min two compounds were obtained by the introduction of the spacer arm at the nitrogen 1 (1) and at the nitrogen 3 (2). Both compounds were purified and hydrolyzed, obtaining the immunizing hapten 5FU1 and the competitor hapten 5FU3. Although the final yield of this reaction is low, we are able to produce both compounds in one simple reaction. Alternatively, another competitor hapten was designed with the alkyl chain at position 6 of the uracil ring. The strategy followed for its synthesis was a cyclization reaction of the modified pyrimidine nucleobase using a microwave-assisted (MW) method. This procedure allowed us to prepare the hapten in a one-pot reaction, avoiding multi-step reactions under harsh experimental conditions.²² Therefore, the precursor 1-ethyl-8-methyl-2-fluoro-3-oxooctanedioate (3), previously synthesized *via* the formation of ethyl fluorooacetate enolate and methyl adipoyl chloride, was treated with urea under solvent free conditions at 160 °C using a microwave to perform the cyclization. After purification by column chromatography, 5FU6 ester (4) was obtained in 12% yield. Finally, compound 6 was hydrolyzed by potassium hydroxide to obtain the desired hapten. All the synthesized compounds were characterized by mass spectrometry and NMR.

5FU1 was covalently coupled through its carboxylic group to the amino acid of the lysines of the HCH using the well-known carbodiimide/*N*-hydroxysuccinimide method. Similarly, all haptens were conjugated to BSA, CONA, OVA and AD to use them as coating antigens in the competitive ELISA. In this case, a different carbodiimide was used to avoid linker recognition. The evaluation of the conjugation yield was performed by MALDI-TOF-MS (see Table S1†).

3.2. Immunoassay development

The conjugate 5FU1-HCH was used for immunizing three New Zealand female rabbits, whose antisera were named As337, As338 and As339. The avidity of these antisera against the competitor antigens was assessed in order to find out the

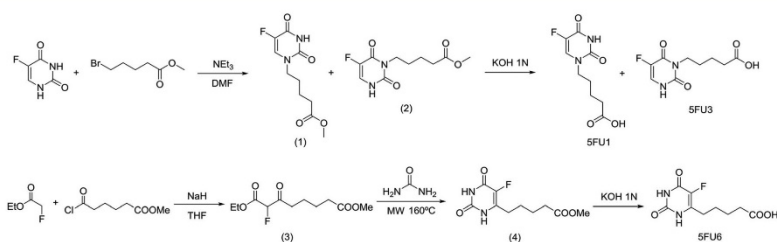


Fig. 1 Schematic representation of the synthesis of the immunogen (5FU1) and competitor haptens (5FU1, 5FU3 and 5FU6).

Paper

Analyst

most appropriate conditions for the development of a competitive immunochemical assay. The concentrations of the immunoreagents were selected by two-dimensional checkerboard titration experiments.²³ Different types of antigens, homologous (5FU1) and heterologous (5FU3 and 5FU6), were tested since it has been reported that the feasibility and selectivity of the antibodies can be modulated with the coating antigen selection.²⁴ Then, the different combinations were studied under a competitive configuration to assess their capability to detect tegafur. 5FU6 conjugates rendered usable assays (Table S2†), and showed that tegafur should be detected under heterologous conditions. Subsequently, As337/5FU6-OVA was selected as the antibody/antigen combination for the assay because of the excellent features and reproducibility observed on the repetitive experiments. Some physicochemical parameters such as pH, ionic strength, Tween 20 concentration and incubation times were tested in order to improve the features of the immunoassay. The results are shown in the ESI (Fig. S2†). In general, no detectability improvement was observed. However, incubation and competition time studies reported similar results for all tested times, consequently allowing us to reduce the competition time down to 10 minutes and decreasing the overall time of the assay by twenty minutes. Finally, the shaking effect in the competition step was also evaluated, reporting a lower IC₅₀ at 600 rpm. The final features of the assay are enclosed in Fig. 2. In summary, the assay shows an IC₅₀ of 35 nM, achieving an LOD of 2.7 nM, much lower than the concentrations found in the blood samples of the treated patients and three orders of magnitude lower than the previously reported assay.¹⁹ The working range was defined to be between 7.5 ± 1.3 and 157.5 ± 5.1 nM (20–80% of the assay response at zero doses). The precision of the assay was determined based on inter-assay and intra-assay variations in the IC₅₀ values and they were expressed as the relative standard deviation of the results obtained from repetitive experiments. The intra-day reproducibility based on the variations between the plates was below 3% (*n* = 3), while the inter-day reproducibility was below 4% (*n* = 3).

3.3. Immunoassay evaluation

To study the specificity of the assay, compounds which are structurally related to tegafur and its metabolites were tested

(see Fig. S3†). Once tegafur is metabolized, it is transformed into 5-fluorouracil (5FU), which can be incorporated into an oligonucleotide sequence as 5-fluoro-2'-deoxyuridine (flouridine), a compound also used as an antimetabolite drug. Both chemical species were selected for cross-reactivity studies. In addition, tegafur brominated forms were also evaluated, jointly with the nucleoside uridine. Other tested compounds were thymine and 5-fluoro-1,3-dimethyluracil, which also contains an alkyl chain at position 1 of the ring as the immunizing hapten. Table 1 shows the IC₅₀ and cross-reactivity results for each tested compound. The antibodies presented high specificity for tegafur, although the recognition pattern reveals a slight affinity for compounds with a residue in position 1. Furthermore, really low cross-reactivity for 5-fluorouracil, its active compound, was found. Consequently, we can conclude that this ELISA could potentially be applied for the determination of tegafur with high specificity.

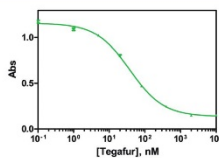
3.4. Matrix studies

Due to the increasing interest in TDM for cytostatic drugs, studies were performed to evaluate potential nonspecific matrix effects. The validation of the assay in plasma samples was done preparing calibration curves at different dilutions in PBST. The results reported that the more diluted the plasma was, the higher the maximal signal of the assay was (Fig. 3, Table S3†). However, not diluting the matrix enables the assay

Table 1 Cross-reactivity of tegafur related compounds using the immunoreagent combination As337/5FU6-OVA

	IC ₅₀ (nM)	% CR ^a
Tegafur (FT)	36	100
5-Fluorouracil (5FU)	9900	0.37
5-Bromouracil (5BrU)	13 310	0.27
5-Fluoro-1,3-dimethyluracil (5FDMU)	>10 000	<0.05
Thymine (T)	>10 000	<0.05
Uridine (Urd)	>10 000	<0.05
5-Fluoro-2'-deoxyuridine (5FUrd)	5867	0.62
5-Bromo-2'-deoxyuridine (5BrUrd)	7934	0.46

^a Cross-reactivity is expressed as a percentage of the relation between the IC₅₀ (nM) of tegafur and the IC₅₀ (nM) of the other compounds tested.



Parameters of the assay (As337/5FU6-OVA)

As dilution	1/7000	Signal _{min}	0.134 ± 0.010
[Competitor]	0.25 µg mL ⁻¹	Signal _{max}	1.157 ± 0.010
Competition time	10 ¹	Slope (m)	-0.915 ± 0.043
Agitation	600 rpm	R ²	0.992 ± 0.001
pH	7.5	IC ₅₀ , nM	35.6 ± 2.6
Ionic strength	15.0 mS/cm	DR ^b , nM	from 7.5 ± 1.3 to 157.5 ± 5.1
Tween 20	0.05 %	LOD, nM	2.7 ± 0.7

Fig. 2 Calibration curve, conditions and features of the tegafur immunoassay. The data presented correspond to the average of six assays performed on four different days. Each assay was built using three well replicates. ^b DR corresponds to dynamic range, calculated as the concentration given between 20 and 80% of the maximum signal.

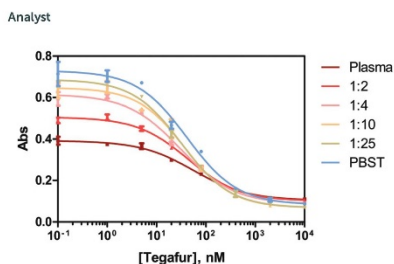


Fig. 3 The matrix effect study. A set of tegafur curves in different plasma dilutions in PBST were tested. Two replicates were assayed in each curve.

to have a better sensitivity and to avoid adding a dilution step. The matrix effect observed was overcome with an analytical protocol modification, thus, by increasing the antisera dilution added to the sample we can obtain the same maximal signal as the calibration curve.²⁵ Therefore, further experiments were carried out in order to find the best dilution of the antisera in plasma. This problem was addressed by comparing the absorbance of PBST with the absorbance of plasma at different antisera dilutions (data not shown). The results reported that, in the case of plasma samples, an antisera dilution three times higher should be used. Therefore, for the following assays the calibration curve in PBST was prepared with an antisera dilution of 1/7000 and for the plasma samples, with a 1/2000 dilution. The parameters of both assays are listed in Fig. S5.† Recovery assays were also carried out with spiked samples, and the results are displayed in Fig. 4. The spiked values closely match the results obtained, plotting a linear regression of a slope of 0.96, which is close to a perfect correlation. Intra-day and inter-day precisions of the recovery in the range of 6 to 100 nM were below 6% in both cases, obtaining a higher precision for lower concentrations.

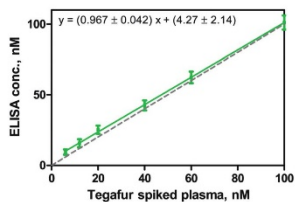


Fig. 4 Results from the recovery study performed in plasma. The graph shows the correlation between the spiked and measured concentration values. The dotted line corresponds to a perfect correlation ($m = 1$). The data correspond to the average of at least three-well replicates from 6 different days.

4. Conclusions

In summary, the proposed ELISA method, which needs no sample treatment, can be applied for therapeutic drug monitoring of tegafur since it is well suited for high throughput analysis. Moreover, antibodies raised against 5FU1 immunizing hapten have been demonstrated to be very specific for tegafur. By combining these antibodies with an appropriate antigen, it has been possible to establish a competitive ELISA that enables specific and accurate detection. Reporting a remarkably low detectability, the assay presents an IC_{50} of 35.6 and an LOD of 2.7 nM, three orders of magnitude lower than that of the previously reported immunoassay. Furthermore, the reported LOD is lower than that of other HPLC and LC-MS/MS methods.

Abbreviations

5BrUrd	5-Bromo-2'-deoxyuridine
5BRU	5-Bromouracil
5FDMU	5-Fluoro-1,3-dimethyluracil
5FUrd	5-Fluoro-2'-deoxyuridine
5FU	5-Fluorouracil
OVA	Albumin from chicken egg white
AD	Aminodextran
BSA	Bovine serum albumin
CONA	Conalbumin from chicken egg
HCH	Hemocyanin from limulus polyphemus hemolymph
DCC	<i>N,N'</i> -Dicyclohexylcarbodiimide
DIC	<i>N,N'</i> -Diisopropylcarbodiimide
FT	Tegafur
TDM	Therapeutic drug monitoring
Urd	Uridine

Acknowledgements

This work has been funded by the Ministry of Economy and Competitiveness (MAT2012-38573-C02-01). The Nb4D group (formerly Applied Molecular Receptors group, AMRg) is a consolidated research group (Grup de Recerca) of the Generalitat de Catalunya and has support from the Departament d'Universitats, Recerca i Societat de la Informació de la Generalitat de Catalunya (expedient: 2014 SGR 1484). CIBER-BBN is an initiative funded by the Spanish National Plan for Scientific and Technical Research and Innovation 2013–2016, Iniciativa Ingenio 2010, Consolider Program, CIBER Actions are financed by the Instituto de Salud Carlos III with assistance from the European Regional Development Fund. Marta Broto wishes to thank the FPI-fellowship (BES-2013-062819) from the Spanish Ministry of Economy and Competitiveness. The Custom Antibody Service (CABS) is acknowledged for the assistance and support on immunoreagent production and characterization of tegafur antibodies.

References

1. A. C. Society, <http://canceratlas.cancer.org/>.
2. B. A. Chabner and T. G. Roberts Jr., *Nat. Rev. Cancer*, 2005, **5**, 65–72.
3. H. Yu, N. Steeghs, C. M. Nijenhuis, J. H. Schellens, J. H. Beijnen and A. D. Huitema, *Clin. Pharmacokinet.*, 2014, **53**, 305–325.
4. K. W. Jones and S. R. Patel, *Am. Fam. Physician*, 2000, **62**, 1607–1612.
5. <https://www.iatdmct.org/>.
6. J. G. Godefroid Maaike, A. von Meyer, H. Parsch, T. Streichert, G. Verstraete Alain and V. Stove, *Clin. Chem. Lab. Med.*, 2014, **52**, e13.
7. M. Broto, R. Galve and M. P. Marco, *Trends Anal. Chem.*, DOI: 10.1016/j.trac.2017.05.005.
8. T. Kosjek and E. Heath, *TrAC, Trends Anal. Chem.*, 2011, **30**, 1065–1087.
9. A. B. van Kuilenburg and J. G. Maring, *Pharmacogenomics*, 2013, **14**, 799–811.
10. R. Pazdur, P. M. Hoff, D. Medgyesy, M. Royce and R. Brito, *Oncology*, 1998, **12**, 48–51.
11. B. Gao, S. Yeap, A. Clements, B. Balakrishnar, M. Wong and H. Gurney, *J. Clin. Oncol.*, 2012, **30**, 4017–4025.
12. C. J. Peer, T. J. McManus, H. I. Hurwitz and W. P. Petros, *J. Chromatogr., B: Biomed. Appl.*, 2012, **898**, 32–37.
13. E. Booka, C. K. Imamura, H. Takeuchi, Y. Hamamoto, D. Gomi, T. Mizukami, T. Ichiyama, K. Tateishi, T. Takahashi, H. Kawakubo, K. Soejima, N. Boku, Y. Tanigawara and Y. Kitagawa, *Gastric Cancer*, 2016, **19**, 876–886.
14. D. Chu, J. Gu, W. Liu, J. Paul Fawcett and Q. Dong, *J. Chromatogr., B: Biomed. Appl.*, 2003, **795**, 377–382.
15. L. Zufia, A. Aldaz, C. Castellanos and J. Giraldez, *Ther. Drug Monit.*, 2003, **25**, 221–228.
16. Y. Gu, R. Lu, D. Si and C. Liu, *Anal. Sci.*, 2009, **25**, 1211–1215.
17. K. Liu, D. Zhong, H. Zou and X. Chen, *J. Pharm. Biomed. Anal.*, 2010, **52**, 550–556.
18. G. Remaud, M. Boisdron-Celle, A. Morel and A. Gamelin, *J. Chromatogr., B: Biomed. Appl.*, 2005, **824**, 153–160.
19. I. Nagayama, *JP Pat* 11337549A, 1999.
20. S. Salamone, J. Courtney and D. Stocker, *US Pat* 2006/0177883, 2006.
21. P. Q. Hu, X. Huang and B. R. W. Von, *WO Pat* 2013/082463A2, 2013.
22. L. N. Burgula, K. Radhakrishnan and L. M. Kundu, *Tetrahedron Lett.*, 2012, **53**, 2639–2642.
23. M. C. Estevez, M. Kreuzer, F. Sanchez-Baeza and M. P. Marco, *Environ. Sci. Technol.*, 2006, **40**, 559–568.
24. A. Oubiña, B. Ballesteros, P. Bou Carrasco, R. Galve, J. Gascón, F. Iglesias, N. Sanvicens and M. P. Marco, in *Techniques and Instrumentation in Analytical Chemistry*, ed. D. Barceló, Elsevier, 2000, vol. 21, pp. 287–339.
25. J. Adrian, H. Font, J.-M. Diserens, F. Sanchez-Baeza and M. P. Marco, *J. Agric. Food Chem.*, 2009, **57**, 385–394.

High throughput immunoassay for the therapeutic drug monitoring of tegafur

Marta Broto^{1,2}, Rita McCabe^{1,2}, Roger Galve^{1,2,#}, M.-Pilar Marco^{1,2}

¹Nanobiotechnology for diagnostics (Nb4D), Department of Chemical and Biomolecular Nanotechnology, Institute for Advanced Chemistry of Catalonia (IQAC) of the Spanish Council for Scientific Research (CSIC).
²CIBER de Bioingeniería, Biomateriales y Nanomedicina (CIBER-BBN), Jordi Girona 18-26, 08034 Barcelona, Spain

[#]To whom correspondence should be addressed. Phone: 934006100 (Ext. 5117). Fax: 932045904. E-mail: roger.galve@iqac.csic.es

SUPPORTING INFORMATION

S1. Synthesis.

S1.1 Reagents and instruments.

The chemicals used in the synthesis of the haptens were obtained from Aldrich Chemical Co. (Milwaukee, WI, USA) or Sigma Chemical Co. (St. Louis, MO, USA). Thin-layer chromatography (TLC) was performed on 0.25 mm, silica gel 60 F254 aluminium sheets (Merck, Darmstadt, Germany). ¹H and ¹³C NMR spectra were obtained with a Varian Mercury-400 spectrometer (400 MHz ¹H and 101 MHz for ¹³C). Liquid chromatography/electrospray ionization/mass spectrometry (LC/ESI/MS) was performed in a Waters (Milford, MA, USA) model composed by an Acquity UPLC system directly interfaced to a Micromass LCT Premier XE MS system equipped with an ESI LockSpray source for monitoring positive ions. Data were processed with MassLynx (V 4.1) software (Waters).

S1.2 Synthetic characterization

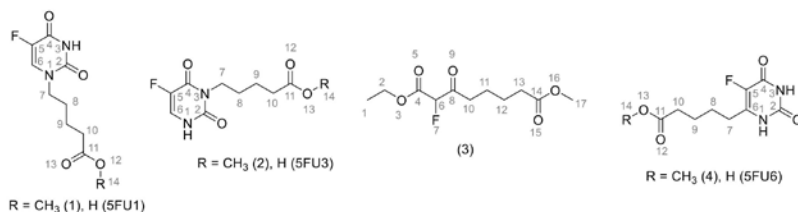


Figure S1. Molecular structure of synthesized compounds. Numbers correspond to NMR assignation.

methyl 5-(5-fluoro-2,4-dioxo-3H-pyrimidin-1-yl)pentanoate (1) and methyl 5-(5-fluoro-2,4-dioxo-1H-pyrimidin-3-yl)pentanoate (2). 5FU1 ester ¹H NMR (400MHz, DMSO-d₆) δ 8.09 (d, *J* = 6.9 Hz, 1H, H6); 3.61 (t, *J* = 6.9 Hz, 2H, H7); 3.58 (s, 3H, H14); 2.33 (t, *J* = 7.2 Hz, 2H, H10); 1.64 – 1.54 (m, 2H, H8); 1.54 – 1.46 (m, 2H, H9)

^{13}C NMR (101MHz, DMSO-d6) δ 173.12 (C11); 157.42 (d, J = 25.8 Hz, C4); 149.98 (C2); 139.56 (d, J = 228.8 Hz, C5); 130.06 (d, J = 33.1 Hz, C6); 51.26 (C14); 47.22 (C7); 32.72 (C10); 21.15 (C9) HRMS (+ESI): m/z calculated for $\text{C}_{10}\text{H}_{14}\text{FN}_2\text{O}_4$ [M + H] $^+$ 245.0938, found 245.0932 (-2.4ppm), (-ESI): m/z calculated for $\text{C}_{10}\text{H}_{12}\text{FN}_2\text{O}_4$ [M - H] $^-$ 243.0781, found 243.0785 (1.6 ppm). 5FU3 ester ^1H NMR (400MHz, DMSO-d6) δ 7.82 (d, J = 5.5 Hz, 1H, H6); 3.76 (t, J = 6.6 Hz, 2H, H7); 3.57 (s, 3H, H14); 2.33 (t, J = 6.9 Hz, 2H, H10); 1.59 - 1.42 (m, 4H, H8 H9) ^{13}C NMR (101MHz, DMSO) δ 173.11 (C11); 157.34 (d, J = 25.1 Hz, C4); 149.82 (C2); 139.39 (d, J = 225.8 Hz, C5); 124.91 (d, J = 31.7 Hz, C6); 51.22 (C7); 39.87 (C14); 32.81 (C10); 26.46 (C8); 21.72 (C9). HRMS (+ESI): m/z calculated for $\text{C}_{10}\text{H}_{14}\text{FN}_2\text{O}_4$ [M + H] $^+$ 245.0938, found 245.0932 (-2.4ppm), (-ESI): m/z calculated for $\text{C}_{10}\text{H}_{12}\text{FN}_2\text{O}_4$ [M - H] $^-$ 243.0781, found 243.0784 (1.2 ppm).

5-(5-fluoro-2,4-dioxo-3H-pyrimidin-1-yl)pentanoic acid (5FU1) and 5-(5-fluoro-2,4-dioxo-1H-pyrimidin-3-yl)pentanoic acid (5FU3). 5FU1 ^1H NMR (400MHz, DMSO-d6) δ 8.10 (d, J = 6.8 Hz, 1H, H6); 3.61 (t, J = 7.0 Hz, 2H, H7); 2.24 (t, J = 7.2 Hz, 2H, H10); 1.65 - 1.53 (m, 2H, H8); 1.53 - 1.37 (m, 2H, H9) ^{13}C NMR (101MHz, DMSO-d6) δ 174.18 (C11); 157.38 (d, J = 25.7 Hz, C4); 149.54 (C2); 139.81 (d, J = 286.3 Hz, C5); 130.06 (d, J = 33.2 Hz, C6); 47.30 (C7); 33.10 (C10); 27.70 (C8), 21.20 (C9). HRMS (+ESI): m/z calculated for $\text{C}_9\text{H}_{12}\text{FN}_2\text{O}_4$ [M + H] $^+$ 231.0781, found 231.0769 (-5.2ppm), (-ESI): m/z calculated for $\text{C}_9\text{H}_{10}\text{FN}_2\text{O}_4$ [M - H] $^-$ 229.0625, found 229.0626 (0.4ppm). 5FU3 ^1H NMR (400MHz, DMSO-d6) δ 11.06 (d, J = 6.4 Hz, 1H, H1); 7.83 (dd, J = 6.3, 5.7 Hz, 1H, H6); 3.76 (t, J = 6.8 Hz, 2H, H7); 2.23 (t, J = 7.0 Hz, 2H, H10); 1.60 - 1.38 (m, 4H, H8 H9) ^{13}C NMR (101MHz, DMSO-d6) δ 174.22 (C11); 157.31 (d, J = 25.2 Hz, C4); 149.80 (C2); 139.37 (d, J = 225.6 Hz, C5); 124.89 (d, J = 31.5 Hz, C6); 39.87 (C7); 33.20 (C10); 26.54 (C8); 21.78 (C9) HRMS (+ESI): m/z calculated for $\text{C}_9\text{H}_{12}\text{FN}_2\text{O}_4$ [M + H] $^+$ 231.0781, found 231.0784 (1.3ppm), (-ESI): m/z calculated for $\text{C}_9\text{H}_{10}\text{FN}_2\text{O}_4$ [M - H] $^-$ 229.0625, found 229.0619 (-2.6ppm).

1-ethyl-8-methyl-2-fluoro-3-oxooctanedioate (3). ^1H NMR (400MHz, CDCl_3) δ 5.13 (d, J = 49.3 Hz, 1H, H6) 4.24 (q, J = 7.2 Hz, 2H, H2) 3.60 (s, 3H, H17) 2.63 (m, 2H, H10) 2.26 (m, 2H, H13) 1.58 (m, 5H, H11 and H12) 1.27 (t, J = 7.1 Hz, 3H, H1) ^{13}C NMR (101MHz, CDCl_3) δ 199.87 (d, J = 22.9 Hz, C8); 172.61 (C14); 163.07 (d, J = 23.6 Hz, C4); 90.32 (d, J = 197.9 Hz, C6); 61.70 (C2); 50.56 (C17); 37.00 (d, J = 0.5 Hz, C10); 32.64 (C13); 23.11 (C12); 21.07 (d, J = 1.7 Hz, C11); 13.00 (C1). HRMS (+ESI): m/z calculated for $\text{C}_{11}\text{H}_{18}\text{FO}_5$ [M + H] $^+$ 249.1138, found 249.1135 (-1.2ppm), (-ESI): m/z calculated for $\text{C}_{11}\text{H}_{16}\text{FO}_5$ [M - H] $^-$ 247.0982, found 247.0979 (-1.2ppm).

methyl 5-(5-fluoro-2,4-dioxo-1H,3H-pyrimidin-6-yl)pentanoate (4). ^1H NMR (400MHz, CD_3OD) δ 3.66 (s, 1H, H14); 2.57 - 2.49 (m, 1H, H7); 2.42 - 2.35 (m, 1H, H10); 1.72 - 1.62 (m, 2H, H8 H9) ^{19}F NMR (400MHz, CD_3OD) δ -174.90 (t, J = 2.7 Hz) ^{13}C NMR (101MHz, CD_3OD) δ 175.45 (C11); 160.04 (d, J = 111.5 Hz, C4); 151.77 (C2); 141.89 (d, J = 25.8 Hz, C6); 138.80 (d, J = 224.5 Hz, C5); 52.07 (C14); 34.15 (C10); 27.78 (C9); 26.95 (C7), 25.22 (C8) HRMS (+ESI): m/z calculated for $\text{C}_{10}\text{H}_{14}\text{FN}_2\text{O}_4$ [M + H] $^+$ 245.0939, found 245.0942 (1.6ppm), (-ESI): m/z calculated for $\text{C}_{10}\text{H}_{12}\text{FN}_2\text{O}_4$ [M - H] $^-$ 243.0781, found 243.0791 (4.1ppm).

5-(5-fluoro-2,4-dioxo-1H,3H-pyrimidin-6-yl)pentanoic acid (5FU6). ^1H NMR (400 MHz, DMSO-d6) δ 12.04 (s, 1H, H-13), 11.40 (d, J = 5.1 Hz, 1H, H-3), 10.77 (s, 1H, H-1), 2.46 - 2.32 (m, 2H, H-7), 2.23 (t, J = 6.9 Hz, 2H, H-10), 1.64 - 1.43 (m, 4H, H-8 H-9). ^{13}C NMR (101 MHz, DMSO-d6) δ 174.27, 157.53 (d, J = 25.9 Hz), 149.82, 140.00 (d, J = 25.7 Hz), 136.92 (d, J = 222.2 Hz), 33.15, 26.27 (d, J = 1.7 Hz), 25.54, 23.72. HRMS (+ESI):

m/z calculated for $C_9H_{12}FN_2O_4 [M + H]^+$ 231.0781, found 231.0787 (2.6 ppm), (-ESI): m/z calculated for $C_9H_{10}FN_2O_4 [M - H]^-$ 229.0625, found 229.0612 (-5.7 ppm).

S2. Immunochemistry.

S2.1 Instruments and General Methods.

The reagents used were obtained from Aldrich Chemical Co. (Milwaukee, WI, USA) and from Sigma Chemical Co. (St. Louis, MO, USA). The matrix-assisted laser desorption ionization time-of-flight mass spectrometer (MALDI-TOF-MS) was a Bruker autoflex III Smartbeam spectrometer (Billerica, Massachusetts). The pH and the conductivity of all buffers and solutions were measured with a pH-meter pH 540 GLP and a conductimeter LF 340, respectively (WTW, Weilheim, Germany). Polystyrene microtiter plates were purchased from Nunc (Maxisorp, Roskilde, Denmark). Dilution plates were purchased from Nirco (Barberà del Vallès, Spain). Washing steps were performed on a Biotek ELx465 (Biotek Inc.). A Heidolph Titramax 1000 vibrating platform shaker (Brinkmann Instruments, Westbury, NY, USA) was used to shake the microplates at 600 rpm. Absorbances were read on a SpectramaxPlus (Molecular Devices, Sunnyvale, CA, USA). The competitive curves were analyzed with a four-parameter logistic equation using the software GraphPad Prism 5.03 (GraphPad Software Inc., San Diego, CA, USA). Normal human plasma was obtained from a pull of non-treated patients (EMD Millipore Corporation, Temecula, CA, USA).

S2.2 Buffers.

Unless otherwise indicated, phosphate buffer saline (PBS) is 0.01 M phosphate buffer in a 0.8% saline solution, pH 7.5. Coating buffer is a 0.05 M carbonate-bicarbonate buffer, pH 9.6. PBST is PBS with 0.05% Tween 20, pH 7.5. Citrate buffer is 0.04 M sodium citrate, pH 5.5. The substrate solution contains 0.01% 3,3',5,5'-tetramethylbenzidine (TMB) and 0.004% H_2O_2 in citrate buffer. Borate buffer is 0.2 M boric acid/sodium borate, pH 8.7.

S2.3 Hapten densities of the bioconjugates

Table S1 Hapten densities of the immunogen and the competitors^a

Immunoreagents	δ -hapten ^b
5FU1-HCH	19 ^c
5FU1-BSA	29
5FU3-BSA	30
5FU6-BSA	21
5FU1-CONA	26
5FU3-CONA	25
5FU6-CONA	17

^aAnalyses were performed by MALDI-TOF-MS. OVA and AD conjugates couldn't be analyzed. ^bMols of hapten per mol of protein. ^cThe immunogen (5FU1-HCH) was characterized using BSA as a protein model.

S2.4 Competitive assays using As337 and different bioconjugates of the hapten 5FU6

Table S2 Immunoassay features of the best competitive ELISAs ^a

Immunoreagents	A _{max}	A _{min}	IC ₅₀ , nM	slope	R ²
As337/5FU6-CONA	0.914	0.145	48.1	-1.143	0.975
As337/5FU6-OVA	1.002	0.109	54.6	-0.772	0.992
As337/5FU6-AD	0.978	0.093	123.6	-0.890	0.992

^aOnly assays showing reasonable parameters and IC₅₀ values are shown. 5FU6-BSA reported really low maximum absorbance.

S2.5 ELISA optimization

Standard calibration curves were carried out at different conditions, varying only one parameter individually. The pH values were studied from 5.5 to 10.5, the conductivity changed from 0 to 50 mS cm⁻¹, the tween 20 concentration was selected between 0 and 0.5%, calcium concentration was optimized from 0 to 8 mM, competition time was tested between 10 and 60 min and incubation time from 0 to 12 h. The value that reported a highest ratio A_{max}-A_{min}/IC₅₀ was selected for following assays.

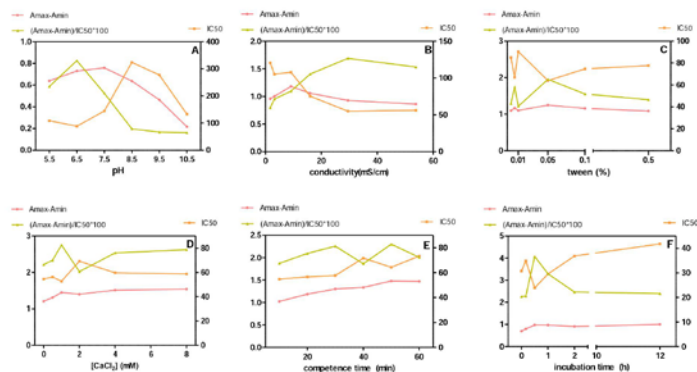


Figure S2 Effect of different physico-chemical parameters on the As337/5FU6-OVA immunoassay. (A) effect of pH; (B) effect of ionic strength (conductivity); (C) concentration of Tween 20; (D) effect of concentration of divalent cations (Ca²⁺); (E) effect of the competition time; (F) effect of the incubation time. At least two-well replicates were employed for each assay. Right axes indicate the value of the IC₅₀. Left axes indicate the difference of absorbance and the ratio (A_{max}-A_{min})/IC₅₀*100. The IC₅₀ values are expressed in nM.

S2.6 Specificity studies

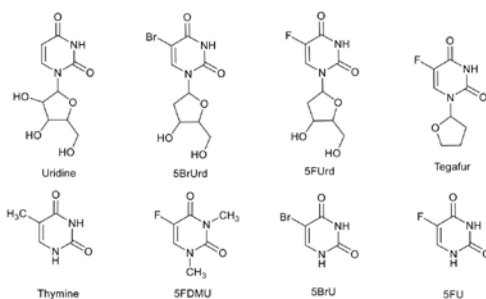
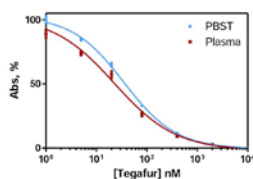


Figure S3. Structures of related tegafur compounds used in the cross-reactivity studies. Abbreviations: 5BrUrd = 5-bromo-2'-deoxyuridine; 5FUrd = 5-fluoro-2'-deoxyuridine; 5FDMU = 5-Fluoro-1,3-dimethyluracil; 5BrU = 5-Bromouracil; 5FU = 5-Fluorouracil.

S2.7 Matrix effect studies

Table S3 Values of the parameters of the non-linear regression of the competence curves in the matrix study.

Parameters	PBST	Plasma	1:2	1:4	1:10	1:25
Amax	0.73 ± 0.02	0.39 ± 0.01	0.51 ± 0.01	0.62 ± 0.01	0.65 ± 0.02	0.69 ± 0.03
Amin	0.08 ± 0.023	0.10 ± 0.01	0.10 ± 0.01	0.09 ± 0.01	0.07 ± 0.02	0.06 ± 0.03
Slope	-0.85 ± 0.13	-0.80 ± 0.09	-0.84 ± 0.09	-0.81 ± 0.09	-0.91 ± 0.13	0.72 ± 0.13
IC ₅₀ (nM)	42 ± 1	57 ± 1	43 ± 1	31 ± 1	38 ± 1	29 ± 1
R ²	0.985	0.985	0.993	0.992	0.987	0.979



Parameters of the assay (As337/5FU6-OVA)

	PBST	Plasma
As dilution	1/7000	1/2000
Bottom	0.055 ± 0.011	0.113 ± 0.016
Top	0.841 ± 0.014	0.741 ± 0.027
Hillslope	-0.837 ± 0.060	-0.709 ± 0.093
IC₅₀, nM	35.4 ± 0.03	22.8 ± 0.08
R²	0.996	0.989

Figure S5. The table shows the features of the inhibition curves of optimized antisera concentration. At least three-well replicates were employed for each curve.

3.5 CHAPTER CONTRIBUTIONS

- Although antibodies against 5FU have shown low affinity, we could modulate immunoassay detectability by production of heterologous competitors. Finally, a competitive ELISA has been developed showing a LOD of 100 nM suitable for TDM.
- Tegafur immunoassay has been developed using a competitor hapten never described before in the literature. The assay has been tested with plasma samples reaching high detectability (LOD of 2.7 nM) and a low crossreactivity. In contrast to previously described immunoassays⁴⁶. Detectability is within real samples requirements⁷².
- For the first time, antibodies able to detect cyclophosphamide have been reported. Hapten was successfully designed trying to expose the cyclophosphamide moiety. Preliminary results reported a LOD of 46 nM in buffer conditions.

3.6 MATERIALS AND METHODS

3.6.1 SYNTHESIS.

- i.* Instruments and general methods. The chemicals used in the synthesis of the haptens were obtained from Aldrich Chemical Co. (Milwaukee, WI, USA) or Sigma Chemical Co. (St. Louis, MO, USA). Thin-layer chromatography (TLC) was performed on 0.25 mm, silica gel 60 F254 aluminum sheets (Merck, Darmstadt, Germany). ¹H and ¹³C NMR spectra were obtained with a Varian Mercury-400 spectrometer (400 MHz ¹H and 101 MHz for ¹³C). Liquid chromatography/electrospray ionization/mass spectrometry (LC/ESI/MS) was performed in a Waters (Milford, MA, USA) model composed by an Acquity UPLC system directly interfaced to a Micromass LCT Premier XE MS system equipped with an ESI LockSpray source for monitoring positive ions. Data were processed with MassLynx (V 4.1) software (Waters).

- ii. *dibenzyl 4,4'-disulfanediyldibutyrate (1)* 4,4'-dithiodibutyric acid (1g, 4 mmol) was placed under inert atmosphere and then thionyl chloride (1.8 mL, 24 mmol) was added and it was allowed to react at 80°C during 30 minutes. Unreacted thionyl chloride was evaporated under reduced pressure, then, 2 mL of benzyl chloride were added. It was allowed to react at r.t. during 90 minutes. Crude was solved in ethyl acetate and extracted three times with NaHCO₃ saturated. Organic phase was dried with MgSO₄, filtered and evaporated under reduced pressure. Liquid obtained was purified by chromatography column with hexane and ethyl acetate to finally obtain 1.47 mg of desired product (yield = 87%, colorless liquid, R_f 0.47 in hexane:ethyl acetate 9.5:0.5) ¹H NMR (400 MHz, Chloroform-*d*) δ 7.36 (d, *J* = 3.7 Hz, 4H), 5.12 (s, 2H), 2.69 (t, *J* = 7.1 Hz, 2H), 2.48 (t, *J* = 7.3 Hz, 2H), 2.04 (q, *J* = 7.2 Hz, 2H). ¹³C NMR (101 MHz, Methanol-*d*₄) δ 174.36, 137.60, 129.53, 129.22, 129.19, 67.26, 38.46, 33.41, 25.37. HRMS (+ESI): *m/z* calculated for C₂₂H₂₇O₄S₂ [M + H]⁺ 419.1351, found 419.1338 (-3.1ppm).
- iii. *benzyl 4-mercaptobutanoate(2)* dibenzyl 4,4'-dithiodibutyrate (714.8 mg, 1.71 mmol) was solved in anhydrous THF and tributylphosphine (630 μL, 2.13 mmol) was added and allowed to react during 2h. Then previously degassed milliQ water was added and allowed to react at 50°C during 30 min. Organic solvent was evaporated under reduced pressure, then HCl 1N was added and extracted three times with ethyl acetate. Organic phases were combined, dried with MgSO₄, filtered and evaporated under reduced pressure. Liquid obtained was purified by chromatography column with hexane and ethyl acetate to finally obtain 694.9 mg of desired product (yield = 97%, colorless liquid, R_f 0.66 in hexane:ethyl acetate 9.5:0.5) ¹H NMR (400 MHz, Methanol-*d*₄) δ 7.44 – 7.18 (m, 4H), 5.10 (d, *J* = 3.7 Hz, 2H), 2.61 – 2.33 (m, 4H), 1.97 – 1.73 (m, 2H). ¹³C NMR (101 MHz, Methanol-*d*₄) δ 174.45, 137.56, 129.51, 129.15, 67.19, 33.44, 30.23, 24.30.
- iv. *benzyl 4-((2-((2-chloroethyl)(2-oxido-1,3,2-oxazaphosphinan-2-yl)amino)ethyl)thio)butanoate (3)* Potassium *tert*-butoxide (707.89 mg, 6.31 mmol) was placed under inert atmosphere, then benzyl thiobutyrate (694.9 mg, 3.30 mmol) and cyclophosphamide monohydrate (838.4 mg, 3.00 mmol) was added solved in 10 mL of anhydrous THF. After one hour, solvent was evaporated until dryness, it

was solved in HCl 1N and extracted three times with ethyl acetate. Organic phases were mixed, dried with MgSO₄, filtered and evaporated under reduced pressure. Liquid obtained was purified by chromatography column with ethyl acetate and methanol to finally obtain 178.2 mg of desired product (yield = 14%, colorless liquid, Rf 0.32 in ethyl acetate:methanol 9:1) **¹H NMR** (400 MHz, Methanol-d₄) δ 7.47 – 7.27 (m, 5H), 5.16 (s, 2H), 4.44 – 4.22 (m, 2H), 3.66 (t, J = 7.3 Hz, 2H), 3.49 – 3.15 (m, 8H), 2.75 – 2.65 (m, 2H), 2.61 (t, J = 7.2 Hz, 2H), 2.53 (t, J = 7.2 Hz, 2H), 2.00 – 1.72 (m, 3H). **¹³C NMR** (101 MHz, Methanol-d₄) δ 174.50, 137.61, 129.53, 129.17, 69.30 (d, J = 6.9 Hz), 67.21, 42.98 (d, J = 1.6 Hz), 42.07 (d, J = 2.7 Hz), 33.69, 31.83, 31.34 (d, J = 1.4 Hz), 26.85 (d, J = 6.3 Hz), 25.91. **HRMS** (+ESI): *m/z* calculated for C₁₈H₂₉N₂O₄PSCI [M + H]⁺ 435.1247, found 435.1228 (-10.6 ppm); (-ESI): *m/z* calculated for C₁₉H₂₉ClN₂O₆PS [(M + HCOOH)-H]⁻ 479.1172, found 479.1140 (-6.7 ppm).

- v. *4-((2-((2-chloroethyl)(2-oxido-1,3,2-oxazaphosphinan-2-yl)amino)ethyl)thio)butanoic acid (CP2-Cl)*. Pd black (180.6 mg) was placed under inert atmosphere and 3 (178.2 mg, 400 μmol) and formic acid (1.32 mL) were added solved in 30 mL of anhydrous methanol. It was allowed to react at r.t. during 1h. Solvent was filtered through celite 545 and solvent was evaporated under reduced pressure. It was solved in HCl 1N and extracted three times with ethyl acetate. Organic phases were mixed, dried with MgSO₄, filtered and evaporated under reduced pressure. (yield = 97%, yellow liquid) **¹H NMR** (400 MHz, Methanol-d₄) δ 4.43 – 4.22 (m, 2H), 3.70 – 3.58 (m, 2H), 3.46 – 3.15 (m, 2H), 2.76 – 2.65 (m, 2H), 2.60 (t, J = 7.2 Hz, 2H), 2.43 (t, J = 7.2 Hz, 2H), 1.96 – 1.74 (m, 4H). **¹³C NMR** (101 MHz, Methanol-d₄) δ 176.79, 69.37 (d, J = 6.9 Hz), 49.36 (d, J = 5.0 Hz), 48.08 (d, J = 4.1 Hz), 42.97 (d, J = 1.7 Hz), 42.10 (d, J = 2.7 Hz), 33.52, 31.92, 31.36 (d, J = 1.6 Hz), 26.87 (d, J = 6.4 Hz), 25.99. **HRMS** (+ESI): *m/z* calculated for C₁₁H₂₃N₂O₄PSCI [M + H]⁺ 345.0805, found 345.0812 (2.0 ppm); (-ESI): *m/z* calculated for C₁₁H₂₁N₂O₄PSCI [M - H]⁻ 343.0648, found 343.0648 (0 ppm)

3.6.2 IMMUNOCHEMISTRY.

- i. *Instruments and general methods.* The chemical reagents used were obtained from Aldrich Chemical Co. (Milwaukee, WI, USA) and from Sigma Chemical Co. (St. Louis, MO, USA). The preparation of the immunoreagents used is described below. The matrix-assisted laser desorption ionization time-of-flight mass spectrometer (MALDI-TOF-MS) was a Bruker autoflex III Smartbeam spectrometer (Billerica, Massachusetts). The pH and the conductivity of all buffers and solutions were measured with a pH-meter pH 540 GLP and a conductimeter LF 340, respectively (WTW, Weilheim, Germany). Polystyrene microtiter plates were purchased from Nunc (Maxisorp, Roskilde, Denmark). Dilution plates were purchased from Nirco (Barberà del Vallés, Spain). Washing steps were performed on a Biotek ELx465 (Biotek Inc.). A Heidolph Titramax 1000 vibrating platform shaker (Brinkmann Instruments, Westbury, NY, USA) was used to shake the microplates at 600 rpm. Absorbances were read on a SpectramaxPlus (Molecular Devices, Sunnyvale, CA, USA). The competitive curves were analyzed with a four-parameter logistic equation using the software GraphPad Prism 5.03 (GraphPad Software Inc., San Diego, CA, USA). Normal human plasma was obtained from a pull of non-treated patients. P
- ii. *Preparation of the immunogens, CP2-Cl-HCH and CXCP-HCH, and competitors, CP2-Cl-BSA, CP2-Cl-CONA, CP2-Cl-OVA, CP2-Cl-AD, CXCP-BSA, CXCP-CONA, CXCP-OVA, CXCP-AD.* The haptens, CP2-Cl and CXCP (10 μ mol) were dissolved in 120 μ L DMF anhydrous. Then, a solution of carbodiimide (25 μ mol) in 60 μ L DMF, N,N'-diisopropylcarbodiimide (DIC) in case of immunizing hapten and N,N'-dicyclohexylcarbodiimide (DCC) in case of competitors, and a solution of N-hydroxysuccinimide (25 μ mol) in 60 μ L DMF were added sequentially. The mixture was stirred for 2 hour until a white precipitate appeared. The suspension was centrifuged at 10000 rpm for 10 min. The supernatant was added dropwise to a solution of 10 mg of protein in 1.8 mL of borate buffer, hemocyanin from limulus polyphemus hemolymph (HCH) in the case of the immunizing hapten and albumin from bovine serum (BSA), conalbumin from chicken egg white (CONA), albumin from chicken egg white (OVA) and aminodextran (AD) in the case of the competitors. The

- reaction mixture was gently stirred for 2 hours at r.t. The protein conjugate was purified by desalting column. Then frozen and lyophilized.
- iii. All of the protein conjugates were stored frozen at $-40\text{ }^{\circ}\text{C}$. Unless otherwise indicated, working aliquots were stored at $4\text{ }^{\circ}\text{C}$ in PBS at 1 mg mL^{-1} . Hapten densities of the bioconjugates were estimated by measuring the molecular weight of the native proteins and the MW of the conjugates by MALDI-TOF-MS. Because HCH is not able to be analyzed by MALDI, simultaneously to preparing the immunogen, the hapten was also conjugated to BSA. However, we assume that this result can be correlated with the hapten density of the immunogen. MALDI spectra were obtained by mixing $2\text{ }\mu\text{L}$ of the freshly prepared matrix (trans-3,5-dimethoxy-4-hydroxycinnamic acid, 10 mg mL^{-1} in ACN/ H_2O 70:30, 0.1% TFA) with $2\text{ }\mu\text{L}$ of a solution of the conjugates or proteins (10 mg mL^{-1} in ACN/ H_2O 70:30, 0.1% TFA). The hapten densities (δ hapten) were calculated according to the following equation: $[\text{MW}(\text{conjugate}) - \text{MW}(\text{protein})] / \text{MW}(\text{hapten})$.
 - iv. *Polyclonal antisera*. As obtained by immunizing female white New Zealand rabbits with CP2-Cl-HCH were named As343, As344 and As345 and with CXCP-HCH were named As 346, 347 and 348. Evolution of the antibody titer was assessed on a non-competitive indirect ELISA, by measuring the binding of serial dilutions of the different antisera to microtiter plates coated with a fixed concentration of hapten-BSA (1 mg mL^{-1}). After 6 immunizations, the animals were exsanguinated, and the blood was collected in vacutainer tubes provided with a serum separation gel. Antisera were obtained by centrifugation at 4°C for 10 min. at 10000 rpm, and stored at $-80\text{ }^{\circ}\text{C}$ in the presence of 0.02% NaN_3 . Unless otherwise indicated, working aliquots were stored at $4\text{ }^{\circ}\text{C}$.
 - v. *Non-competitive indirect ELISA*. The screening of the avidity of the antisera (As343-348) with the 8 antigens (CP2-Cl-BSA, CP2-Cl-CONA, CP2-Cl-OVA, CP2-Cl-AD, CXCP-BSA, CXCP-CONA, CXCP-OVA, CXCP-AD) was evaluated. Two-dimensional titration assays (2D-assay) were carried out, based on the measurement of the binding of serial dilutions of the antisera ($1/1000$ to $1/512000$, and zero, $100\text{ }\mu\text{L well}^{-1}$) against different concentration of the antigens ($1\text{ }\mu\text{g mL}^{-1}$ to 0.5 ng mL^{-1} , and zero, $100\text{ }\mu\text{L well}^{-1}$). From these experiments, optimum concentrations for coating

antigens and antisera dilutions were chosen to generate around 0.7-1 units of absorbance.

- vi. *Competitive ELISA CXCP-BSA/As343*. Microtiter plates were coated with the antigen CXCP-BSA (0.0625 $\mu\text{g}/\text{mL}$ in coating buffer, 100 $\mu\text{L}/\text{well}$), overnight at 4 °C and covered with adhesive plate sealers. The next day, the plates were washed four times with PBST (300 $\mu\text{L}/\text{well}$), and the solution of cyclophosphamide (from 10 to 0 μM in PBST) or the samples, were added (50 $\mu\text{L}/\text{well}$), followed by the solution of antisera As343 (1/8000 in PBST, 50 $\mu\text{L}/\text{well}$). After 30 min at r.t., the plates were washed as before, and a solution of anti-IgG-HRP (1/6000 in PBST) was added to the wells (100 $\mu\text{L}/\text{well}$) and incubated for 30 minutes at r.t. The plates were washed again, and the substrate solution was added (100 $\mu\text{L}/\text{well}$). Color development was stopped after 30 min at r.t. with 4 N H_2SO_4 (50 $\mu\text{L}/\text{well}$), and the absorbances were read at 450 nm. The standard curves were fitted to a four-parameter equation according to the following formula: $y = B(A - B)/[1 - (x/C)^D]$, where A is the maximal absorbance, B is the minimum absorbance, C is the concentration producing 50% of the maximal absorbance, and D is the slope at the inflection point of the sigmoid curve. Unless otherwise indicated, data presented correspond to the average of at least two well replicates.

4 MONOPLEXED BIOBARCODE ASSAY DEVELOPMENT

4.1 CHAPTER OBJECTIVES



Figure 4.1 Structure of chapter 4 related to the different sections

The specific objective of this chapter (Figure 4.1) is the development of a biobarcode strategy for the detection of a low molecular weight molecule (acenocoumarol, ACL) and a protein (C-reactive protein, CRP). The bioreceptors for the specific detection of both compounds were already produced or validated in our group. Thus, our objective was focused on the establishment of the analytical platform. Figure 4.1 shows the general overview of this chapter. Two main milestones were pursued, the conjugation and characterization of the

different particles using the immunoreagents, and the optimization of the parameters of the assays for each particle combination.

4.2 INTRODUCTION

Analytical diagnostic is in need of innovative testing strategies implementation to fulfil clinical challenges.

4.2.1 CODING OLIGONUCLEOTIDES

Designed DNA molecules are emerging as an application for diagnostics platforms⁷³. DNA has special characteristics that include capabilities to hybridize with its complementary, its four-base system pairing and stability along a wide range of environmental parameters, cheap and systematic synthesis, and the huge possibilities of strand functionalization. Oligonucleotides could play an important role as versatile labels being coupled to other sensing systems, providing high performance amplification processes⁷⁴.

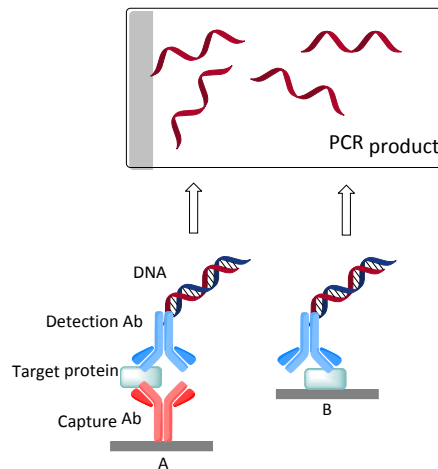


Figure 4.2 The most popular IPCR formats. (a) Sandwich format detection with a primary antibody adsorbed to the microwell and a secondary antibody linked to the DNA tag. (b) Direct detection format.

Oligonucleotide first application in immunoassay based platforms was immuno-PCR⁷⁵ (IPCR). This new approach was based on oligonucleotide labeled antibodies. Then oligonucleotide sequences could be amplified via quantitative PCR techniques (Figure 4.2).

This strategy has been used for many practical applications. Despite the detectability amplification of the system, five orders of magnitude lower than conventional ELISA, quantitative PCR required highly standardized protocols and required the implementation of real-time PCR⁷⁶. Furthermore, amplification factor is limited by the ratio tag:antibody, which is usually 1:1; thus amplification comes from the PCR and not the assay itself. Other amplification techniques have recently focused on combining immunoassays and immobilization on particle surfaces⁷⁷ to increase tag:antibody ratio; one example is the biobarcode.

4.2.2 BIOBARCODE

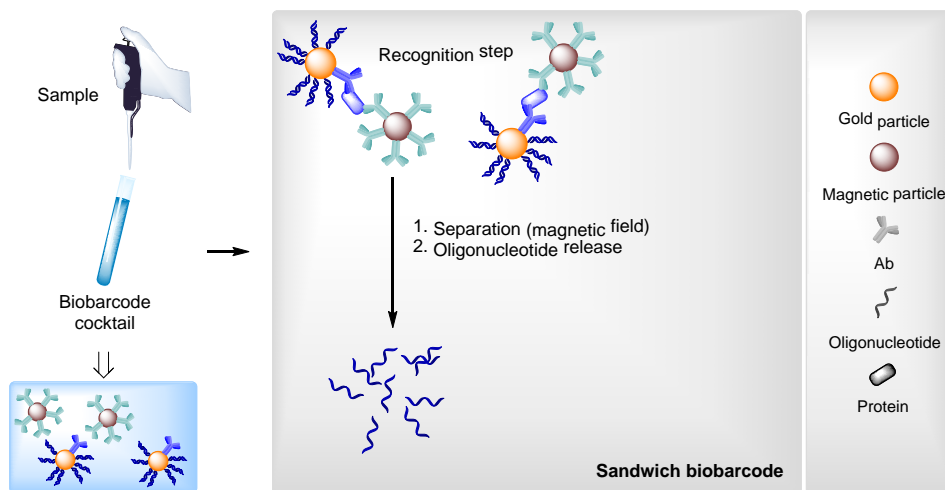


Figure 4.3 Scheme showing the biobarcode assay method.

Biobarcode was designed as an alternative for signal amplification intended to use a PCR-less approach. This platform was first introduced by Nam *et al.* in 2003 achieving a detectability as low as 30 aM⁷⁸.

This technology is based on using multifunctional oligonucleotide encoded particles, modified with a bioreceptor as an encoded probe, and a receptor-

functionalized magnetic particle (Figure 4.3). Thus, after magnetic separation of the complexed probes, biobarcode can be released as signaling readout. The final signal is not the direct interaction between the target analyte and the bioreceptor since it is translated to a reference coding oligonucleotide^{78, 79}. Thus, the quantification of this coding oligonucleotide is equivalent to the analyte concentration. The particle probe carries a large number of oligonucleotides, being possible to increase the ratio tag:antibody up to 1:100. Consequently, there is a substantial amplification of the final signal⁸⁰. Not only an increase of sensitivity could be achieved but the background signal can be reduced via complex isolation. Moreover, particle specific functionalization enables the platform multiplexation^{10, 11}.

In Table 4.1 a list of single molecule biobarcode assays is presented. Multiplexed biobarcode assays have also been developed for proteins¹⁰, bacteria and virus⁸¹⁻⁸³, cells⁸⁴, DNA¹¹ and miRNA⁹, but will be deeply discussed in section 5.1.

As can be observed in the table, almost all previously developed biobarcode assays have been designed in a sandwich format, the main one for protein detection. Other immunoassay formats have been seldom reported, there's only one competitive assay suitable for the detection of a low molecular weight molecule⁸⁵. Most reported assays have focused on the detection of proteins functionalizing both particles with specific antibodies⁷⁸, and using a complementary strand for DNA and/or RNA sequence quantification⁷⁹. Aptamer-based detection particles have also been designed using an oligonucleotide sequence as both barcode and bioreceptor⁸⁶.

In case of magnetic particles, different sizes and functionalizations have been used with successful results. Alternatively, encoded probes deal with a main fundamental challenge, they should be functionalized with a specific bioreceptor while containing the coding oligonucleotides. Gold and polystyrene particle cores have been evaluated, each of them providing specific characteristics. Gold particles⁷ present the advantage of the specific interaction with thiol groups (thiol functionalized oligonucleotides) and the unspecific adsorption of proteins. Thus, these particles propose easy functionalization protocols for both components. Whereas, polystyrene particles have been proposed for a higher loading capacity⁸⁷ since particles can have a bigger size.

Table 4.1 Developed biobarcode assays for a single analyte

Target type	Analyte	Assay format	Signaling readout	LOD	Ref
Protein	PSA ^a	Sandwich	Silver enhancement	30 aM, 12 fM	78, 88
		Sandwich	On-chip silver enhancement	500 aM	89
		Sandwich	Fluorescence	300 aM	87
	IgG	Sandwich	Purine base detection	0.1 ng/mL	90
		Sandwich	DNA microarray	1 pg/mL	91
	ADDLs ^b	Sandwich	Silver enhancement	100 aM	92
	Cytokines	Sandwich	Colorimetric particle aggregation	30 aM	93
	IgE	Sandwich	Chemiluminescence	4.6 pM	86
Ricin	Sandwich	PCR	0.01 fg/mL	94	
Virus (protein)	HCV ^c antigen	Sandwich	Nanogap electrode	1 ng/mL	95
	HIV-1 p24 antigen	Sandwich	On-chip silver enhancement	0.1 pg/mL	96
	AIV ^d	Sandwich	Fluorescence	1:128x10 ⁻⁵ dilution	97
	Respiratory syncytial virus	Sandwich	PCR	8.3 PFU/mL	98
	Bluetongue virus	Sandwich	PCR	0.1 fg/mL	99
Bacteria (protein)	<i>Staphylococcus aureus</i>	Sandwich	Electrochemical	5x10 ³ CFU/mL	100
DNA	Anthrax lethal factor	Sandwich	Silver enhancement	500 zM	79
	<i>Salmonella</i> Enteritidis Iel ^e	Sandwich	Fluorescence	0.2 fM	8
	Exotoxin A	Sandwich	Fluorescence	1.2 ng/mL	101
miRNA	miRNA-21	Sandwich	Enzyme-assisted strand cycle	52.5 zM	12
Small molecule	17 β -estradiol	Sandwich	Fluorescence	6.37x10 ⁻⁶ ng/mL	102
	Triazophos	Competitive	PCR	0.02 ng/mL	85

a) PSA, prostate specific antigen b) ADDLs, amyloid- β -derived diffusible ligands c) HCV, hepatitis C virus d) AIV, avian influenza virus e) Iel, insertion element gene

Concerning coding oligonucleotides release and quantification, several strategies have been reported. Firstly, oligonucleotide release has been addressed either by dehybridization from the particle⁷⁸, meaning that two oligonucleotide sequences are required, or either by breaking the gold-thiol interaction by ligand exchange treatment⁷ or core particle dissolution⁹. Secondly, different oligonucleotide quantification methods have been conducted via PCR⁹⁸, silver enhancement arrays⁷⁸ and capillary electrophoresis⁸². However another

implemented strategy has been used by tagging oligonucleotides with fluorophores⁸⁷, allowing direct detection of the fluorescence by hybridization on a DNA-microarray^{7, 91}.

4.2.3 PROOF OF CONCEPT, CARDIOVASCULAR DISEASES

Cardiovascular diseases accounted for 31% of all the global deaths in 2012, making them the leading cause of death worldwide¹⁰³. They are a group of disorders of the heart and blood vessels that include some diseases like coronary heart disease and cerebrovascular disease. Most of them are caused by an accumulation of fatty deposits on the inner walls of the blood vessels, called atherosclerosis. Otherwise, rheumatic heart disease is produced by streptococcal infection and congenital heart disease is presented at birth.

Due to the high CVDs incidence, two CVDs-related analytes were selected for the development of a monoplexed biobarcode assay. Targets selected were a low molecular weight molecule (ACL), and the C-reactive protein (CRP), both of them described below.

4.2.3.1 Acenocoumarol (ACL)

Acenocoumarol, also known as nicoumalone or Sintrom[®], is a vitamin K antagonist drug used for long-term treatment of thromboembolic events (Figure 4.4). It has a narrow therapeutic window and there is high dose-response variability, mainly caused by a genetic polymorphism¹⁰⁴. Furthermore, overdosing can produce bleeding complications or recurrent thrombosis.

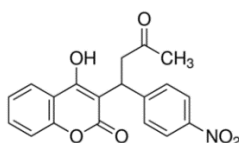


Figure 4.4 Acenocoumarol chemical structure

Due to its clinical features, ACL is routinely monitored in healthcare centers. Its monitoring is usually based in chromatographic methods^{105, 106}, which, as stated before, are time consuming and require qualified personnel. For this reason,

antibodies for ACL recognition were previously raised and validated in our group to produce a high throughput quantification assay. The immunoassay developed reported a LOD of 5 nM and low crossreactivity with parent and related compounds.

4.2.3.2 C-reactive protein (CRP)

Biomolecules that promote atherosclerosis are known as risk factors. Due to the high incidence of CVDs, increasing numbers of biomarkers are being proposed as risk factors for disease stage evaluation, C-reactive protein among them. It is a pentameric protein (Figure 4.5) that can be found in blood. Evidence is mounting that plasma CRP deposited onto inflamed tissue breaks in biologically active monomeric subunits, which have been attributed to a range of proinflammatory effects. Consequently, CRP has been stated as a risk factor for cardiovascular diseases¹⁰⁷, and in addition has been suggested as a better marker than LDL cholesterol¹⁰⁸.

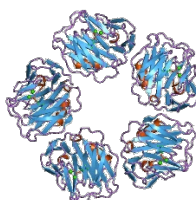


Figure 4.5 CRP chemical structure

CRP plasma levels have been proposed for risk assessment as: low risk < 1 mg/mL, average risk 1-3 mg/mL, high risk 3-10 mg/mL and very high risk > 10 mg/mL¹⁰⁹. A lot of analytical platforms have been used for CRP quantification¹¹⁰ including immunoassays, surface plasmon resonance (SPR) and assays using molecular imprinted polymers as non-natural receptors; some of them have also have been commercialized¹¹¹. Nevertheless, future research should focus on integrated and multiplexed sensing platforms with co-existing biomarkers¹¹².

4.3 RESULTS AND DISCUSSION

In order to develop a biobarcode assay, we need to design the system and the signaling readout. Our assay would be characterized by three main components (Figure 4.6):

1. **Encoded probes**, oligonucleotide encoded particles, will be used to identify the target biomarker and provide amplification of the signal through the release of the coding oligonucleotides attached to the nanoparticles. Oligonucleotides would be functionalized with a fluorophore as signaling readout.
2. **Magnetic particles**, will allow selective extraction/isolation of biomarker targets or biocomplexes from complex matrices.
3. **Multiplexed DNA-microarray** will capture the coding oligonucleotides, which provide a fluorophore group, released by the encoded probes.

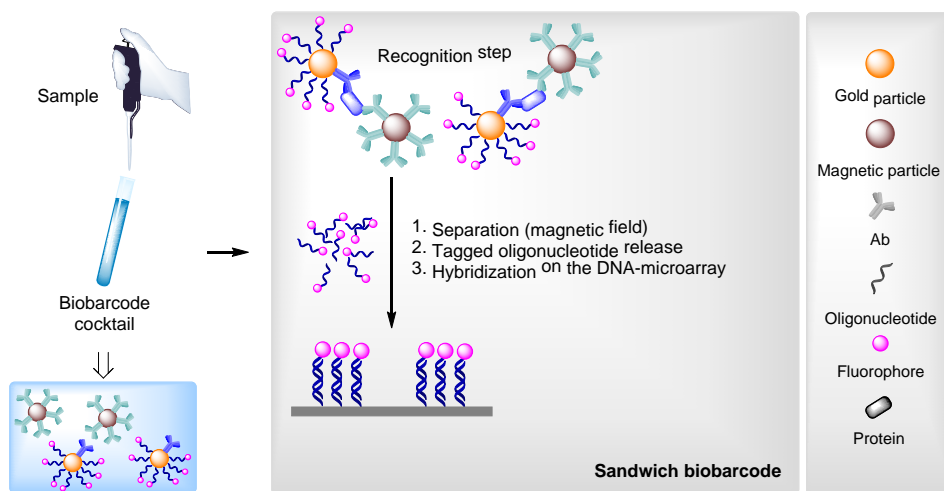


Figure 4.6 Schematic diagram of the sandwich biobarcode strategy

But prior to develop the assay, we must establish the microarray conditions and conjugation procedures for both particles. Particle functionalization requirements have to be taken into account before developing these procedures, specially encoded probes that will be functionalized with both

coding oligonucleotide and bioreceptor. Since we want to develop a universal platform, encoded probes should provide functional groups for antigen or hapten conjugation in case of competitive formats or antibody functionalization in case of sandwich format.

4.3.1 DNA MICROARRAY

Microarray concept was first introduced in the late 80s¹¹³, which is a tidy arrangement of bioreagents or samples. DNA microarray have leaded a revolution in diagnostics due to their major stability and elevated specificity of the hybridization process that takes place between two single complementary DNA strands¹¹⁴. DNA microarray was selected as a signaling readout since it reports a limit of detection two orders of magnitude lower than fluorescence in solution and, eventually, it can be multiplexed.

Glass surface was selected for microarray due to its high chemical and physical resistance, it has low intrinsic fluorescence and shows high transmission which are crucial characteristics for our fluorescent readout. Moreover, it is easy to obtain, its surface is normally flat with few wrinkles, rigid, transparent and without pores, allowing a more favorable kinetic reaction.

Glass slides (75x25 mm size) were printed with 24 microarrays. The chemistry selected for covalent binding of DNA sequences was 3-Glycidyloxypropyl)trimethoxysilane (GPTMS), that provides an epoxy group (Figure 4.7A) that will react with the amino terminal group of the DNA sequence that want to be spotted.

Hence, after a washing step with piranha solution, slides are immersed in NaOH 10% to deprotonate hydroxyl groups and then pure GPTMS is allowed to react with the glass. Afterwards, the DNA strands are added with the aid of a nanodrop dispensator, a microspotter, forming micrometric active zones.

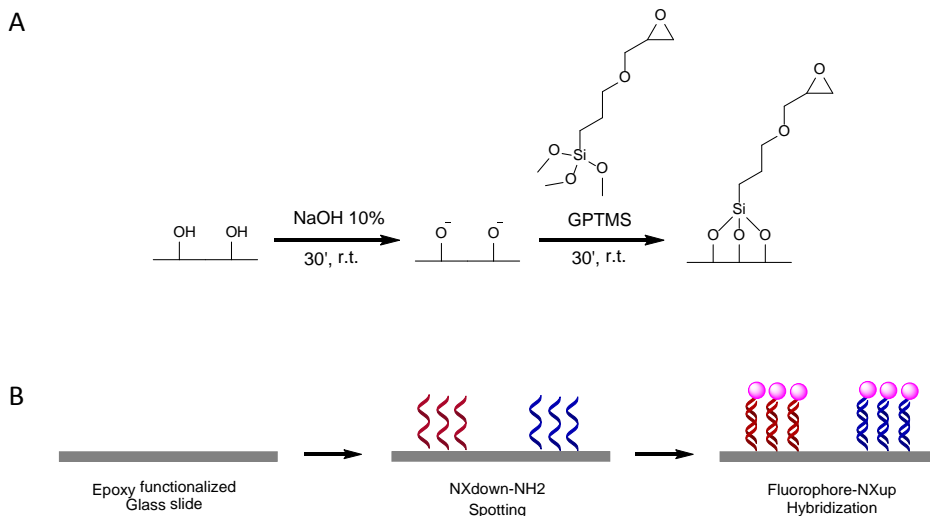


Figure 4.7 A) Glass slide functionalization with GPTMS. B) DNA microarray, coding oligonucleotide quantification strategy.

Nucleotide sequences used were previously designed in our group¹¹⁵. Two complementary pairs of single stranded DNA were used (N2 and N4, up and down), they had 50% of G/C content and the same nucleotide composition to supply all pairs with similar hybridization properties. The specificity of the hybridization was studied in a microarray multiplex format (Figure 4.7B) reporting no cross-hybridization between them. All protocols and procedures related to slide derivatization and functionalization can be found in section 4.4.

Once the slide has been already functionalized, they are kept at low temperature until use. The microarray assay was run by placing the slides in an ArrayIt® multi-well platform (see Figure 4.8). In this manner, each slide was divided in 24 wells (8 wells in each of the 3 columns). In each well a determined number of spots were printed depending on the experiment. Different configurations are possible which can be programmed in the spotter.



Figure 4.8. All material needed for the different steps involved in fluorescent microarray development: print, assemble, measure, analyze and data treatment.

4.3.2 MAGNETIC PARTICLES FUNCTIONALIZATION AND CHARACTERIZATION

Magnetic particles (MP) had to be functionalized with the specific antibodies. First of all, antisera solution should be precipitated using ammonium sulfate and then purified by protein A affinity column (specific for rabbit antibodies), in order to remove the rest of proteins present in antisera solution. Antisera purification provides a mixture of IgGs produced by the animal host, in which a 10% are specific for our analyte. Afterwards, functionalization procedure was performed following a similar protocol to the one supplied by the manufacturers. The particles selected had a size of 1 μm and were already functionalized with Tosyl groups, good leaving groups able to react with any amino group of the antibodies. The procedure reports yields higher than 80%. Protocol related to MP functionalization can be found in section 4.4.

4.3.3 ENCODED PROBES FUNCTIONALIZATION AND CHARACTERIZATION

4.3.3.1 Gold nanoparticles functionalization and characterization

All procedures included in this chapter can be found in section 4.6.

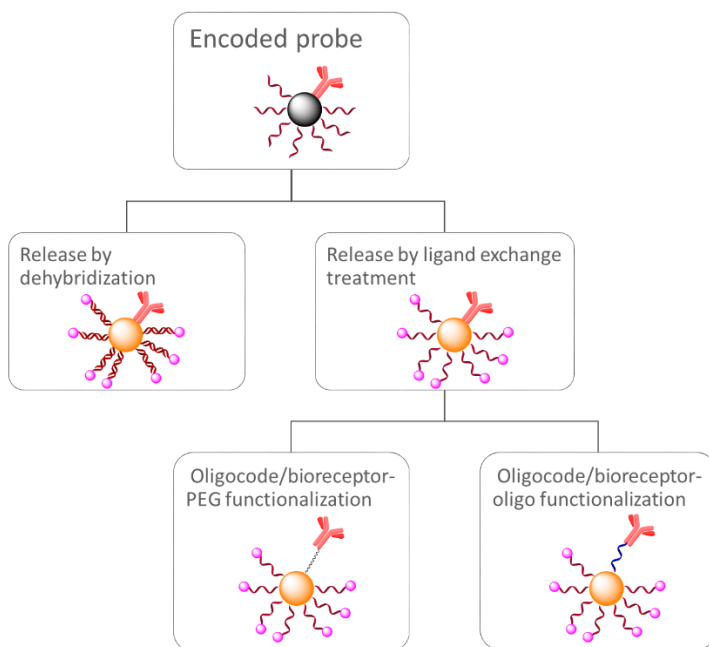


Figure 4.9 Graph showing previous attempts for gold nanoparticle functionalization with both bioreceptor and coding oligonucleotide.

Originally, gold nanoparticle (AuNPs) functionalization was started by Nuria Tort and Gloria Colom in their PhD thesis. In Figure 4.9 there's a graph showing main strategies used for gold particle functionalization. Design was thought to functionalize particles with bioreceptor and coding oligonucleotides. First, the fluorescence release by dehybridization was studied, as it has been already reported in the literature, but the procedure unexpectedly lack of robust and many oligo sequences were required. Secondly, fluorescent-tagged oligonucleotides were addressed by ligand exchange treatment. This strategy was tested functionalizing particles with a mixed monolayer, containing both the coding oligonucleotides and a PEG sequence that provides functional groups for the covalent link of the bioreceptor. Unfortunately, this procedure also lacked reproducibility regarding particle preparation, and reported a really low signal. Taking into account previous procedures, our preliminary attempt was focused on functionalizing particles with a mixed monolayer of oligonucleotides.

Our first objective was the establishment of a procedure for mixed monolayer preparation. Furthermore, a secondary objective was also addressed, the development of an assay in a competitive format since biobarcode in this format

has been seldom reported before. This assay design was based on a magnetic particle functionalized with specific antibodies and an encoded gold probe (eAuP) that had both oligonucleotide sequences: one conjugated to the hapten for the biorecognition, and the other functionalized with a fluorophore as the coding sequence (Figure 4.10).

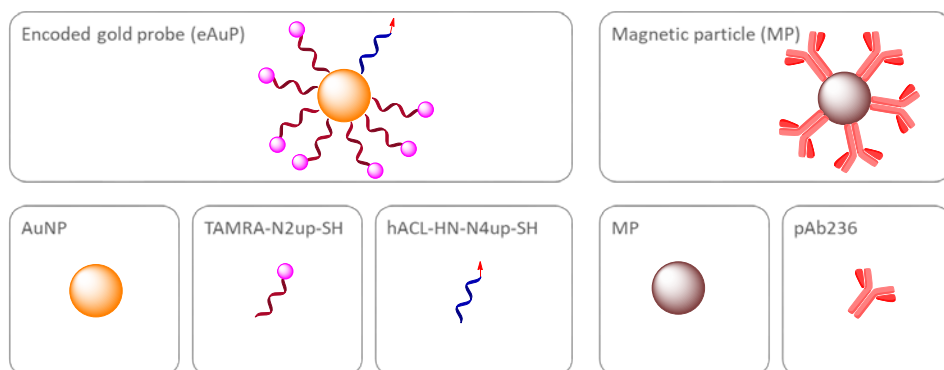


Figure 4.10 Scheme showing the design of the biobarcode assay for the detection of small molecules. Most reagents were already prepared or are commercially available.

AuNPs and thiolated oligonucleotides were selected due to Au-S self-assembly. Nanoparticles were coated with two different oligonucleotide sequences: TAMRA-N2up-SH as the fluorophore functionalized barcode (allows detection and amplification of the signal⁸⁷), and hACL-N4up-SH as the oligonucleotide sequence functionalized with the acenocoumarol hapten (hACL) (the responsible of the biorecognition). Both N2up and N4up sequences were 20-mer oligonucleotides with the same content of G-C bases to confer them similar properties. First, hACL was conjugated to an oligonucleotide sequence (H₂N-N4up-S-S-OH) for subsequent conjugation to AuNPs. Then, oligonucleotide conjugation to AuNPs and release was studied to finally introduce hapten and characterize the particles.

4.3.3.1.1 Hapten conjugation

hACL, hapten of acenocoumarol, was conjugated to an oligonucleotide sequence, H₂N-N4up-S-S-OH (Figure 4.11). This oligonucleotide sequence was designed with an amino group in the 5'-end for the conjugation with the hapten and a thiol group in the 3'-end for the interaction with the gold nanoparticle. This thiol group was protected forming a disulfide bond to avoid possible reactions in

the conjugation step. The conjugation strategy used was the well-known carbodiimide methodology (DCC/NHS). Then, the product was purified by HPLC being able to separate unreacted hapten and oligonucleotide from the conjugated one. Next, the produced oligonucleotide conjugate was characterized by MALDI-TOF-MS reporting a mass only three units lower than the calculated one, which is within technique variability. Finally, disulfide bond was reduced with dithiothreitol treatment.

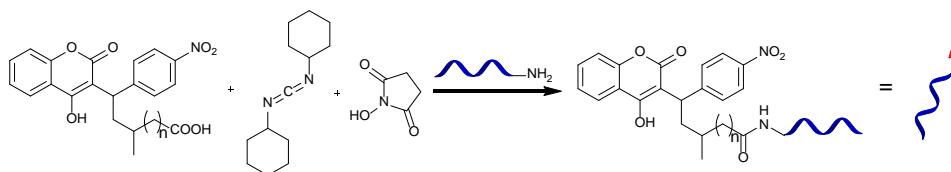


Figure 4.11 Acenocoumarol hapten, hACL, conjugation to oligonucleotide sequence.

4.3.3.1.2 AuNPs synthesis

AuNPs synthesis was done following the Turkevich method¹¹⁶, based on citrate reduction of gold salt. Sodium citrate not only reduces gold but solvates the particles. Particles were characterized by transmission electron microscope (TEM) and UV-Vis, both methods reported 16-nm diameter with a polydispersity lower than 9 %, and demonstrated high stability along time.

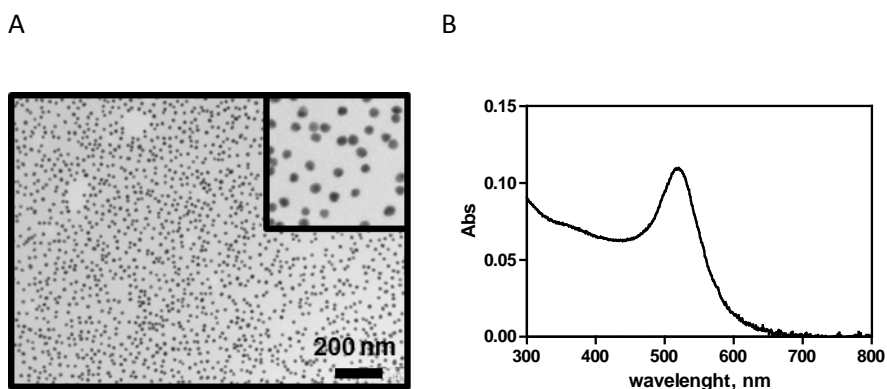


Figure 4.12 A) TEM image of produced AuNPs (16 nm). B) UV-Vis spectra of the particle solution. Maximum absorbance corresponds to 520 nm, which can be correlated with particle size (16 nm) and particle concentration through the Lambert-Beer law.

4.3.3.1.3 AuNPs biofunctionalization and oligonucleotide release

AuNPs are usually functionalized via the salt-aging strategy¹¹⁷, however, it is time consuming. A pH-assisted methodology¹¹⁸ was reported which shortened conjugation time from days to minutes. This approach was based on the addition of a low pH buffer that reduces the repulsion between chains allowing a maximal loading. Furthermore, sodium dodecyl sulfate (SDS) present in the buffer keeps particles from aggregation, provides better stability and adds washing efficiency. Then, oligonucleotide release from the particles was done with a ligand exchange treatment, with the reagent dithiothreitol (DTT). Several parameters like conjugation time, release time, release temperature, DTT concentration and the concentration of oligonucleotides were optimized (Figure 4.13). A Final quantity of 80 molecules of oligonucleotide per particle was obtained, inside the same range as salt aging method¹¹⁹.

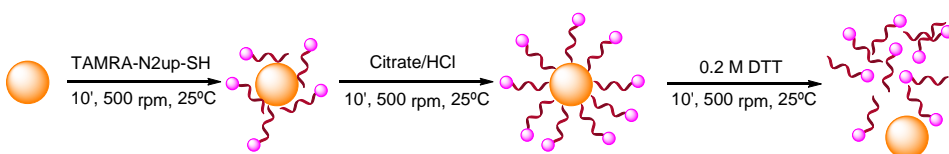


Figure 4.13 Scheme showing conjugation and release procedure for AuNPs

Once conjugation procedure was established, we proceed to functionalize the particles with both coding and hapten sequences. Modulating the percentage of both sequences we were able to modulate the percentage of them on the surface of the particles. We selected only a 10% of hapten sequences, which would provide 70 sequences of coding oligonucleotide per particle achieving a biobarcode amplification factor of 1:70, similar to previous approaches⁷⁸.

4.3.3.1.4 eAuP validation

First of all, buffer properties were evaluated in order to find suitable conditions for eAuP stability and antigen-antibody interaction. Parameters like SDS concentration, Tween 20 concentration and conductivity, which are crucial for eAuP stability, were varied in ELISA to see how they affected to the antigen-antibody interaction. Results reported that SDS can't be used in the interaction step since it disrupts non-covalent bonds of the proteins or antibodies and

denature them. In addition, conductivity should be low to avoid particle aggregation, showing a peak of signal at 5 mS/cm. Optimal concentration of tween 20 and BSA were 0.05 to 0.3 % and 0 to 0.3 % respectively.

Afterwards, particle characterization was conducted running a competitive assay on its surface (eAuP-ELISA) using an enzyme-linked secondary antibody for the colorimetric response. The calibration curve of the assay reported an IC_{50} of 3.7 nM (Figure 4.14), similar to the ELISA results. Thus, confirming that particles had been correctly functionalized, were able to interact with the antibodies, and presented inhibition in the presence of the analyte.

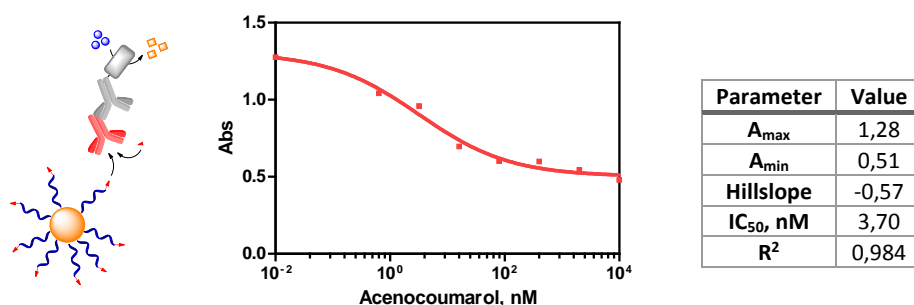


Figure 4.14 Calibration curve of ELISA assay on eAuPs. The data has been extracted from the four-parameter equation used to fit the standard curves.

Despite the successful results obtained with these particles, subsequent assays between MPs and eAuPs reported unspecific adsorption. Particle concentration was evaluated carrying a 2D checkerboard assays. Concentrations found were used for the competitive assays, but unfortunately it was found there was unspecific interaction of non-haptenized encoded probes with the antibodies (eAuPs functionalized only with TAMRA-N2up interacted unspecifically with MPs).

All possible sources of unspecificity, and strategies evaluated to reduce it, are listed below:

1. **Washing buffer:** At the beginning, the same buffer was used for competition and washing steps, different surfactants and additives were added into the washing buffer to remove eAuPs coupled by electrostatic interactions. Cationic and anionic surfactants, and also a certain percentage of organic solvent were tried.

- Interaction buffer:** as explained before, this buffer was optimized for the antibody recognition of the hapten functionalized probes. Some variations concerning BSA, salinity or the tween 20 concentration were introduced in the interaction buffer with similar results. Otherwise, magnetic particles were coated with a polyurethane layer and capped with BSA, leaving free secondary amines. Amines could be protonated at neutral pH, which would interact with the negative charge of oligonucleotides. Increasing pH could reduce this effect but results were not successful.
- Magnetic particles:** magnetic particle conjugation was modified to introduce different residues. A different capping procedure could avoid unspecific electrostatic interaction. Capping was tried with β -alanine, to obtain a carboxylic residue, PEG-NH₂ and also ethanolamine. All capping procedures reported the same results. Then, other particle brands were evaluated that provided different particle size, coating or magnetic properties. Moreover, a different batch of antibodies (As337, also raised against acenocoumarol hapten) was used for particle functionalization. All approaches reported the same results.
- Encoded gold probes:** eAuPs were the last component to be evaluated, unspecific adsorption of the fluorophore was studied without successful results. Another approach was PEG passivation of particles¹²⁰, Figure 4.15. The hypothesis was that oligonucleotides were not conjugated producing a monolayer. There could be some spaces that could interact with proteins. It has long been known that proteins interact unspecifically with gold. PEG passivation could prevent interaction and add stability due to hydrophilic properties. Nevertheless, neither this approach solved the problem presented.

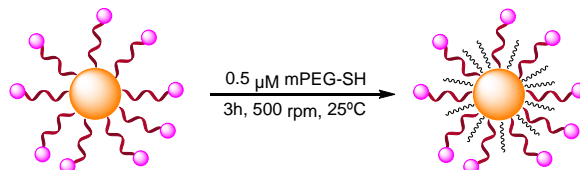


Figure 4.15 Preparation of prefucionalized PEG-coated eAuPs

All possible alternatives were already evaluated, consequently, the last option was removing gold particles.

4.3.3.2 Polystyrene microparticles functionalization and characterization

As explained before, all strategies approached for gold nanoparticles functionalization did not report reliable results. Polystyrene particles were selected to be used as encoded probes. Polystyrene particles (PSP) have already been used for biobarcode development⁸⁷ They can have a bigger particle size that could allow a higher oligonucleotide loading and, consequently, a larger amplification factor. In this case, assay design had to be slightly modified (Figure 4.16). Coding oligonucleotides (TAMRA-N2up-SS-NH₂) required a fluorophore in the 5'-end, an internal modification of a disulfide bond for subsequent cleavage with DTT, and an amino group in the 3'-end for the conjugation to the particles. Alternatively, antigen used for ELISA development was also conjugated to the particles without any further synthesis steps.

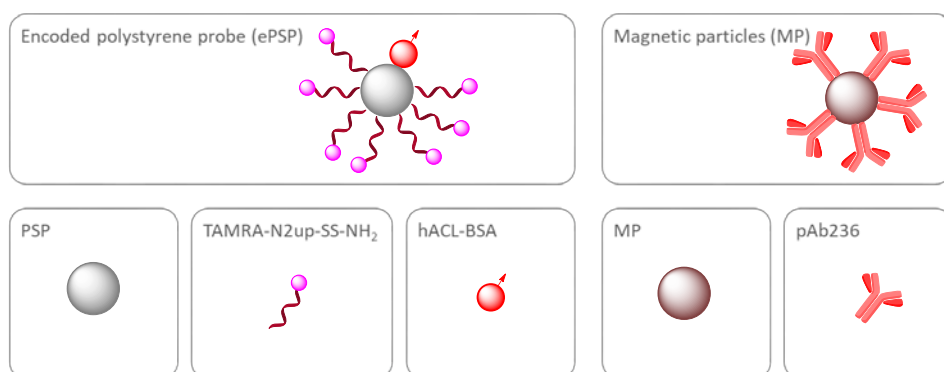


Figure 4.16 Scheme showing the design of the biobarcode assay for the detection of small molecules with PSP.

Some physicochemical parameters such as carbodiimide concentration, pH, ionic strength, temperature, and reaction time were tested in order to improve conjugation yield. ELISA and fluorescence quantification were used for evaluation of unbound reagents present in supernatant.

After the functionalization procedure, the specificity of the particles was evaluated comparing the interactions of unspecific and specific particles in a biobarcode format. Results for particle functionalization and specific interaction is detailed in section 4.4.1

4.3.4 ESTABLISHMENT OF A NP-BASED BIOBARCODE ASSAY FOR ACENOCOUMAROL

Results obtained in this section were collected in a publication and can be found in section 4.4.1.

Development of the indirect competitive biobarcode assay for acenocoumarol was accomplished since all procedures for DNA microarray and particle functionalization were already established.

4.3.5 ESTABLISHMENT OF A NP-BASED BIOBARCODE ASSAY FOR C-REACTIVE PROTEIN

Results obtained in this section were collected in a publication and can be found in section 4.4.2.

Biobarcode for CRP detection was carried out in sandwich format. In that case, both ePSP and MP were functionalized with two different specific antibodies (Figure 4.17).

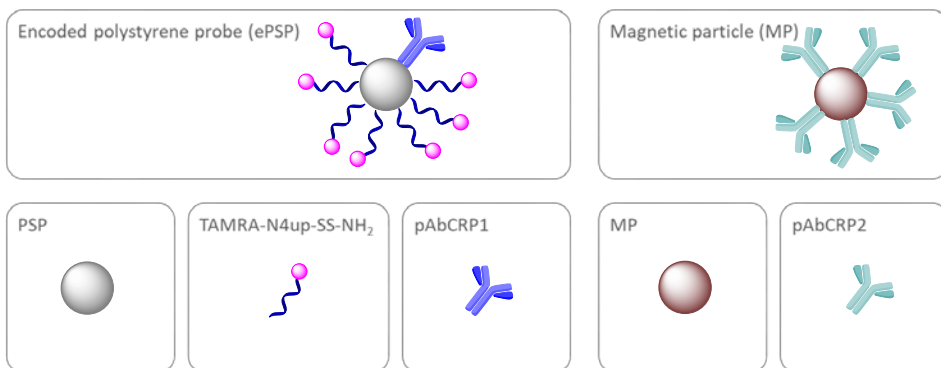


Figure 4.17 Scheme showing the design of the biobarcode assay for the detection of proteins with PSP.

Protocols already established for particle functionalization were used with successful results.

4.4 RELATED PUBLICATIONS

4.4.1 PUBLICATION III: BIOBARCODE ASSAY FOR THE ORAL ANTICOAGULANT ACENOCOUMAROL

Biobarcode Assay for the Oral Anticoagulant Acenocoumarol

Marta Broto, J.-Pablo Salvador, Roger Galve and M.-Pilar Marco

Submitted

This publication describes the development of a competitive indirect biobarcode assay for acenocoumarol quantification in plasma samples. First, assay design is deeply discussed, as well as, particle functionalization. Second, assay development is evaluated and challenged by plasma samples. Finally, signal amplification and working range modulation are demonstrated by the use of tailored particles.

Biobarcode Assay for the Oral Anticoagulant Acenocoumarol

Marta Broto^{1,2}, J.-Pablo Salvador^{1,2}, Roger Galve^{1,2,*} and M.-Pilar
Marco^{1,2}

¹*Nanobiotechnology for Diagnostics (Nb4D), Institute for Advanced Chemistry of Catalonia of the Spanish Council for Scientific Research (IQAC-CSIC).* ²*CIBER de Bioingeniería, Biomateriales y Nanomedicina (CIBER-BBN). Jordi Girona 18-26, 08034-Barcelona, Spain*

*To whom correspondence should be sent:

Roger Galve

IQAC-CSIC

Jordi Girona, 18-26

08034-Barcelona, Spain

Phone: 93 4006180

FAX: 93 2045904

E-mail: roger.galve@cid.csic.es

ABSTRACT

A novel approach for therapeutic drug monitoring of oral anticoagulants (OA) in clinical samples is reported, based on a *NP-based biobarcode* assay. The proposed strategy uses specific antibodies for acenocumarol (ACL) covalently bound to magnetic particles (pAb236-MP) and a bioconjugate competitor (hACL-BSA) linked to encoded polystyrene probes (hACL-BSA-*e*PSP) on a classical competitive immunochemical format. By using this scheme ACL can be detected in low nM range (LOD, 0.96 ± 0.26 , N= 3, in buffer) even in complex samples such as serum or plasma (LOD 3.84 ± 1.04). The assay shows a high reproducibility (%CV 1.1 day-to-day) and is robust, as it is demonstrated by the fact that ACL can be quantified in complex biological samples with a very good accuracy (slope= 0.97 and $R^2=0.91$, of the linear regression obtained when analyzing spiked *vs* measured values). Moreover, we have demonstrated that the biobarcode approach has the potential to overcome one of the main challenges of the multiplexed diagnostic, which is the possibility to measure in a single run biomarker targets present at different concentration ranges. Thus, it has been proven that the signal and the detectability can be modulated by just modifying the oligonucleotide load of the encoded probes. This fact opens the door for combining in the same assay encoded probes with the necessary oligonucleotide load to achieve the detectability required for each biomarker target.

KEYWORDS

NP-based Biobarcode, small molecule, acenocoumarol, therapeutic drug monitoring, oral anticoagulants, immunoassay

INTRODUCTION

Biobarcode assays emerged some years ago as a new generation of innovative approaches for assay signal amplification. *Biobarcode* refers to biomolecules that have specific features that made them suitable to become a code. Thus, the characteristic structure of DNA molecules based on four bases, allows designing an extraordinary wide number of different oligonucleotide sequences and, therefore, their use as *biobarcodes*¹. The nucleotide bases are complementary two-by-two, which allows the specific binding to complementary sequence. These properties, combined with DNA versatile synthesis, permits the introduction of diverse functionalities and make designed DNA an exceptional option for *biobarcode* assays, particularly immunoassays². Oligonucleotide sequences were first introduced in immunoassays as signaling readout, for amplification purposes, developing immuno-PCR³. Antibodies were labeled with oligonucleotide sequences instead of enzymes, providing increased detectability. However, this approach has not been routinely applied due to the requirement of highly standardized protocols, special instruments and qualified personnel.

The *biobarcode assay* concept, as we understand it today, was reported for the first time in 2002 by Mirkin's group (Nam *et al.*⁴), demonstrating that PSA (prostate-specific antigen) could be detected down to 30 aM concentration, six orders of magnitude more sensitive than the clinically

accepted assay methods. The principle behind *biobarcode assays* is the use of bioreceptors attached to nanoparticles (NP) that contains a large number of specific nucleotide sequences (encoded probes). Every different bioreceptor is attached to encoded probes with a unique oligonucleotide sequence and, in this manner, the binding of a particular analyte is encoded. Since every NP is loaded with a large number of nucleotides (i.e. 360 on a 30 nm particle⁵) the signal for the detection of a particular target analyte is amplified. After the binding event, the bound oligonucleotides are released and subsequently detected through different means. This PCR-less technique, has the ability to achieve countless distinctive labels and signal amplification due the large surface/volume ratio of nanoparticles. Moreover, these *NP-based biobarcode assay*, usually employ biofunctionalized magnetic particles as capture probes that allow capturing/concentrating the target analytes present in the sample^{10,11}. Both, the magnetic particle and the DNA encoded probes form a complex via sandwich with the target analyte, usually a protein or a particular DNA or RNA sequence, that can be isolated by the application of a magnetic field. This strategy has been found to increase sensitivity, reduce background signal (since oligonucleotide quantification is matrix free) and potential for high multiplexing⁶⁻⁷. Otherwise, oligonucleotide detection/quantification strategies include DNA-microarray based on silver enhancement of gold nanoparticles⁸, oligonucleotide digestion coupled to electrochemical detection of purine bases⁹, fluorophore functionalization of coding sequences¹⁰, colorimetric particle aggregation¹¹, immunoPCR¹², capillary electrophoresis¹³ and Raman or SERS¹⁴ technologies among others. Each of them provide different advantages and drawbacks, while microarray remains the best strategy for simultaneous detection of a large number of

sequences and is ideal for high-throughput analysis, conversely, fluorescence spectroscopy can allow time reduction and *in situ* detection.

The PCR-less *NP-based biobarcode assay* approach has been used for proteins¹⁵, DNA¹⁵, pathogens¹⁶, cells¹⁷ and miRNA¹⁸ detection, but their application to the detection and quantification of small molecules is scarce¹⁹. Thus, some attempts have pursued determination of small molecules such as dopamine²⁰ or norepinephrine¹⁴ using *biobarcode*s, either on a sandwich immunochemical format based on antibody competition²⁰ or either based on antigen competition²¹⁻²². However, both having one of the immunoreagents coated in a well-plate, limiting its applicability for multiplexed purposes. It has not been until very recently, that *NP-based biobarcode* formats, performed as described above, have been used for determination of small molecules. Hence, 17 β -estradiol *NP-based biobarcode* was the first assay reported using this format. A LOD of 6.37 fg mL⁻¹ was reached using an immunochemical format with two antibodies competing for the target analyte¹⁹, instead of employing a bioconjugate competitor as it is usual in the immunochemical field. A bioconjugate competitor immunochemical format for triazophos detection has been lately reported by the same authors but require real-time PCR²³, to reach a LOD of 0.02 ng mL⁻¹.

With this scenario, we report here for the first time a PCR-less *NP-based biobarcode* assay for acenocumarol (ACL), a frequently used oral anticoagulant (OA), using a bioconjugate competitor immunochemical format according to the scheme shown in (Figure 1). ACL is a vitamin K antagonist (VKAs) that belong to coumarin derivatives group as also does warfarin and phenprocoumon. Although new OAs have appeared, vitamin K antagonists are still used by millions of patients worldwide for the

primary and secondary prevention of venous and arterial thromboembolic events. They are highly efficient drugs, however, their complex pharmacokinetics and pharmacodynamics together with the remarkable variability in the dose-response relationship, as well as, their narrow therapeutic index determine a high risk of bleeding complications (up to 10-17% of the patients treated with these drugs²⁴) or recurrent thrombosis. Appropriate management of patients under VKAs treatment calls for efficient laboratory and clinical monitoring of these drugs. Chromatographic methods are the most frequently used tools for the detection of these drugs or their metabolites in plasma, but the main drawback is the need of sample pretreatment (either solid phase extraction, sample derivatization or sample clean-up)²⁵ which make them not suitable for routine pharmacokinetic and pharmacodynamics studies of many samples from each of the patients treated.

EXPERIMENTAL SECTION

Materials and Instruments: Polystyrene particles (PSP) were carboxy modified Dyed Microspheres (K1 050 noir) were supplied by Estapor[®] (Millipore Corp., Billerica, MA, USA). The magnetic particles (MP), Dynabeads MyOne Tosylactivated, and the magnetic rack Magnarack[™] were obtained from Invitrogen (Life technologies[™], Paisley, UK). The pre-cleaned plain slides were purchased from Corning[®] (Corning Inc., New York, NY, USA). Functionalized slides were spotted with a BioOdyssey Calligrapher MiniArrayer (Bio-Rad Laboratories, Inc. USA). Measurements were recorded on a ScanArray Gx PLUS (Perkin Elmer, USA) with a Cy3 optical filter with 5- μ m resolution. Slide gaskets were purchased from ArrayIt Corporation (Sunnyvale, CA, USA). U-bottom

polystyrene microplates were purchased from Nirco (Barberà del Vallès, Spain). IKA[®] MS 3 basic shaker with a MS 3.4 Microtiter attachment (IKA[®], Staufen, Germany) was used to shake the microplates at 800 rpm. A thermos-shaker (TS-100C Biosan, Riga, Latvia) was used to shake Eppendorfs. Eppendorfs were centrifuged with a Legend Micro 21, 10 min, 17500G (Thermo Fisher Scientific Inc.) and plates were centrifuged with a Centrifuge 5810 R, 10 min, 3220 G (Eppendorf, Hamburg, Germany). The pH and the conductivity of all buffers and solutions were measured with a 540 GLP pH meter and an LF 340 conductimeter (WTW, Weilheim, Germany), respectively. Absorbance and fluorescence were read on a Spectramax Plus and a Spextramax Gemini XPS (Molecular Devices, Sunnyvale, CA, USA), respectively. Microscope images were recorded with a Cytoviva (Auburn, AL, USA) coupled to an Olympus VX43 with a 100X Dage objective and software used was Exponent7 Dage MTI XL16 45.

Chemicals and biochemicals. The chemical reagents used were obtained from Aldrich Chemical Co. (Milwaukee, WI, USA) and from Sigma Chemical Co. (St. Louis, MO, USA). N2down-NH₂ oligonucleotide sequence, [AmC6F]CGGAGGTACATTCGACTTGA, was purchased from Sigma Chemical Co. (St. Louis, MO, USA) and TAMRA-N2up-SS-NH₂, [TAMRA]TCAAGTCGAATGTACCTCCG5[ThiolC6SS][AminolinkC6], was obtained from Biomers (GmbH, Ulm, Germany). The immunoreagents used for ACL detection (Protein A purified antibody pAb236 and antigen hACL-BSA) were developed in our laboratory and their preparation and characterization will be described elsewhere. The ACL stock solution was prepared at 10 mM in DMSO and stored at 4°C.

Clinical Samples: The serum samples (Human Serum, Normal, S1-100) used were obtained from EMD Millipore (Millipore Corp., Billerica, MA, USA) and consisted on a pool of sera from healthy normal humans. Normal human plasma was obtained from a pull of non-treated patients.

General procedures: On the scanner measurements, the laser power and PMT were set to 90% and 60%, respectively. The spots were measured by F543_Mean-B543 (Mean Cy3 foreground intensity minus mean Cy3 background intensity). Fluorescence intensity values were expressed normalized or in relative units as average and standard deviation of five replicate wells. The competitive curves were analyzed with a four-parameter logistic equation using software (GraphPad Prism version 5.03 for Windows, GraphPad Software, San Diego, California, USA). The standard curve was fitted to a four-parameter equation according to the following formula: $Y = [(A - B) / (1 + (x/C)^D)] + B$, where A is the maximal fluorescence, B the minimum fluorescence, C the concentration producing 50% of the difference between A and B (or IC₅₀), and D the slope at the inflection point of the sigmoid curve. The limit of detection (LOD) was defined as the concentration producing 90% of the maximal fluorescence (IC₉₀), and working range was defined as the concentration producing 20% to 80% of the maximal fluorescence (IC₂₀-IC₈₀). All the incubation steps performed on the U-bottomed microplates were performed at 25 °C and 800 rpm using the microtiter shaker.

Buffers. PBS was 0.01 M phosphate buffer in a 0.8% saline solution (137 mmol L⁻¹ NaCl, 2.7 mmol L⁻¹ KCl), and the pH was 7.5. PBST was PBS with 0.05% Tween 20. PSPs coupling buffer was 100 mM carbonate buffer pH 9. MP A buffer was 0.1 M borate buffer (pH 9.5). MP C buffer was 3 M ammonium sulphate in MP A buffer (pH 9.5). MP blocking buffer was

PBST with 0.5 % BSA. MP storage buffer was PBST with 0.1 % BSA. Printing buffer comprised 150 mM sodium phosphate and 0.01 % sodium dodecyl sulphate (SDS) and the pH was 8.5. Hybridization buffer was 10 mM TRIS, 1 mM EDTA, 1M NaCl and the pH was 7.2.

Microarray printing. Slides were cleaned by immersing them in piranha solution ($\text{H}_2\text{SO}_4:\text{H}_2\text{O}_2$ 7:3) during 30 min; washed with purified water and immersed in NaOH 10 % during 30 min; washed with water and ethanol and dried. Activation of the slides was performed by immersing them on (3-glycidoxypropyl)methyldiethoxysilane during 30 min. Afterwards, slides were washed with ethanol and dried. These epoxidized slides can be stored in the dessicator for long periods of time. Finally, the oligonucleotide ($\text{N}2_{\text{down}}\text{-NH}_2$, 200 ng mL⁻¹ in printing buffer) was spotted onto substrates in a high-humidity chamber, maintained for 30 min at room temperature and finally stored overnight at 4°C. Each glass slide was printed with 24 (8 x 3) microarrays. A 5 x 1 spot matrix was printed on each grid (five spots replicated).

Encoded polystyrene probes (ePSP) functionalization. Polystyrene particles (PSPs, 10% w/v solution, 40 μL) were washed twice with PSPs coupling buffer (500 μL) and subsequently, a solution of a combination of oligonucleotide probes (TAMRA- $\text{N}2_{\text{up}}\text{-SS-NH}_2$, 0.13 μM) and ACL antigen (hACL-BSA bioconjugate) at different molar ratios (TAMRA- $\text{N}2_{\text{up}}\text{-SS-NH}_2$:hACL-BSA, 1:0, 1:2, 2:2 or 4:2, hACL-BSA, 320 μL in PSPs coupling buffer) followed by a solution of EDC (500 mM, 80 μL in PSPs coupling buffer) were added and the mixture allowed to react at 25 °C for 3 h under shaking (750 rpm). Afterwards, the supernatant was removed and the efficiency of the coupling reaction was checked by analyzing the remaining hACL-BSA bioconjugate and the oligonucleotide probes by

ELISA and by fluorescence (543 nm excitation, 575 nm emission), respectively. A conjugation yield of 20 % of hACL-BSA and 70 % of TAMRA-N2up-SS-NH₂ was obtained. The suspension was then washed twice with PBST and stored in 400 μ L of PBS at 4°C for at least 1 month.

Oligonucleotide release. ePSPs stock solution (25 μ L) was treated with 0.2 M DTT (100 μ L, hybridation buffer) and allowed to react for 1 h using the shaker (750 rpm). The suspension was then centrifuged and the supernatant used to quantify the fluorescence released as described above. A release yield of 50 % was obtained under these conditions.

Magnetic particles (MP) functionalization. ACL specific (pAb236) and nonspecific (pAbPRE, from preimmune sera) antibodies were covalently coupled to magnetic particles (MP) following the manufacturer supplier procedure with slight modifications. Briefly, Dynabeads MyOne Tosylactivated (100 mg mL⁻¹, 200 μ L) were washed with MP A buffer (3 x 300 μ L) and a solution of pAb236 (400 μ L, 2 mg mL⁻¹ in MP A buffer) was added followed by MP C buffer (200 μ L). The mixture was allowed to react protected from light overnight at 37°C under shaking 750 rpm. The day after, the supernatant was removed and analyzed by the Bradford protein test to estimate the efficiency of the coupling. A conjugation yield of 80 % was obtained. Next, the biofunctionalized particles were resuspended in MP blocking buffer and allowed to stand overnight again, before the supernatant was removed and particles were washed with of MP storage buffer (1000 μ Lx 2) and finally resuspended in 1000 μ L for storage at 4°C for at least 2 months. Specific particles were named pAb236-MP and unspecific particles, pAbPRE-MP, were named NEG-MP.

Two-dimensional Checkerboard Titration Experiments (2D-assay). The binding of serial dilutions of the pAb236-MP suspension (from 0 to 2

mg mL⁻¹) against different dilutions of the ePSP (from 0.0038 to 0.1 %) were evaluated incubating their mixtures for half an hour. Afterwards, the microplates were washed (4 x 200 µL, PBST), a solution of 0.2 M DTT (in hybridization buffer, 100 µL/well) was added and the mixtures allowed to react for 1 h at RT under shaking (800 rpm). The microplates were then centrifuged and supernatant, with the released oligonucleotide probes, transferred to a previously washed (4 x 200 µL) DNA microarray slide and allowed to hybridize for 30 min at RT (500 rpm). Then slide was washed once more (4 x 200 µL) with PBST and one last time with milliQ water (200 µL) without the gasket. From these experiments, optimum concentrations for both particles were chosen.

Non-competitive NP-based biobarcode assay. The screening of the avidity of the pAb236, immobilized on the MP, for the encoded probes was evaluated by incubating the pAb236-MP and the NEG-MP (2.5 mg mL⁻¹ in PBST) with ePSP 1:0 and 1:2 (0.05 % w/v in PBST). Subsequently, the biocomplexes formed were processed as described above on the 2D-assay for measuring the released oligonucleotide probes on the DNA microarray.

Competitive NP-based biobarcode assay. Before starting, both the pAb236-MP and the ePSPs were washed with PBST (2 x 10 times its volume). The standards (ACL, 2000 to 0 nM in PBST, 50 µL) or the samples (diluted in the same buffer) were mixed with the pAb236-MP (25 µL, 0.25 mg mL⁻¹ in PBST) and the ePSPs (25 µL, 0.008 % w/v in PBST) and incubated. Subsequently, the biocomplexes formed were processed as described above on the 2D-assay for measuring the released oligonucleotide probes on the DNA microarray.

Matrix effect studies. Non-specific interferences produced by the plasma and serum were assessed by preparing calibration curves at different matrix dilutions (1, 1/2, 1/4, 1/8, 1/16 and 0).

Recovery studies. The recovery of the analyte concentration was assessed with samples prepared by spiking blank plasma or serum samples at 6 different concentrations of ACL (from 0 to 200 nM) and analyzed them five times on different days. The ACL concentration in the samples was calculated by interpolating the fluorescent signal recorded on a calibration curve processed in the same way as the samples. The results were fitted to a linear regression curve between the spiked and the measured concentration values.

RESULTS AND DISCUSSION

Biofunctionalized ePSPs. Carboxy-PSPs were used instead of the usually employed gold nanoparticles^{5,8} for their bigger particle size that could allow higher oligonucleotide loading, and thus a larger amplification factor¹⁰. The sequences of the N2 oligonucleotides used in this study were previously designed to have near 50% content of GC, which ensures a stable hybridization with the complementary oligonucleotide sequences of the DNA microarray²⁶. Carboxy-PSPs were biofunctionalized with hACL-BSA, the bioconjugate competitor used for the competitive immunochemical assay, and codified with the oligonucleotide TAMRA-N2up-SS-NH₂. This oligonucleotide was provided of a fluorophore (5-(and-6)-carboxytetramethylrhodamine, TAMRA) at the 5'-end for signal generation on the DNA microarray¹⁰, a disulfide bond next to the 3'-end to allow release from the particle by ligand exchange with DTT and an amino group at the 3'-end for its covalent attachment to the carboxy modified

PSPs. Both, the bioconjugate competitor and the oligonucleotide probe were linked to the carboxy-PSPs forming an amide bond using EDC. Encoded probes showing increasing oligonucleotide loads (600, 1400 and 3100 strands per ePSP) were prepared by employing distinct hACL-BSA:TAMRA-N2*up*-SS-NH₂ molar ratios (1:2, 2:2 and 4:2, respectively) at a constant hACL-BSA ratio of 800 molecules per ePSP. In the same manner, a negative encoded probe (NEG-ePSP) was also prepared lacking the bioconjugated competitor. Regardless of the antigen or oligonucleotide concentrations used the ePSPs biofunctionalization yield remained constant at 20% and 70%, respectively.

Biofunctionalized MPs. The beads were functionalized with pAb236 through a SN2 reaction of the amino groups of the antibody molecule and the tosyl groups of the magnetic beads. In the same way, nonspecific polyclonal antibodies obtained from pre-immune serum were used to prepare negative MPs (NEG-MP) for specificity studies. A conjugation yield around 80% was obtained in all cases.

Fluorescent DNA-microarray. Microarrays were manufactured on epoxy-silyanized glass slides by covalently attaching the oligonucleotide N2*down*-NH₂ through its amino group in the 5'-end. This oligonucleotide had the exactly complementary sequence to the TAMRA-N2*up*-SS-NH₂ used to codify the probes. The assay showed a LOD of 6 pM in terms of TAMRA-N2*up*-SS-NH₂, which was found to be very good for our purposes.

Signal amplification. One of the major challenges in multiplexing *in vitro* diagnostics is to be able to analyze in a single run substances that are present in a particular sample at very different concentration ranges. The principle behind biobarcode allows envisaging the possibility to modulate signal amplification. With this purpose, ePSPs with increasing oligonucleotide

loads (600, 1400 and 3100 oligo/ePSP) and the same load of bioconjugate competitor were prepared, characterized and used to run biobarcode assays. Suitable concentration of encoded probes and biofunctionalized magnetic beads were established through 2D assays as described in the experimental section (see figure S1 in the Supporting Information document). As it can be observed in Figure 2.A, using the same concentration of particles the signal is significantly amplified from around 20000 RFUs (600-ePSP) to 51000 RFUS (3100-ePSP). Moreover, the IC_{50} remained very similar on the three biobarcode assays (IC_{50} values between 75 and 96 nM, see Table 1 (assays I, II and III)). However, by adjusting on each case the concentration of particles after running 2D-assays and selecting more suitable conditions for a maximum signal of around 20000 RFUs, the detectability could be improved to an IC_{50} of 18.6 ± 1.1 nM, see Table 1 (assays IV and V), pointing to the possibility of increasing even more the assay detectability by raising the amount of loaded oligonucleotide strands (see figure 2.B). Even though we functionalized particles with only 600, 1400 and 3100 oligo/ePSP, Wang et al.⁹ accomplished to detect IgG molecules at 13 fM (2 pg mL^{-1} in $50 \text{ }\mu\text{L}$ volume) using 500 nm ePSPs loaded with 75000 dG₂₅ oligonucleotides, proving that ePSPs loading could be further increased achieving increased sensitivity.

Specificity of the biobarcode. The specificity of the binding interaction was assessed by carrying out parallel assays with particles that did not contain the specific immunoreagents for ACL detection. For this purpose, NEG-MP and NEG-ePSP were used on an assay in which they had to interact with the corresponding specific counter particles. As it can be seen in Figure 3 the results showed that the binding interaction is specific, and that none unspecific adsorptions are observed between the biofunctionalizaed

particles. Thus, the signal was close to zero when the MPs or the ePSPs lacked the specific pAb236 antibody and the hACL-BSA, respectively.

Biobarcode particle complexes. Formation of the ePSP-MP complexes could be assessed by microscopy being possible to observe the formation of the particle complexes, mainly formed by 3 ePSPs per each MP (see Figure 4.A).

NP-based Biobarcode assay. Under the final conditions (2.5 mg mL⁻¹ concentration of pAb236-MPs and a 0.008% (w/v) of 1400-ePSPs) an IC₅₀ of 17.5 ± 0.2 nM and a LOD of 0.96 ± 0.26 (n = 3) were obtained, which are values lower than the usual concentrations found in plasma or serum samples from OA treated patients (30-300 nM)²⁷. Figure 4.B and Table 1 (Assay VI) shows the calibration curve obtained and the assay features. Assay reported a high interday reproducibility with a %CV of 1.1 (n = 4).

Implementation of the biobarcode assay for ACL to the analysis of clinical samples. On a first instance the potential nonspecific interferences of plasma and serum samples in the biobarcode assay were assessed by running calibration curves in these samples. Although a slight decrease of the signal was observed, this undesirable effect disappears after a just four times dilution of the samples with the assay buffer being able to obtain calibration curves with very similar immunoassay features to those recorded in buffer (see Figure 5.A and Table 2). Thus, the working range of the ACL biobarcode assay run in plasma was 12.8 to 228.4 nM (taking into account the dilution with the buffer) in the same range that the ACL concentrations reported in plasma samples obtained from treated patients (30 to 300 nM²⁷), which points to the possibility to directly analyze plasma samples without the need of clean-up or preconcentration steps. Furthermore, only 12.5 µL of sample were required to carry out the assay. These results and the LOD

accomplished in four-times diluted plasma (3.84 ± 1.04 nM) is comparable to the microplate-based ELISA using the same immunoreagents.

Finally, accuracy studies were performed by measuring ACL spiked plasma and serum samples. As it can be observed in Figure 5.B, the results obtained were very good. In both types of samples the measured results match very well the concentrations spiked, as it is demonstrated by the slope values of the linear regressions that were 0.97 in serum and 1.04 in plasma, near of the ideal correlation ($X=Y$, slope= 1) with acceptable regression coefficients.

CONCLUSIONS

A NP-based biobarcode coupled to fluorescent DNA-microarray has been developed for ACL based on a classical immobilized bioconjugate competitor immunochemical format, able to quantify this OA within the concentration range usually found in the plasma of treated patients. Thus, the LOD (3.84 ± 1.04 nM) is below the usual ACL concentrations reported on plasma from treated patients (30-300 nM) which fit within the linear range of the assay. The ACL biobarcode assay reported here was found to be reproducible and robust, as it is demonstrated by the low variability of the analytical parameters of the calibration curve (%CV 1.1, interday for the IC_{50} value). Moreover, complex biological samples such as serum or plasma can be directly measured without additional sample treatments with a very good accuracy. Thus, linear regression studies performed with spiked serum samples show a slope of 0.97 with a R^2 of 0.91. Furthermore, with this NP-based biobarcode assay we have demonstrated that the signal can be amplified and the working range modulated by modifying the oligonucleotide load of oligonucleotide probes. The results point to the

possibility to face one of the most important diagnostic challenges of the multiplexed analysis, which is the possibility to measure in a single run biomarker targets present at different concentration ranges.

ASSOCIATED CONTENT

Additional information as noted in text. The Supporting Information is available free of charge on the ACS Publications website at DOI:

AUTHOR INFORMATION

Corresponding Author

#To whom correspondence should be addressed. Phone: 934006100 (Ext. 5117). Fax: 932045904. E-mail: roger.galve@iqac.csic.es

ACKNOWLEDGMENT

This work has been funded by the ministry of Economy and Competitiveness (MAT2012-38573-C02-01). The Nb4D group (formerly Applied Molecular Receptors group, AMRg) is a consolidated research group (Grup de Recerca) of the Generalitat de Catalunya and has support from the Departament d'Universitats, Recerca i Societat de la Informació de la Generalitat de Catalunya (expedient : 2014 SGR 1484). CIBER-BBN is an initiative funded by the Spanish National Plan for Scientific and Technical Research and Innovation 2013-2016, Iniciativa Ingenio 2010, Consolider Program, CIBER Actions are financed by the Instituto de Salud Carlos III with assistance from the European Regional Development Fund. Marta Broto wishes to thank the FPI-fellowship (BES-2013-062819) from the Spanish Ministry of Economy and Competitiveness. The ICTS “NANOBIOSIS”, and particularly the Custom Antibody Service (CAbS,

IQAC-CSIC, CIBER-BBN), is acknowledged for the assistance and support related to the immunoreagents used in this work.

REFERENCES

1. Condon, A., Designed DNA molecules: principles and applications of molecular nanotechnology. *Nat Rev Genet* **2006**, *7* (7), 565-575.
2. Noel, V.; Piro, B.; Reisberg, S., DNA for Non-nucleic Acid Sensing. In *RNA and DNA Diagnostics*, Erdmann, V. A.; Jurga, S.; Barciszewski, J., Eds. Springer International Publishing: 2015; pp 81-106.
3. Sano, T.; Smith, C. L.; Cantor, C. R., Immuno-PCR very sensitive antigen-detection by means of specific antibody-dna conjugates. *Science* **1992**, *258* (5079), 120-122.
4. Nam, J.-M.; Park, S.-J.; Mirkin, C. A., Bio-Barcodes Based on Oligonucleotide-Modified Nanoparticles. *Journal of the American Chemical Society* **2002**, *124* (15), 3820-3821.
5. Nam, J.-M.; Stoeva, S. I.; Mirkin, C. A., Bio-Bar-Code-Based DNA Detection with PCR-like Sensitivity. *Journal of the American Chemical Society* **2004**, *126* (19), 5932-5933.
6. Stoeva, S. I.; Lee, J.-S.; Smith, J. E.; Rosen, S. T.; Mirkin, C. A., Multiplexed Detection of Protein Cancer Markers with Biobarcode Nanoparticle Probes. *Journal of the American Chemical Society* **2006**, *128* (26), 8378-8379.
7. Stoeva, S. I.; Lee, J.-S.; Thaxton, C. S.; Mirkin, C. A., Multiplexed DNA Detection with Biobarcode Nanoparticle Probes. *Angewandte Chemie International Edition* **2006**, *45* (20), 3303-3306.
8. Nam, J.-M.; Thaxton, C. S.; Mirkin, C. A., Nanoparticle-Based Bio-Bar Codes for the Ultrasensitive Detection of Proteins. *Science* **2003**, *301* (5641), 1884-1886.
9. Wang, J.; Liu, G.; Munge, B.; Lin, L.; Zhu, Q., DNA-Based Amplified Bioelectronic Detection and Coding of Proteins. *Angewandte Chemie International Edition* **2004**, *43* (16), 2158-2161.
10. Oh, B.-K.; Nam, J.-M.; Lee, S. W.; Mirkin, C. A., A Fluorophore-Based Bio-Barcode Amplification Assay for Proteins. *Small* **2006**, *2* (1), 103-108.
11. Nam, J.-M.; Wise, A. R.; Groves, J. T., Colorimetric Bio-Barcode Amplification Assay for Cytokines. *Analytical Chemistry* **2005**, *77* (21), 6985-6988.

12. Perez, J. W.; Vargis, E. A.; Russ, P. K.; Haselton, F. R.; Wright, D. W., Detection of respiratory syncytial virus using nanoparticle amplified immuno-polymerase chain reaction. *Analytical Biochemistry* **2011**, *410* (1), 141-148.
13. Jung, J. H.; Kim, G.-Y.; Seo, T. S., An integrated passive micromixer-magnetic separation-capillary electrophoresis microdevice for rapid and multiplex pathogen detection at the single-cell level. *Lab on a Chip* **2011**, *11* (20), 3465-3470.
14. An, J. H.; Lee, K. J.; Choi, J. W., Gold Nanoparticles-Based Barcode Analysis for Detection of Norepinephrine. *J. Biomed. Nanotechnol.* **2016**, *12* (2), 357-365.
15. Hill Haley, D.; Mirkin Chad, A., The bio-barcode assay for the detection of protein and nucleic acid targets using DTT-induced ligand exchange. *Nature Protocols* **2006**, *1* (1), 324-336.
16. Cho, M.; Chung, S.; Jung, J. H.; Rhie, G.-e.; Jeon, J. H.; Seo, T. S., Combination of biobarcode assay with on-chip capillary electrophoresis for ultrasensitive and multiplex biological agent detection. *Biosensors and Bioelectronics* **2014**, *61* (0), 172-176.
17. Chung, S.; Cho, M.; Hwan Jung, J.; Seok Seo, T., Highly sensitive detection of cancer cells based on the DNA barcode assay and microcapillary electrophoretic analysis. *ELECTROPHORESIS* **2014**, *35* (10), 1504-1508.
18. Lee, H.; Park, J.-E.; Nam, J.-M., Bio-barcode gel assay for microRNA. *Nat Commun* **2014**, *5*.
19. Du, L.; Ji, W.; Zhang, Y.; Zhang, C.; Liu, G.; Wang, S., An ultrasensitive detection of 17[small beta]-estradiol using a gold nanoparticle-based fluorescence immunoassay. *Analyst* **2015**, *140* (6), 2001-2007.
20. An, J. H.; Choi, D.-K.; Lee, K.-J.; Choi, J.-W., Surface-enhanced Raman spectroscopy detection of dopamine by DNA Targeting amplification assay in Parkisons's model. *Biosensors and Bioelectronics* **2015**, *67*, 739-746.
21. Tang, Y.; Wang, H.; Xiang, J.; Chen, Y.; He, W.; Deng, N.; Yang, H., A sensitive immunosorbent bio-barcode assay combining PCR with icELISA for detection of gonyautoxin 2/3. *Analytica Chimica Acta* **2010**, *657* (2), 210-214.
22. Tang, Y.; Yan, L.; Xiang, J.-j.; Wang, W.-z.; Yang, H.-y., An immunoassay based on bio-barcode method for quantitative detection of semicarbazide. *Eur Food Res Technol* **2011**, *232* (6), 963-969.
23. Du, P.; Jin, M.; Chen, G.; Zhang, C.; Jiang, Z.; Zhang, Y.; Zou, P.; She, Y.; Jin, F.; Shao, H.; Wang, S.; Zheng, L.; Wang, J., A Competitive

Bio-Barcode Amplification Immunoassay for Small Molecules Based on Nanoparticles. *Scientific Reports* **2016**, *6*, 38114.

24. Stehle, S.; Kirchheiner, J.; Lazar, A.; Fuhr, U., Pharmacogenetics of oral anticoagulants: a basis for dose individualization. *Clin*

Pharmacokinet **2008**, *47* (9), 565-94.

25. Vecchione, G.; Casetta, B.; Tomaiuolo, M.; Grandone, E.; Margaglione, M., A rapid method for the quantification of the enantiomers of Warfarin, Phenprocoumon and Acenocoumarol by two-dimensional-enantioselective liquid chromatography/electrospray tandem mass spectrometry. *Journal of Chromatography B-Analytical Technologies in the Biomedical and Life Sciences* **2007**, *850* (1-2), 507-514.

26. Tort, N.; Salvador, J. P.; Marco, M. P.; Eritja, R.; Poch, M.; Martínez, E.; Samitier, J., Fluorescence site-encoded DNA addressable hapten microarray for anabolic androgenic steroids. *TrAC Trends in Analytical Chemistry* **2009**, *28* (6), 718-728.

27. Ufer, M., Comparative pharmacokinetics of vitamin K antagonists: warfarin, phenprocoumon and acenocoumarol. *Clin Pharmacokinet* **2005**, *44* (12), 1227-46.

FIGURES

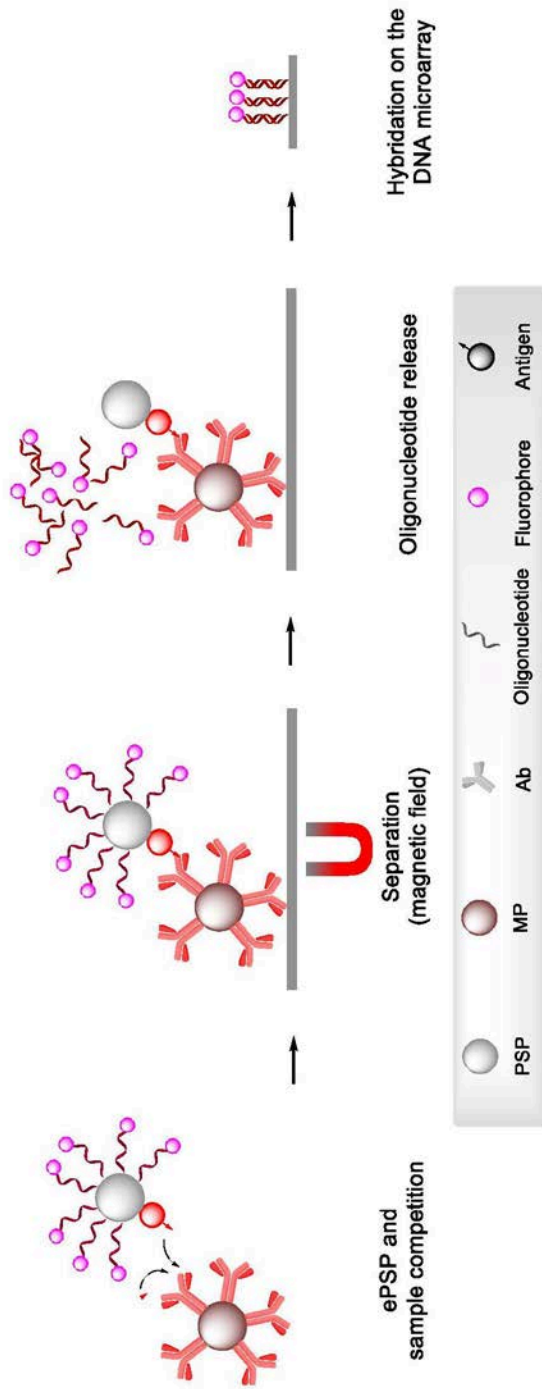
Figure 1. Schematic diagram of the NP-based biobarcode strategy used in this study.

Figure 2. A. Graph showing how the signal can be amplified by increasing the oligonucleotide load of the ePSPs. Particles with three oligonucleotide loads (600, 1400 and 3100) and a fixed load of hACL-BSA bioconjugate competitor were prepared, characterized and used to run the biobarcode assays for ACL using the same conditions. The graph shows the calibration curves of these three assays where it can be observed that the signal is proportional to the oligonucleotide load and the parameters resulting from the adjust using the four-parameter logistic equation are shown in Table 1 (Assay I, II and III). The % CV at the middle point of the assay is 1.6. **B.** Graph showing how the detectability can be modulated by adjusting the concentration values of the biofunctionalized encoded probes and magnetic beads. An increase of almost 4 times has been accomplished by using the 1400-ePSP, instead of the 600-ePSP, accomplishing the same signal (~20000 RFUs). Parameters of the equation are shown in Table I (Assay IV and V).

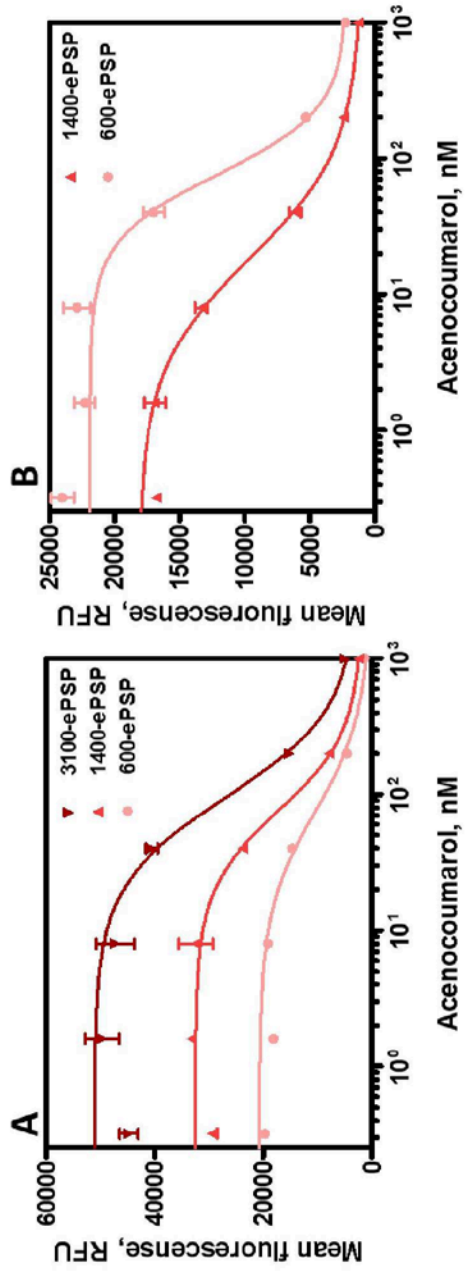
Figure 3. Bar graph showing the lack of non-specific binding between the particles employed in the assay. Encoded particles with (ePSP) and without (NEG-ePSP) the bioconjugate competitor of the ACL immunochemical assay were mixed with the pAb236-MPs and the NEG-MPs. Only in the assay that used the specific biofunctionalized particles provided a significant signal. For the rest of the assays, the signal recorded was negligible.

Figure 4. A. Images obtained with the Cytoviva (100X) microscope showing formation of the ePSP-MP complexes. (i) Image of the ePSPs (500 nm size). (ii) Image of the MP (1 μm size). (iii) Image of the ePSP-MP complex formed by 3 ePSPs and 1 MP. **B.** Calibration curve of the biobarcode assay of ACL run in buffer. The data presented correspond to the average of three assays performed three different days. On every assay, each calibration point was measured five times. A LOD of 0.96 nM was accomplished. The %CV at the middle point of the assay is 1.1.

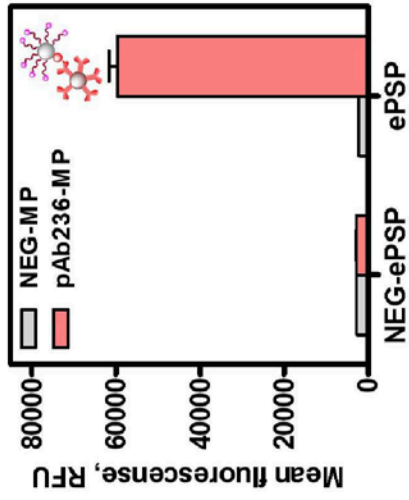
Figure 5. A. Calibration curves of the biobarcode assays run in buffer, serum and plasma. Clinical samples were diluted 4 times with the assay buffer before running the assay. **B.** Results from the accuracy study performed using blind samples prepared by spiking plasma and serum. The graph shows the correlation between the spiked and measured concentration values. The dotted line corresponds to a perfect correlation ($m=1$). The samples, diluted $\frac{1}{4}$ in buffer, were quantified using calibration curves prepared in buffer. The data correspond to the average of at least four different days. The % CV at the middle point of the assay is 12% for serum and 18% for plasma.



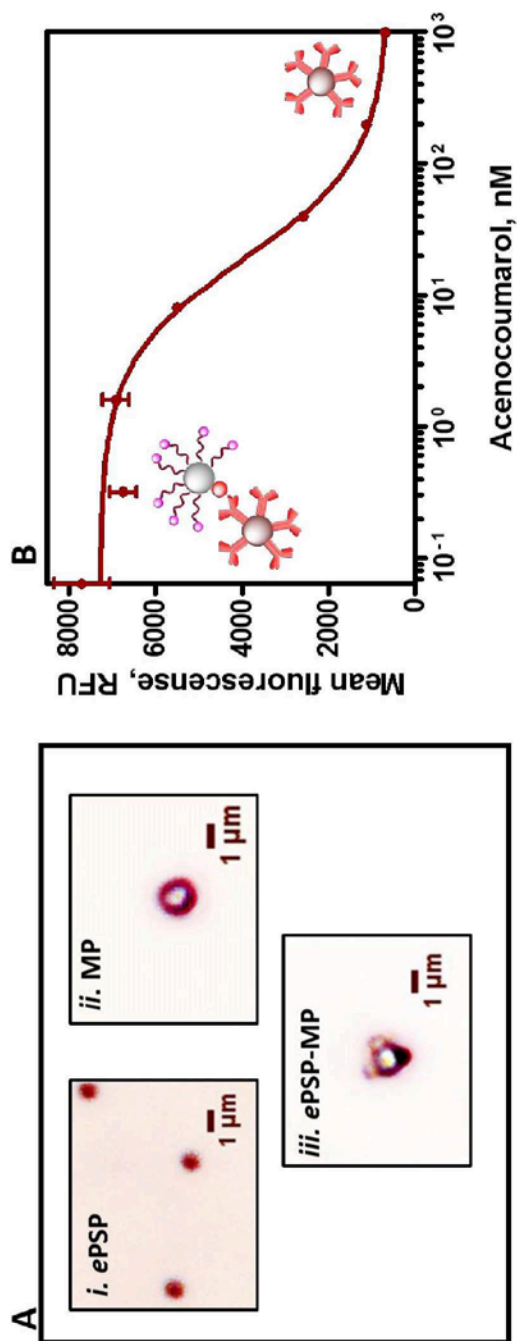
Broto *et al.*, Figure 1

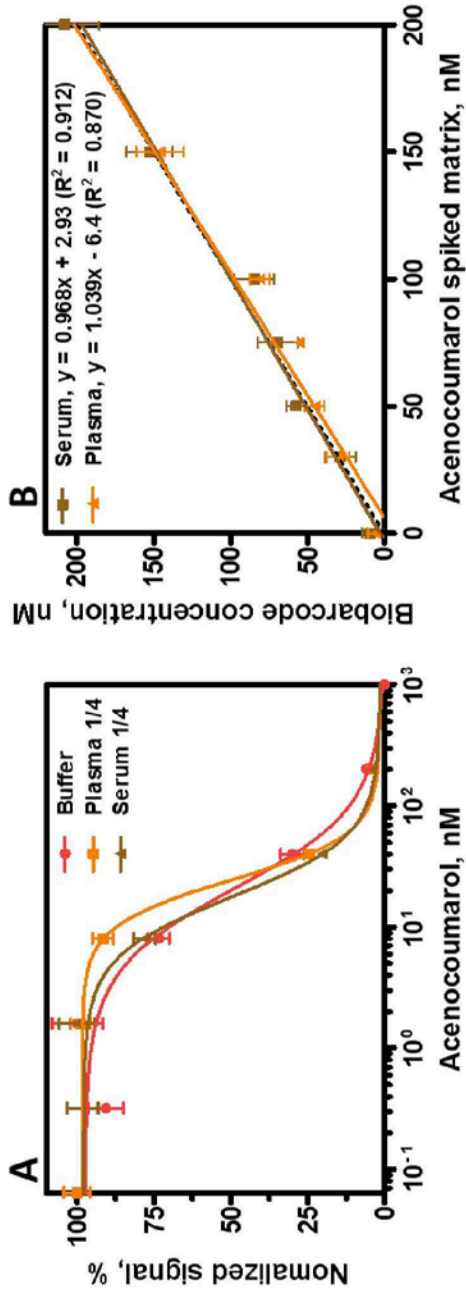


Broto *et al.*, Figure 2



Broto *et al.*, Figure 3

Broto *et al.*, Figure 4



Broto et al. Figure 5

Table 1. ACL biobarcode assay parameters run with ePSP

Assays	I ^a	II ^a	III ^a	IV ^a	V ^a	VI ^b
DNA/ePSP	600	1400	3100	600	1400	1400
% ePSPs	0.0125	0.0125	0.0125	0.02	0.008	0.008
mg/mL MP	0.5	0.5	0.5	0.5	0.25	0.25
RFU_{min}	226 ± 142.3	1841 ± 1864	2584 ± 4183	2199 ± 1200	1047 ± 539	624 ± 317
RFU_{max}	20724 ± 461	32558 ± 692	51100 ± 1339	21899 ± 546	18135 ± 380	7299 ± 186
m	-1.19 ± 0.24	-1.50 ± 0.30	-1.33 ± 0.33	-1.81 ± 0.40	-1.05 ± 0.13	-1.03 ± 0.10
R²	0.94	0.93	0.90	0.93	0.97	0.947 ± 0.027
IC₅₀, nM	75.2 ± 1.2	76.5 ± 1.2	95.9 ± 1.3	76.5 ± 1.2	18.6 ± 1.1	17.5 ± 0.2
IC₂₀, nM	167.0	176.9	195.0	152.2	60.6	57.1 ± 4.5
IC₈₀, nM	8.5	25.6	5.9	24.6	3.6	3.28 ± 0.81

The data has been extracted from the four-parameter equation used to fit the standard curves. The IC₂₀ and IC₈₀ values have been used to define the working range of the assay. ^aData shows the average a standard deviation of the parameters of assays using 5 replicates for each concentration of ACL standard measured. ^bData shown is the average of assays run on 3 different days. On each day, the assay was run using 5 replicates for each ACL concentration. All ePSP had the same amount of antigen, 800 molecules per ePSP.

Table 2. Acenocumarol biobarcode assay parameters when run in clinical samples

	Buffer	Plasma 1/4*	Serum 1/4*
RFU_{min}	364.5	1383	1295
RFU_{max}	11537	12646	13513
m	-1.28	-1.75	-1.50
R²	0.97	0.97	0.95
IC₅₀, nM	22.3	17.8	15.6

The data has been extracted from the four-parameter equation used to fit the standard curves. It shows the average and standard deviation of the parameters of assays using 5 replicates for each concentration of ACL standard measured. *Final IC₅₀ values should be multiplied by four since samples are diluted in a 1/4 factor.

Biobarcode Assay for the Oral Anticoagulant Acenocoumarol

SUPPORTING INFORMATION

Marta Broto^{1,2}, J.-Pablo Salvador^{1,2}, Roger Galve^{1,2,*} and M.-Pilar Marco^{1,2}

¹*Nanobiotechnology for Diagnostics (Nb4D), Institute for Advanced Chemistry of Catalonia of the Spanish Council for Scientific Research (IQAC-CSIC).* ²*CIBER de Bioingeniería, Biomateriales y Nanomedicina (CIBER-BBN). Jordi Girona 18-26, 08034-Barcelona, Spain*

*To whom correspondence should be sent:

Roger Galve

IQAC-CSIC

Jordi Girona, 18-26

08034-Barcelona, Spain

Phone: 93 4006180

FAX: 93 2045904

E-mail: roger.galve@cid.csic.es

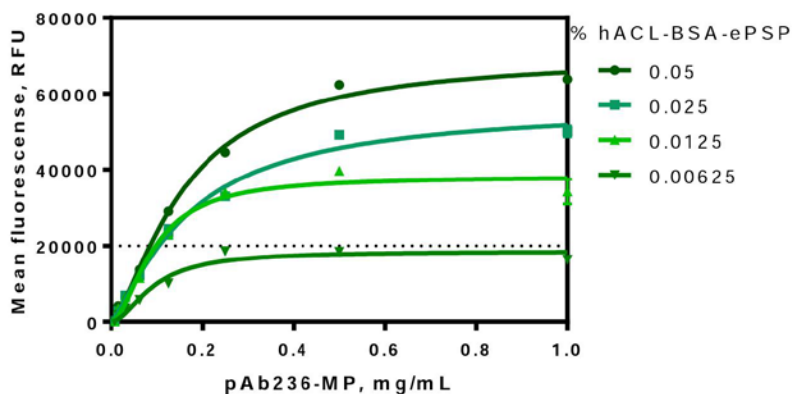


Figure S1 Graph showing the results of the two-dimensional checkerboard titration experiments for the NP-based biobarcode assay using biofunctionalized *e*PSPs and MPs. A saturation of the concentration of pAb236-MPs was observed at at 0.25 mg ml^{-1} . The concentration of hACL-BSA-*e*PSPs was selected according the fluorescence desired.

4.4.2 PUBLICATION IV: SANDWICH NP-BASED BIOBARCODE ASSAY FOR QUANTIFICATION C-REACTIVE PROTEIN IN PLASMA SAMPLES

**Sandwich NP-based Biobarcode Assay for quantification C-reactive Protein
in Plasma Samples**

Marta Broto, Roger Galve and M.-Pilar Marco

Submitted

This publication describes the development of a biobarcode assay in sandwich format for C-reactive protein. This publication focuses on assay development and assay validation for plasma samples. Furthermore, assay has been used for real sample analysis and compared with a reference methodology with successful results.

**Sandwich NP-based Biobarcode Assay for quantification
C-reactive Protein in Plasma Samples**

Marta Broto^{1,2}, Roger Galve^{1,2, *}, M.-Pilar Marco^{1,2}.

¹Nanobiotechnology for diagnostics (Nb4D), Department of Chemical and Biomolecular Nanotechnology, Institute for Advanced Chemistry of Catalonia (IQAC) of the Spanish Council for Scientific Research (CSIC).

²CIBER de Bioingeniería, Biomateriales y Nanomedicina (CIBER-BBN),
Jordi Girona 18-26, 08034 Barcelona, Spain

Abstract

A *NP-based biobarcode* for C-reactive protein (CRP) quantification in plasma samples is reported for the first time. The assay uses capture antibody functionalized magnetic beads (pAbCRP2-MP), multifunctional oligonucleotide encoded probes modified with a detection antibody (pAbCRP1-ePSP), and a fluorescent DNA microarray. Thus, magnetic beads are added to the sample to form immunocomplexes that will be isolated, to then add the codified particles to form a sandwich complex with both particles and the target protein, subsequently the complexes are treated to release the oligonucleotide codes, which are finally hybridized in a fluorescent DNA microarray. The assay has been implemented to the analysis of plasma samples being able to quantify this biomarker within 900 ng mL^{-1} to 12500 ng mL^{-1} with an excellent accuracy (mean of recovery of $99.5 \pm 4.2\%$, $N = 3$). The *CRP biobarcode* has been used on a small pilot clinical study in which plasma samples from patients suffering different pathologies, most of them related to cardiovascular diseases (CVDs), have been analyzed and the results compared to a reference method demonstrating that the assay developed can be useful for monitoring this biomarker on patients being suspicious to be under risk to suffer CVDs or other diseases involving inflammatory processes.

Keywords

NP-based biobarcode, sandwich immunoassay, C-reactive protein, CRP, antibody, biomarker, cardiovascular diseases, plasma sample

1 Introduction

C-reactive protein (CRP) is an annular homopentameric protein that participates in the systemic response to inflammation, it is mainly synthesized in the liver in response to factors released by macrophages and T cells, subsequently it deposits onto inflamed tissue and breaks into biologically active monomeric subunits (mCRP), to which have been attributed a range of proinflammatory effects[1]. Between other diseases, high levels of CRP in blood may be related to an inflammation of the arteries of the heart, indicating risk to suffer a heart attack. Because of the high prevalence of cardiovascular diseases (CVDs) in developed countries, routine measurement of CRP levels is being contemplated as a strategy to reduce deaths caused by these diseases. CVDs are a group of heart and blood vessels disorders , which include coronary heart disease (CHD), cerebrovascular disease and peripheral arterial disease among others. CVDs are the number 1 cause of death worldwide according to the World Health Organization (WHO)[2] accounting for 31% (17.5 million people) of all the global deaths in 2012. The latest available data[3] states that CVD causes more than 4 million deaths each year across Europe, accounting for 45% of all deaths, being CHD and cerebrovascular diseases the most common causes.

Under the leadership of WHO, all Member States agreed to reduce the number of deaths caused by non-communicable diseases (NCD) such as CVDs. Reduction of identified risks factors (hypertension, alcohol, physical inactivity, overweight, etc) and early diagnostic are between the global targets. Over the past 20 years, there has been an accelerating growth in the application of proteomics in cardiovascular biomedicine seeking for biomarkers offering information of the physiological status in this respect.

As result, plethora of different proteins have been identified providing information of the disease status (B-type natriuretic peptide (BNP) for heart failure or acute coronary syndrome; creatinine-kinase- myocardial band (CK-MB), myoglobin (MYO) or Troponin I (cTnI) for acute myocardial infarct or myocardial necrosis, etc) or the risk to suffer such disorders[4-8]. Between the last group, circulating CRP levels are clinically used to predict the occurrence of cardiovascular events and to assist in the selection of therapies based on more accurate risk assessment of individuals at intermediate risk[9-13]. Moreover, as inflammatory biomarker CRP may add prognostic information comparable to well recognized risk factors such as blood pressure or cholesterol. Values <1 , 1 to 3 , and >3 mg L⁻¹ indicate lower, average, or higher relative cardiovascular risk, respectively[10, 12]. Several assays have been developed for CRP quantification in blood samples[14] including immunoassays, biosensors such as surface plasmon resonance (SPR) or assays based on the use of molecularly imprinted polymers (MIPs). In addition, many methodologies and strategies for CRP detection and quantification have been commercialized. Brouwer *et al.* evaluated eight of the most representative ones in terms of analytical quality[15]. Their analysis concluded that CRP strips are suitable for semi-quantitative analysis but the Smart CRP test and Alere Afinion™ CRP test would be preferred as quantitative methods. Furthermore, CRP has been used as proof-of-concept to demonstrate the potential of new bioanalytical strategies [16-19] for point-of-care (POC) assay development. The combination of CRP testing on multiplexed platforms in which other CVD biomarkers could also be measured simultaneously, would undoubtedly enhance its predictive risk factor value[20]. However, notwithstanding the

research efforts to develop CVD multiplexed diagnostic methods[21-25], their implementation on clinical practice has been still scarce.

Biobarcode has recently emerged as a new bioanalytical technique with excellent capabilities for multiplexation[26-30], reaching also high sensitivity (as low as zM[31]). This technology, in the case of protein detection, is based in using multifunctional oligonucleotide encoded probes modified with a detection antibody, magnetic particles functionalized with a capture antibody and a DNA detection method. Several strategies have been evaluated as signaling readout, nevertheless, microarray[32] and capillary electrophoresis[33] remain the best options for future multiplexed analysis. This strategy has been used to detect cancer biomarkers[29, 32, 34], bacteria [33, 35, 36] and virus[37-41], but to our knowledge nobody has reported its implementation to diagnose CVDs. In this study, we report the development and evaluation of a *NP-based biobarcode* strategy for C-reactive protein detection as a preliminary stage to subsequently implement this approach to the development of a multiplexed platform for more reliable diagnostics of CVDs.

2 Experimental

2.1 Materials and Instruments

Polystyrene particles (PSP) were carboxy modified Dyed Microspheres (K1 050 noir) were supplied by Estapor[®] (Millipore Corp., Billerica, MA, USA). The magnetic particles (MP), Dynabeads MyOne Tosylactivated, and the magnetic rack Magnarack[™] were obtained from Invitrogen (life technologies[™], Paisley, UK). The pre-cleaned plain slides were purchased from Corning[®] (Corning Inc., New York, NY, USA). Functionalized slides

were spotted with a BioOdyssey Calligrapher MiniArrayer (Bio-Rad Laboratories, Inc. USA). Measurements were recorded on a ScanArray Gx PLUS (Perkin Elmer, USA) with a Cy3 optical filter with 5- μ m resolution. Slide gaskets were purchased from ArrayIt Coporation (Sunnyvale, CA, USA). U-bottom polystyrene microplates were purchased from Nirco (Barberà del Vallès, Spain). IKA[®] MS 3 basic shaker with a MS 3.4 Microtiter attachment (IKA[®], Staufen, Germany) was used to shake the microplates at 800 rpm. A thermos-shaker (TS-100C Biosan, Riga, Latvia) was used to shake Eppendorfs. Eppendorfs were centrifuged with a Legend Micro 21, 10 min, 17500G (Thermo Fisher Scientific Inc.) and plates were centrifuged with a Centrifuge 5810 R, 10 min, 3220 G (Eppendorf, Hamburg, Germany). The pH and the conductivity of all buffers and solutions were measured with a 540 GLP pH meter and an LF 340 conductimeter (WTW, Weilheim, Germany), respectively. Absorbance and fluorescence were read on a Spectramax Plus and a Spextramax Gemini XPS (Molecular Devices, Sunnyvale, CA, USA), respectively.

2.2 *Chemicals and biochemicals*

The chemical reagents used were obtained from Aldrich Chemical Co. (Milwaukee, WI, USA) and from Sigma Chemical Co. (St. Louis, MO, USA). N₄down-NH₂ oligonucleotide sequence, [AmC6F]TCCAGCGTTAGTGTACAGAG, was purchased from Sigma Chemical Co. (St. Louis, MO, USA) and TAMRA-N₄up-SS-NH₂, [TAMRA]CTCTGTACACTAACGCTGGA[ThiolC6SS][AminolinkC6], was obtained from Biomers (GmbH, Ulm, Germany). The two antibodies for CRP (pAbCRP1 and pAbCRP2) were supplied by Audit Diagnostics (Cork, Ireland).

2.3 *Clinical samples*

Blank plasma samples were commercially available from a pull of healthy patients. Moreover, clinical plasma samples from patients showing different pathologies were provided by Institut d'Investigació Germans Trias i Pujol (IGTP). These plasma samples were already analyzed at the IGTP for CRP concentration using a Siemens Dimensions analyzer based on LOCI[®] chemiluminescent technology.

2.4 *General procedures*

On the scanner measurements, the laser power and PMT were set to 95% and 67%, respectively. The spots were measured by F543_Mean-B543 (Mean Cy3 foreground intensity minus mean Cy3 background intensity). Fluorescence intensity values were expressed normalized or in relative units as average and standard deviation of five replicate spots. The standard curve was fitted to a linear regression according to the following formula: $Y = mX + n$ (GraphPad Prism version 5.03 for Windows, GraphPad Software, San Diego, California, USA), where m is the slope and n the Y-intercept. The limit of detection (LOD) was calculated as the mean of blank values plus three times its standard deviation. Limit of quantification (LOQ) was calculated as ten times the standard deviation of blank values. The assays were carried out three times within three different days. All the incubation steps performed on the U-bottomed microplates were performed at 25 °C and 800 rpm using the microtiter shaker.

2.5 *Buffers*

Phosphate buffer saline (PBS) is 0.01 M phosphate buffer in a 0.8% saline solution, pH 7.5. Coating buffer is a 0.05 M carbonate-bicarbonate buffer,

pH 9.6. PBST is PBS with 0.05% Tween 20, pH 7.5. Citrate buffer is 0.04 M sodium citrate, pH 5.5. The substrate solution contains 0.01% 3,3',5,5'-tetramethylbenzidine (TMB) and 0.004% H₂O₂ in citrate buffer. PSPs coupling buffer was 100 mM carbonate buffer pH 9. MP A buffer was 0.1 M borate buffer (pH 9.5). MP C buffer was 3 M ammonium sulphate in A buffer (pH 9.5). MP blocking buffer was PBST with 0.5 % BSA. MP storage buffer was PBST with 0.1 % BSA. Printing buffer comprised 150 mM sodium phosphate (pH 8.5) and 0.01 % sodium dodecyl sulphate. Hybridization buffer was 10 mM TRIS, 1 mM EDTA, 1M NaCl (pH 7.2).

2.6 CRP ELISA development

All information concerning CRP analysis in ELISA format is enclosed in the supporting information.

2.7 Microarray printing

Slides were cleaned immersing them in piranha solution (H₂SO₄:H₂O₂ 7:3) during 30 min; washed with purified water and immersed in NaOH 10 % during 30 min; washed with water and ethanol and dried to finally be activated with (3-glycidoxypropyl)methyldiethoxysilane during 30 min. Afterwards, slides were washed with ethanol and dried. These epoxidized slides can be stored in the desiccator for long periods of time. Finally, oligonucleotide chains (N₄down-NH₂, 200 ng mL⁻¹ in printing buffer) were spotted onto substrates in a high-humidity chamber, maintained for 30 min at room temperature and finally stored overnight at 4°C. Each glass slide contained 24 (8 x 3) spotting grids. A 5 x 1 spot matrix was printed on each grid (five spots replicated).

2.8 *Preparation of the pAbCRP1 biofunctionalized encoded polystyrene probes (pAbCRP1-ePSP)*

Polystyrene particles (PSPs, 10% w/v solution, 40 μ L) were washed twice with PSPs coupling buffer (500 μ L) and subsequently, a solution of a combination of oligonucleotide probes and pAbCRP1 (TAMRA-N4up-SS-NH₂, 0.27 μ M, and pAbCRP1, 0.54 μ M, 320 μ L in PSPs coupling buffer) was added followed by a solution of EDC (500 mM, 80 μ L in PSPs coupling buffer) were added and the mixture allowed to react at 25 °C for 3 h under shaking (750 rpm). Afterwards, the supernatant was removed and the efficiency of the coupling reaction was checked by analyzing the remaining pAbCRP1 and the oligonucleotides by ELISA and fluorescence (543 nm excitation, 575 nm emission), respectively. A conjugation yield of 70 % of pAbCRP1 and 38 % of TAMRA-N4up-SS-NH₂ was obtained, 1 % w/v. The suspension was then washed twice with PBST and stored in 400 μ L of PBS at 4°C. Under these conditions the biofunctionalized beads were stable for at least 1 month.

2.9 *Oligonucleotide release*

ePSPs stock solution (25 μ L) was treated with 0.2 M DTT (100 μ L, hybridation buffer) and allowed to react for 1 h at RT using the shaker (750 rpm). The suspension was then centrifuged and the supernatant used to quantify the fluorescence released as described above. A release yield of 79 % was obtained under these conditions.

2.10 *Preparation of the pAbCRP2-MPs*

pAbCRP2 were covalently coupled to magnetic particles (MP) following the manufacturer supplier procedure with slight modifications. Briefly,

Dynabeads MyOne Tosylactivated (100 mg mL^{-1} , $200 \text{ }\mu\text{L}$) were washed with MP A buffer ($3 \times 300 \text{ }\mu\text{L}$) and a solution of pAbCRP2 ($400 \text{ }\mu\text{L}$, 0.5 mg mL^{-1} in MP A buffer) was added followed by MP C buffer ($200 \text{ }\mu\text{L}$). The mixture was allowed to react protected from light overnight at 37°C under shaking 750 rpm . The day after the supernatant was removed and analyzed by the Bradford protein test to estimate the efficiency of the coupling. A conjugation yield of 96% was obtained. Next, the biofunctionalized particles were resuspended in MP blocking buffer and allowed to stand overnight again, before the supernatant was removed and particles were washed with of MP storage buffer ($1000 \text{ }\mu\text{L} \times 2$) and finally resuspended in $1000 \text{ }\mu\text{L}$ for storage at 4°C . Under these conditions the biofunctionalized beads were stable for at least two months.

2.11 Two-dimensional Checkerboard Titration Experiments (2D-assay)

The binding of serial dilutions of the pAbCRP2-MP suspension (from 0 to 2 mg mL^{-1}) against different dilutions of the pAbCRP1-ePSP (from 0.013 to 0.05%) were evaluated during $30'$, at RT. Afterwards, the microplates were washed ($4 \times 200 \text{ }\mu\text{L}$, PBST), a solution of 0.2 M DTT (in hybridation buffer, $100 \text{ }\mu\text{L}/\text{well}$) was added and the mixtures allowed to react for 1 h at RT under shaking (800 rpm). The microplates were then centrifuged and supernatant, with the released oligonucleotide probes, transferred to a previously washed ($4 \times 200 \text{ }\mu\text{L}$) DNA microarray slide and allowed to hybridize for 30 min at RT (500 rpm). Then slide was washed once more ($4 \times 200 \text{ }\mu\text{L}$) with PBST and one last time with milliQ water ($200 \text{ }\mu\text{L}$) without the gasket. From these experiments, optimum concentrations for both particles were chosen. By using a concentration of 0.5 mg mL^{-1} of MP and 0.05% of ePSP a fluorescent signal of around 10000 RFU was recorded

2.12 Sandwich biobarcode assay

Before starting, both the pAbCRP2-MP and the pAbCRP1-ePSPs were washed with PBST (2 x10 times its volume). The standards (CRP, from 250 to 0 ng mL⁻¹ in PBST, 50 µL) or the samples (diluted 1/50 in the same buffer) were mixed with the pAbCRP2-MP (25 µL, 0.5 mg mL⁻¹ in PBST) and allowed to interact for 30', r.t. Afterwards, the microplates were washed (4 x200 µL, PBST), the and pAbCRP1-ePSPs (0.05 % w/v in PBST, 100 µL) were added and incubated, then biocomplexes were processed as described above for the two-dimensional assay for measuring the released oligonucleotide probes on the DNA microarray.

2.13 Matrix effect studies, accuracy studies and analysis of clinical samples

Non-specific interferences produced by the plasma were assessed by preparing calibration curves in this matrix diluted 50 times with the assay buffer. The accuracy of the method was assessed by spiking blank plasma or serum samples at 5 different concentrations (from 5000 to 1000 ng mL⁻¹) and analyzed them with the biobarcode. The sample concentration was calculated interpolating the results to CRP calibration curve prepared in PBST. The measured and spiked concentration values were fitted to a linear regression curve. Finally, human plasma samples from the Hospital Germans Tries i Pujol were diluted 1/50 with PBST and then analyzed with the sandwich *NP-based biobarcode* assay. Results were compared with those obtained using the Siemens Dimension analyzer and ELISA.

3 Results and discussion

3.1 Preparation of multifunctional particles (*pAbCRP1-ePSP* and *pAbCRP2-MP*)

Carboxy-PSPs particles were functionalized with TAMRA-N₂up-SS-NH₂, as fluorescent oligonucleotide code, and pAbCRP1, as detection antibody, using EDC to activate the carboxylic groups of the particles. The oligonucleotide sequence was previously designed[42] to ensure stable hybridization with the complementary sequences of the DNA microarray used for detection. Moreover, at the 5'-end it is linked to 5-carboxytetramethylrhodamine (TAMRA) for signal generation. The biofunctionalization yield was found to be 38% and 70% for the oligonucleotides and the antibody, respectively. About 1800 DNA strands per ePSP was obtained using the conditions described in the experimental section, which provided sufficient amplification capability[32]. On the other hand, commercially available tosyl-activated MP were functionalized with pAbCRP2, used as capture antibody, with a 96 % conjugation yield.

3.2 CRP Biobarcode assay

The assay was designed as a two-step format (Figure 1). On a first instance, the CRP was captured with the pAbCRP2-MPs, and, secondly, pAbCRP1-ePSPs was added for detection of the immunocomplexes formed. Subsequently, the oligonucleotides were released via ligand exchange by treatment with dithiothreitol (DTT) breaking the disulfide bond in the 3'-end of the oligonucleotides. The released sequences were then allowed to hybridize with their complementary oligonucleotides immobilized on the DNA-microarray. The fluorescent signal recorded in the microarray was

dependent on the concentration of CRP being possible to calibrate the assay using a linear regression equation. Under the conditions established, the *CRP biobarcode assay* shows a working range between 250 and 18 ng mL⁻¹ with a LOD of 11 ng mL⁻¹. That is below the physiological levels reported for this biomarker, even on healthy individuals (< 1000 ng L⁻¹). Figure 2 shows the calibration curve adjusted to a linear regression while Table 1 shows the analytical parameters.

3.3 *Implementation of the CRP biobarcode assay to the analysis of clinical samples*

Because of the high sensitivity of the assay, it was necessary to dilute the plasma samples with the assay buffer in order to place the quantification range of the assay within the usual CRP concentration range with clinical value (10000 – 1000 ng mL⁻¹ [10, 12]). Considering the analytical features, samples had to be diluted at least 50 times, in such way the working range of the assay would move from 250 and 18 ng mL⁻¹ to 12500 – 900 ng mL⁻¹. Using these conditions calibrations curves were built with blank plasma showing analytical features identical to those of the assay run in buffer (see Figure 2), indicating the absence of nonspecific or specific interferences.

Subsequently, studies were performed to assess CRP biobarcode assay accuracy. With this purpose, blank plasma samples were spiked with CRP and measured with the assay. The results shown in Figure 3 and Table S1 demonstrate that the CRP biobarcode quantifies this biomarker with an excellent accuracy. As it can be observed, the regression analysis shows a very good correlation ($R^2=0,983$) with a slope close to 1. A mean recovery of 99.5% with a relative standard deviation (RSD) of 4.2% (N = 3) was obtained for all samples analyzed, with the only exception of a sample

spiked at a concentration close to the detection limit, in which case the recovery was 75% (see table S2 in the Supporting Information). These results pointed to the suitability of the method to analyze clinical samples.

3.4 Clinical Evaluation of the CRP Biobarcode Assay

Clinical samples from different patients showing symptoms related to CVDs and other pathologies involving inflammatory processes (gastric disorders, urinary infections, etc) were collected and analyzed with the CRP biobarcode assay. The results were compared to those obtained with a commercial laboratory benchtop automated analyzer (High Sensitivity C-Reactive Protein (hsCRP) assay in a Siemens Dimension Analyzer) and in our group by ELISA (see supplementary information). The results obtained are shown in Figure 4, where it can be observed the excellent correlation found between those obtained with the benchtop analyzer (green bars), the microplate ELISA (blue bars) and the *CRP biobarcode assay* (orange bars). It should be noticed that some samples from patients readily showing a CVD could not be analyzed for CRP at the hospital due to the high sample load. Even though, our assay showed that these samples contained high CRP concentrations in consonance with the diagnostic made. Hence, patients 2-6 diagnosed to have suffered AMI showed values between 3000 and 10000 ng mL⁻¹ or even higher. Patient number 7, suffering chest pain, but not showing increase of the S and T waves, also had high CRP levels. Similarly, for those suffering cardiac arrest (patient 11), hypertension (patient 12), heart failure (patient 13), ischemia (patient 14) or thoracic pain (patient 19). Patients suffering gastric disorders or urinary infections also showed extremely high levels, due to the implication of CRP in inflammatory processes. Thus, these results demonstrate the CRP biobarcode assay

developed in this work could be an excellent tool for monitoring this biomarker on patients suffering CVDs or other inflammatory processes.

4 Conclusions

The sandwich *NP-based biobarcode* assay developed for CRP shows a detectability with is sufficient for directly measuring this biomarker in complex samples such as plasma. Due to the number of oligonucleotide strands (~1800), used as codes, on the detection probe, every binding event is amplified before the detection on the DNA microarray. Because of this fact, the LOD achieved (11.0 ng mL^{-1}) is much below of the CRP concentration found in the plasma of healthy patients, which allows diluting the sample 50 times before the analysis avoiding in this way potential nonspecific (matrix effect) or specific interferences (physiological CRP levels of healthy patients). Thus the assay can directly quantify CRP within a range ($12500 - 900 \text{ ng mL}^{-1}$) in which variation of the levels provide a relevant information and a clinical value regarding the use of CRP as risk-predictive CVD biomarker and other diseases involving inflammatory processes. The small clinical study performed demonstrates the that the CRP biobarcode assay could be used for performing reliable measurements of this biomarker in plasma samples. Furthermore, it shows the potential of implementation in a multiplexed biobarcode assay by combining the biofunctional encode particles synthesized in this study with other sets particles bearing different oligonucleotide codes.

5 Author information

Corresponding Author

#To whom correspondence should be addressed. Phone: 934006100 (Ext. 5119). Fax: 932045904. E-mail: roger.galve@cid.csic.es

6 Acknowledgement

This work has been funded by the ministry of Economy and Competitiveness (MAT2012-38573-C02-01). The Nb4D group (formerly Applied Molecular Receptors group, AMRg) is a consolidated research group (Grup de Recerca) of the Generalitat de Catalunya and has support from the Departament d'Universitats, Recerca i Societat de la Informació de la Generalitat de Catalunya (expedient : 2014 SGR 1484). CIBER-BBN is an initiative funded by the Spanish National Plan for Scientific and Technical Research and Innovation 2013-2016, Iniciativa Ingenio 2010, Consolider Program, CIBER Actions are financed by the Instituto de Salud Carlos III with assistance from the European Regional Development Fund. Audit Diagnostics is acknowledged by supplying specific antibodies for CRP detection. The ICTS "NANOBIOSIS", and particularly the Custom Antibody Service (CAbs, IQAC-CSIC, CIBER-BBN), is acknowledged for the assistance and support related to the immunoreagents used in this work. Institut d'Investigació Germans Trias i Pujol (IGTP) is acknowledged for the clinical samples supplies. Marta Broto wishes to thank the FPI-fellowship (BES-2013-062819) from the Spanish Ministry of Economy and Competitiveness.

7 References

- [1] B. Rhodes, B.G. Furnrohr, T.J. Vyse, C-reactive protein in rheumatology: biology and genetics, *Nat Rev Rheumatol*, 7 (2011) 282-289.
- [2] W.H. Organization, The top 10 causes of death, 2016.
- [3] N. Townsend, L. Wilson, P. Bhatnagar, K. Wickramasinghe, M. Rayner, M. Nichols, Cardiovascular disease in Europe: epidemiological update 2016, *European Heart Journal*, 37 (2016) 3232-3245.
- [4] R. Cemin, M. Daves, Pre-analytic variability in cardiovascular biomarker testing, *Journal of Thoracic Disease*, 7 (2015) E395-E401.
- [5] K. Kotani, M.-C. Serban, P. Penson, G. Lippi, M. Banach, Evidence-based assessment of lipoprotein(a) as a risk biomarker for cardiovascular diseases - Some answers and still many questions, *Critical Reviews in Clinical Laboratory Sciences*, 53 (2016) 370-378.
- [6] M.P.Y. Lam, P. Ping, E. Murphy, Proteomics Research in Cardiovascular Medicine and Biomarker Discovery, *Journal of the American College of Cardiology*, 68 (2016) 2819-2830.
- [7] J. Tunon, C. Barbas, L. Blanco-Colio, E. Burillo, O. Lorenzo, J. Luis Martin-Ventura, S. Mas, F. Javier Ruperez, J. Egido, Proteomics and metabolomics in biomarker discovery for cardiovascular diseases: progress and potential, *Expert Review of Proteomics*, 13 (2016) 857-871.
- [8] E. Braunwald Biomarkers in Heart Failure, *New England Journal of Medicine*, 358 (2008) 2148-2159.
- [9] E. Rietzschel, M. De Buyzere, High-sensitive C-reactive protein: universal prognostic and causative biomarker in heart disease?, *Biomarkers in Medicine*, 6 (2012) 19-34.
- [10] F.G. Hage, C-reactive protein and hypertension, *Journal of Human Hypertension*, 28 (2014) 410-415.
- [11] P.A. Stone, J. Kazil, The relationships between serum C-reactive protein level and risk and progression of coronary and carotid atherosclerosis, *Seminars in Vascular Surgery*, 27 (2014) 138-142.
- [12] P.M. Ridker, A Test in Context High-Sensitivity C-Reactive Protein, *Journal of the American College of Cardiology*, 67 (2016) 712-+.
- [13] P.M. Ridker, From C-Reactive Protein to Interleukin-6 to Interleukin-1 Moving Upstream To Identify Novel Targets for Atheroprotection, *Circulation Research*, 118 (2016) 145-156.
- [14] M. Algarra, D. Gomes, J.C. Esteves da Silva, Current analytical strategies for C-reactive protein quantification in blood, *Clin Chim Acta*, 415 (2013) 1-9.

- [15] N. Brouwer, J. van Pelt, Validation and evaluation of eight commercially available point of care CRP methods, *Clinica Chimica Acta*, 439 (2015) 195-201.
- [16] H.H. Lee, M. Bae, S.-H. Jo, J.-K. Shin, D.H. Son, C.-H. Won, J.-H. Lee, Differential-mode HEMT-based biosensor for real-time and label-free detection of C-reactive protein, *Sensors and Actuators B: Chemical*, 234 (2016) 316-323.
- [17] R.J. Huttunen, T. Nareoja, L. Mariani, H. Harma, Residual nanoparticle label immunosensor for wash-free C-reactive protein detection in blood, *Biosens Bioelectron*, 83 (2016) 54-59.
- [18] S.K. Vashist, T. van Oordt, E.M. Schneider, R. Zengerle, F. von Stetten, J.H. Luong, A smartphone-based colorimetric reader for bioanalytical applications using the screen-based bottom illumination provided by gadgets, *Biosens Bioelectron*, 67 (2015) 248-255.
- [19] S. Sridevi, K.S. Vasu, S. Asokan, A.K. Sood, Sensitive detection of C-reactive protein using optical fiber Bragg gratings, *Biosens Bioelectron*, 65 (2015) 251-256.
- [20] B. Zethelius, L. Berglund, J. Sundstrom, E. Ingelsson, S. Basu, A. Larsson, P. Venge, J. Arnlov, Use of multiple biomarkers to improve the prediction of death from cardiovascular causes, *The New England journal of medicine*, 358 (2008) 2107-2116.
- [21] C.A. Marquette, F. Bouteille, B.P. Corgier, A. Degiuli, L.J. Blum, Disposable screen-printed chemiluminescent biochips for the simultaneous determination of four point-of-care relevant proteins, *Analytical and Bioanalytical Chemistry*, 393 (2009) 1191-1198.
- [22] F. Zhou, M. Lu, W. Wang, Z.P. Bian, J.R. Zhang, J.J. Zhu, Electrochemical immunosensor for simultaneous detection of dual cardiac markers based on a poly(dimethylsiloxane)-gold nanoparticles composite microfluidic chip: a proof of principle, *Clin Chem*, 56 (2010) 1701-1707.
- [23] G.-J. Zhang, Z.H.H. Luo, M.J. Huang, J.A.J. Ang, T.G. Kang, H. Ji, An integrated chip for rapid, sensitive, and multiplexed detection of cardiac biomarkers from fingerprick blood, *Biosensors and Bioelectronics*, 28 (2011) 459-463.
- [24] J. Park, V. Sunkara, T.-H. Kim, H. Hwang, Y.-K. Cho, Lab-on-a-Disc for Fully Integrated Multiplex Immunoassays, *Analytical Chemistry*, 84 (2012) 2133-2140.
- [25] G. Koukouvinos, P. Petrou, K. Misiakos, D. Drygiannakis, I. Raptis, G. Stefanitsis, S. Martini, D. Nikita, D. Goustouridis, I. Moser, G. Jobst, S. Kakabakos, Simultaneous determination of CRP and D-dimer in human blood plasma samples with White Light Reflectance Spectroscopy, *Biosens Bioelectron*, 84 (2016) 89-96.

- [26] D. Hill Haley, A. Mirkin Chad, The bio-barcode assay for the detection of protein and nucleic acid targets using DTT-induced ligand exchange, *Nature Protocols*, 1 (2006) 324-336.
- [27] D. Zhang, D.J. Carr, E.C. Alocilja, Fluorescent bio-barcode DNA assay for the detection of *Salmonella enterica* serovar Enteritidis, *Biosensors and Bioelectronics*, 24 (2009) 1377-1381.
- [28] H. Lee, J.-E. Park, J.-M. Nam, Bio-barcode gel assay for microRNA, *Nat Commun*, 5 (2014).
- [29] S.I. Stoeva, J.-S. Lee, J.E. Smith, S.T. Rosen, C.A. Mirkin, Multiplexed Detection of Protein Cancer Markers with Biobarcode Nanoparticle Probes, *Journal of the American Chemical Society*, 128 (2006) 8378-8379.
- [30] S.I. Stoeva, J.-S. Lee, C.S. Thaxton, C.A. Mirkin, Multiplexed DNA Detection with Biobarcode Nanoparticle Probes, *Angewandte Chemie International Edition*, 45 (2006) 3303-3306.
- [31] H. Dong, X. Meng, W. Dai, Y. Cao, H. Lu, S. Zhou, X. Zhang, Highly Sensitive and Selective MicroRNA Detection Based on DNA-Bio-Bar-Code and Enzyme-Assisted Strand Cycle Exponential Signal Amplification, *Analytical Chemistry*, 87 (2015) 4334-4340.
- [32] J.-M. Nam, C.S. Thaxton, C.A. Mirkin, Nanoparticle-Based Bio-Bar Codes for the Ultrasensitive Detection of Proteins, *Science*, 301 (2003) 1884-1886.
- [33] J.H. Jung, G.-Y. Kim, T.S. Seo, An integrated passive micromixer-magnetic separation-capillary electrophoresis microdevice for rapid and multiplex pathogen detection at the single-cell level, *Lab on a Chip*, 11 (2011) 3465-3470.
- [34] C.S. Thaxton, R. Elghanian, A.D. Thomas, S.I. Stoeva, J.S. Lee, N.D. Smith, A.J. Schaeffer, H. Klocker, W. Horninger, G. Bartsch, C.A. Mirkin, Nanoparticle-based bio-barcode assay redefines "undetectable" PSA and biochemical recurrence after radical prostatectomy, *Proc Natl Acad Sci U S A*, 106 (2009) 18437-18442.
- [35] M. Cho, S. Chung, J.H. Jung, G.-e. Rhie, J.H. Jeon, T.S. Seo, Combination of biobarcode assay with on-chip capillary electrophoresis for ultrasensitive and multiplex biological agent detection, *Biosensors and Bioelectronics*, 61 (2014) 172-176.
- [36] M. Cho, S. Chung, Y.T. Kim, J.H. Jung, D.H. Kim, T.S. Seo, A fully integrated microdevice for biobarcode assay based biological agent detection, *Lab on a Chip*, 15 (2015) 2744-2748.
- [37] T.-L. Chang, C.-Y. Tsai, C.-C. Sun, C.-C. Chen, L.-S. Kuo, P.-H. Chen, Ultrasensitive electrical detection of protein using nanogap

electrodes and nanoparticle-based DNA amplification, *Biosensors and Bioelectronics*, 22 (2007) 3139-3145.

[38] S.X. Tang, J.Q. Zhao, J.J. Storhoff, P.J. Norris, R.F. Little, R. Yarchoan, S.L. Stramer, T. Patno, M. Domanus, A. Dhar, C.A. Mirkin, I.K. Hewlett, Nanoparticle-based biobarcode amplification assay (BCA) for sensitive and early detection of human immunodeficiency type 1 capsid (p24) antigen, *AIDS-Journal of Acquired Immune Deficiency Syndromes*, 46 (2007) 231-237.

[39] C. Cao, R. Dhumpa, D.D. Bang, Z. Ghavifekr, J. Hogberg, A. Wolff, Detection of avian influenza virus by fluorescent DNA barcode-based immunoassay with sensitivity comparable to PCR, *Analyst*, 135 (2010) 337-342.

[40] J.W. Perez, E.A. Vargis, P.K. Russ, F.R. Haselton, D.W. Wright, Detection of respiratory syncytial virus using nanoparticle amplified immuno-polymerase chain reaction, *Analytical Biochemistry*, 410 (2011) 141-148.

[41] H.-q. Yin, M.-x. Jia, L.-j. Shi, S. Yang, L.-y. Zhang, Q.-m. Zhang, S.-q. Wang, G. Li, J.-g. Zhang, Nanoparticle-based bio-barcode assay for the detection of bluetongue virus, *Journal of Virological Methods*, 178 (2011) 225-228.

[42] N. Tort, J.P. Salvador, M.P. Marco, R. Eritja, M. Poch, E. Martínez, J. Samitier, Fluorescence site-encoded DNA addressable hapten microarray for anabolic androgenic steroids, *TrAC Trends in Analytical Chemistry*, 28 (2009) 718-728.

Figure legends

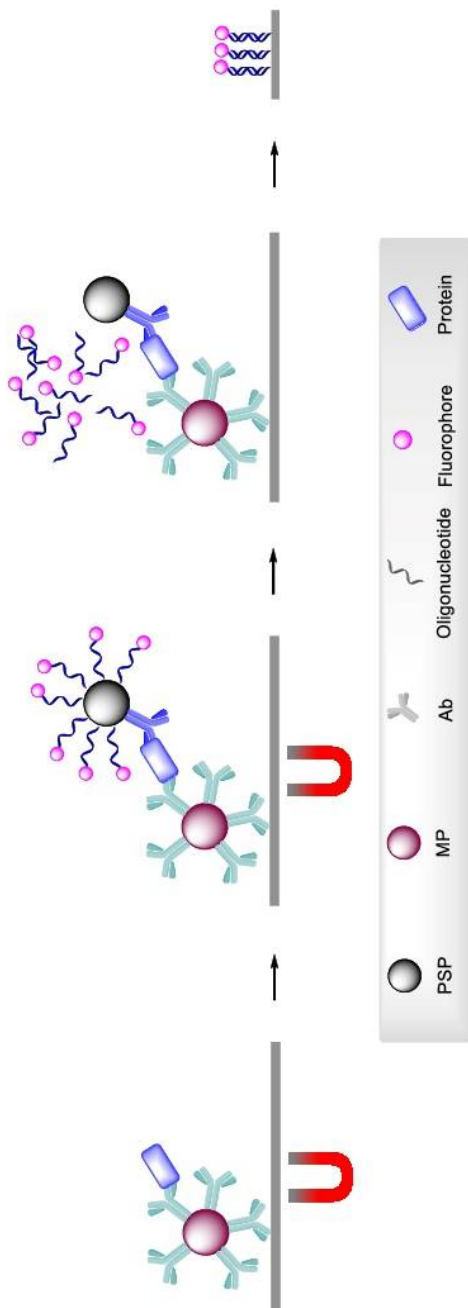
Figure 1. Schematic diagram of the sandwich nanoparticle-based biobarcode assay for small molecules. First, pAbCRP2-MP are mixed with the sample, then, unbound reagent or sample matrix is removed and subsequently pAbCRP1-ePSP are added to form the complex. Finally, coding oligonucleotides are released and hybridized in a DNA-microarray where a fluorescent signal is recorded.

Figure 2. Calibration curves of the NP-based biobarcode assay for CRP detection run in buffer and plasma at a 1/50 dilution with PBS. Each concentration point corresponds to the average of three assays performed three different days. On each assay, each calibration point was measured five times. The data was adjusted to a linear regression. The analytical parameters can be found in table 1.

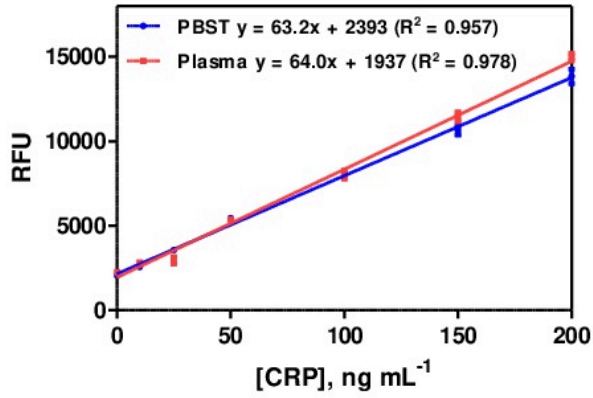
Figure 3. Results from the accuracy study performed in plasma. The graph shows the correlation between the CRP spiked and measured concentration values. The dotted line corresponds to an ideal correlation ($m=1$). The samples, diluted 1/50 in buffer, were quantified using calibration curves prepared in buffer. The data correspond to the average of at least five replicates obtained in three different days. The average of the %CV is 9.2.

Figure 4. Results from the pilot clinical study in which plasma samples from patients suffering different pathologies were measured with the CRP *biobarcode assay* developed. The results obtained (orange bars) were compared to those obtained by microplate ELISA (blue bars), using the same immunoreagents, and with a Siemens Dimension Analyzer (green bars). For the ELISA the data shown correspond to the average of three-well replicates. For the CRP biobarcode, the results shown are the average

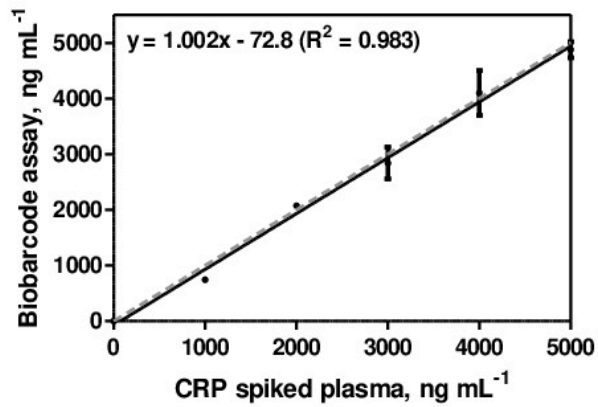
of 5 measurements. The results of the benchtop analyzer correspond to a single measurement. Horizontal dotted lines separate low, medium, high and very high risk of cardiovascular diseases. Patients are grouped depending on the illnesses.



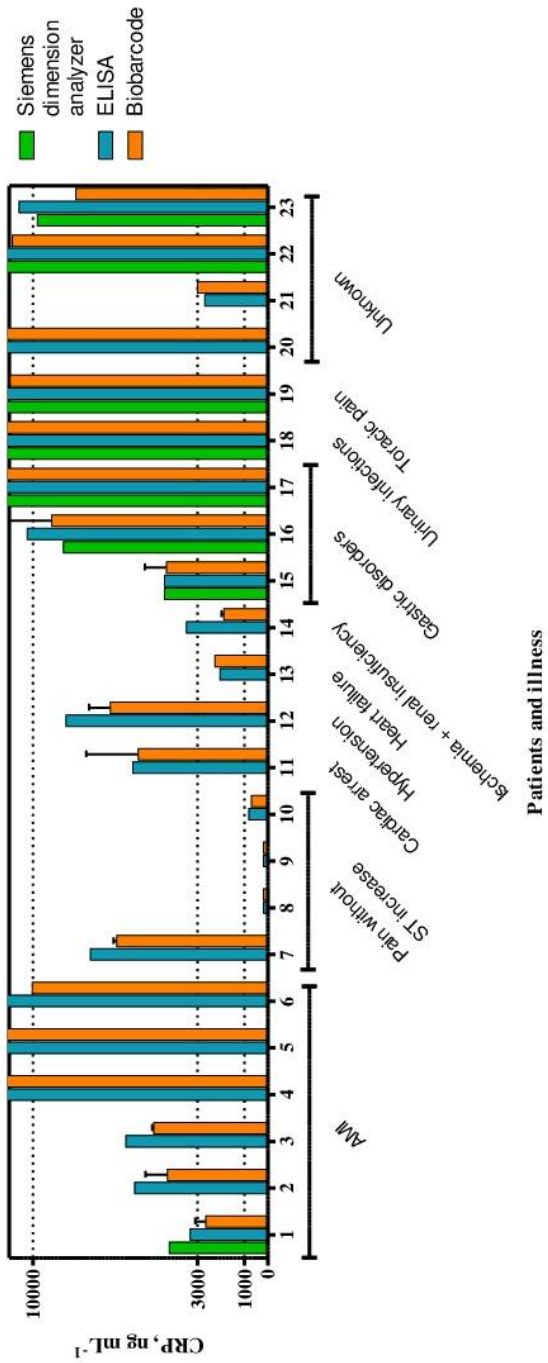
Broto *et al* Figure 1



Broto *et al.* Figure 2



Broto *et al.* Figure 3



Broto *et al.* Figure 4

Tables

Table 1. CRP biobarcode assay parameters run with ePSP

	Buffer ^a	Plasma ^b
Slope	63.2 ± 4.49	64.0
Y-intercept	2393 ± 221	1937
R²	0.957 ± 0.03	0.978
LOL, ng mL⁻¹	250.0	-
LOQ, ng mL⁻¹	18.0	-
LOD, ng mL⁻¹	11.0	-

The data has been extracted from the linear regression to fit the standard curve. ^aData shown is the average of assays run on 3 different days. On each day, the assay was run using 5 replicates for each CRP concentration. ^bData shows the average standard deviation of the parameters of assays using 5 replicates for each concentration of CRP standard measured.

Sandwich NP-based Biobarcode Assay for quantification C-reactive Protein in Plasma Samples

SUPPORTING INFORMATION

Marta Broto^{1,2}, Roger Galve^{1,2,*}, M.-Pilar Marco^{1,2},

¹Nanobiotechnology for diagnostics (Nb4D), Department of Chemical and Biomolecular Nanotechnology, Institute for Advanced Chemistry of Catalonia (IQAC) of the Spanish Council for Scientific Research (CSIC).

²CIBER de Bioingeniería, Biomateriales y Nanomedicina (CIBER-BBN), Jordi Girona 18-26, 08034 Barcelona, Spain

EXPERIMENTAL PROCEDURES

CRP ELISA development

Preparation of pAbCRP1-biotin. of EZ-Link Sulfo-NHS-LC-LC-Biotin (10 mM in milliQ water, 30 μL) were added to pAbCRP1 (2 mg mL^{-1} in PBS, 1 mL) and allowed to react 30', 800 rpm, r.t. Then, the mixture was purified by passing the solution through a Sephadex G-25 desalting column and eluting with milliQ. Collected fractions were frozen and lyophilized to yield 1.19 mg of pAbCRP1-biotin (60%).

Non-competitive sandwich ELISA. The screening of the avidity of the antisera pAbCRP2 with pAbCRP1 was evaluated through two-dimensional titration assays (2D-assay), based on the measurement of the binding of serial dilutions of the capture antibody (pAbCRP2 5 – 0.04 $\mu\text{g mL}^{-1}$, and zero, 100 $\mu\text{L well}^{-1}$) and different concentration of the detection antibody (pAbCRP1-biotin 8 $\mu\text{g mL}^{-1}$ to 0.12 $\mu\text{g mL}^{-1}$, and zero, 100 $\mu\text{L well}^{-1}$) to a fixed concentration of CRP (20 ng mL^{-1}). From these experiments, optimum concentrations for capture and detection antibodies were chosen to generate around 0.7-1 units of absorbance.

Sandwich ELISA pAbCRP2/pAbCRP1-biotin. Microtiter plates were coated with the capture antibody (0.3 $\mu\text{g mL}^{-1}$ in coating buffer, 100 $\mu\text{L well}^{-1}$), overnight at 4 °C and covered with adhesive plate sealers. The next day, the coated plates were washed four times with PBST (300 $\mu\text{L well}^{-1}$) followed and plasma samples or standard curve (CRP from 6 to 0.1 nM) were added (100 $\mu\text{L well}^{-1}$) and incubated for 30' at r.t.. The plates were washed as before, followed by the addition of detection antibody (pAbCRP1-biotin 0.25 $\mu\text{g mL}^{-1}$, 100 $\mu\text{L well}^{-1}$) for another 30' at r.t.. The plates were washed as before, and a solution of Streptavidin-HRP (1/6000 in PBST) was added to the wells (100 $\mu\text{L well}^{-1}$) and incubated for 30 minutes at r.t. The plates were washed again, and the substrate solution was added (100 $\mu\text{L well}^{-1}$). Color development was stopped after 30 min at r.t. with 4 N H_2SO_4 (50 μL

well⁻¹), and the absorbances were read at 450 nm. The standard curve was fitted to a linear regression according to the following formula: $Y = mX + n$ (GraphPad Prism version 5.03 for Windows, GraphPad Software, San Diego, California, USA), where m is the slope and n the Y-intercept. Limit of quantification (LOQ) was calculated as ten times the standard deviation of blank values. The assays were carried out three times within three different days. The main features of the final assay were described as the mean of all the replicates.

Matrix Effect Studies. Non-specific interferences produced by plasma were assessed by preparing standard curves at different plasma dilutions (1/400, 1/600, 1/800).

Analysis of clinical samples by ELISA. The analysis of the real sample concentration was assessed by diluting plasma 1/10000. The sample concentrations were calculated interpolating the results to CRP linear regression prepared in PBST.

RESULTS

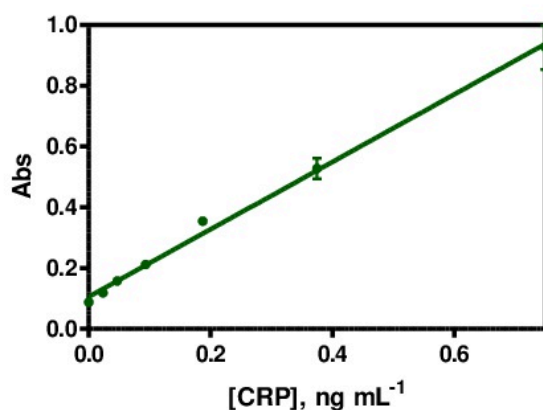
CRP ELISA

Figure S1 Calibration curve of the CRP ELISA. The data was adjusted to a linear regression. Each concentration point corresponds to the average of three replicates. The analytical parameters can be found in Table S1.

Table S1. Features of the CRP ELISA in buffer

Slope	1.11 ± 0.03
Y-intercept	0.105 ± 0.008
R²	0.987
LOL, ng mL⁻¹	0.7
LOQ, ng mL⁻¹	0.022

The data has been extracted from the linear regression to fit the standard curve. Data shows the average standard deviation of the parameters of assays using 3 replicates for each concentration of CRP standard measured.

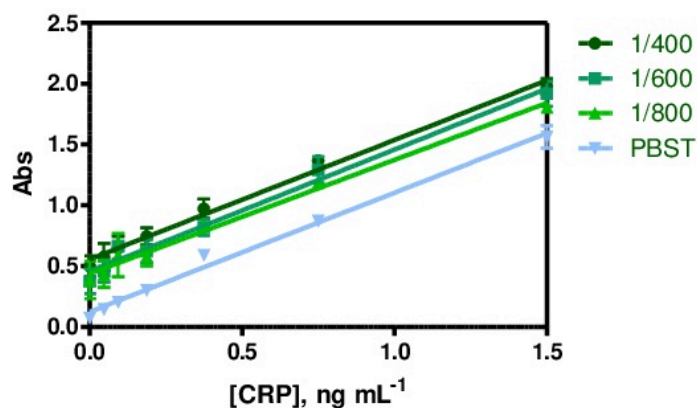
Matrix Effect Studies.

Figure S3 Matrix effect evaluation of the CRP ELISA. The data was adjusted to a linear regression. Each concentration point corresponds to the average of three replicates. Results reported that there is no matrix effect below 1/400 matrix dilution since slope is the same for plasma and PBST, Y intercept reported that real CRP concentration in plasma is 176 ng mL^{-1} .

Recovery results.

Table S2. Results from the accuracy study performed in plasma.

Spiked concentration, ng mL^{-1}	Biobarcode assay, ng mL^{-1}	Recovery, %
1000	746	75
2000	2074	104
3000	2840	95
4000	4099	102
5000	4874	97

The data correspond to the average of at least five replicates obtained in three different days. The average of the %CV is 9.2.

4.5 CHAPTER CONTRIBUTIONS

- An indirect competitive biobarcode assay has been reported for the first time. The assay has been applied to the detection and quantification of acenocoumarol in plasma and serum samples at nM range.
- Modulating the oligonucleotide charge on ePSPs we were allowed to demonstrate the remarkable capability of the biobarcode platform of amplifying the assay signal, and consequently modulate the working range depending the target requirements.
- A NP-based biobarcode assay in a sandwich format for C-reactive protein in plasma samples has been developed. Excellent results were obtained by challenging the platform with human samples of non-healthy patients and comparing them with a reference assay.

4.6 MATERIALS AND METHODS

4.6.1 IMMUNOCHEMISTRY

- Materials and methods.* The chemical reagents used in the synthesis were obtained from Aldrich Chemical Co. (Milwaukee, WI, USA) and from Sigma Chemical Co. (St. Louis, MO, USA). N2down-NH₂ oligonucleotide sequence, [AmC6F]CGGAGGTACATTCGACTTGA and TAMRA-N2up-SH, [TAMRA]TCAAGTCGAATGTACCTCCG5[ThiC3], was purchased from Sigma Chemical Co. (St. Louis, MO, USA), H₂N-N4up-SS-OH, was supplied by NACg (Nucleic Acid Chemistry group). TS-100C (Biosan, Riga, Latvia) was used to shake Eppendorfs. Eppendorfs were centrifuged with a Legend Micro 21, 10 min, 17500G (Thermo Fisher Scientific Inc.). Absorbance and fluorescence were read on a Spectramax Plus and a Spectramax Gemini XPS (Molecular Devices, Sunnyvale, CA, USA). The preparation of the immunoreagents used (hapten hACL, antibody pAb236 and antigen hACL-BSA) will be described elsewhere.
- Buffers.* Citrate/HCl buffer is 500 nM pH 3. PB/SDS is 10 mM, pH 7, 0.01 % SDS. Hybridation buffer is 10 mM TRIS, 1 mM EDTA and 1M NaCl pH

- 7.2. PBST-BSA is 10 mM PB, 0.2% NaCl, 0.1% tween, 0.1% BSA and pH 7. PBS was 0.01 M phosphate buffer in a 0.8% saline solution (137 mmol/L NaCl, 2.7 mmol/L KCl), and the pH was 7.5. PBST was PBS with 0.05% Tween 20. PSPs coupling buffer was 100 mM carbonate buffer pH 9. Citrate buffer is 0.04 M sodium citrate, pH 5.5. The substrate solution contains 0.01% 3,3',5,5'-tetramethylbenzidine (TMB) and 0.004% H₂O₂ in citrate buffer. Borate buffer is 0.2 M boric acid/sodium borate, pH 8.7.
- iii. *Hapten conjugation.* 2.9 μmol of hACL hapten, were mixed with 7.25 μmol (2.5 equivalents) of DCC and NHS in 100 μL of anh. DMF and allowed to react for 3h at r.t., 750 rpm. Activated hapten was added to 45.7 nmol of H₂N-N4up-SS-OH in 300 μL of Borate buffer and allowed to react overnight at r.t., 750 rpm. Resulting product was concentrated and purified by HPLC, HPLC at 2 mL/min, using gradients of A: H₂O/ACN (95:5) 0.1 M TEEAc and B: H₂O/ACN (30:70) 0.1 M TEEAc (lineal from 100% to 70% of A during 15 min). t_R(hACL): 2 min, t_R (H₂N-N4up-SS-OH): 8 min, t_R(product, hACL-N4up-SS-OH): 13 min. The detection was followed at 260 and 300 nm. Final product, 67% yield, was characterized by MALDI-TOS-MS (m/z calculated for hACL-N4up-SS-OH: 6911, m/z found for hACL-N4up-SS-OH: 6914). Oligonucleotide was deprotected by treatment of dithiothreitol 0.2 M followed by NAP-5 column purification prior to use.
- iv. *AuNPs synthesis.* 500 μL of gold (III) chloride trihydrate 0.1 M in milliQ were added to 150 mL of milliQ water. It was brought to boiling with the highest stirring velocity, subsequently, 4.5 mL of sodium citrate 1 % was injected to the solution. After 30' at boiling temperature it was cooled and stored in the fridge. Finally, particles were characterized by TEM and UV-Vis spectroscopy from 300 to 800 nm. Particle size of 16 nm and polydispersion < 9 % was reported.
- v. *AuNPs biofunctionalization.* A solution of 259 pmol of oligonucleotide in 200 μL of milliQ was prepared and added to 1 mL of AuNPs stock during 10', 25°C, 500 rpm. Then, 20 μL of Citrate/HCl buffer were added and allowed to react 10' more. Subsequently, reaction mixture was splited in 200 μL aliquots and centrifuged during 10' at 17500 G, resulting pellets were resuspended and washed twice with PB/SDS. Finally, particles were characterized by UV-Vis spectra using lamber-beer equation to

determine particle concentration, in case of 16nm-particles:
 $Abs(520\text{ nm}) = 0.195 c(\text{AuNPs}, nM) + 0.039$.

- vi. *Oligonucleotide release.* 50 μL of functionalized particles were mixed with 250 μL of dithiothreitol 0.2 M in hybridization buffer and let 10', 25°C, 500 rpm. Then, particles were centrifuged (10', 17500 G) and supernatant fluorescence was measured (excitation 543 nm, emission 575 nm).
- vii. *Buffer optimization by ELISA assay.* Microtiter plates were coated with the antigen hACL-BSA (1/16000 in coating buffer, 100 μL /well), overnight at 4 °C and covered with adhesive plate sealers. The next day, the plates were washed four times with PBST (300 μL /well) the solution of antisera As236 (1/8000 in PB varying SDS, NaCl, Tween and BSA content, 100 μL /well). After 30 min at r.t., the plates were washed as before, and a solution of anti-IgG-HRP (1/6000 in PBST) was added to the wells (100 μL /well) and incubated for 30 minutes at r.t. The plates were washed again, and the substrate solution was added (100 μL /well). Color development was stopped after 30 min at r.t. with 4 N H_2SO_4 (50 μL /well), and the absorbance was read at 450 nm.
- viii. *AuNPs-ELISA.* 50 μL of particles were placed in a 1.5-mL Eppendorf, then were centrifuged (10', 17500 G) and supernatant was removed. 200 μL of primary antibody solution, 25 ng/mL of pAb236 in PBST-BSA, were added and allowed to react 30', 25°C, 500 rpm. Afterwards, particles were washed twice with 200 μL of PBST-BSA and 200 μL of AntiIgG-HRP 1/6000 in PBST-BSA were added and let for 30', 25°C, 500 rpm. Finally, particles were washed again twice, 100 μL of substrate solution was added during 30', 25°C, 500 rpm to finally stop the reaction with 50 μL of H_2SO_4 4N. Resulting solution was transferred to a dilution plate and absorbance was read at 450 nm.
- ix. *AuNPs-Biobarcode 2D-assay.* Two-dimensional titration assays based on a non-competitive indirect format were carried out, measurements of the binding of serial concentrations of MP (from 0 to 3 mg/mL) against different dilutions of the AuNPs (from 0.15 to 0.0375, and 0 nM) were evaluated.
- x. *PEG-coated AuNPs.* 76.9 μL of AuNPs 1.3 nM was centrifuged (10', 17500 G) and 100 μL of mPEG350-SH 1 μM were added. It was allowed to react 3h, 500 rpm and 25°C and then washed twice with PB/SDS.

5 MULTIPLEXED AND MULTIMODAL BIOBARCODE ASSAY DEVELOPMENT

5.1 CHAPTER OBJECTIVE

After demonstration of the feasibility of the NP-based biobarcode strategy and how it can be used for different chemical nature compounds (low molecular weight compounds and proteins), this chapter (Figure 5.1) addressed the implementation of both assays in one-single platform. We will evaluate the multiplexation of both assays, firstly performed individually and subsequently optimized together for quantification of both target compounds at the same time within the same sample dilution.

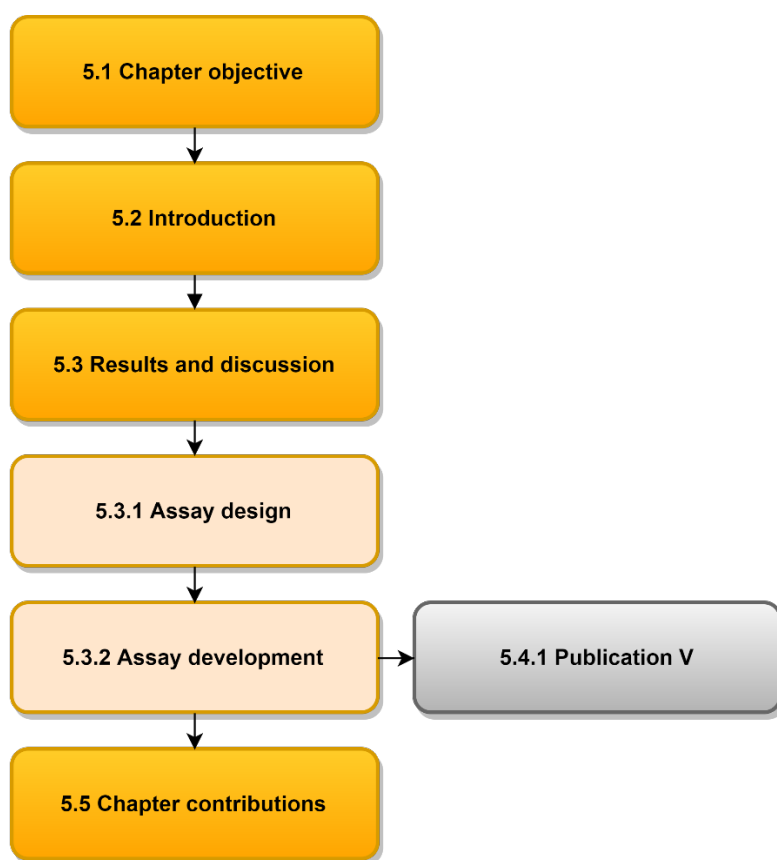


Figure 5.1 Structure of chapter 5 related to the different sections

5.2 INTRODUCTION

There is a need for multiplexed analytical techniques, they should be fast, robust, easy-to use and be able to detect compounds of different chemical nature (multimodality) and at a different range of concentration. These assays could provide huge advantages in personalized medicine addressing disease diagnosis, stratification and treatment. As explained in section 2.1, multiplexed assay basis is mainly the capacity to discriminate between different analytes. Various kinds of assay platforms have been introduced such as spatial localization or multiple labels⁶ (Figure 5.2). In the next section most important platforms will be discussed.

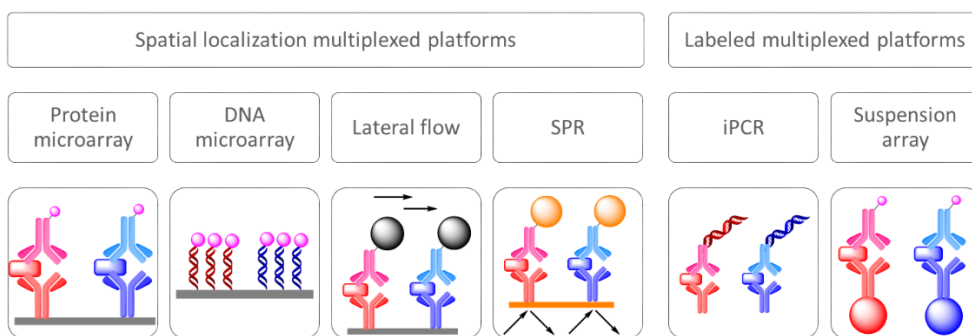


Figure 5.2 Schematic representation of main multiplexed platforms

5.2.1 SPATIALLY LOCALIZED MULTIPLEXED PLATFORMS

On one hand, an example of spatial localization is biospecific probes patterned on 2D surfaces. Analysis of multiple biomarkers on the protein microarray has been achieved by various readout technologies such as fluorescence, optical waveguide, charge-coupled divide camera, chemiluminiscence, electrical, electrochemical and surface plasmon resonance measurements.

Examples of spatial localization multiplexed platforms include microarray or lateral flow biosensors. Microarray permits the characterization from hundreds to thousands of proteins or DNA sequences at the same time. Protein microarray has been widely used for basic research¹²¹ as protein expression profiling, biomarker discovery, post-translational modification and protein interaction

with other molecules. Concerning clinical research, serological studies have been conducted. DNA microarray have been used for rapid sequencing and analysis of genes¹²², enabling the study of subtle changes in many genes at the same time, or infectious diseases¹²³. Sandwich microarray studies have also been performed, similarly to sandwich ELISA, but spatially localized¹²⁴. Comparable LOD and accuracy have been reported, but there's still need for printing process optimization and assay automation. Although microarray has been used for screening of hundreds of compounds at the same time, multimodality is yet to be addressed.

Other multiplexed platforms are lateral flow biosensors⁴, which are self-operating devices. They are rapid assays that, after sample addition, it encounters a series of reaction zones as it migrates across the device membrane by capillarity. These reaction zones become a readable output. Nevertheless, main limitations of lateral flow development are sensitivity and specificity. Surface plasmon resonance (SPR), that sometimes uses gold tagged bioreceptors as signal amplification¹²⁵, has also been applied in multiplexed detection³.

5.2.2 LABELED MULTIPLEXED PLATFORMS

On the other hand, multiple labels are used in suspension systems based on multiple bioconjugated labels or encoded carriers like particles. Quantum dots (QDs), semiconductor particles with various emission spectra, gold nanoparticles and magnetic nanoparticles have been widely used with this purpose⁸⁰. Particles can have different shapes and composition, their very small size imparts physical and chemical properties that are very different from those of the same material in bulk form. These properties include a large surface to volume ratio, enhanced or hindered particle aggregation depending on the type of surface modification, enhanced photoemission, high electrical and heat conductivity, and improved surface catalytic activity¹²⁶.

As an examples of labeled platforms, the Immuno-PCR technology¹²⁷ has become a key procedure in molecular diagnostics but it is limited by DNA sequences quantification, its cost and analysis time. Furthermore, both external and internal qualitative controls must be rigorously applied¹²⁸. If we focus on particles labeling, suspension array platforms¹²⁹ usually use particles with different

spectral addresses and separate them by flow cytometry. One example is the use of QD for a microbead-based flow cytometric immunoassay using QD fluorescent labels¹³⁰. Nevertheless, working range cannot be easily modulated according each analyte requirement.

5.2.3 MULTIPLEXED BIOBARCODE

In order to develop a universal platform, we proposed biobarcode as this gold standard technique. In section 4.2.2, biobarcode basis was introduced using particles coated with oligonucleotides as barcodes for quantification of different compounds. In Table 5.1, a list of multiplexed biobarcode assays can be found. Although the platform has been proven reliable for detection of multiple analytes, up to five targets including proteins, cells and DNA, multimodality has never been addressed.

Table 5.1 Developed biobarcode assays for multiple analytes

Target type	Analyte	Assay format	Signaling readout	LOD	Ref
Protein	Prostate specific antigen Hepatocellular carcinoma marker Testicular cancer marker	Sandwich	Silver enhancement	170 fM	10
	Staphylococcus aureus Escherichia coli Salmonella typhimurium	Sandwich	Capillary electrophoresis	1 CFU	81
	Bacillus anthracis Francisella tularensis Yersinia pestis Vaccinia virus Botulinum toxin A	Sandwich	Capillary electrophoresis	50 CFU/mL 12.5 ag/mL	82, 83
Cells	MCF-4 (breast cancer) SW620 (colorectal cancer)	Sandwich	Capillary electrophoresis	50 cells/mL	84
DNA	Hepatitis B virus Variola Virus Ebola virus Human immunodeficiency virus	Sandwich	Silver enhancement	500 fM	11
miRNA	miR-205 miR-21 miR-155	Sandwich	Capillary electrophoresis	aM	9

Among all developed multiplexed biobarcode, they were applied in buffer^{11, 81, 84} and in serum samples^{10, 82}, which proves its usefulness in biological matrices. Furthermore, these systems have been miniaturized⁸³, proving its potential as PoC (point of care) platforms. Concerning multiplexing readout, capillary electrophoresis has been the strategy selected for most multiplexed assays, since it is easily miniaturized. Another strategy based on DNA microarray hybridization coupled to silver enhancement has also been developed. However, fluorophore functionalized oligonucleotides have never been used for multiplexed biobarcode development.

5.3 RESULTS AND DISCUSSION

Monoplexed biobarcode were previously developed, section 4.3.4 and 4.3.5. The assay is based on using encoded polystyrene probes functionalized with specific bioreceptors, and magnetic particles functionalized with the specific antibodies. Thus, after a recognition step, immunocomplexes can be isolated to release coding oligonucleotides and hybridize them in a DNA-microarray for subsequent quantification. Results reported reproducible assays for small molecule detection in a competitive format and for protein detection in sandwich format. Now, the main objective was the implementation of both assays in one (Figure 5.3).

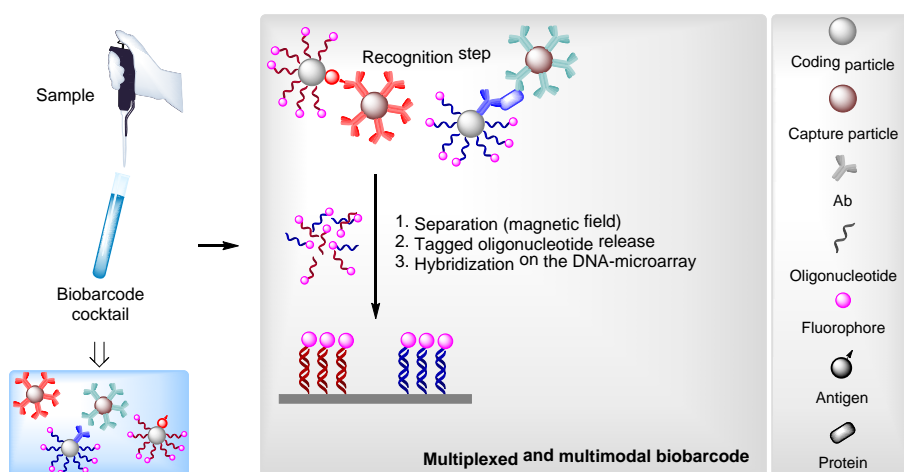


Figure 5.3 Schematic diagram of the multiplexed and multimodal biobarcode strategy.

5.3.1 ASSAY DESIGN

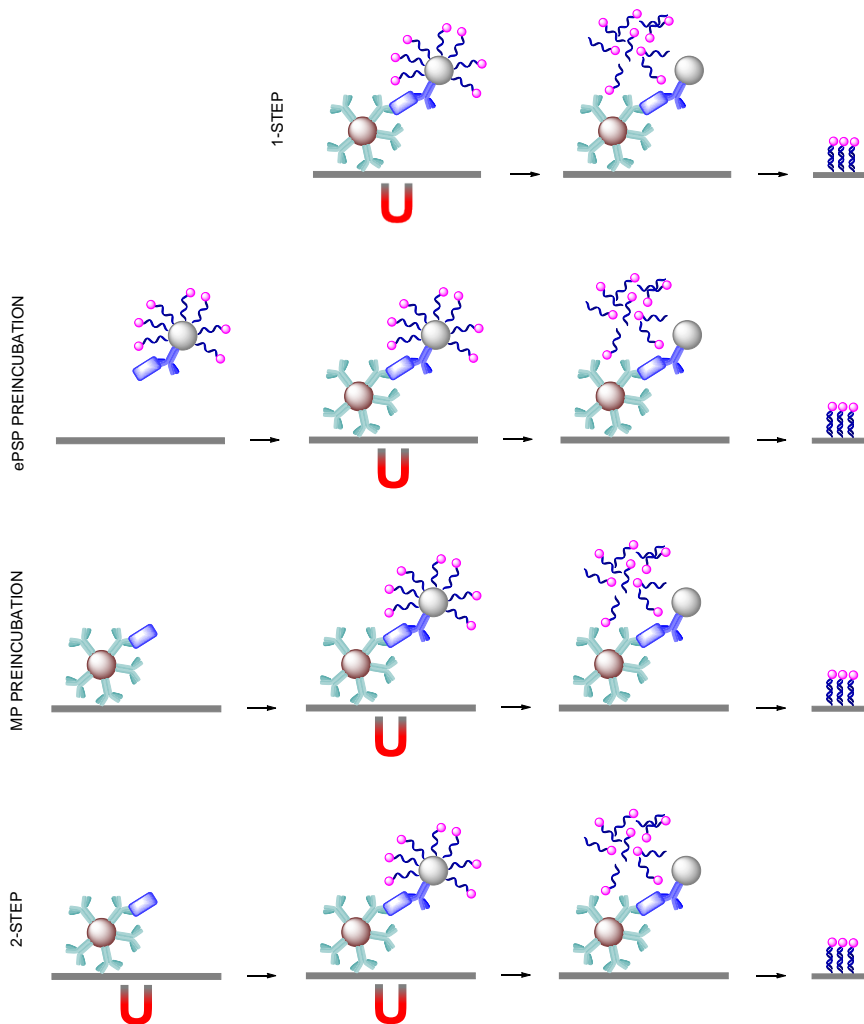


Figure 5.4 Scheme of the step designs evaluated. Scheme is showing assays for sandwich format, in case of competitive format ePSPs are functionalized with an antigen instead of an antibody. The magnets represent a washing step.

Acenocoumarol was previously designed in one-step assay, competitive format, but CRP was designed as two-step assay, sandwich format. Usually sandwich assay is designed in two-steps to avoid matrix effect produced during the interaction between capture antibody and target analyte. First, one-step or two-step assay had to be selected. Both competitive and sandwich assays were evaluated at different step designs. Assays were designed in two-step, one-step,

MP-incubation and ePSP-incubation (Figure 5.4). Incubation refers to mixing the sample with the particles just before adding the other particles. The reason is try to favor the interaction of the target analyte to a certain receptor.

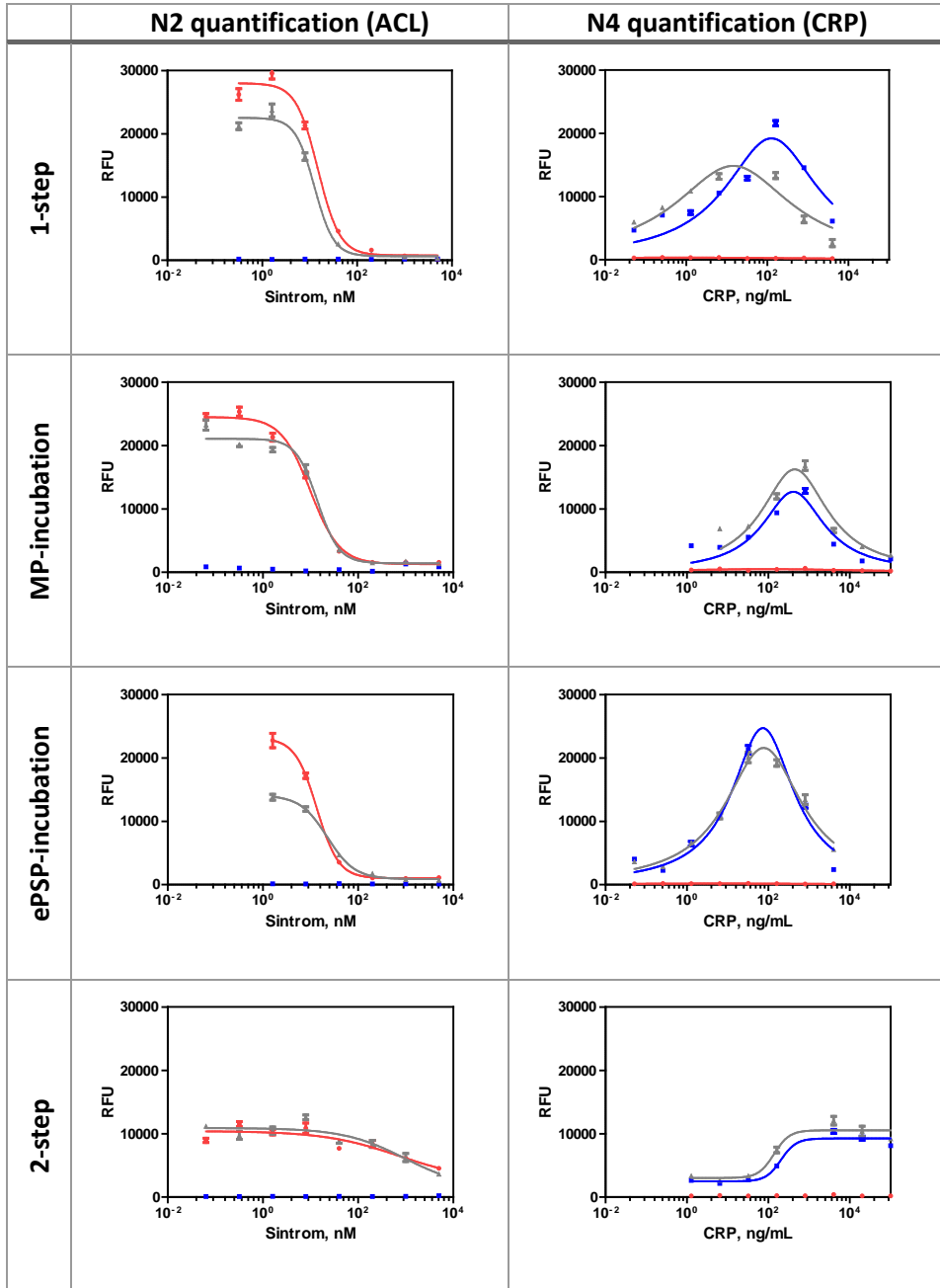


Figure 5.5 Comparison of N2 quantification and N4 quantification in different step design. Red: ACL monoplex assay, blue: CRP monoplex assay, grey: multiplexed assay. Particles concentration were 0.5 mg/mL of pAb236-MP and 0.0125 % w/v of N2-ePSPs for ACL and 0.1 mg/mL of pAbCRP2-MP and 0.05 % w/v of N4-ePSPs for CRP. Each concentration point corresponds to the average of an assay; each calibration point was measured five times.

All step designs were evaluated for ACL and CRP particles, and mixing both particles at the same time. Thus, we not only compared assay steps but checked if particle mixture behaved like monoplex assay. ePSPs were encoded with N2 oligonucleotide for ACL and with N4 for CRP, due to when hybridizing them on the DNA-microarray we could quantify each of them separately.

Results, shown in Figure 5.5, reported a lower fluorescence in the 2-step format, probably by the loss of particles during the washes. Two-step assay for small molecules reports an IC_{50} drastically increased and won't be suitable for multiplexed assay. Although, all experiments in 1-step reported similar results, sandwich assay in 1-step produce the prozone effect. Prozone effect is a false-negative result from a sandwich immunoassay due to very high concentrations of the analyte^{131, 132}. Even though CRP assay won't provide full coverage of the CRP concentration range¹³³, we chose this format since we were able to detect both ACL and CRP. In addition, in a multiplexed assay, the quantification of different compounds will reduce the effect of false negatives²¹ allowing the use of one-step sandwich assay.

Multiplexed and monoplex assays reported the same assay parameters in all cases, proving that there is no crossreactivity between particles and that multiplexed assay of proteins and small molecules is possible. Furthermore, when quantifying N2 signal, N4-ePSPs reported no signal and vice versa, confirming that there is no crossreactivity between N2 and N4 oligonucleotide sequences.

5.3.2 ASSAY DEVELOPMENT

Having selected assay steps, we proceed to the development of the multiplexed assay for ACL and CRP within each compound requirements. Results are enclosed in section 5.4.1. Part of this work have been carried out by Rita McCabe.

5.4 RELATED PUBLICATIONS

5.4.1 PUBLICATION V: A MULTIPLEXED AND MULTIMODAL BIOBARCODE, SIMULTANEOUS TAILORED DETECTION OF SMALL MOLECULES AND PROTEINS

A Multiplexed and Multimodal Biobarcode, simultaneous tailored detection of small molecules and proteins

Marta Broto, Rita McCabe, Roger Galve and M.-Pilar Marco

Submitted

This publication describes, for the first time, the development of a multiplexed and multimodal assay. It is able to quantify two compounds of different chemical nature inside its clinical sample requirements. This work has been carried out with the help of Rita McCabe. She helped with particle preparation and assay development.

A Multiplexed and Multimodal Biobarcode, simultaneously tailored detection of small molecules and proteins

Marta Broto, Rita McCabe, Roger Galve, M.-Pilar Marco*

M. Broto^{1,2}, R. McCabe^{1,2}, R. Galve^{1,2,*}, M.-P. Marco^{1,2}

¹Nanobiotechnology for diagnostics (Nb4D), Department of Chemical and Biomolecular Nanotechnology, Institute for Advanced Chemistry of Catalonia (IQAC) of the Spanish Council for Scientific Research (CSIC).

²CIBER de Bioingeniería, Biomateriales y Nanomedicina (CIBER-BBN), Jordi Girona 18-26, 08034 Barcelona, Spain

*To whom correspondence should be addressed. Phone: 934006100 (Ext. 5117). Fax: 932045904. E-mail: roger.galve@iqac.csic.es

Keywords

Biobarcode, multiplexed, multimodal, indirect competitive, sandwich, acenocoumarol, C-reactive protein

Abstract

For the first time, we report a multiplexed and multimodal NP-based biobarcode assay. The strategy is based on: (1) encoded polystyrene particles (ePSP) functionalized either with an antigen, for a competitive assay format, or with an antibody, for a sandwich assay format, (2) magnetic particles (MP) functionalized with specific antibodies and (3) DNA-microarray for the selective quantification of each coding oligonucleotide. Thus, this assay design was used for the simultaneous detection of two different biomarkers related to cardiovascular diseases, a small molecular weight compound (acenocoumarol, ACL) and a protein (C-reactive protein, CRP), achieving LODs of 3.6 Nm AND 78.4 $\mu\text{g mL}^{-1}$ respectively. In addition, the platform capability for quantifying spiked buffer has been demonstrated reproducible, obtaining recoveries around 110 and 96%. We have demonstrated the feasibility of this strategy as a tool for the multiplexed detection of different chemical nature compounds at different concentration ranges.

Manuscript

Multiplexed bioanalytical techniques have become crucial in clinical diagnostics for different applications: identification of pathogenic diseases within a single run to reduce diagnostic time[1], analysis of disease biomarker panel for a better disease stratification[2] and therapeutic drug-response monitoring to certify the success of a treatment[3]. These applications require the quantification of many targets at the same time. Some bioanalytical techniques have been developed including DNA[4] or protein[5] microarrays, spatially localized ELISA[6], lateral flow biosensors[7], immuno-PCR[8], SPR[9], or recently, microbead based systems for label-based platforms[10]. Each method has its particular advantages and drawbacks. Despite the huge effort done towards the multiplexed revolution, there remains a gap in the development of multimodal techniques. Bioanalytical techniques must face two main challenges: the quantification of many compounds at the same time, either proteins, small molecules, DNA or cells, plus overcoming the fact that they can be present in the sample at different concentration ranges (e.g. mg/mL for serum albumin to few pg/mL for interleukins). Thus, these techniques should be multiplexed, multimodal and able to quantify the target analyte at its appropriate working range. This last objective, to our knowledge, has seldom been addressed. Even though the assay is multiplexed, if the working range is not optimized the sample will need several dilutions to fit the required concentrations for each analyte, losing the multiplexed advantages of a single run. In this communication, we propose a NP-based biobarcode assay combining multiplexed and multimodal techniques. We have developed a NP-based biobarcode for the quantification of two analytes related with cardiovascular diseases (CVDs), a low molecular weight compound (acenocoumarol, ACL) and the C-reactive protein (CRP), at different concentration ranges.

Biobarcode was first reported in 2003[11]. This platform consists on a magnetic particle, that can be isolated by a magnetic field, and an encoded particle that will provide the signal amplification. Several biobarcode assays have been developed for the multiplexed detection[12-15]. In this work, we have designed magnetic particles (MP) with specific antibodies, encoded polystyrene probes (ePSP) with either an antigen or an antibody attached, depending on the assay format, and an oligonucleotide sequence to function as a barcode. Then, after the specific interactions of the particle pairs,

coding nanoprobe can be released and hybridized in a DNA-microarray for subsequent quantification (Figure 1). The signal readout is provided by a fluorophore attached to the coding oligonucleotide. ACL and CRP were selected as a proof of concept since they are related to CVDs, which represent the first cause of death worldwide[16]. ACL is an anticoagulant drug subjected to therapeutic drug monitoring (TDM) due to its narrow therapeutic window and the incidence of bleeding complications of up to 17% of the patients[17]. CRP is an inflammatory-related protein stated as an early stage CVD risk biomarker[18].

First, two complementary pairs of single stranded DNA were designed[19] as coding oligonucleotides (N2 and N4, up and down). They had 50% of G/C content and the same nucleotide composition to supply all pairs with similar hybridization properties. The specificity of the hybridization was studied in a microarray multiplex format reporting no cross-hybridization between them. Then, ePSP were functionalized with the coding oligonucleotides, the antigen in the case of ACL and the detection antibody for the CRP, via activation of a carboxylic group of the particles. Summarizing, ACL ePSPs were functionalized with the specific barcode (N2) and the antigen hACL-BSA while CRP ePSPs were functionalized with the barcode (N4) and the antibody pAbCRP1. Both N2 and N4 oligonucleotide sequences were provided with a fluorophore at the 5'-end, a disulfide bond next to the 3'-end to allow the release with dithiothreitol (DTT) and an amino group at the 3'-end for covalent attachment onto the ePSPs. MP were functionalized with the capture specific antibodies pAb236 and pAbCRP2, respectively for ACL and CRP. Particles were characterized by evaluating the unbound bioreceptor in the supernatant washes. Oligonucleotide sequences showed between 75-85% yields, reporting higher yields when a higher quantity of oligonucleotide was added. Antigen conjugation reported a yield of 33%, in contrast to the 100% antibody conjugation yield. The main explanation for this behavior is that the antigen had already been conjugated to the target hapten via primary amines, reducing its availability for conjugation with the particle. Regarding the antibodies coupled to MPs, in the case of ACL, a low concentration of antibody was coated, while for CRP an excess of antibody was coated reaching MP saturation and reporting a lower conjugation yield (53%).

Next, a suitable concentration of both encoded probe and magnetic particles were chosen with 2D checkerboard assays. Our first objective was to prove

that the multiplexed assay behaved as monoplexed assays. Calibration curves were prepared with ACL specific particles and CRP specific particles, separately and both ACL and CRP particles mixed in the same well. The comparison (Figure S1 and Table S1) reported similar detectability results for both monoplexed and multiplexed assays in the same order of magnitude. CRP assay in the mixture of particles reported a slight increase of signal but a similar slope and IC_{50} . Furthermore, no signal was obtained from CRP when quantifying N2 oligonucleotide neither ACL when quantifying N4 oligonucleotide confirming that there is no cross-reactivity between sequences. In conclusion, we can work with the particle mixture reporting the same results as obtained monoplexed assays.

Subsequently, assay working range had to be established for both compounds to fit human sample requirements (30 – 300 nM for ACL[20] and 1000 – 3000 ng/mL for CRP [21]). Due to our experience within biobarcode development and working range modulation, we could maintain detectability of ACL [ref ACL], but tailored the detectability of CRP within a 7-fold decrease from our previous developed assay [ref CRP]. We worsened the CRP assay detectability by increasing the quantity of antibodies attached on the MP. Obviously, the assay required a higher concentration of analyte for its saturation. Figure 2 shows the calibration curve obtained and the assay features. ACL assay is in a competitive format showing an inhibition curve. CRP assay is a one-step sandwich format showing a prozone effect at high concentrations of the analyte[22, 23]. Prozone effect is a false-negative result that limits the assay coverage of CRP concentration range[24]. Despite the limitation of CRP above a certain concentration, multiplexed assays are able to reduce the effect of false-negatives analyzing more than one biomarker[25]. Consequently, under the final conditions, a working range of 6.9 to 29.4 nM of ACL and 109.9 to 368.8 ng/mL of CRP were obtained, fitting human samples within a 1/10 dilution.

Finally, to demonstrate the potential of our developed assay, 8 blind samples were prepared spiking PBST with different concentration of ACL and CRP, as it can be observed in Figure 3.A. Good recoveries were obtained with all of the samples, even samples E and G that were only spiked with ACL or CRP respectively, reporting zero concentration of the other analyte. A mean recovery of 110% and 96% were obtained for both compounds. Furthermore, spiked and found concentrations comparison (Figure 3.B and

3C) reported a really good accuracy. Both compounds matched the spiked concentrations with slopes of 1.110 and 0.966, for ACL and CRP respectively, with an acceptable regression coefficient.

In conclusion, we have been able to develop a multiplexed and multimodal NP-based assay for the quantification of a low molecular weight drug, acenocoumarol, and a protein, CRP. Calibration curves showed a LOD of 3.6 nM and 78.4 ng/mL. Detectability has been modulated to fit human samples requirements within a sole dilution, 1/10. The assay has been challenged with blind samples in buffer, reporting an accuracy with a slope of 1.110 and 0.966, respectively.

Experimental section

Materials and Instruments: Polystyrene particles (PSP) were carboxy modified Dyed Microspheres (K1 050 noir) were supplied by Estapor[®] (Millipore Corp., Billerica, MA, USA). The magnetic particles (MP), Dynabeads MyOne Tosylactivated, and the magnetic rack Magnarack[™] were obtained from Invitrogen (Life technologies[™], Paisley, UK). The pre-cleaned plain slides were purchased from Corning[®] (Corning Inc., New York, NY, USA). Functionalized slides were spotted with a BioOdyssey Calligrapher MiniArrayer (Bio-Rad Laboratories, Inc. USA). Measurements were recorded on a ScanArray Gx PLUS (Perkin Elmer, USA) with a Cy3 optical filter with 5- μ m resolution. Slide gaskets were purchased from ArrayIt Coporation (Sunnyvale, CA, USA). U-bottom polystyrene microplates were purchased from Nirco (Barberà del Vallès, Spain). IKA[®] MS 3 basic shaker with a MS 3.4 Microtiter attachment (IKA[®], Staufen, Germany) was used to shake the microplates at 800 rpm. A thermo-shaker (TS-100C Biosan, Riga, Latvia) was used to shake Eppendorfs. Eppendorfs were centrifuged with a Legend Micro 21, for 10 min, at 17500G (Thermo Fisher Scientific Inc.) and plates were centrifuged with a Centrifuge 5810 R, for 10 min, at 3220 G (Eppendorf, Hamburg, Germany). The pH and the conductivity of all buffers and solutions were measured with a 540 GLP pH meter and an LF 340 conductimeter (WTW, Weilheim, Germany), respectively. Absorbance and fluorescence were read on a Spectramax Plus and a Spectramax Gemini XPS (Molecular Devices, Sunnyvale, CA, USA), respectively.

Chemicals and biochemicals. The chemical reagents used were obtained from Aldrich Chemical Co. (Milwaukee, WI, USA) and from Sigma

Chemical Co. (St. Louis, MO, USA). N2_{down}-NH₂ and N4_{down}-NH₂ oligonucleotide sequences, [AmC6F] CGGAGGTACATTCTGACTTGA and [AmC6F] TCCAGCGTTAGTGTACAGAG, were purchased from Sigma Chemical Co. (St. Louis, MO, USA) and TAMRA-N2_{up}-SS-NH₂ and TAMRA-N4_{up}-SS-NH₂, [TAMRA] TCAAGTCGAATGTACCTCCG [ThiolC6SS] [AminolinkC6] and [TAMRA] CTCTGTACTAACGCTGGA [ThiolC6SS] [AminolinkC6], were obtained from Biomers (GmbH, Ulm, Germany). The immunoreagents used for ACL detection (Protein A purified antibody pAb236 and antigen hACL-BSA) were developed in our laboratory. The ACL stock solution was prepared at 10 mM in DMSO and stored at 4°C. The two antibodies for CRP (pAbCRP1 and pAbCRP2) were supplied by Audit Diagnostics (Cork, Ireland). The CRP stock, 2700 µg/mL, was purchased from Fitzgerald (Acton, MA, USA).

General procedures: On the scanner measurements, the laser power and PMT were set at 90% and 70%, respectively. The spots were measured by F543_Mean-B543 (Mean Cy3 foreground intensity minus mean Cy3 background intensity). Fluorescence intensity values were expressed normalized or in relative units as average and standard deviation of five replicate wells. The competitive curves were analyzed with a four-parameter logistic equation using software (GraphPad Prism version 5.03 for Windows, GraphPad Software, San Diego, California, USA). The standard curve was fitted to a four-parameter equation according to the following formula: $Y = [(A - B) / (1 + (x/C)^D)] + B$, where A is the maximal fluorescence, B the minimum fluorescence, C the concentration producing 50% of the difference between A and B (or IC₅₀), and D the slope at the inflection point of the sigmoid curve. The limit of detection (LOD) was defined as the concentration producing 90% or 10% of the maximal fluorescence (IC₉₀ or IC₁₀) for competitive and sandwich formats respectively, and working range was defined as the concentration producing 20% to 80% of the maximal fluorescence (IC₂₀-IC₈₀). All the incubation steps performed on the U-bottomed microplates were performed at 25 °C and 800 rpm using the microtiter shaker.

Buffers. PBS was 0.01 M phosphate buffer in a 0.8% saline solution (137 mmol L⁻¹ NaCl, 2.7 mmol L⁻¹ KCl), and the pH was 7.5. PBST was PBS with 0.05% Tween 20. PSPs coupling buffer was 100 mM carbonate buffer pH 9. MP A buffer was 0.1 M borate buffer (pH 9.5). MP C buffer was 3 M

ammonium sulphate in MP A buffer (pH 9.5). MP blocking buffer was PBST with 0.5 % BSA. MP storage buffer was PBST with 0.1 % BSA. Printing buffer comprised 150 mM sodium phosphate and 0.01 % sodium dodecyl sulphate (SDS) and the pH was 8.5. Hybridization buffer was 10 mM TRIS, 1 mM EDTA, 1M NaCl and the pH was 7.2.

Microarray printing. Slides were cleaned by immersing them in piranha solution ($\text{H}_2\text{SO}_4:\text{H}_2\text{O}_2$ 7:3) during 30 min; washed with purified water and immersed in 10% NaOH for 30 min; washed with water and ethanol and dried. The activation of the slides was performed by immersing them in (3-glycidoxypropyl)methyldiethoxysilane during 30 min. Afterwards, the slides were washed with ethanol and dried. These epoxidized slides can be stored in a dessicator for long periods of time. Finally, the oligonucleotide ($\text{N}2_{\text{down}}\text{-NH}_2$ and $\text{N}4_{\text{down}}\text{-NH}_2$, 200 ng mL^{-1} in printing buffer) was spotted onto substrates in a high-humidity chamber, maintained for 30 min at room temperature and finally stored overnight at 4°C . Each glass slide was printed with 24 (8 x 3) microarrays. A 5 x 4 spot matrix was printed on each grid (ten spots replicated per sequence).

Encoded polystyrene particles (ePSP). Polystyrene particles (PSPs, 10% w/v solution, $40 \mu\text{L}$) were washed twice with PSPs coupling buffer ($500 \mu\text{L}$). Subsequently, a solution of a combination of oligonucleotide probes and bioreceptor (TAMRA- $\text{N}2_{\text{up}}\text{-SS-NH}_2$, $0.60 \mu\text{M}$, and hACL-BSA bioconjugate, $0.07 \mu\text{M}$, in $320 \mu\text{L}$ of PSPs coupling buffer for ACL PSP and TAMRA- $\text{N}4_{\text{up}}\text{-SS-NH}_2$, $0.34 \mu\text{M}$, and pAbCRP1, $0.13 \mu\text{M}$, in $320 \mu\text{L}$ of PSPs coupling buffer for CRP PSP) followed by a solution of EDC (500 mM , $80 \mu\text{L}$ in PSPs coupling buffer) were added and the mixture was allowed to react at 25°C for 3 h under shaking conditions/ subjected to shaking (750 rpm). Afterwards, the supernatant was removed and the efficiency of the coupling reaction was checked by analyzing the remaining bioreceptor and oligonucleotide probes by ELISA and by fluorescence (543 nm excitation, 575 nm emission), respectively. A conjugation yield of 85 % of TAMRA- $\text{N}2_{\text{up}}\text{-SS-NH}_2$, 33% of BSA-hACL, 75 % of TAMRA- $\text{N}4_{\text{up}}\text{-SS-NH}_2$ and 100 % of pAbCRP1 were obtained. The suspension was then washed twice with PBST and stored in $400 \mu\text{L}$ of PBS at 4°C for at least 1 month.

Oligonucleotide release. PSPs functionalized solution ($25 \mu\text{L}$) was treated with DTT (0.2 M , $100 \mu\text{L}$ of hybridization buffer) and allowed to react for 1

h at 60°C using the shaker (750 rpm). The suspension was then centrifuged and the supernatant was used to quantify the fluorescence released as described above. A release yield of 49 % and 47% were obtained respectively for each oligonucleotide.

Magnetic particles (MP). ACL specific (pAb236) and CRP specific (pAbCRP2) antibodies were covalently coupled to magnetic particles (MP) following the manufacturer supplier procedure with slight modifications. Briefly, Dynabeads MyOne Tosylactivated (100 mg mL⁻¹, 200 µL) were washed with MP A buffer (2 x 1000 µL) and a solution of pAb236 (400 µL, 0.75 mg mL⁻¹ in MP A buffer) or pAbCRP2 (400 µL, 3 mg mL⁻¹ in MP A buffer) was added followed by the addition of MP C buffer (200 µL). The mixture was allowed to react protected from light overnight at 37°C under shaking 750 rpm. The day after the supernatant was removed and analyzed by the Bradford protein test to estimate the efficiency of the coupling reaction/procedure. A conjugation yield of 100 % and 69 % was obtained respectively for pAb236 and pAbCRP1. Next, the biofunctionalized particles were resuspended in MP blocking buffer and allowed to stand? overnight again, before the supernatant was removed and particles were washed with MP storage buffer (1000 µL x 2) and finally resuspended in 1000 µL for storage at 4°C for at least two months.

Two-dimensional Checkerboard Titration Experiments (2D-assay). The binding of MP (from 0 to 2 mg mL⁻¹) to PSP (from 0.013 to 0.05 %) was evaluated through different concentrations, prepared with serial dilutions, of the NP. Afterwards the microplates were washed (4 x 200 µL, PBST), a solution of 0.2 M DTT (in hybridation buffer, 100 µL/well) was added and the mixtures were allowed to react for 1 h at 60°C subject to shaking (800 rpm). The microplates were then centrifuged and the supernatant, where the released oligonucleotide probes were found, was transferred to a previously washed (4 x 200 µL) DNA microarray slide and allowed to hybridize for 30 min at RT (500 rpm). Then, the slide was washed once more (4 x 200 µL) with PBST and one last time with milliQ water (200 µL) outside the gasket. From these experiments, optimum concentrations for both particles were chosen.

Competitive indirect biobarcode assay. Before starting, both the MP and the PSP were washed with PBST (2 x 10 times its volume). The standards (ACL, 500 to 0 nM in PBST, and CRP, 1600 to 0 ng mL⁻¹, 50 µL) or the

samples (diluted 1/12 in PBST) were mixed with the MP (25 μL , 0.5 mg mL^{-1} for ACL and 1 mg mL^{-1} for CRP in PBST) and the PSP (25 μL , 0.0125 % w/v for ACL and 0.05 % w/v for CRP in PBST) and incubated. Then, the biocomplexes were processed as described above for the non-competitive assay to measure the released oligonucleotide probes on the DNA microarray.

Recovery studies. The recovery of the analyte concentration was assessed with samples prepared by spiking PBST at 7 different concentrations of ACL (from 0 to 300 nM) and CRP (from 1000 to 3000 ng/mL). These were analyzed three times. The ACL and CRP concentration found in the samples was calculated by interpolating the fluorescent signal recorded on a calibration curve, which was processed the same way as the samples. The results were fitted to a linear regression curve representing the relationship between the spiked and the measured concentration values.

Supporting Information

Supporting Information is available the Wiley Online Library or from the author.

Acknowledgements

This work has been funded by the ministry of Economy and Competitiveness (MAT2012-38573-C02-01). The Nb4D group (formerly Applied Molecular Receptors group, AMRg) is a consolidated research group (Grup de Recerca) of the Generalitat de Catalunya and has support from the Departament d'Universitats, Recerca i Societat de la Informació de la Generalitat de Catalunya (expedient : 2014 SGR 1484). CIBER-BBN is an initiative funded by the Spanish National Plan for Scientific and Technical Research and Innovation 2013-2016, Iniciativa Ingenio 2010, Consolider Program, CIBER Actions are financed by the Instituto de Salud Carlos III with assistance from the European Regional Development Fund. Marta Broto wishes to thank the FPI-fellowship (BES-2013-062819) from the Spanish Ministry of Economy and Competitiveness.

References

1. Deshpande, A.; White, P. S., *Expert Review of Molecular Diagnostics* **2012**, *12* (6), 645-659. DOI 10.1586/erm.12.60.
2. Gupta, V. B.; Sundaram, R.; Martins, R. N., *Alzheimer's Research & Therapy* **2013**, *5* (3), 31-31. DOI 10.1186/alzrt185.

3. McKeating, K. S.; Aube, A.; Masson, J.-F., *Analyst* **2016**, *141* (2), 429-449. DOI 10.1039/c5an01861g.
4. Donatin, E.; Drancourt, M., *Médecine et Maladies Infectieuses* **2012**, *42* (10), 453-459. DOI <http://dx.doi.org/10.1016/j.medmal.2012.07.017>.
5. Moore, C. D.; Ajala, O. Z.; Zhu, H., *Current Opinion in Chemical Biology* **2016**, *30*, 21-27. DOI <http://dx.doi.org/10.1016/j.cbpa.2015.10.013>.
6. Tighe, P. J.; Ryder, R. R.; Todd, I.; Fairclough, L. C., *Proteomics Clinical Applications* **2015**, *9* (3-4), 406-422. DOI 10.1002/prca.201400130.
7. Li, J.; Macdonald, J., *Biosensors & Bioelectronics* **2016**, *83*, 177-192. DOI 10.1016/j.bios.2016.04.021.
8. Ryazantsev, D. Y.; Voronina, D. V.; Zavriev, S. K., *Biochemistry (Moscow)* **2016**, *81* (13), 1754-1770. DOI 10.1134/s0006297916130113.
9. Spindel, S.; Sapsford, K. E., *Sensors* **2014**, *14* (12), 22313-22341. DOI 10.3390/s141222313.
10. Lee-Montiel, F. T.; Li, P.; Imoukhuede, P. I., *Nanoscale* **2015**, *7* (44), 18504-18514. DOI 10.1039/C5NR01455G.
11. Nam, J.-M.; Thaxton, C. S.; Mirkin, C. A., *Science* **2003**, *301* (5641), 1884-1886.
12. Cho, M.; Chung, S.; Kim, Y. T.; Jung, J. H.; Kim, D. H.; Seo, T. S., *Lab on a Chip* **2015**, *15* (13), 2744-2748. DOI 10.1039/C5LC00355E.
13. Lee, H.; Park, J.-E.; Nam, J.-M., *Nat Commun* **2014**, *5*. DOI 10.1038/ncomms4367.
14. Stoeva, S. I.; Lee, J.-S.; Smith, J. E.; Rosen, S. T.; Mirkin, C. A., *Journal of the American Chemical Society* **2006**, *128* (26), 8378-8379. DOI 10.1021/ja0613106.
15. Stoeva, S. I.; Lee, J.-S.; Thaxton, C. S.; Mirkin, C. A., *Angewandte Chemie International Edition* **2006**, *45* (20), 3303-3306. DOI 10.1002/anie.200600124.
16. Organization, W. H. The top 10 causes of death. <http://www.who.int/mediacentre/factsheets/fs310/en/>.
17. Stehle, S.; Kirchheiner, J.; Lazar, A.; Fuhr, U., *Clin Pharmacokinet* **2008**, *47* (9), 565-94.
18. Black, S.; Kushner, I.; Samols, D., *The Journal of biological chemistry* **2004**, *279* (47), 48487-90. DOI 10.1074/jbc.R400025200.
19. Tort, N.; Salvador, J. P.; Marco, M. P.; Eritja, R.; Poch, M.; Martínez, E.; Samitier, J., *TrAC Trends in Analytical Chemistry* **2009**, *28* (6), 718-728. DOI <http://dx.doi.org/10.1016/j.trac.2009.04.003>.

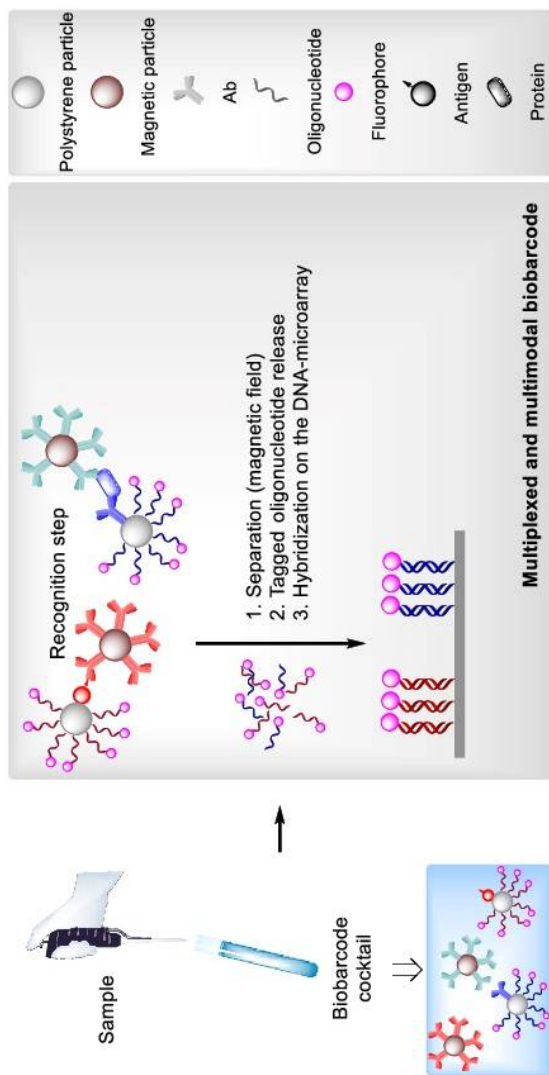
20. Ufer, M., *Clin Pharmacokinet* **2005**, *44* (12), 1227-46. DOI 10.2165/00003088-200544120-00003.
21. Myers, G. L.; Christenson, R. H.; Cushman, M.; Ballantyne, C. M.; Cooper, G. R.; Pfeiffer, C. M.; Grundy, S. M.; Labarthe, D. R.; Levy, D.; Rifai, N.; Wilson, P. W., *Clin Chem* **2009**, *55* (2), 378-84. DOI 10.1373/clinchem.2008.115899.
22. Amarasiri Fernando, S.; Wilson, G. S., *Journal of Immunological Methods* **1992**, *151* (1), 47-66. DOI [http://dx.doi.org/10.1016/0022-1759\(92\)90104-2](http://dx.doi.org/10.1016/0022-1759(92)90104-2).
23. Rodbard, D.; Feldman, Y.; Jaffe, M. L.; Miles, L. E. M., *Immunochemistry* **1978**, *15* (2), 77-82. DOI [http://dx.doi.org/10.1016/0161-5890\(78\)90046-9](http://dx.doi.org/10.1016/0161-5890(78)90046-9).
24. Oh, Y. K.; Joung, H.-A.; Han, H. S.; Suk, H.-J.; Kim, M.-G., *Biosensors and Bioelectronics* **2014**, *61*, 285-289. DOI <http://dx.doi.org/10.1016/j.bios.2014.04.032>.
25. Rusling, J. F.; Kumar, C. V.; Gutkind, J. S.; Patel, V., *Analyst* **2010**, *135* (10), 2496-2511. DOI 10.1039/C0AN00204F.

Figures

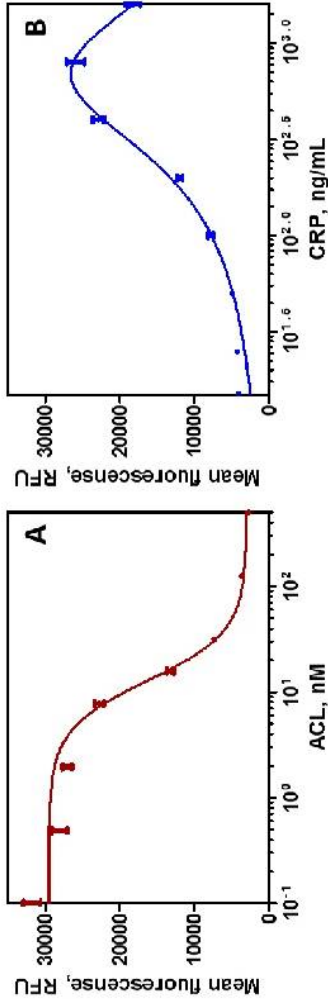
Figure 1. A schematic representation of a multiplexed and multimodal biobarcode assay. The sample is mixed with the particle probes. Then, the immunocomplexes formed are isolated and the oligonucleotide codes are released and hybridized in a glass microarray for subsequent quantification.

Figure 2. Calibration curve of the biobarcode assay for ACL (**A**) and CRP (**B**) run in buffer. The data presented corresponds to the average of three assays performed throughout three different days. On every assay, each calibration point was measured five times. The parameters have been extracted from the four-parameter equation used to fit the standard curves. ^aDR corresponds to the working range, calculated as the concentration given between 20 and 80% of the maximum absorbance. The CV% at the middle point of the assay is 7.1 for ACL and 21.0 for CRP.

Figure 3. Results from the accuracy study performed using blind samples prepared by spiking PBST. **A.** The graph shows the spiked concentration of 8 different samples with different quantities of ACL and CRP and the concentration found. The samples, diluted 1/10, were quantified using calibration curves prepared in buffer. The data correspond to the average of at least three different assays. **B. C.** The graph shows the correlation between the spiked and measured concentration values for ACL (**B**) and CRP (**C**). The dotted line corresponds to a perfect correlation ($m=1$). The samples, diluted 1/10, were quantified using calibration curves prepared in buffer. The data correspond to the average of at least three different assays. The % CV at the middle point of the assay is 28.3 for ACL and 21.3 for CRP.



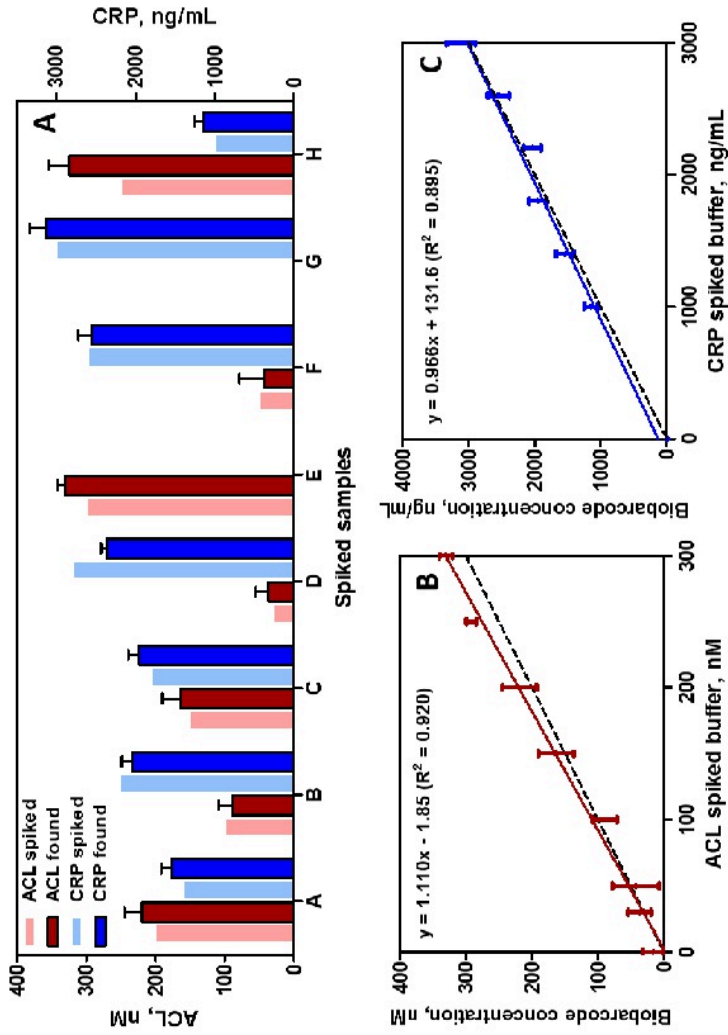
Broto et al. **Figure 1**



Multiplexed biobarcode assay parameters

Assays	ACL	CRP
DNA/ePSP	600	1400
% ePSPs	0.0125	0.0125
mg/mL MP	0.5	0.5
RFU_{min}	2662 ± 89	4101 ± 906
RFU_{max}	27414 ± 2405	31316 ± 10345
m	-2,29 ± 0.69	2,35 ± 0.55
R^2	0.91 ± 0.03	0.95 ± 0.03
IC_{50} , nM or ng/mL	15.6 ± 1.1	238.7 ± 50.2
DR^2 , nM or ng/mL	From 6.9 ± 1.2 to 29.4 ± 6.5	From 109.9 ± 9.9 to 368.8 ± 71.8
LOD, nM or ng/mL	3.6 ± 1.2	78.4 ± 14.9

Broto et al. **Figure 2**



Broto et al. **Figure 3**

Supporting Information

A Multiplexed and Multimodal Biobarcode, simultaneous tailored detection of small molecules and proteins

M. Broto^{1,2}, R. McCabe^{1,2}, R. Galve^{1,2,*}, M.-P. Marco^{1,2}

¹Nanobiotechnology for diagnostics (Nb4D), Department of Chemical and Biomolecular Nanotechnology, Institute for Advanced Chemistry of Catalonia (IQAC) of the Spanish Council for Scientific Research (CSIC).

²CIBER de Bioingeniería, Biomateriales y Nanomedicina (CIBER-BBN), Jordi Girona 18-26, 08034 Barcelona, Spain

*To whom correspondence should be addressed. Phone: 934006100 (Ext. 5117). Fax: 932045904. E-mail: roger.galve@iqac.csic.es

Monoplexed and multiplexed comparison

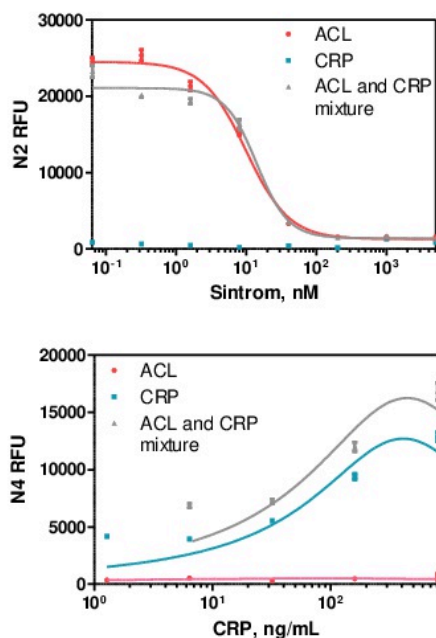


Figure S1. Comparison of calibration curves of monoplexed assays with the mixture of particles. The data was adjusted to a four-parameter logistic equation. Each concentration point corresponds to the average of five replicates. The analytical parameters can be found in Table S1.

Table S1. Monoplexed and multiplexed calibration curve comparison

	ACL	ACL mixture	CRP mixture	CRP
mg/mL MP	0.5	0.5	1	1
% PSPs	0.0125	0.0125	0.05	0.05
RFU_{min}	1287	1411	3951	6837
RFU_{max}	24485	21061	13901	17240
<i>m</i>	-1.416	-1.925	2.134	2.209
R²	0.980	0.970	0.957	0.900
IC₅₀, nM or ng/mL	9.9	14.0	136.4	161.8

The data has been extracted from the four-parameter equation used to fit the standard curves. It shows the average of the parameters of assays using 5 replicates for each concentration of ACL standard measured.

5.5 CHAPTER CONTRIBUTIONS

- Multiplexed and multimodal biobarcode assay has proven achievable. Multiplexed results were comparable to monoplexed ones; these results confirm biobarcode as a golden platform for multiplexed analysis.
- Furthermore, exciting results were obtained in accuracy results for the quantification of both target analytes, succeeding at detecting compounds at different concentration ranges.

6 CONCLUSIONS

- In spite of the extraordinary effort made synthesizing an immunizing hapten preserving all the important chemical groups (5FU6) and two other haptens (5FU1 and 5FU3) with also excellent features for raising antibodies, it has been difficult to establish a competitive immunochemical assay for 5FU. At the time of writing this thesis we have not been able to find an explanation for this fact, since the antibodies obtained showed a very high avidity for the immunizing haptens, which showed only small chemical differences with 5FU. However, trying to increment the heterology of the competitor bioconjugate did favour the recognition of the target.
- Surprisingly, tegafur, a prodrug of 5FU with a tetrahydrofuran group at position 1, was able to compete effectively in the assay using the antibodies raised against hapten 5FU1, allowing its detection on a competitive immunochemical format with LOD near 3 nM. This fact has raised the possibility that the hapten 5FU1 could have been rearranged under the conditions used for its bioconjugation to HCH leading to an unexpected structure bearing a ring at position 1. This fact would need to be investigated in more detail.
- A new hapten for CP (CP2-Cl) has been reported for the first time. This hapten is designed trying to expose the cyclophosphamide moiety instead of the mustard one. This hapten has been used to raise antibodies that combined with an heterologous competitor lead to a competitive immunoassay with a LOD of 46 nM.
- Biofunctionalization of polystyrene particles with oligonucleotides bearing a disulphide bond in the 5'-end is a simple procedure to prepare encoded probes and allows using them on biobarcode assays on an efficient manner, by just releasing the coding oligonucleotide with dithiothreitol (DTT) instead of using double stranded DNA to encode the particles as described by other authors. Moreover, the procedure established allows preparing multifunctional probes in which the ratio between the bioreceptor molecules and the oligonucleotide codes could be easily varied in a reproducible manner.
- It has been possible for almost the first time to develop a biobarcode assay based on a competitive immunochemical format. The assay allows detecting the oral anticoagulant acenocoumarol, in serum and plasma samples without any other sample treatment. Also, to establish a

biobarcode assay for the pentameric C-reactive protein (CRP) using a sandwich immunochemical format. The biobarcode assay has found to be useful for measuring the biomarker in plasma samples.

- The possibility to modulate signal amplification and working range of the biobarcode assays has been demonstrated, by just varying the load of the oligonucleotides on the encoded probes. This fact opens the door to the development of multiplexed biobarcode platforms able to overcome one of the main challenges of this type of bioanalytical techniques: the possibility to measure simultaneously analytes present on a sample at different concentration ranges.
- We have demonstrated that the biobarcode strategy allows detecting different chemical entities at the same time since any binding reaction is finally converted to DNA by the release of the oligonucleotides of the codified particles. The released oligonucleotides are finally measured on DNA microarray. Thus, acenocoumarol and CRP have been measured simultaneously on a biobarcode multiplexed platform with comparable detectability to the previously developed single biobarcode assays.

7 RESUM

(Aquest apartat està redactat en català d'acord amb un dels requisits establerts en l'article 37 de la normativa reguladora del doctorat a l'empara del RD 99/2011 i de la Comissió de Doctorat de la Facultat de Química. "Quan la totalitat de la tesi es presenta en una llengua diferent de les especificades al programa de doctorat, s'exigeix que es presenti un resum que no sigui inferior a un 10% del volum redactat en l'altra llengua").

L'estructura del resum en català es pot observar a la Figura 7.1.

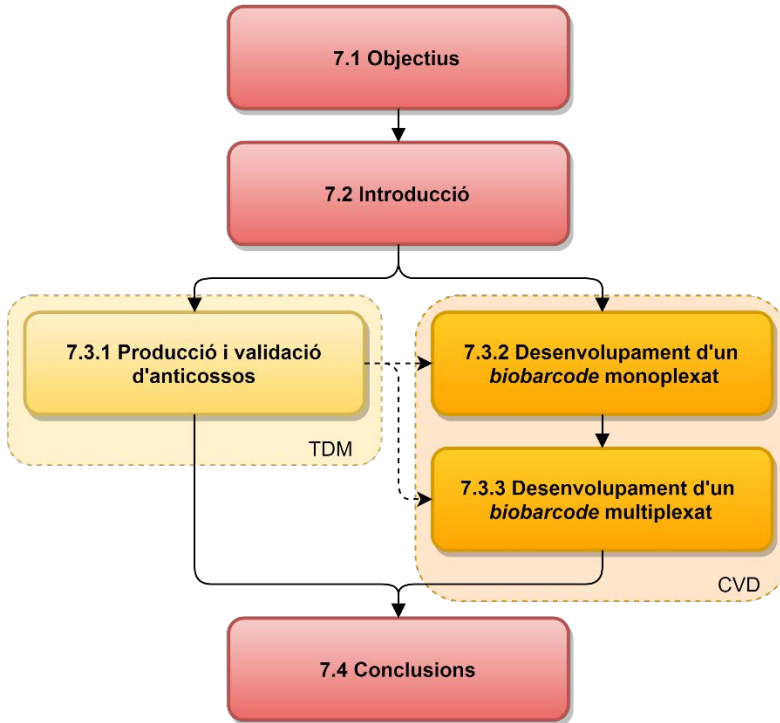


Figura 7.1 Estructura del capítol en relació amb les seves seccions.

7.1 OBJECTIUS

El principal objectiu de la tesi és demostrar la universalitat del sistema *biobarcode*, utilitzar oligonucleòtids com a codis de barres per detectar analits de diferent naturalesa química. El *biobarcode* és una tècnica desenvolupada recentment que ha demostrat que pot detectar múltiples biomarcadors en una mateixa plataforma codificada per seqüències d'oligonucleòtids.

Per tal d'abordar l'objectiu principal, cal desenvolupar uns objectius secundaris:

1. Establir un procediment per preparar partícules codificades d'una manera reproducible. Amb aquest objectiu, anticossos o antigens i seqüències d'oligonucleòtids per cada analit s'enllaçaran covalentment a les partícules, cadascun en un percentatge específic.

2. Estudiar el mètode més eficient per alliberar les seqüències d'oligonucleòtids de les partícules codificades per tal d'aconseguir un màxim rendiment.
3. Avaluar la possibilitat de modular l'amplificació de la senyal de la plataforma variant la càrrega d'oligonucleòtid codificant sobre la partícula.
4. Desenvolupament i avaluació de l'assaig *biobarcode* per cadascun dels analits escollits. Aquesta tasca inclourà l'ús d'immunoreactius produïts per proteïnes i molècules petites, i serà de vital importància la consideració de les necessitats de detectabilitat d'aquestes molècules.
5. Avaluar la possibilitat de desenvolupar un assaig multiplexat que combini les diferents partícules amb l'objectiu de quantificar simultàniament diferents molècules en una sola mesura.

7.2 INTRODUCCIÓ

Un dispositiu mèdic per a la diagnosi *in vitro* es defineix com qualsevol reactiu, instrument, aparell o sistema dissenyat per tal d'analitzar mostres clíniques, com sang o teixits, amb la finalitat d'aportar informació sobre el contingut de la mostra.

Actualment, la majoria de tècniques utilitzades en diagnosi són tècniques cromatogràfiques i PCR (reacció de polimerasa en cadena). El principal inconvenient d'aquestes tècniques és la durada dels anàlisis, la necessitat de personal qualificat i un preu elevat. Donades aquestes circumstàncies, és necessari el desenvolupament de noves tècniques que siguin fiables, de baix cost, sensibles, ràpides i fàcils d'utilitzar. Les tècniques bioanalítiques compleixen amb tots aquests requisits, aquestes utilitzen un element de natura biològica per tal de dur a terme el reconeixement de l'analit.

Per altra banda, la medicina personalitzada està adquirint una certa importància en l'àmbit clínic. Una de les principals característiques que ha tenir un dispositiu de diagnòstic per abordar la medicina personalitzada és l'anàlisi de diferents compostos a la vegada. Aquesta necessitat ve donada per tres principals problemàtiques: la identificació d'organismes patògens, l'anàlisi d'un panell de

biomarcadors per una certa malaltia i el monitoratge terapèutic de l'administració de fàrmacs¹⁴. Primer, la identificació de múltiples patògens en un sol anàlisi permetria reduir el temps d'anàlisi i d'identificació del patogen, permetent començar el tractament en estadis inicials de la infecció⁵. Segon, s'ha demostrat que per certes malalties un únic biomarcador no és suficient per determinar l'estat del pacient o la progressió de la malaltia¹⁶⁻²⁰. Analitzar més d'un biomarcador podria aportar un diagnosi de la malaltia més acurat i, a més, reduir el nombre de falsos negatius o positius²¹. Per últim, el monitoratge terapèutic es centra en la quantificació de la concentració de un fàrmac en fluids biològics per tal d'avaluar la possible resposta i ajustar la dosi²². Per altra banda, el monitoratge de biomarcadors de resposta a un cert tractament permet confirmar l'eficàcia d'aquest²⁵. Així, el monitoratge del fàrmac i el biomarcador de resposta podrien permetre el control necessari per assegurar l'èxit del tractament²⁵.

7.2.1 TÈCNiques BIOANALÍTiques MULTIPLEXADES

Les tècniques multiplexades han d'enfrontar-se amb diverses necessitats. Els compostos a analitzar poden ser de diferent naturalesa química: no només les proteïnes però les molècules petites i els miRNA estan prenent rellevància. Aquests poden estar presents en intervals de concentració molt diferents, per exemple, 41 mg/mL per algunes albúmines i pocs pg/mL per interleuquines en sang, més de nou ordres de magnitud. Així, per tal d'abordar la medicina personalitzada calen assajos multiplexats i multimodals.

A l'hora de dissenyar assajos multiplexats, aquests s'han dissenyat basats en dos principals plataformes com són la localització espacial en superfícies 2D, o bé la utilització de marcadors⁶. Per una banda, la localització espacial de reactius en superfícies 2D, també anomenat bioxip, s'ha aconseguit desenvolupar amb diferents tècniques de lectura com fluorescència, fibra òptica, quimioluminescència, elèctrica, o electroquímica. Per altra banda, s'han desenvolupat sistemes en suspensió els quals utilitzen marcadors o partícules codificades per discernir entre un analit o un altre. Entre les partícules utilitzades n'hi ha de diferents tipus com els *quantum dots* (partícules semiconductores amb diferents espectres d'emissió), partícules d'or i partícules magnètiques⁸⁰.

Tot i la gran quantitat de propostes de assajos multiplexats, encara no s'ha desenvolupat cap assaig que uneixi les característiques necessàries per ser la tècnica definitiva per la medicina personalitzada. El principal desavantatge de la majoria de plataformes és la detecció d'un sol tipus de naturalesa química. Amb aquest objectiu, en aquesta tesi es proposa el *biobarcode*, una assaig bioanalític que s'ha demostrat que es pot aplicar per la detecció de compostos de diferent naturalesa química⁷⁻⁹, diferents compostos a la vegada^{10, 11} i, a més, arribant a detectar concentracions tant baixes com zM¹².

7.2.1.1 Biobarcode

Les seqüències d'ADN tenen unes característiques especials com la seva capacitat d'hibridar amb la seva complementària, el sistema basat només en 4 bases aparellables, la seva síntesi automatitzada i la possible funcionalització amb marcadors.

Combinant els avantatges de les seqüències d'ADN amb plataformes de detecció es pot aconseguir l'amplificació de la detecció d'aquestes plataformes⁷⁴. Per exemple, la primera aplicació de seqüències d'ADN va ser en els assajos immuno-PCR⁷⁵, on l'anticòs secundari de l'immunoassaig estava marcat amb una seqüència d'oligonucleòtid que podia ser amplificada via PCR i aconseguir una amplificació de la senyal. Tot i així, l'amplificació estava limitada pel ràtio ADN:anticòs, que acostuma a ser 1:1, per aquest motiu es va combinar aquest sistema amb la biofuncionalització de partícules, un exemple és el *biobarcode*.

El *biobarcode* es va dissenyar com una alternativa al immuno-PCR que eliminés la PCR, ja que necessita personal qualificat. Aquesta tecnologia es basa en el disseny de partícules codificades funcionalitzades amb un bioreceptor de detecció i una seqüència d'ADN codificant, i per altra banda, partícules magnètiques funcionalitzades amb un bioreceptor de captura. Així, després de l'aïllament per magnetisme dels complexos formats, es poden alliberar les seqüències d'ADN i quantificar-les (Figura 7.2). En aquest cas, s'aconsegueix un ràtio ADN:anticòs de 1:100⁸⁰.

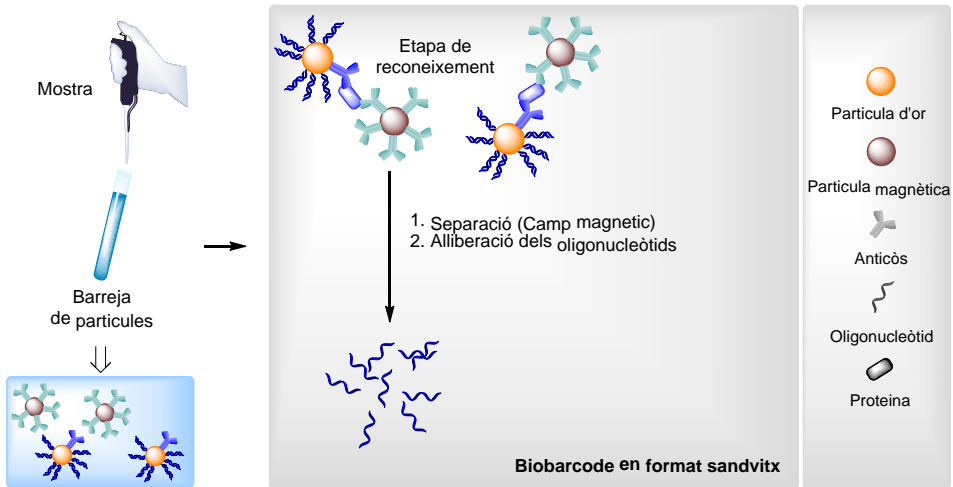


Figura 7.2 Esquema de l'assaig *biobarcode*

La plataforma *biobarcode* s'ha aplicat per la detecció de proteïnes¹⁰, bacteries i virus⁸¹⁻⁸³, cèl·lules⁸⁴, ADN¹¹ i miRNA⁹. A més també s'ha multiplexat funcionalitzant les partícules codificants amb diferents oligonucleòtids^{10, 11, 81, 82, 84}. Fent una revisió de la literatura es pot veure que hi ha dues estratègies majoritàries d'alliberació de les seqüències d'oligonucleòtid: o bé via deshibridació, el que comporta la utilització de dues seqüències complementàries, o bé trencant el pont tiol-or quan les partícules codificants són d'or. Pel que fa la quantificació d'oligonucleòtids alliberats, s'han utilitzat diferents tècniques com PCR⁹⁸, bioxip realçat amb plata⁷⁸, electroforesis capil·lar⁸² o oligonucleòtids funcionalitzats amb una molècula fluorescent⁸⁷. En el cas dels assajos multiplexats, l'estratègia de lectura ha estat l'electroforesi capil·lar i el bioxip d'ADN acoblat a realçament amb plata.

Tot i els molts avantatges que ofereix aquesta plataforma, mai s'ha descrit un assaig multimodal.

7.3 RESULTATS I DISCUSSIÓ

7.3.1 PRODUCCIÓ I VALIDACIÓ D'ANTICOSSOS

Com a prova de concepte es van voler desenvolupar anticossos per a la posterior implementació en un assaig *biobarcode*. Aquests anticossos es van desenvolupar per la detecció de compostos citostàtics, aquests són compostos químics utilitzats per tractar el càncer, la segona causa de mort al món²⁷. Els fàrmacs citostàtics tenen una finestra terapèutica molt estreta i per aquest motiu el seu monitoratge està altament recomanat²⁸. Els fàrmacs seleccionats van ser el 5-fluorouracil (5FU) i la ciclofosfamida (CP).

7.3.1.1 5-fluorouracil i tegafur

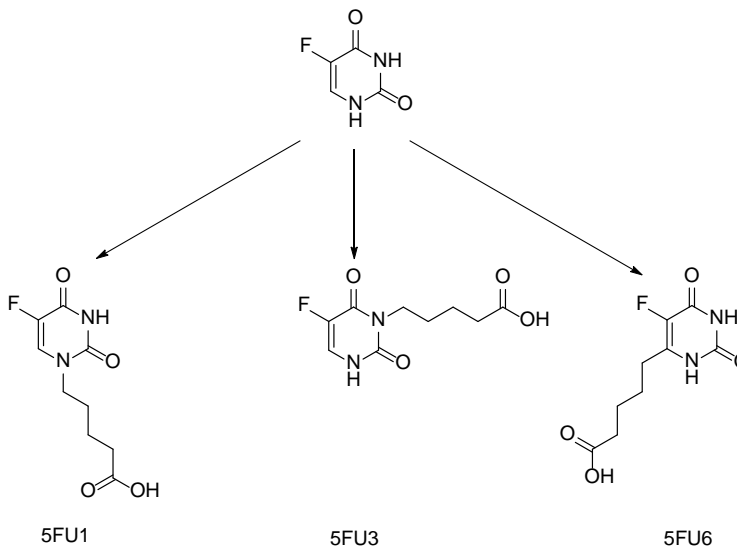


Figura 7.3 Estructura del 5FU i disseny dels seus haptens

Per tal de produir anticossos en contra d'una molècula petita cal conjuguar-la a una proteïna portadora capaç d'activar el sistema immunitari. Per aquest motiu cal sintetitzar un hapten, una molècula molt semblant al compost desitjat però amb un braç espaiador que proveirà el grup funcional per conjuguar la molècula a la

proteïna. En el cas del 5-fluorouracil es van dissenyar tres haptens amb el braç espaiador en les posicions 1, 3 i 6 de l'anell (Figura 7.3).

Els haptens 5FU1 i 5FU3 es van sintetitzar a la vegada mitjançant la introducció del braç metil bromoalerat. La trietilamina⁵⁸ va ser necessària per tal de desprotonar els nitrògens de l'uracil. Els dos compostos es van separar exitosament amb una columna cromatogràfica i subseqüentment els àcids es van desprotegir per tractament bàsic. Per altra banda, l'haptè 5FU6 es va sintetitzar en tres etapes: primer, la síntesi del α -fluoro- β -cetoèster; segon, la formació de l'anell per un tractament amb microones en presència de urea, el rendiment obtingut (10%) va ser baix però cap altra opció avaluada va reportar un rendiment més alt; i per últim, es va desprotegir l'àcid amb tractament bàsic. La síntesi de tots els haptens esta esquematitzada en la Figura 7.4.

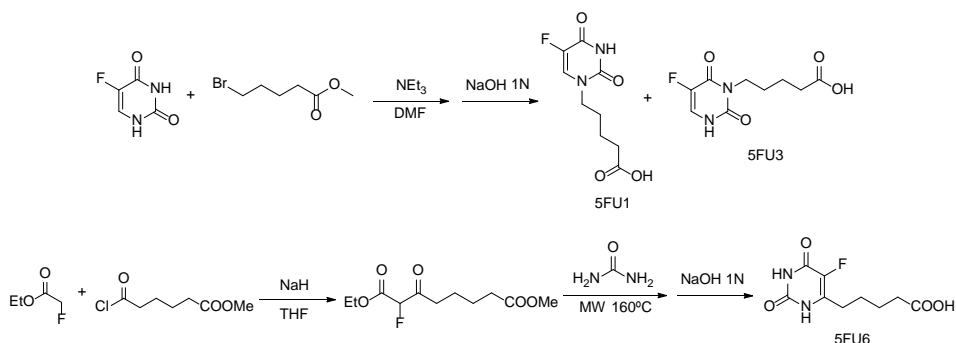
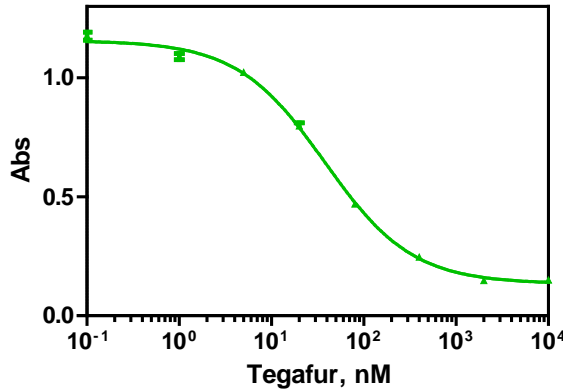


Figura 7.4 Síntesi dels haptens del 5FU

Tots els haptens es van conjuguar a una proteïna portadora per tal d'immunitzar conills i produir anticossos policlonals. Cada immunogen es va injectar a tres conills diferents. A més, el títol dels anticossos es va avaluar amb un assaig ELISA, després de la primera immunització s'estaven produint anticossos específics per l'immunogen.

Un cop obtinguts els anticossos es va procedir a desenvolupar un assaig immunoquímic per validar els anticossos. Amb l'objectiu de detectar molècules petites cal dissenyar l'assaig de manera competitiva. Així, l'antigen o competidor entapissat competeix amb l'analit pel centre actiu de l'anticòs. Es van avaluar les condicions necessàries per fer un assaig per detectar el 5FU, es van combinar els tres haptens conjugats a 4 proteïnes portadores diferents i els 9 antisèrums

produïts. Per desgracia, cap de les combinacions obtingudes va demostrar afinitat per l'analit, l'afinitat del anticòs per l'antigen era massa alta.



Paràmetres de l'assaig per detectar tegafur

Dilució As	1/7000	Senyal _{min}	0.134 ± 0.010
[Competidor]	0.25 µg mL ⁻¹	Senyal _{max}	1.157 ± 0.010
Temps competència	10'	Pendent	-0.915 ± 0.043
Agitació	600 rpm	R ²	0.992 ± 0.001
pH	7.5	EC ₅₀ , nM	35.6 ± 2.6
Força iònica	15.0 mS/cm	IT ^a , nM	de 7.5 ± 1.3 a 157.5 ± 5.1
Tween 20	0.05 %	LOD, nM	2.7 ± 0.7

Figura 7.5 Corba de calibració, condicions i paràmetres de l'immunoassaig per el tegafur. Les dades representades corresponen a la mitjana de sis assajos desenvolupats en 4 dies diferents, tres rèpliques per assaig. ^aIT correspon al interval de treball, calculat com la concentració donada entre el 20 i el 80 % de senyal.

En busca d'una solució al problema de la baixa afinitat dels anticossos per el fàrmac es van avaluar diferent metabòlits, profàrmacs i molècules semblants al 5FU. Els resultats van demostrar que una certa combinació d'antigen-anticòs era adequada per la detecció del tegafur, un profàrmac del 5FU. Un cop seleccionat el tegafur com analit, es va procedir a l'avaluació dels paràmetres físico-químics que afecten l'immunoassaig. També es va avaluar la precisió i l'exactitud de l'assaig desenvolupat amb mostres de plasma. Els paràmetres finals de l'assaig estan recollits en la Figura 7.5.

L'assaig del tegafur va demostrar ser reproduïble i sensible per quantificar el tegafur en mostres de plasma, amb un LOD de 2.7 nM no va mostrar reactivitat creuada amb altres compostos similars.

Com a últim recurs també es van avaluar uns competidors produïts amb haptens altament heteròlegs comparats amb l'haptè d'immunització. Aquest haptens posseïen heterologia en l'anell del uracil i també en la posició del braç espaiador (posició 1 i 3). Els resultats van demostrar que la combinació d'un haptè heteròleg pel que fa l'anell uracil però homòleg en la posició del braç espaiador mostrava una menor afinitat per el competidor i amb aquesta combinació de immunoreactius es va desenvolupar un assaig amb una EC_{50} de 1600 nM per el 5FU.

7.3.1.2 Ciclofosfamida

En el cas de la ciclofosfamida (CP) es van dissenyar dos haptens, el CP2-Cl per exposar l'anell de la CP, en canvi el CP3 exposant la mostassa, també present en altres metabòlits⁵⁴ (Figura 7.6).

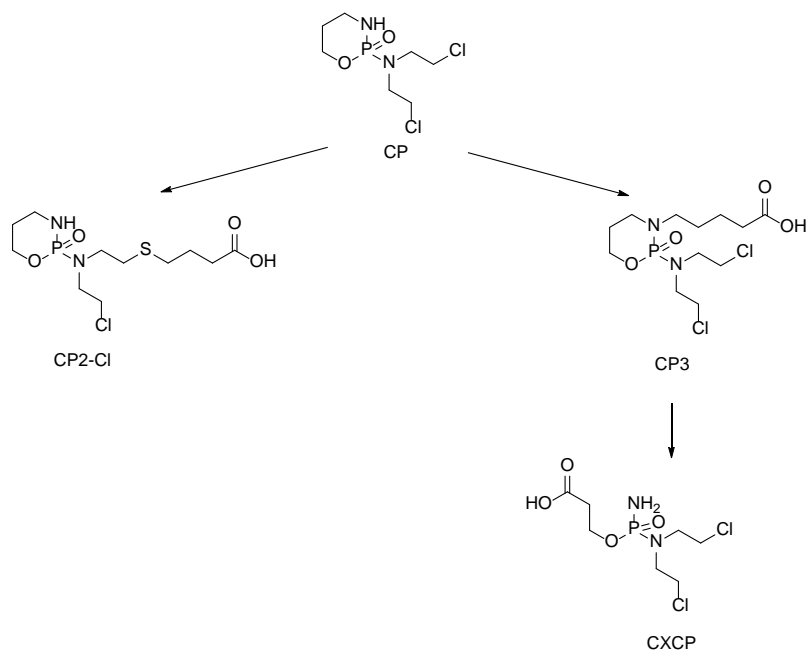


Figura 7.6 Estructura de la CP i disseny dels haptens

La síntesi de l'haptè CP2-Cl es va fer utilitzant un àcid protegit amb el grup benzil per evitar la desprotecció de l'àcid en medi bàsic que pot trencar l'anell de la CP. Llavors es va preparar el braç espaiador amb un tiol, per reaccionar amb la CP, i

un àcid protegit amb un grup benzil. Un cop sintetitzat, es va procedir a la incorporació a la ciclofosfamida utilitzant una base no nucleòfila i la desprotecció per hidrogenació catalítica (Figura 7.7).

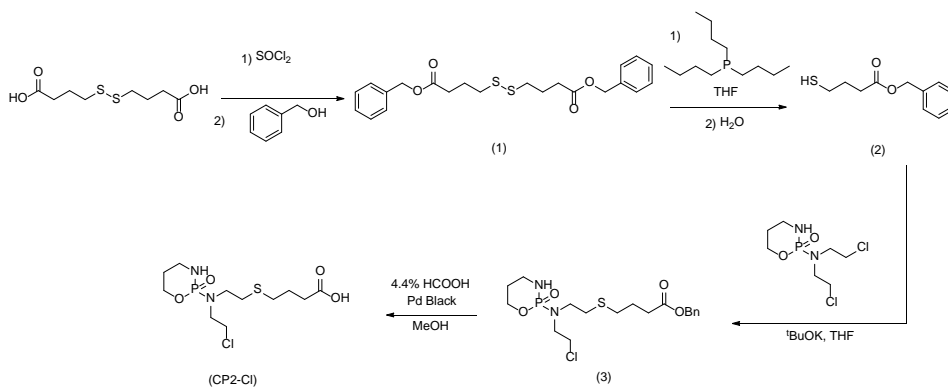
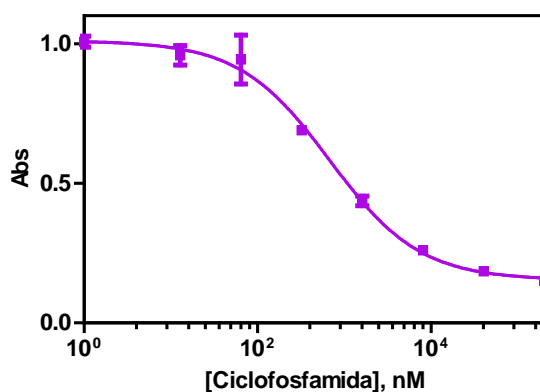


Figura 7.7 Disseny i síntesi del haptè CP2-Cl



Paràmetres de l'assaig per detectar ciclofosfamida

Dilució As	1/8000	Senyal _{min}	1.16 ± 0.02
[Competidor]	0.0625 µg mL ⁻¹	Senyal _{max}	0.18 ± 0.03
Temps competència	30'	Pendent	-0.79 ± 0.08
pH	7.5	R ²	0,997
Força iònica	15.0 mS/cm	EC ₅₀ , nM	676 ± 1
Tween 20	0.05 %	LOD, nM	46 ± 1

Figura 7.8 Corba de calibració, condicions i paràmetres de l'immunoassaig per la ciclofosfamida. Les dades representades corresponen a la mitjana de tres rèpliques.

Per altra banda la producció de l'haptè CP3 es va complicar per la impossibilitat de utilitzar una base que no trenqués l'anell de la ciclofosfamida, per aquest

motiu, un metabòlit es va escollir com haptè. Aquest metabòlit, la carboxifosfamida (CXCP), conté la mostassa i també un àcid terminal per poder conjuguar-lo a una proteïna portadora.

Tot seguit, la producció dels anticossos es va desenvolupar igual que en el cas del 5FU. Els resultats del títol van demostrar la producció d'anticossos específics per la ciclofosfamida. A més, també es van preparar competidors amb els dos haptens i 4 proteïnes portadores diferents. Els resultats van demostrar que una combinació d'un dels anticossos i un competidor heteròleg eren la combinació idònia per quantificar la CP amb un límit de detecció de 46 nM (Figura 7.8).

7.3.2 DESENVOLUPAMENT D'UN *BIOBARCODE* MONOPLEXAT

Degut als problemes obtinguts en el desenvolupament d'anticossos en contra fàrmacs cancerígens, com a prova de concepte per desenvolupar un *biobarcode* monoplexat es van escollir compostos relacionats amb malalties cardiovasculars (CVDs), la primera causa de mort al món. Els anticossos utilitzats ja havien estat validats prèviament al grup. Els compostos són l'acenocoumarol, un fàrmac anticoagulant, i la proteïna C-reactiva, un marcador de risc cardiovascular.

Per desenvolupar un *biobarcode*, tal com s'ha descrit a la introducció, cal dissenyar les partícules que utilitzarem i com es procedirà amb la lectura de la senyal. Donat que gairebé mai abans s'ha descrit un assaig *biobarcode* per a molècula petita, en format competitiu, es va decidir començar amb aquest objectiu. Els components que cal posar a punt són:

1. **Partícules codificades (ePSP):** aquestes han d'estar funcionalitzades amb un bioreceptor, o competidor en el cas d'un assaig competitiu, i la seqüència d'oligonucleòtid codificant. Les partícules d'or es van escollir com a partícules codificades per la seva facilitat de funcionalització amb oligonucleòtids funcionalitzats amb un grup tiol, però presenten adsorció inespecífica a proteïnes que no va poder ser controlada. Per aquest motiu, es van escollir les partícules de poliestirè⁸⁷. Aquestes ja s'han utilitzat amb anterioritat pel desenvolupament d'aquest tipus d'assajos i mostren un mida de partícula prou gran que permet l'amplificació de la senyal i poca adsorció inespecífica a proteïnes. A més,

el poliestirè pot ser funcionalitzat amb diferents grups funcionals, es van escollir grups carboxil que permetran la conjugació de la proteïna portadora del competidor i també l'oligonucleòtid mitjançant un grup amino. La seqüència codificant es va dissenyar amb un fluoròfor terminal per la posterior lectura de la senyal, un grup disulfur per l'alliberació de la partícula amb el tractament d'un reactiu intercanviador de lligands i un grup amino terminal per la conjugació a la partícula. Diferents paràmetres com la concentració de carbodiimida, el pH i la força iònica es van optimitzar per a un màxim rendiment de conjugació. Com a resultat, les partícules van ser activades amb una carbodiimida i tant el competidor i l'oligonucleòtid van ser conjugats amb un rendiment del 20% i el 70% respectivament. Per altra banda, l'alliberació de l'oligonucleòtid de les partícules es va optimitzar aconseguint una màxima alliberació amb el tractament amb dithiothreitol 0.2 M.

2. **Partícules magnètiques (MP):** com a partícules magnètiques es van seleccionar unes partícules que ja estan prèviament funcionalitzades amb grups tosil. Aquestes partícules s'han de funcionalitzar amb anticossos específics per el compost a detectar, en aquest cas el rendiment de conjugació va ser superior al 80 %.
3. **Bioxip d'ADN:** el bioxip es va seleccionar com a mètode de quantificació de les seqüències de oligonucleòtid per la seva capacitat de multiplexació i la lectura directa de les seqüències funcionalitzades amb un grup fluoròfor. Portaobjectes de vidre es van funcionalitzar amb grups epòxid, i amb l'ajuda d'un aparell de deposició de microgotes es van imprimir les seqüències complementaries a les utilitzades per les partícules codificades (Figura 7.9). Les seqüències complementàries estan funcionalitzades amb un grup amino terminal que permet la fàcil conjugació al portaobjectes de vidre per reacció amb els grups epòxid.

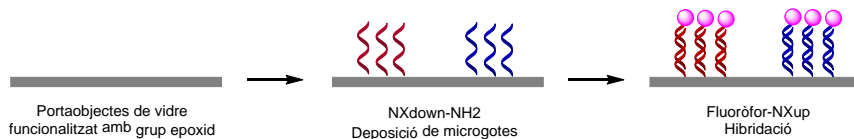


Figura 7.9 Bioxip de ADN, quantificació de les seqüències codificants

Un cop tots els components necessaris per a la producció del *biobarcode* van estar preparats es va procedir al desenvolupament de l'assaig. Primer, el

biobarcode està dissenyat per tal de poder modular la detectabilitat del assaig, per aquest motiu, es van fer diferents proves per comprovar si modificant la càrrega d'oligonucleòtid a la partícula codificant érem capaços de modificar la senyal i la detectabilitat. Els resultats obtinguts van ser excel·lents, augmentant la càrrega s'obté una senyal més alta (si augmentem la càrrega de les partícules de 600 a 3100 seqüències la senyal augmenta de 20000 a 45000 RFU). A més, modulant la concentració de les partícules codificades associades a cada càrrega de partícula som capaços de canviar l'interval de treball i la detectabilitat (Figura 7.10). La capacitat d'aquest assaig de modular la detectabilitat no ha sigut descrita amb anterioritat.

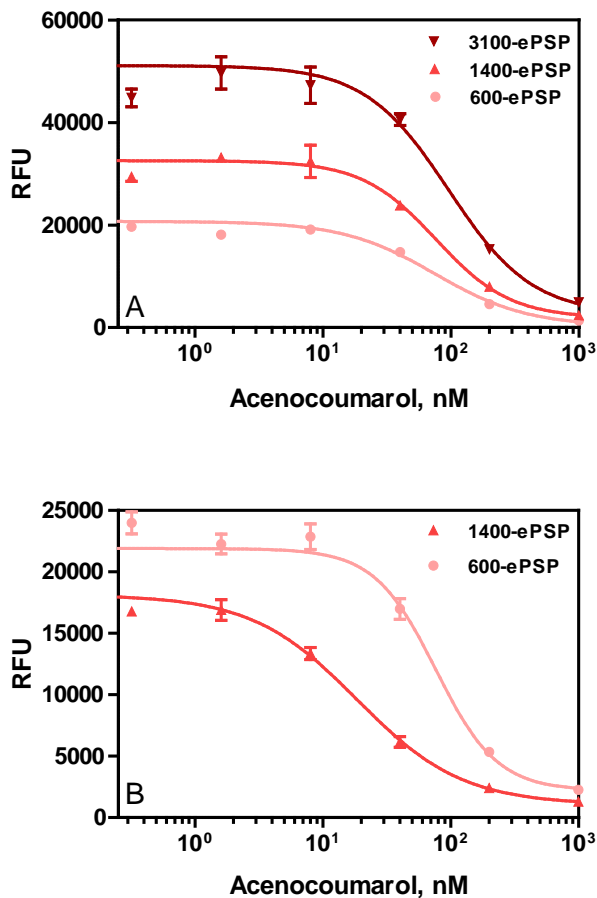
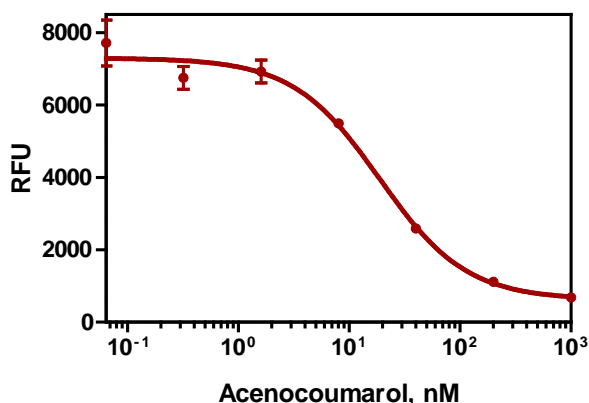


Figura 7.10 Avantatges del Sistema *biobarcode*. A. Capacitat de amplificar la senyal. B. Capacitat de modular el interval de treball i la detectabilitat.

Segon, es va comprovar que les partícules no interaccionessin entre si inespecificament, després es va desenvolupar la recta de calibrat (Figura 7.11) amb una detectabilitat semblant a l'obtinguda amb l'assaig ELISA.



Paràmetres del *biobarcode* per detectar l'acenocoumarol

[ADN] a les ePSP	1407 ADN/ePSP	Senyal _{min}	624 ± 317
[Ag] a les ePSP	669 Ag/ePSP	Senyal _{max}	7299 ± 186
[PSP]	0.008 %	Pendent	-1.03 ± 0.10
[pAb] al stock de MP	0.69 mg/mL	R ²	0.947 ± 0.027
[MP]	0.25 mg/mL	EC ₅₀ , nM	17.5 ± 0.2
		Interval de treball, nM	de 3.28 ± 0.81 a 57.1 ± 4.5
		LOD, nM	0.96 ± 0.26

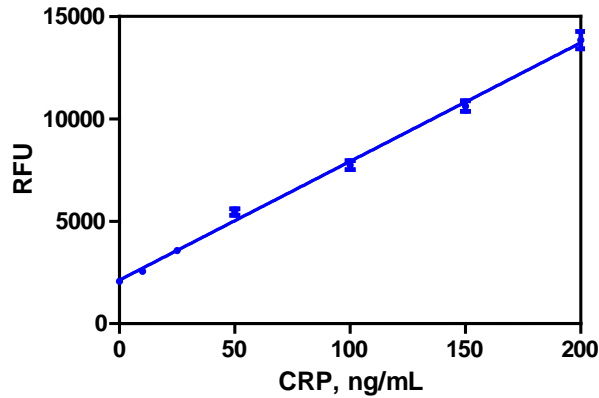
Figura 7.11 Corba de calibració, condicions i paràmetres del *biobarcode* per al acenocoumarol.

Les dades han sigut extretes de la regressió sigmoïdal de quatre paràmetres que s'ajusta a la corba. Les dades representades són la mitjana de tres assajos duts a terme en tres dies diferents, cinc rèpliques cada dia.

Finalment, es va aplicar aquest assaig per a la detecció de l'acenocoumarol en mostres de plasma, amb una dilució ¼ vam ser capaços d'eliminar l'efecte matriu i detectar el fàrmac dins dels nivells necessaris (30-300 nM).

Un cop desenvolupat l'assaig per a molècula petita i demostrada la capacitat per modular l'interval de treball, es va procedir a desenvolupar el assaig monoplexat per a proteïna. Per aquest assaig es van utilitzar els mateixos procediments de funcionalització que per a l'assaig de l'acenocoumarol. Els paràmetres de l'assaig obtingut estan recollits a la Figura 7.12.A.

A



Paràmetres del *biobarcode* per detectar la CRP

[ADN] a les ePSP	1804 ADN/ePSP	Pendent	63.2 ± 4.49
[pAb] a les ePSP	2812 Ab/ePSP	Intersecció	2393 ± 221
[PSP]	0.05 %	R ²	0.957 ± 0.03
[pAb] al stock de MP	0.23 mg mL^{-1}	LOL, ng mL ⁻¹	250.0
[MP]	0.5 mg mL^{-1}	LOQ, ng mL ⁻¹	18.0
		LOD, ng mL ⁻¹	11.0

B

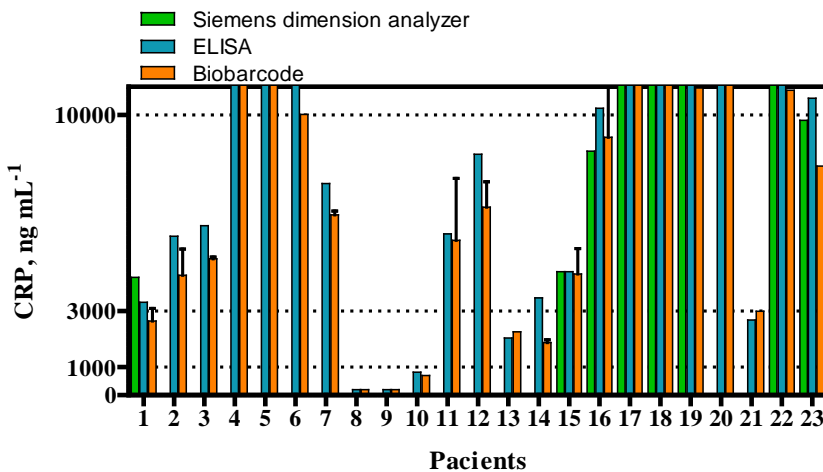


Figura 7.12 A. Corba de calibració, condicions i paràmetres del *biobarcode* per l'acencoumarol.

Les dades han sigut extretes de la regressió sigmoïdal de quatre paràmetres que s'ajusta a la corba. Les dades representades són la mitjana de tres assajos duts a terme en tres dies diferents, cinc rèpliques cada dia. **B.** Comparació de la quantificació del *biobarcode* amb l'ELISA i una assaig

de referència (Siemens dimensió analyzer). Les dades representades són la mitjana d'un assaig de cinc rèpliques pel *biobarcode*, tres rèpliques per l'ELISA.

Degut als bons resultats obtinguts, aquest assaig es va provar en mostres de plasma. Es va observar que amb una dilució 1/40 no hi havia efecte matriu i es podien quantificar les mostres dins les necessitats de les mostres clíniques. A més, l'assaig es va posar a prova amb mostres reals i es va comparar amb l'ELISA i un assaig de referència. Els resultats, van mostrar com la quantificació de les mostres reportava uns resultats molt semblants a l'assaig de referència (Figura 7.12.B).

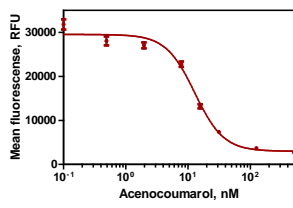
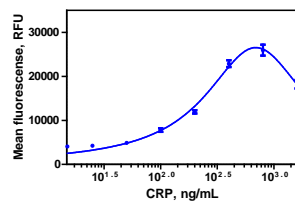
7.3.3 DESENVOLUPAMENT D'UN *BIOBARCODE* MULTIPLEXAT

Un cop ja teníem establerts els assajos monoplexats, es va procedir al desenvolupament de l'assaig multiplexat. Primer, es va avaluar el disseny de l'assaig. Es va optar per desenvolupar l'assaig en una sola etapa, aquest disseny és òptim per l'assaig competitiu del ACL. En el cas de la detecció del CRP, format sandvitx en una sola etapa, es dona l'efecte prozone. Aquest efecte està produït per altes concentracions d'analit^{131, 132} i pot portar a falsos negatius, per aquest motiu l'interval de concentració analitzat resta limitat per sota de una certa concentració. Tenint en compte que en un assaig multiplexat s'analitzen més d'un compost a la vegada, l'efecte dels falsos negatius es veurà disminuït²¹.

Segon, es va procedir a preparar les corbes de calibrat amb la barreja de reactius per als dos assajos monoplexats. Els resultats van mostrar uns excel·lents paràmetres amb uns límits de detecció de 3.6 ± 1.2 nM per al ACL i de 78.4 ± 14.9 per a la CRP (Taula 7.1).

Per últim, amb les rectes de calibrat establertes es va procedir a analitzar 8 mostres amb concentracions variables de ACL i CRP. Aquestes mostres van ser dopades a l'interval de treball donat per les mostres clíniques (30-300 nM per ACL i 1000-3000 ng/mL per CRP). Independentment de les concentracions dopades de cada analit, vam ser capaços de quantificar-les amb èxit (Figura 7.13). A més, la recta de relació entre concentració trobada i dopada té una pendent de 1.161 ($R^2 = 0.900$) per al ACL i de 0.966 ($R^2 = 0.895$) per a la CRP.

Taula 7.1 Paràmetres de l'assaig *biobarcode* multiplexat

Assays	ACL	CRP
		
ADN/ePSP	600	1400
% ePSPs	0.0125	0.0125
mg/mL MP	0.5	0.5
RFU_{min}	2662 ± 89	4404 ± 906
RFU_{max}	27414 ± 2405	31316 ± 10345
<i>m</i>	-2,29 ± 0.69	2,35 ± 0.55
R²	0.91 ± 0.03	0.95 ± 0.03
IC₅₀, nM or ng/mL	15.6 ± 1.1	238.7 ± 50.2
IT^a, nM or ng/mL	From 6.9 ± 1.2 to 29.4 ± 6.5	From 109.9 ± 9.9 to 368.8 ± 71.8
LOD, nM or ng/mL	3.6 ± 1.2	78.4 ± 14.9

Les dades han sigut extretes de la equació logística de quatre parametres que s'ajusta als punts. Es mostra la mitjana i la desviació estàndard d'assajos duts a terme en tres dies diferents, 5 repliques per dia. ^aIT correspon a interval de treball, calculat com la concentració entre el 20 i el 80% de la senyal màxima.

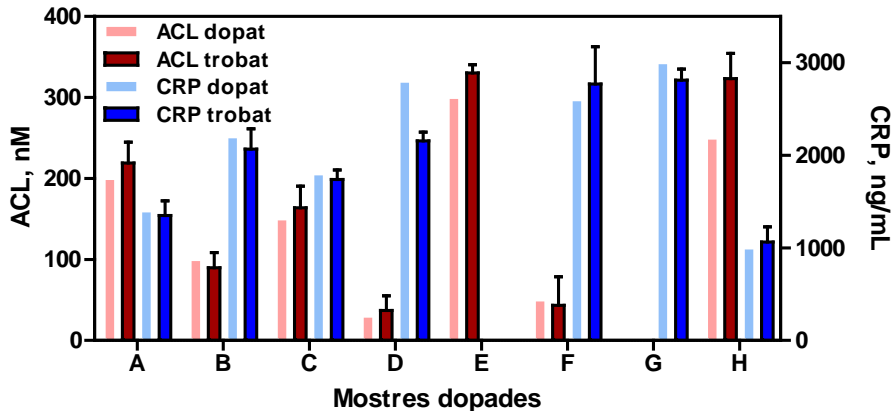


Figura 7.13 Grafica mostrant les concentracions trobades en 8 mostres dopades amb diferents concentracions de ACL i CRP. Els resultats són la mitja dels anàlisis de tres assajos, amb 5 repliques cada un.

Així queda demostrada, no només la capacitat de modulació del interval de treball, sinó la capacitat de detectar més d'un compost de diferent naturalesa química.

7.4 CONCLUSIONS

- Tot i l'esforç fet sintetitzant un haptè d'immunització que preservés tot els grups químics importants (5FU6), i dos haptens més (5FU1 i 5FU3) amb propietats excel·lents per produir anticossos, ha sigut difícil establir un assaig immunoquímic competitiu per al 5FU. A l'hora d'escriure aquesta tesi no hem sigut capaços de trobar una explicació a aquests fet, ja que els anticossos van mostrar una bona avidesa per els haptens de immunització, que només presentaven petites diferències químiques amb el 5FU. Tot i això, incrementant l'heterologia del competidor es va poder afavorir el reconeixement del analit.
- Sorprenentment, el tegafur, un profàrmac del 5FU amb un tetrahidrofurà en la posició 1, va ser capaç de competir en l'assaig utilitzant anticossos produïts en contra de l'haptè 5FU1, permetent la seva detecció en un format immunoquímic competitiu amb un LOD prop de 3 nM. Aquest fet porta a la possibilitat que l'haptè 5FU1 es pot haver reorganitzat sota les condicions utilitzades per la seva conjugació a l'HCH conduint a un comportament similar a un anell en la posició 1. Aquest fet necessita ser investigat en més detall.
- Un nou haptè per la CP (CP2-CI) s'ha descrit per primer cop. Aquest haptè es va dissenyar per tal d'exposar la fracció de l'anell fosfamida en comptes de la mostassa. L'haptè s'ha utilitzat per produir anticossos que combinats amb un competidor heteròleg s'ha obtingut un immunoassaig competitiu amb un LOD de 46 nM.
- La biofuncionalització de partícules de poliestirè amb oligonucleòtids proveïts d'un pont disulfur a l'extrem 5' es un procediment simple per preparar les sondes codificades. Aquest ens permet utilitzar les partícules en assajos *biobarcode* de una manera eficient, només alliberant els oligonucleòtids amb DTT en comptes de utilitzar una doble cadena d'ADN per codificar les partícules com s'ha descrit per altres

autors. A més, el procediment permet la multifuncionalització de les sondes en el qual el ratio entre la molècula bioreceptora i els oligonucleòtids codificants poden ser variats de una manera reproduïble.

- Ha sigut possible, gairebé per primera vegada, el desenvolupament d'un assaig *biobarcode* basat en un format immunoquímic competitiu. L'assaig permet la detecció d'un anticoagulant oral, acenocoumarol, en mostres de sèrum i plasma sense cap altre tractament de mostra. A més, el desenvolupament d'un assaig *biobarcode* per la proteïna C-reactiva (CRP) utilitzant un format immunoquímic sandvitx. L'assaig ha mostrat ser útil per quantificar el biomarcador en mostres de plasma.
- S'ha demostrat la possibilitat de modular l'amplificació de la senyal i l'interval de treball del assaig *biobarcode*, només variant la càrrega d'oligonucleòtids en les sondes codificants. Aquest fet obre la porta al desenvolupament de plataformes *biobarcode* multiplexades capaces de solucionar un dels principals reptes d'aquestes tècniques bioanalítiques que és la mesura simultània d'analits presents en una mostra a diferents intervals de concentració.
- S'ha demostrat que el *biobarcode* permet detectar diferents entitats químiques a la vegada ja que qualsevol interacció es tradueix a una seqüència d'ADN per l'alliberació dels oligonucleòtids de les sondes codificades. Els oligonucleòtids alliberats són, finalment, mesurats amb un bioxip d'ADN. Així l'acenocoumarol i la proteïna C-reactiva s'han mesurat simultàniament en una plataforma de *biobarcode* multiplexat amb una detectabilitat comparable als assajos monoplexats.

8 ANNEX. NANOCARRIER SYSTEM FOR 5- FLUOROURACIL DRUG DELIVERY

This work was developed as a part of a research stage in Prof. Mitragotri group of the University of California Santa Barbara. The scientific objective was the preparation of a drug delivery system for cytostatic drugs, promoted by the application of the knowledge acquired by biobarcode development to another field of interest.

8.1 CHAPTER OBJECTIVE

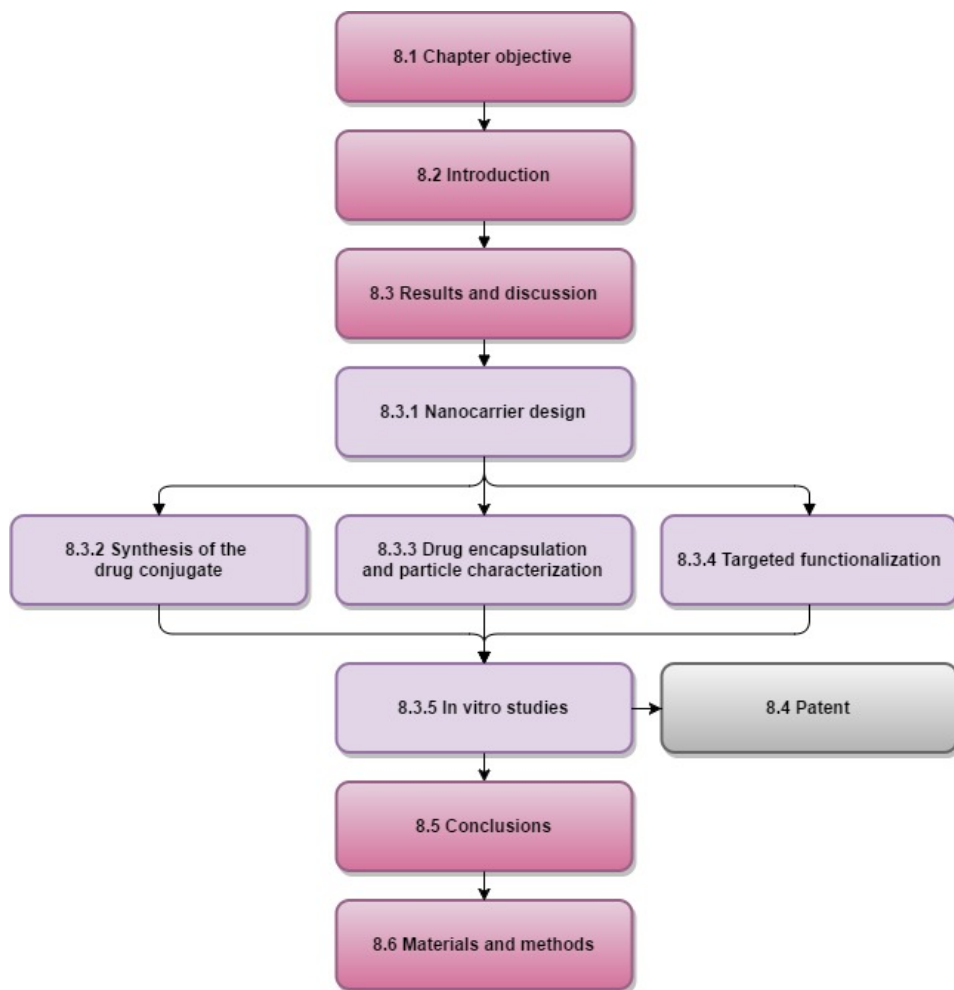


Figure 8.1 Structure of chapter 8 related to the different sections

The main objective of the research stage was the preparation of a drug delivery system for a cytostatic drug. The carrier system for 5FU was already designed in Mitragotri's group, it was developed for the coencapsulation of synergistic ratios of doxorubicin and 5FU in liposomes¹³⁴. Consequently, specific tasks addressed the further optimization of 5FU derivative synthesis and encapsulation efficiency and functionalization of liposomes with targeting antibodies for specific cell lines (Figure 8.1).

8.2 INTRODUCTION

Nanoparticles have emerged as a profitable modality for the treatment of various diseases, including cancer, cardiovascular and inflammatory diseases, but in this chapter, we will focus mainly in cancer carriers. Carriers main purpose is delivering therapeutic agents in a safer and more efficient manner. Particles offer the capability of 1) encapsulate poorly soluble drugs, 2) protect therapeutic molecules and 3) modify their pharmacokinetics and pharmacodynamics¹³⁵.

Several carriers have been designed (Figure 8.2) such as liposomes, polymeric nanoparticle, micelles and dendrimers. Carrier development has focused on small-molecule drugs. Protein and peptide delivery is still in its early stages of development¹³⁶. Main challenges developing nanoparticle carriers for disease treatment are facing with elonged circulation time, which can be accomplished via pegylation¹³⁷; enhance tissue penetration¹³⁸, challenged by biological transport barriers; and the use of other substances for specific tissue targeting¹³⁹.

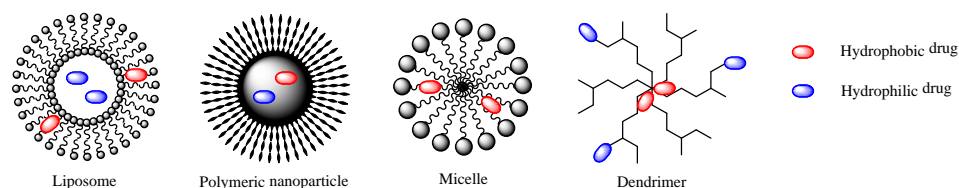


Figure 8.2 Different types of nanocarriers

8.2.1 LIPOSOMES

Liposomes have been approved for cancer since the mid-1990s and mainly used to solubilize drugs, leading to biodistributions that favor higher uptake by the tumor than the free drug. Main advantages are enhanced biocompatibility, extended systemic circulation and the ability to accumulate in tumor via the enhanced permeability effect (EPR)¹⁴⁰. Furthermore, they fulfil clinical manufacturing requirements like low interbatch variability, ease of synthesis, scalability and biocompatibility¹³⁹.

Liposome membrane composition can be tailored by means of physicochemical properties such as charge, fluidity and permeability only modifying the ratio of constituent lipids¹⁴¹. Furthermore, liposome characteristics not only offer the possibility of encapsulation of several types of molecules but can also be functionalized with targeting ligands to enhance the selective targeting of tumours¹³⁹ (Figure 8.3).

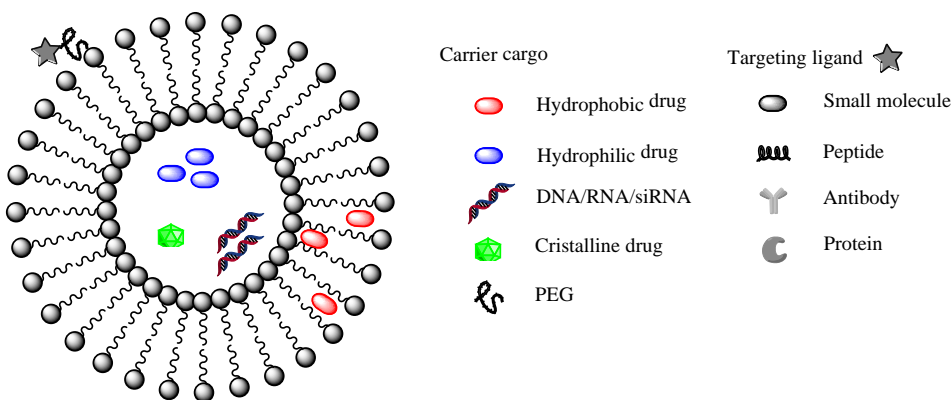


Figure 8.3 Structural and design considerations for liposomal drug delivery

As can be concluded from the literature review, liposomes offer a huge variety of loading strategies and functionalities making them a versatile carrier for coencapsulation of drugs with different chemical properties.

Active targeting, also called ligand mediated targeting, has been trying to play a major role in personalized cancer medicine and has also addressed liposome functionalization. Nanoparticle small size drives nanocarriers into tumors via the EPR effect, but ligands on the surface of the carrier system are supposed to be specifically retained and uptaken by the targeted disease cell. Usually, ligands

that bind to receptors or surface molecules are selected with this aim to increase particle-cell interaction and enhance internalization without affecting biodistribution¹³⁵. Nevertheless, other problems that should be faced for targeted liposome production are administration route, higher clearance rate, unspecific targeting due to serum protein binding and hindered tumor penetration¹³⁹.

8.2.2 LIPOSOMES FOR 5FU ENCAPSULATION

5-fluorouracil is the most widely used cytostatic drug. Several attempts to encapsulate 5FU have been reported in the literature since 1981¹⁴²⁻¹⁴⁹. Most of the publications focus on the optimization of encapsulation efficiency (EE) evaluating all possible encapsulation procedures. In 2003 da Costa *et Al.*, published a study of passive and active encapsulation reporting that reverse-phase evaporation method resulted in the largest 5FU EE¹⁴⁶. Despite the extensive study developed, only a 6% of EE was achieved.

Alternatives for higher EE have been also studied. For example, Kaiser *et Al.* designed drug entrapment with vesicular phospholipid gels, due to its high lipid content it increases ratio of aqueous volume inside the vesicle in comparison with the surrounding volume, being able to reach EE as high as 40%¹⁴⁷. Another approach has been the use of 5FU derivatives to improve its physicochemical, biopharmaceutical and pharmacokinetic properties; 1-substituted 5FU derivatives have been evaluated differing in the residue either alkyl chain¹⁴⁹ or a sugar moiety¹³⁴.

8.3 RESULTS AND DISCUSSION

Firstly, nanocarriers were prepared and characterized. Physico-chemical properties were evaluated since they are crucial for particle performance. Then, further studies to prepare targeted delivery systems were addressed. And finally, *in vitro* studies were performed to evaluate the activity of these nanocarriers. All experimental procedures related to this chapter can be found in section 8.6.

8.3.1 NANOCARRIER DESIGN

In this methodology, designed cationic liposomes used a pH-gradient passive encapsulation that would allow the coencapsulation with other cytostatic drugs¹⁵⁰. The active loading engine arises from the weak base exchange with the ammonium ions (Figure 8.4). The stability of the ammonium ion gradient is produced by the low permeability of sulfate counterion, which also will stabilize encapsulated drug.

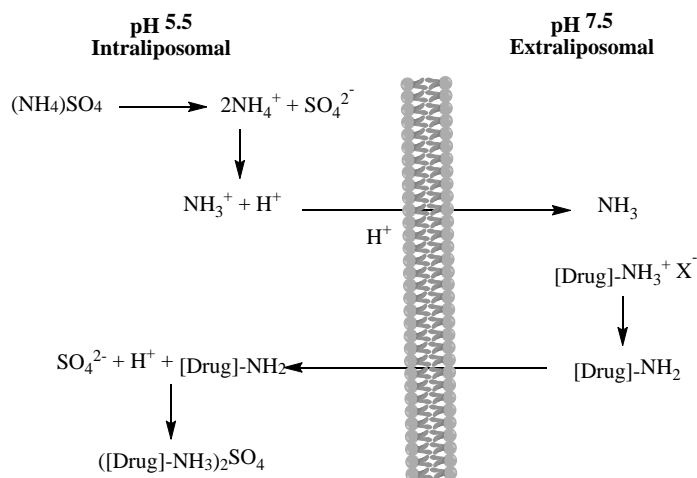


Figure 8.4 Scheme showing the encapsulation mechanism by ammonium sulfate gradient

To be able to use this pH gradient we needed to make 5FU an amphipathic weak base. This was achieved conjugating 5FU with tryptophan molecules that provide the drug with the characteristics required. Free amines of tryptophan, with a pKa of 9.39, have the capability to form salts in presence of ammonium sulfate, and indole ring of tryptophan provides a non-polar region to make the compound amphipathic.

Liposome composition was formed by 4 main components. DSPC (1,2-Distearoyl-sn-glycero-3-phosphocholine) is the main lipidic component, DSPE-PEG (1,2-distearoyl-sn-glycero-3-phosphoethanolamine-N-[polyethylene glycol-2000]) is a PEGylated lipid to prolong circulation time of the liposome and avoid immune detection¹³⁷, cholesterol confers higher stability to the lipid bilayer and DOTAP (N-[1-(2,3-Dioleoyloxy)propyl]-N,N,N-trimethylammonium methyl-sulfate) is a cationic lipid. Cationic lipids exhibit unique abilities to fuse with cell membranes

and intracellularly release payloads¹⁵¹ and show high affinity for the negatively-charged fenestrae in tumor vasculature¹⁵². The final composition was as follows: DSPC: DSPE-PEG(2000)Amine or DSPE-PEG(2000)Carboxy: Cholesterol: DOTAP with the ratio 75:5:10:10¹³⁴.

8.3.2 SYNTHESIS OF THE DRUG CONJUGATE

Some 5FU analogues were designed by Kathrin M. Camacho in her doctoral thesis¹⁵³ for liposome encapsulation via ammonium sulphate gradient. Modifications were based on introducing a tryptophan in position 1 of the fluorouracil ring or using a 5FU metabolite, 5-fluorouridine, to incorporate tryptophan in the hydroxyl groups of its sugar moiety. Encapsulation efficiency of both compounds was 3.2 % and 26.6 % respectively, thus, 5-fluorouridine conjugated to tryptophan (5FURW) was selected as the drug conjugate.

From that point, synthesis of the drug carrier was optimized using activated tryptophan with the amino group protected with Boc to avoid side reactions and provide an easy deprotection with acid treatment (Figure 8.5). First, 5-fluorouridine was mixed one-pot with an excess of two equivalents of activated tryptophan (Boc-Trp-N-carboxyanhydride) per hydroxyl group and a catalytic amount of 4-Dimethylaminopyridine. Desired compound (5FURBocW) was isolated from unreacted tryptophan by column chromatography with a yield of 94%. Secondly, protected compound was treated with TFA 10 % in DCM for Boc protecting group release. TFA salt of the desired compound (5FURW) was obtained after precipitation with a 75% yield. Both compounds were characterized by NMR, mass spectra and UV-Vis.

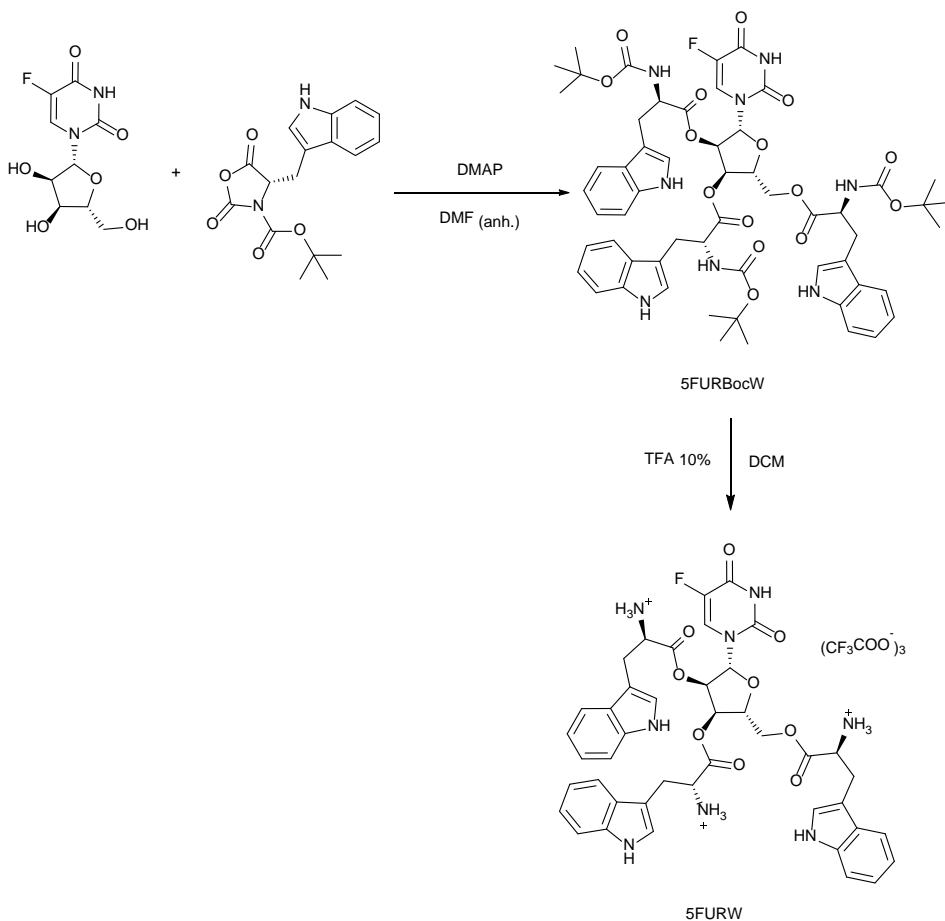


Figure 8.5 Diagram showing the 5-fluorouracil prodrug synthesized for encapsulation

8.3.3 DRUG ENCAPSULATION AND PARTICLE CHARACTERIZATION

In order to encapsulate 5FURW, liposomes were prepared via the thin lipid film formation. This work was done with the help of Debra Wu. After the formation of the liposomes and passing them through the extruder to obtain monodisperse 100 nm liposomes the external solvent was changed using a size exclusion column, thus, creating a pH gradient between the inner and outer solutions of the liposome. The procedure for encapsulation was based in a transmembrane ammonium sulfate gradient for the entrapment of amphipathic weak bases. The problem we found is that the described procedure, for doxorubicin, uses an external pH of 7.5 at which the drug is insoluble since it is its isoelectric pH. It has

been reported that even the engine for encapsulation is a pH gradient, higher differences between pH do not necessarily improve EE¹⁵⁰. Consequently, to overcome the encapsulation problem, several pHs were tested, the best encapsulation yield was obtained with an external pH of 6.5. At this pH, the drug is completely soluble and also keeps a pH gradient with the inner buffer of the liposomes. Then, the quantity of added drug was increased to raise the loading capacity, observing a saturation peak at 60 mg/mL and aggregation of liposomes at higher concentration of drug. Finally, encapsulation time was optimized reporting a 20 % of loading capacity (LC) after 2h. To our knowledge, LC is a better indicator than EE to measure drug internalization since it is compared to lipid concentration and is not a function of the concentration added in the external media. This yield is in the same range of other encapsulation procedures for 5FU reported in the literature^{134, 147, 148}, there's no loading improvement but pH gradient will allow the coencapsulation with other cytostatic drugs.

Particle sizing and ζ -potential measurements were performed using PBS as buffer to maintain constant the conductivity and particle solvation. Results demonstrated low polydisperse liposome batches with a mean diameter of 110 nm. A reduction in size to 83 nm was observed after encapsulation procedure. Otherwise, ζ -potential measurements showed a positive charge of 6 mV for amino functionalized liposomes and a negative charge of -6 mV for carboxy functionalized liposomes. These values were not modified after encapsulation of the drug.

Otherwise, drug release was evaluated along time at different pHs, pH 7.5 was selected since it is the blood pH and lower pHs are known to be cancer tissue pH¹⁵⁴. The results obtained showed a non-pH-dependent release of the drug, expected results according to lipidic composition of the liposome. The crucial factor determining pH-sensitive formulations is the presence of dioleoylphosphatidylethanolamine (DOPE) which is able to undergo destabilization upon acidification¹⁵⁵. Nevertheless, after 12h almost 50% of the drug was released and after 24 h 90% of the drug was released at 37°C (Figure 8.6). This results contrast with previous results obtained with anthracycline encapsulation that reported a shelf life of 6 months¹⁵⁰, probably due to the lack of π -stacking of planar aromatic rings presented by doxorubicin.

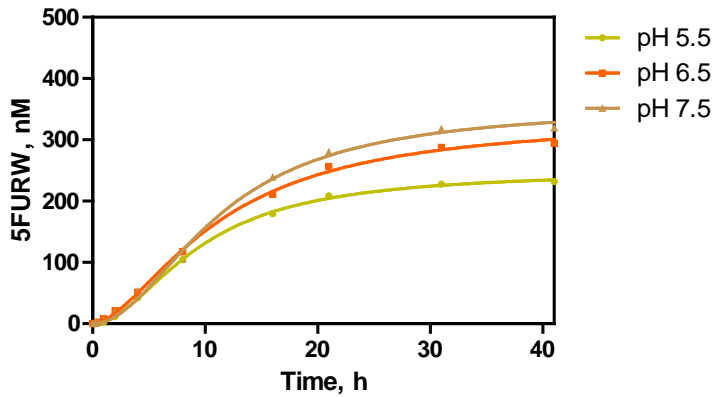


Figure 8.6 Release of drug of both amino particles along time. Release was produced with PBS at different pH at 37°C.

8.3.4 TARGETED FUNCTIONALIZATION

The functionalization of particles was designed via activation of the antibodies or the particles (Figure 8.7).

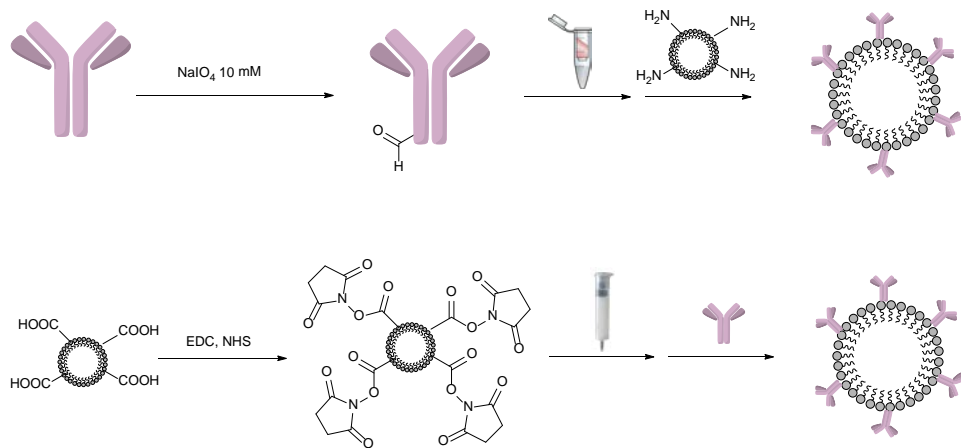


Figure 8.7 Graphic scheme of the conjugation procedures of antibodies for both amino and carboxy functionalized particles

Amino particles were designed to be conjugated with aldehyde functionalized antibodies that can form an enamine with amino groups of the liposomes. This

aldehyde functionalized antibodies were prepared using sodium periodate that oxidizes selectively the sugars of the heavy chain of the antibodies¹⁵⁶. Carboxy particles were activated using the well-known carbodiimide strategy and N-hydroxysuccinimide¹⁵⁷. The quantity of antibody added to the particles was calculated to produce a 25% of surface coverage of the particles, taking into account that if we consider antibodies as spheres of 16 nm on the surface of a 100 nm liposome we could fit 81 antibodies. First attempts were carried out with unspecific mouse IgG, and the analysis of the conjugation was done using mouse IgG ELISA on the final liposomes. Unexpectedly, both proposed strategies reported a really low yield, approximately 10% (approximately one antibody per liposome). An extensive review of the literature proved that these procedures work for both amino functionalized liposomes¹⁵⁸⁻¹⁶⁰ and carboxy functionalized liposomes^{148, 161-163} for a range of buffer conditions, thus it remains unclear which is the cause of this low yield.

8.3.5 *IN VITRO* STUDIES

MTT assays¹⁶⁴ were carried out to evaluate new drug conjugate and prepared liposome activity, those assays evaluate cell metabolic viability. Two breast cancer cell lines (of mouse and human, 4T1 and MDA-MB-231 respectively) were tested with the synthesized 5FURW, compared with 5FU and also with encapsulated drug in liposomes functionalized with amino and carboxyl groups (Figure 6). Targeted liposomes were not evaluated since antibody conjugation was really low.

For 4T1, murine breast cancer cell line, 5FURW was 2.5-fold more active than 5FU, for MDA-MB-231, human breast cancer, it was 127-fold higher. It is clear that much additional work is required before a complete understanding of this result can be reached, for example comparing the results also with cell metabolic inhibition of 5-fluorouridine. Concerning the encapsulated drug, for MDA-MB-231 it is 1.5 and 6-fold less active than 5FURW, for amino and carboxy functionalized liposomes; in addition, for 4T1 cell line it is just 2-fold less active. Further *in vivo* experiments should be conducted to evaluate this slight less activity because it could be easily overcome by EPR effect.

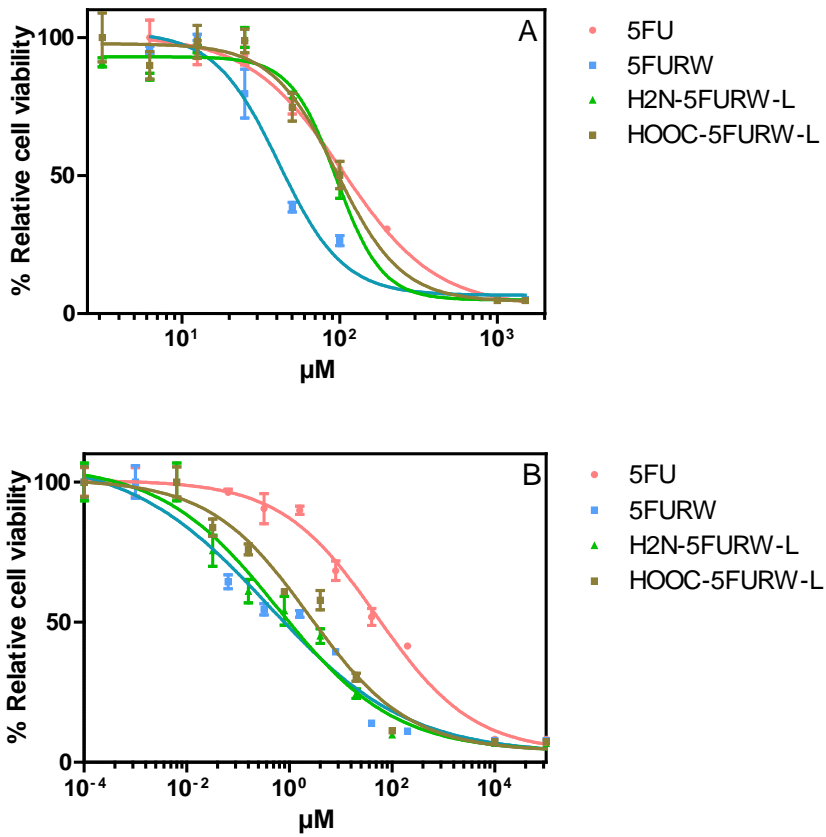


Figure 8.8 Inhibition curves of cell activity due to the presence of the drug and the liposomes for two different cell lines. A and B correspond to 4T1 and MDA-MB-231 cell lines respectively. Each concentration point corresponds to the average of three replicates.

8.4 RELATED PUBLICATIONS

Drug formulations for cancer treatment

S. Mitragotri, K. M. Camacho, S. Menegatti, M. Broto

Patent in preparation, UC Case No. 2016-246 (2)

This patent describes the encapsulation of synergistic combinations of doxorubicin and 5FU analog (DADOFIL). Synergistic combination of this two drugs encapsulated on liposomes reported 90% reduction in tumor growth of murine carcinoma in vivo with the treatment of remarkably low doses. My main contribution to this patent has been the optimization of the synthesis procedure of the drug conjugate.

8.5 CONCLUSIONS

5FU analog has been encapsulated into liposomes using a pH gradient method. This 5FU analog consisted on 5-fluorouridine conjugated with three tryptophans (5FURW) providing the molecule with amphipathic weak base characteristics. A new synthetic route for 5FURW has been proposed and reported reproducible, furthermore, this analog encapsulation strategy has been optimized reporting a loading capacity of 20%. In vitro studies reported a higher activity against tumoral cells from newly synthesized analog, 5FURW, than from 5FU.

8.6 MATERIALS AND METHODS

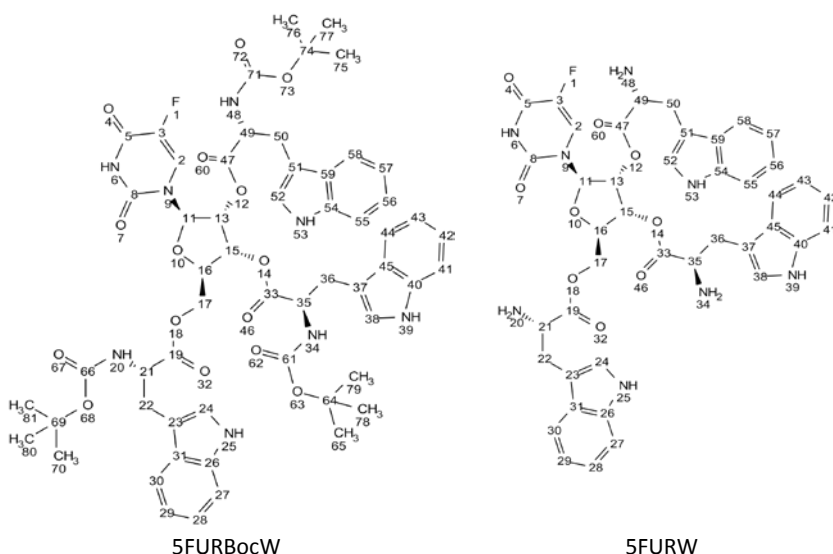


Figure 8.9 Molecular structure of synthesized compounds: 5FURBocW (5) and 5FURW (6). Numbers correspond to NMR assignment.

Synthesis of 5FURBocW. 5FUrd (48.50 mg, 184.98 μmol), Boc-Trp-N-carboxyanhydride (274.98 mg, 832.40 μmol) and DMAP (6.78 mg, 55.49 μmol) was solved in 10 mL of anhydrous DMF and allowed to react overnight at r.t. under inert atmosphere. The mixture was evaporated until dryness and resulting oil was extracted with a mixture of HCl 1N and Ethyl acetate 1:1. The organic layer was separated, dried with MgSO_4 , filtered and finally evaporated. Liquid obtained was purified by chromatography column with dichloromethane and ethyl acetate to finally obtain a yellow liquid (194.4 mg, 94% yield). UV-Vis (MeOH): 270 nm. TLC (dichloromethane:ethyl acetate 5:95) Rf 0.71. ^1H NMR (600 MHz, DMSO-d_6) δ 11.96 (s, 1H, H6), 10.80 (s, 3H, H25 H39 H53), 8.21 – 7.92 (m, 1H, H2), 7.62 – 6.65 (m, 15H, tryptophan aromatic protons), 5.96 (d, J = 5.4 Hz, 1H, H16), 5.73 (m, 1H, H11), 5.56 (m, 1H, H15), 5.35 (m, 1H, H13), 4.37 – 4.07 (m, 6H, H21 H35 H49), 3.21 – 2.85 (m, 6H, H22 H36 H50), 1.46 – 1.16 (m, 21H, tBu protons). MALDI-TOF: m/z calculated for $\text{C}_{57}\text{H}_{65}\text{FN}_8\text{NaO}_{15}^+$ [M + Na] $^+$ 1143.44, found 1143.20.

Synthesis of 5FURW. 5FURBocW (78.9 mg, 70.4 μmol) were solved in 3 mL of dichloromethane and 200 μL of TFA were added to achieve a concentration of 10% of TFA. After half an hour solvent was evaporated until dryness. Product was redissolved in ethyl acetate and precipitated with dichloromethane. Finally, the desired product was obtained by filtration and washed with dichloromethane. A white powder (43.1 mg, 75% yield) was obtained. UV-Vis: 270 nm. TLC (dichloromethane:ethyl acetate 5:95) Rf 0.00. ^1H NMR (600 MHz, DMSO-d_6) δ 12.10 (s, 1H, H6), 11.10 (m, 3H, H25 H39 H53), 8.80 – 8.33 (m, 6H, H20 H34 H48), 8.11 (d, J = 6.8 Hz, 1H, H2), 7.65 – 6.83 (m, 15H, aromatic tryptophan protons), 5.93 (d, J = 5.2 Hz, 1H, H11), 5.80 – 5.69 (m, 1H, H13), 5.50 (m, 2H, H15 H16), 4.47 – 4.19 (m, 5H, H17 H21 H35 H49), 3.54 – 3.10 (m, 6H, H22 H36 H50). MALDI-TOF: m/z calculated for $\text{C}_{42}\text{H}_{42}\text{FN}_8\text{O}_9^+$ [M + H] $^+$ 821.31, found 821.11.

Buffers. Unless otherwise indicated, phosphate buffer saline (PBS) is 0.01 M phosphate buffer in a 0.8% saline solution, pH 6.5. Ammonium sulfate solution is 150 mM pH 5.5.

Liposome preparation. Liposomes were prepared utilizing the conventional thin film evaporation method. Liposomes were prepared using DSPC:PEG-DSPE:DOTAP:Chol in a ratio of 75:5:10:10¹³⁴. Lipids were co-dissolved in chloroform in a round-bottomed flask, and organic solvent was removed using a

rotary evaporator at reduced pressure at 60 °C (5 °C above the lipid transition temperature) in order to form a thin lipid film. The film was subsequently hydrated in ammonium sulfate at 60°C and passed 21 times through an extruder (Avestin LiposoFast Extruder) with 100 nm polycarbonate filters. A transmembrane ammonium sulfate gradient was generated by passing liposomes through a Sephadex G-25 PD-10 column equilibrated with PBS pH 6.5. Then, 200 µL of 5FURW solution (60 mg/mL) was added to 1 mL of liposome solution (12 mM of lipid concentration). To remove free drug, liposomes were finally passed through a Sephadex G-25 PD-10 column.

Liposome characterization. Lipid concentration was calculated with Stewart assay¹⁶⁵. To measure drug encapsulation, 50 µL of drug-loaded liposomes was dissolved in 950 µL methanol through vortexing and sonication. The dissolved liposomes were centrifuged at 12000 G for 20 min to allow the lipids to pellet. The supernatant was collected and its absorbance was measured at 270 nm to quantify 5FURW concentration. Encapsulation efficiency is reported as the mol % of drug initial versus final applying a correction for particle loss, loading capacity is reported as the % mol of drug with respect to mols of lipids.

$$EE \% = \frac{[5FURW]_{final} * \frac{[Lipid]_{initial}}{[Lipid]_{final}}}{[5FURW]_{initial}} * 100$$

$$LC \% = \frac{[5FURW]_{final}}{[Lipid]_{final}} * 100$$

Figure 8.10 Equations used to calculate encapsulation efficiency and loading capacity.

Liposome sizes and ζ potentials were determined utilizing dynamic light scattering and electrophoretic light scattering, respectively, on a Malvern ZetaSizer NanoZS. Samples were diluted 100× in PBS immediately prior analysis, and each measurement is reported as an average of 2 independent sets of at least 20 runs each \pm SD.

Cell culture. All cell lines were obtained by ATCC® and maintained in a humidified CO₂ incubator at 37 °C. MDA-MB-231 human breast cancer cells and 4T1 murine breast cancer cells were cultured in RPMI1640 medium (Thermo Scientific). All above cells were supplemented with 10% fetal bovine serum (FBS;

ThermoScientific) and supplemented with 1% penicillin/streptomycin (Thermo Scientific).

Cancer cell growth inhibition. In vitro anticancer efficacy of drug-loaded liposomes was determined using MTT cell viability assay. MDA-MB-431 or 4T1 cells were seeded in a 96-well cell culture plate at a density of 5000 cells/well or in a total volume of 100 μ L media and allowed to adhere overnight. Media was then replaced with fresh media containing liposomes and incubated for 72 h. Parameters were optimized such that untreated cells reached 70% confluency after treatment. After incubation with liposomes, media was aspirated and replaced with 100 μ L of MTT (0.5 mg/mL, 3-(4,5-dimethylthiazol-2-yl)-2,5-diphenyltetrazolium bromide) in media for 4 h at room temperature. Finally, media was aspirated and DMSO was added (100 μ L/well). The absorbance was read at 570 nm after 2 min shaking. D_{50} concentrations were determined by fitting experimental data to a four-parameter equation according to the following formula: $y = B(A - B)/[1 - (x/C)^D]$, where A is the maximal absorbance, B is the minimum absorbance, C is the concentration producing 50% of the maximal absorbance, and D is the slope at the inflection point of the sigmoid curve. Unless otherwise indicated, data presented correspond to the average of at least two well replicates.

9 BIBLIOGRAPHY

1. F. Dati, *Journal*, 2003, **41**, 1289.
2. T. Tian, J. Wang and X. Zhou, *Organic & Biomolecular Chemistry*, 2015, **13**, 2226-2238.
3. S. Spindel and K. E. Sapsford, *Sensors*, 2014, **14**, 22313-22341.
4. J. Li and J. Macdonald, *Biosensors & Bioelectronics*, 2016, **83**, 177-192.
5. A. Deshpande and P. S. White, *Expert Review of Molecular Diagnostics*, 2012, **12**, 645-659.
6. J. Park, V. Sunkara, T. H. Kim, H. Hwang and Y. K. Cho, *Anal Chem*, 2012, **84**, 2133-2140.
7. H. D. Hill and C. A. Mirkin, *Nat Protoc*, 2006, **1**, 324-336.
8. D. Zhang, D. J. Carr and E. C. Alocilja, *Biosens Bioelectron*, 2009, **24**, 1377-1381.
9. H. Lee, J. E. Park and J. M. Nam, *Nat Commun*, 2014, **5**, 3367.
10. S. I. Stoeva, J. S. Lee, J. E. Smith, S. T. Rosen and C. A. Mirkin, *J Am Chem Soc*, 2006, **128**, 8378-8379.
11. S. I. Stoeva, J. S. Lee, C. S. Thaxton and C. A. Mirkin, *Angew Chem Int Ed Engl*, 2006, **45**, 3303-3306.
12. H. Dong, X. Meng, W. Dai, Y. Cao, H. Lu, S. Zhou and X. Zhang, *Anal Chem*, 2015, **87**, 4334-4340.
13. P. J. Tighe, R. R. Ryder, I. Todd and L. C. Fairclough, *Proteomics Clinical Applications*, 2015, **9**, 406-422.
14. B. Sanavio and S. Krol, *Frontiers in bioengineering and biotechnology*, 2015, **3**, 20-20.
15. K. E. Jones, N. G. Patel, M. A. Levy, A. Storeygard, D. Balk, J. L. Gittleman and P. Daszak, *Nature*, 2008, **451**, 990-993.
16. V. B. Gupta, R. Sundaram and R. N. Martins, *Alzheimer's Research & Therapy*, 2013, **5**, 31-31.
17. B. Zethelius, L. Berglund, J. Sundstrom, E. Ingelsson, S. Basu, A. Larsson, P. Venge and J. Arnlov, *The New England journal of medicine*, 2008, **358**, 2107-2116.
18. T. J. Wang , P. Gona , M. G. Larson , G. H. Tofler , D. Levy , C. Newton-Cheh , P. F. Jacques , N. Rifal , J. Selhub , S. J. Robins , E. J. Benjamin , R. B. D'Agostino and R. S. Vasan *New England Journal of Medicine*, 2006, **355**, 2631-2639.
19. C.-S. Ang, J. Phung and E. C. Nice, *Biomedical Chromatography*, 2011, **25**, 82-99.
20. M. T. Weigel and M. Dowsett, *Endocrine-Related Cancer*, 2010, **17**, R245-R262.
21. J. F. Rusling, C. V. Kumar, J. S. Gutkind and V. Patel, *Analyst*, 2010, **135**, 2496-2511.
22. P. Y. Muller and M. N. Milton, *Nat Rev Drug Discov*, 2012, **11**, 751-761.
23. E. Marrer and F. Dieterle, *Chem. Biol. Drug Des.*, 2007, **69**, 381-394.
24. G. Lavezzari and A. W. Womack, *Clin. Pharmacol. Ther.*, 2016, **99**, 208-213.
25. K. S. McKeating, A. Aube and J.-F. Masson, *Analyst*, 2016, **141**, 429-449.
26. G. McMahon and R. O'Connor, *Bioanalysis*, 2009, **1**, 507-511.
27. A. C. Society, (<http://canceratlas.cancer.org/>).
28. J. H. Beumer, *Clin. Pharmacol. Ther.*, 2013, **93**, 228-230.
29. K. W. Jones and S. R. Patel, *American family physician*, 2000, **62**, 1607-1612, 1614.
30. C. Bardin, G. Veal, A. Paci, E. Chatelut, A. Astier, D. Leveque, N. Widmer and J. Beijnen, *Eur. J. Cancer*, 2014, **50**, 2005-2009.
31. A. Paci, G. Veal, C. Bardin, D. Leveque, N. Widmer, J. Beijnen, A. Astier and E. Chatelut, *Eur. J. Cancer*, 2014, **50**, 2010-2019.
32. R. Pazdur, P. M. Hoff, D. Medgyesy, M. Royce and R. Brito, *Oncology (Williston Park, N.Y.)*, 1998, **12**, 48-51.
33. T. Kosjek and E. Heath, *TrAC Trends in Analytical Chemistry*, 2011, **30**, 1065-1087.
34. M. W. Saif, A. Choma, S. J. Salamone and E. Chu, *J Natl Cancer Inst*, 2009, **101**, 1543-1552.
35. A. B. van Kuilenburg and J. G. Maring, *Pharmacogenomics*, 2013, **14**, 799-811.
36. J. J. Lee, J. H. Beumer and E. Chu, *Cancer Chemother Pharmacol*, 2016, **78**, 447-464.
37. E. Gamelin, R. Delva, J. Jacob, Y. Merrouche, J. L. Raoul, D. Pezet, E. Dorval, G. Piot, A. Morel and M. Boisdron-Celle, *J Clin Oncol*, 2008, **26**, 2099-2105.

38. D. B. Longley, D. P. Harkin and P. G. Johnston, *Nat. Rev. Cancer*, 2003, **3**, 330-338.
39. S. Nussbaumer, P. Bonnabry, J. L. Veuthey and S. Fleury-Souverain, *Talanta*, 2011, **85**, 2265-2289.
40. J. H. Beumer, M. Boisdron-Celle, W. Clarke, J. B. Courtney, M. J. Egorin, E. Gamelin, R. L. Harney, C. Hammett-Stabler, S. Lepp, Y. Li, G. D. Lundell, G. McMillin, G. Milano and S. J. Salamone, *Ther Drug Monit*, 2009, **31**, 688-694.
41. S. J. Salamone, C. N. Benfield, J. B. Courtney, R. L. Harney, D. R. Kozo, Y. Li and G. D. Lundell, *Journal of Clinical Oncology*, 2011, **29**, 1.
42. P. H. J. White, M. Bonen, M. K. Bamat, R. von Borstel; Wellstat Diagnostics, LLC, Gaithersburg, MD; Wellstat Therapeutics Corporation, Gaithersburg, MD, presented in part at the J Clin Oncol, 2011.
43. P. Q. Hu, X. Huang and B. R. W. Von, *Journal*, 2013.
44. D. Koyuncu Zeybek, B. Demir, B. Zeybek and S. Pekyardimci, *Talanta*, 2015, **144**, 793-800.
45. M. Satyanarayana, K. Y. Goud, K. K. Reddy and K. V. Gobi, *Electrochimica Acta*, 2015, **178**, 608-616.
46. JP11337549A, 1999.
47. S. Salamone, J. Courtney and D. Stocker, *Journal*, 2006.
48. M. E. de Jonge, A. D. Huitema, A. C. Tukker, S. M. van Dam, S. Rodenhuis and J. H. Beijnen, *Clin Cancer Res*, 2005, **11**, 273-283.
49. A. Emadi, R. J. Jones and R. A. Brodsky, *Nature Reviews Clinical Oncology*, 2009, **6**, 638-647.
50. M. E. de Jonge, A. D. Huitema, S. Rodenhuis and J. H. Beijnen, *Clin Pharmacokinet*, 2005, **44**, 1135-1164.
51. M. Canal-Raffin, K. Khennoufa, B. Martinez, Y. Goujon, C. Folch, D. Ducint, K. Titier, P. Brochard, C. Verdun-Esquer and M. Molimard, *Journal of Chromatography B*, 2016, **1038**, 109-117.
52. F. A. Weaver, A. R. Torkelson, W. A. Zygmunt and H. P. Browder, *J Pharm Sci*, 1978, **67**, 1009-1012.
53. A. C. Begg and K. A. Smith, *Br J Cancer*, 1984, **49**, 49-55.
54. US20060024748A1, 2006.
55. S. Carrara, A. Cavallini, V. Erokhin and G. De Micheli, *Biosens Bioelectron*, 2011, **26**, 3914-3919.
56. O. McCarthy, A. Musso-Buendia, M. Kaiser, R. Brun, L. M. Ruiz-Perez, N. G. Johansson, D. G. Pacanowska and I. H. Gilbert, *European Journal of Medicinal Chemistry*, 2009, **44**, 678-688.
57. W. A. El-Sayed and A. A. H. Abdel-Rahman, *Z. Naturforsch., B: J. Chem. Sci.*, 2010, **65**, 57-66.
58. S. G. Zhou, M. X. Xu, S. Y. Ye, D. S. Li, J. Xu, P. Mao and J. Xiong, *J. Chem. Res*, 2012, DOI: 10.3184/174751912x13282923623804, 114-117.
59. M. c. Parlato, C. Mugnaini, M. L. Renzulli, F. Corelli and M. Botta, *ARKIVOC (Gainesville, FL, U. S.)*, 2004, DOI: 10.3998/ark.5550190.0005.530, 349-363.
60. C. Dugave, J. Dubois, S. Bory, M. Gaudry and A. Marquet, *Bull. Soc. Chim. Fr.*, 1991, 381-386.
61. M. T. Abdel-Aal, *Arch. Pharmacol Res.*, 2010, **33**, 797-805.
62. L. N. Burgula, K. Radhakrishnan and L. M. Kundu, *Tetrahedron Letters*, 2012, **53**, 2639-2642.
63. N. Markova, V. Enchev and I. Timtcheva, *The journal of physical chemistry. A*, 2005, **109**, 1981-1988.
64. F. Peral and D. Troitiño, *Journal of Molecular Structure: THEOCHEM*, 2010, **944**, 1-11.
65. V. K. Rastogi and M. A. Palafox, *Spectrochim. Acta, Part A*, 2011, **79**, 970-977.

66. G. S. Abdrakhimova, M. Y. Ovchinnikov, A. N. Lobov, L. V. Spirikhin, S. P. Ivanov and S. L. Khursan, *Journal of Physical Organic Chemistry*, 2014, **27**, 876-883.
67. S. M. Bayomi and A. A. Al-Badr, in *Analytical Profiles of Drug Substances*, eds. A. A. A.-B. G. A. F. H. G. B. Klaus Florey and T. G. Lee, Academic Press, 1990, vol. Volume 18, pp. 599-639.
68. M. Broto, S. Matas, R. Babington, M. P. Marco and R. Galve, *Food Control*, 2015, **51**, 381-389.
69. B. ElAmin, G. M. Anantharamaiah, G. P. Royer and G. E. Means, *The Journal of Organic Chemistry*, 1979, **44**, 3442-3444.
70. WO2010085377A2, 2010.
71. US2006024748-A1; WO2006020263-A2; EP1774331-A2; CN101052877-A; JP2008508281-W; JP4521029-B2; JP2010189414-A; WO2006020263-A3; CN101052877-B; CA2572671-C.
72. G. D. Heggie, J.-P. Sommadossi, D. S. Cross, W. J. Huster and R. B. Diasio, *Cancer Research*, 1987, **47**, 2203-2206.
73. A. Condon, *Nat Rev Genet*, 2006, **7**, 565-575.
74. V. Noel, B. Piro and S. Reisberg, in *RNA and DNA Diagnostics*, eds. V. A. Erdmann, S. Jurga and J. Barciszewski, Springer International Publishing, 2015, DOI: 10.1007/978-3-319-17305-4_4, ch. 4, pp. 81-106.
75. T. Sano, C. Smith and C. Cantor, *Science*, 1992, **258**, 120-122.
76. F. Akter, M. Mie and E. Kobatake, *Sensors and Actuators B: Chemical*, 2014, **202**, 1248-1256.
77. S. Brakmann, *Angewandte Chemie International Edition*, 2004, **43**, 5730-5734.
78. J. M. Nam, C. S. Thaxton and C. A. Mirkin, *Science*, 2003, **301**, 1884-1886.
79. J. M. Nam, S. I. Stoeva and C. A. Mirkin, *J Am Chem Soc*, 2004, **126**, 5932-5933.
80. K. K. Jain, *Clinica Chimica Acta*, 2005, **358**, 37-54.
81. J. H. Jung, G. Y. Kim and T. S. Seo, *Lab Chip*, 2011, **11**, 3465-3470.
82. M. Cho, S. Chung, J. H. Jung, G. E. Rhie, J. H. Jeon and T. S. Seo, *Biosens Bioelectron*, 2014, **61**, 172-176.
83. M. Cho, S. Chung, Y. T. Kim, J. H. Jung, D. H. Kim and T. S. Seo, *Lab Chip*, 2015, **15**, 2744-2748.
84. S. Chung, M. Cho, J. Hwan Jung and T. Seok Seo, *Electrophoresis*, 2014, **35**, 1504-1508.
85. P. Du, M. Jin, G. Chen, C. Zhang, Z. Jiang, Y. Zhang, P. Zou, Y. She, F. Jin, H. Shao, S. Wang, L. Zheng and J. Wang, *Sci Rep*, 2016, **6**, 38114.
86. Q. Peng, Z. Cao, C. Lau, M. Kai and J. Lu, *Analyst*, 2011, **136**, 140-147.
87. B. K. Oh, J. M. Nam, S. W. Lee and C. A. Mirkin, *Small*, 2006, **2**, 103-108.
88. C. S. Thaxton, R. Elghanian, A. D. Thomas, S. I. Stoeva, J. S. Lee, N. D. Smith, A. J. Schaeffer, H. Klocker, W. Horninger, G. Bartsch and C. A. Mirkin, *Proc Natl Acad Sci U S A*, 2009, **106**, 18437-18442.
89. E. D. Goluch, J.-M. Nam, D. G. Georganopoulou, T. N. Chiesl, K. A. Shaikh, K. S. Ryu, A. E. Barron, C. A. Mirkin and C. Liu, *Lab on a Chip*, 2006, **6**, 1293-1299.
90. J. Wang, G. Liu, B. Munge, L. Lin and Q. Zhu, *Angew Chem Int Ed Engl*, 2004, **43**, 2158-2161.
91. Z. Liu, B. Zhou, H. Wang, F. Lu, T. Liu, C. Song and X. Leng, *J Nanopart Res*, 2013, **15**.
92. D. G. Georganopoulou, L. Chang, J.-M. Nam, C. S. Thaxton, E. J. Mufson, W. L. Klein and C. A. Mirkin, *Proceedings of the National Academy of Sciences of the United States of America*, 2005, **102**, 2273-2276.
93. J. M. Nam, A. R. Wise and J. T. Groves, *Anal Chem*, 2005, **77**, 6985-6988.
94. H.-q. Yin, M.-x. Jia, L.-j. Shi, J. Liu, R. Wang, M.-m. Lv, Y.-y. Ma, X. Zhao and J.-g. Zhang, *Journal of Immunotoxicology*, 2014, **11**, 291-295.

95. T. L. Chang, C. Y. Tsai, C. C. Sun, C. C. Chen, L. S. Kuo and P. H. Chen, *Biosens Bioelectron*, 2007, **22**, 3139-3145.
96. S. Tang, J. Zhao, J. J. Storhoff, P. J. Norris, R. F. Little, R. Yarchoan, S. L. Stramer, T. Patno, M. Domanus, A. Dhar, C. A. Mirkin and I. K. Hewlett, *J Acquir Immune Defic Syndr*, 2007, **46**, 231-237.
97. C. Cao, R. Dhumpa, D. D. Bang, Z. Ghavifekr, J. Hogberg and A. Wolff, *Analyst*, 2010, **135**, 337-342.
98. J. W. Perez, E. A. Vargis, P. K. Russ, F. R. Haselton and D. W. Wright, *Anal Biochem*, 2011, **410**, 141-148.
99. H. Q. Yin, M. X. Jia, L. J. Shi, S. Yang, L. Y. Zhang, Q. M. Zhang, S. Q. Wang, G. Li and J. G. Zhang, *J Virol Methods*, 2011, **178**, 225-228.
100. K. Cihalova, S. Dostalova, D. Hegerova, S. Skalickova, M. Vaculovicova, R. Kizek and P. Kopel, *Mendelnet 2015*, 2015, 448-452.
101. B. Amini, M. Kamali, M. Salouti and P. Yaghmaei, *Biosensors and Bioelectronics*, 2017, **92**, 679-686.
102. L. Du, W. Ji, Y. Zhang, C. Zhang, G. Liu and S. Wang, *Analyst*, 2015, **140**, 2001-2007.
103. W. H. Organization, The top 10 causes of death, <http://www.who.int/mediacentre/factsheets/fs310/en/>).
104. S. Stehle, J. Kirchheiner, A. Lazar and U. Fuhr, *Clin Pharmacokinet*, 2008, **47**, 565-594.
105. G. Vecchione, B. Casetta, M. Tomaiuolo, E. Grandone and M. Margaglione, *Journal of chromatography. B, Analytical technologies in the biomedical and life sciences*, 2007, **850**, 507-514.
106. R. Ceresole, M. A. Rosasco, C. C. Forastieri and A. I. Segall, *Journal of Liquid Chromatography & Related Technologies*, 2008, **31**, 179-187.
107. S. Black, I. Kushner and D. Samols, *The Journal of biological chemistry*, 2004, **279**, 48487-48490.
108. P. M. Ridker and N. Cook, *Circulation*, 2004, **109**, 1955-1959.
109. P. M. Ridker, *Circulation*, 2003, **107**, 363-369.
110. M. Algarra, D. Gomes and J. C. Esteves da Silva, *Clin Chim Acta*, 2013, **415**, 1-9.
111. N. Brouwer and J. van Pelt, *Clin Chim Acta*, 2015, **439**, 195-201.
112. S. K. Vashist, A. G. Venkatesh, E. M. Schneider, C. Beaudoin, P. B. Lupp and J. H. T. Luong, *Biotechnology Advances*, 2016, **34**, 272-290.
113. R. Ekins, F. Chu and E. Biggart, *Analytica Chimica Acta*, 1989, **227**, 73-96.
114. A. C. Pease, D. Solas, E. J. Sullivan, M. T. Cronin, C. P. Holmes and S. P. Fodor, *Proceedings of the National Academy of Sciences of the United States of America*, 1994, **91**, 5022-5026.
115. N. Tort, J. P. Salvador, A. Aviñó, R. Eritja, J. Comelles, E. Martínez, J. Samitier and M. P. Marco, *Bioconjugate Chemistry*, 2012, **23**, 2183-2191.
116. J. Kimling, M. Maier, B. Okenve, V. Kotaidis, H. Ballot and A. Plech, *The Journal of Physical Chemistry B*, 2006, **110**, 15700-15707.
117. T. A. Taton, in *Current Protocols in Nucleic Acid Chemistry*, John Wiley & Sons, Inc., 2001, DOI: 10.1002/0471142700.nc1202s09.
118. X. Zhang, M. R. Servos and J. Liu, *Journal of the American Chemical Society*, 2012, **134**, 7266-7269.
119. S. Xu, H. Yuan, A. Xu, J. Wang and L. Wu, *Langmuir*, 2011, **27**, 13629-13634.
120. M. Schollbach, F. Zhang, F. Roosen-Runge, M. W. A. Skoda, R. M. J. Jacobs and F. Schreiber, *Journal of Colloid and Interface Science*, 2014, **426**, 31-38.
121. C. D. Moore, O. Z. Ajala and H. Zhu, *Current Opinion in Chemical Biology*, 2016, **30**, 21-27.
122. K. K. Jain, *Molecular Diagnosis & Therapy*, 2010, **14**, 141-147.
123. E. Donatin and M. Drancourt, *Médecine et Maladies Infectieuses*, 2012, **42**, 453-459.

124. U. B. Nielsen and B. H. Geierstanger, *Journal of Immunological Methods*, 2004, **290**, 107-120.
125. F. Fernandez, D. G. Pinacho, F. Sanchez-Baeza and M. P. Marco, *Journal of Agricultural and Food Chemistry*, 2011, **59**, 5036-5043.
126. H. M. E. Azzazy and M. M. H. Mansour, *Clinica Chimica Acta*, 2009, **403**, 1-8.
127. M. Spengler, M. Adler and C. M. Niemeyer, *Analyst*, 2015, **140**, 6175-6194.
128. E. M. Elnifro, A. M. Ashshi, R. J. Cooper and P. E. Klapper, *Clinical Microbiology Reviews*, 2000, **13**, 559-570.
129. Y. Leng, K. Sun, X. Chen and W. Li, *Chemical Society Reviews*, 2015, **44**, 5552-5595.
130. H. W. Yu, I. S. Kim, R. Niessner and D. Knopp, *Anal Chim Acta*, 2012, **750**, 191-198.
131. S. Amarasiri Fernando and G. S. Wilson, *Journal of Immunological Methods*, 1992, **151**, 47-66.
132. D. Rodbard, Y. Feldman, M. L. Jaffe and L. E. M. Miles, *Immunochemistry*, 1978, **15**, 77-82.
133. Y. K. Oh, H.-A. Joung, H. S. Han, H.-J. Suk and M.-G. Kim, *Biosensors and Bioelectronics*, 2014, **61**, 285-289.
134. K. M. Camacho, S. Menegatti, D. R. Vogus, A. Pusuluri, Z. Fuchs, M. Jarvis, M. Zakrewsky, M. A. Evans, R. Chen and S. Mitragotri, *J Control Release*, 2016, DOI: 10.1016/j.jconrel.2016.03.027.
135. N. Bertrand, J. Wu, X. Xu, N. Kamaly and O. C. Farokhzad, *Adv Drug Deliv Rev*, 2014, **66**, 2-25.
136. S. Mitragotri, P. A. Burke and R. Langer, *Nat Rev Drug Discov*, 2014, **13**, 655-672.
137. T. S. Levchenko, R. Rammohan, A. N. Lukyanov, K. R. Whiteman and V. P. Torchilin, *International Journal of Pharmaceutics*, 2002, **240**, 95-102.
138. S. Barua and S. Mitragotri, *Nano Today*, 2014, **9**, 223-243.
139. G. T. Noble, J. F. Stefanick, J. D. Ashley, T. Kiziltepe and B. Bilgicer, *Trends Biotechnol*, 2014, **32**, 32-45.
140. M. Slingerland, H.-J. Guchelaar and H. Gelderblom, *Drug Discovery Today*, 2012, **17**, 160-166.
141. Y. Malam, M. Loizidou and A. M. Seifalian, *Trends in Pharmacological Sciences*, **30**, 592-599.
142. A. Mazumder, *Indian Journal of Biochemistry & Biophysics*, 1981, **18**, 120-123.
143. B. C. Joondeph, G. A. Peyman, B. Khoobehi and B. Y. Yue, *Ophthalmic Surg*, 1988, **19**, 252-256.
144. B. Elorza, M. A. Elorza, G. Frutos and J. R. Chantres, *Biochimica et biophysica acta*, 1993, **1153**, 135-142.
145. M. Fresta, A. Villari, G. Puglisi and G. Cavallaro, *International Journal of Pharmaceutics*, 1993, **99**, 145-156.
146. C. A. M. da Costa and A. M. Moraes, *Acta Scientiarum Technology*, 2003, **25**, 53-61.
147. N. Kaiser, A. Kimpfler, U. Massing, A. M. Burger, H. H. Fiebig, M. Brandl and R. Schubert, *Int J Pharm*, 2003, **256**, 123-131.
148. V. Soni, D. V. Kohli and S. K. Jain, *Journal of Drug Targeting*, 2008, **16**, 73-78.
149. M. Petaccia, M. Condello, L. Giansanti, A. La Bella, F. Leonelli, S. Meschini, D. Gradella Villalva, E. Pellegrini, F. Ceccacci, L. Galantini and G. Mancini, *MedChemComm*, 2015, **6**, 1639-1642.
150. G. Haran, R. Cohen, L. K. Bar and Y. Barenholz, *Biochimica et Biophysica Acta (BBA) - Biomembranes*, 1993, **1151**, 201-215.
151. Y. Liu, L. C. Mounkes, H. D. Liggitt, C. S. Brown, I. Solodin, T. D. Heath and R. J. Debs, *Nature biotechnology*, 1997, **15**, 167-173.
152. G. Thurston, J. W. McLean, M. Rizen, P. Baluk, A. Haskell, T. J. Murphy, D. Hanahan and D. M. McDonald, *J Clin Invest*, 1998, **101**, 1401-1413.

153. K. M. Camacho, University of California, Santa Barbara, 2015.
154. S. Manchun, C. R. Dass and P. Sriamornsak, *Life Sciences*, 2012, **90**, 381-387.
155. I.-Y. Kim, Y.-S. Kang, D. S. Lee, H.-J. Park, E.-K. Choi, Y.-K. Oh, H.-J. Son and J.-S. Kim, *Journal of Controlled Release*, 2009, **140**, 55-60.
156. S. M. Ansell, T. O. Harasym, P. G. Tardi, S. S. Buchkowsky, M. B. Bally and P. R. Cullis, *Methods in molecular medicine*, 2000, **25**, 51-68.
157. S. Viswanathan, C. Rani and C. Delerue-Matos, *Analytica Chimica Acta*, 2012, **726**, 79-84.
158. D. E. Lopes de Menezes, L. M. Pilarski and T. M. Allen, *Cancer Research*, 1998, **58**, 3320-3330.
159. M. Hong, S. Zhu, Y. Jiang, G. Tang and Y. Pei, *Journal of Controlled Release*, 2009, **133**, 96-102.
160. P. Simard and J. C. Leroux, *Int J Pharm*, 2009, **381**, 86-96.
161. R. Suzuki, T. Takizawa, Y. Kuwata, M. Mutoh, N. Ishiguro, N. Utoguchi, A. Shinohara, M. Eriguchi, H. Yanagie and K. Maruyama, *Int J Pharm*, 2008, **346**, 143-150.
162. X. Ying, H. Wen, W.-L. Lu, J. Du, J. Guo, W. Tian, Y. Men, Y. Zhang, R.-J. Li, T.-Y. Yang, D.-W. Shang, J.-N. Lou, L.-R. Zhang and Q. Zhang, *Journal of Controlled Release*, 2010, **141**, 183-192.
163. R. Nieto Montesinos, A. Béduneau, A. Lamprecht and Y. Pellequer, *Molecular Pharmaceutics*, 2015, **12**, 3829-3838.
164. T. Mosmann, *Journal of Immunological Methods*, 1983, **65**, 55-63.
165. J. C. M. Stewart, *Analytical Biochemistry*, 1980, **104**, 10-14.

10 ACRONYMS, ABBREVIATIONS AND TABLES

10.1 ACRONYMS AND ABBREVIATIONS

1,3MeU6	1,3-Dimethyl-2,6-dioxo-1,2,3,6-tetrahydropyrimidine-4-carboxylic acid
3MeDHU6	1-methyl-L-4,5-dihydroorotic acid
4OHCP	4-hydroxycyclophosphamide
5BrdUrd	5-bromo-2'-deoxyuridine
5BrU	5-bromouracil
5BrU1	5-Bromo-2,4-dioxo-3,4-dihydropyrimidin-1(2H-yl)acetic acid
5FDMU	1,3-dimethyl-5-fluorouracil
5FdUrd	5-fluoro-2'-deoxyuridine
5FU	5-fluorouracil
5FU1	5-(5-fluoro-2,4-dioxo-3H-pyrimidin-1-yl)pentanoic acid
5FU3	5-(5-fluoro-2,4-dioxo-1H-pyrimidin-3-yl)pentanoic acid
5FU6	5-(5-fluoro-2,4-dioxo-1H,3H-pyrimidin-6-yl)pentanoic acid
5FURBocW	(2R,3R,4R,5R)-2-(((tert-butoxycarbonyl)-L-tryptophyl)oxy)methyl)-5-(5-fluoro-2,4-dioxo-3,4-dihydropyrimidin-1(2H-yl)tetrahydrofuran-3,4-diyl (2R,2'R)-bis(2-((tert-butoxycarbonyl)amino)-3-(1H-indol-3-yl)propanoate)
5FUrd	5-fluorouridine
5FURW	(2R,3R,4R,5R)-2-(((L-tryptophyl)oxy)methyl)-5-(5-fluoro-2,4-dioxo-3,4-dihydropyrimidin-1(2H-yl)tetrahydrofuran-3,4-diyl (2R,2'R)-bis(2-amino-3-(1H-indol-3-yl)propanoate)
Ab	Antibody
Abs	Absorbance
ACL	Acenocoumarol
ACN	Acetonitrile
AD	Aminodextran
ADDLs	Amyloid- β -derived diffusible ligands
Ag	Antigen
AIV	Avian influenza virus
ALDH	Aldehyde dehydrogenase 1
AldoCP	Aldophosphamide
Amax	Maximum absorbance
Amin	Minimum absorbance
As	Antiserum
AuNP	Gold nanoparticle

BSA	Bovine Serum Albumin
C	Cytosine
cELISA	Competitive enzyme linked immunosorbent assay
CETEMMSA	Technological business center of Mataro and Maresme
CONA	Conalbumin from chicken egg white
CP	Cyclophosphamide
CRP	C-Reactive Protein
CSIC	Spanish Council for Scientific Research
CVD	Cardiovascular Diseases
CXCP	Carboxyphosphamide
DCC	N,N'-dicyclohexylcarbodiimide
DHFU	Dihydrofluorouracil
DIC	N,N'-diisopropylcarbodiimide
DMF	N-dimethylformamide
DMSO	Dimethylsulfoxide
DNA	Deoxyribonucleic acid
DOPE	dioleylphosphatidylethanolamine
DOTAP	N-[1-(2,3-Dioleoyloxy)propyl]-N,N,N-trimethylammonium methyl-sulfate
DPD	Dihydropyrimidine dehydrogenase
DSPC	1,2-Distearoyl-sn-glycero-3-phosphocholine
DSPE-PEG	1,2-distearoyl-sn-glycero-3-phosphoethanolamine-N-[polyethylene glycol-2000]
DTT	Dithiothreitol
EDC	1-Ethyl-3-(3-dimethylaminopropyl)carbodiimide
EDTA	EthyleneDiamineTetraacetic Acid
EE	Encapsulation efficiency
ELISA	Enzyme-Linked ImmunoSorbent Assay
EPR	Enhanced permeability effect
ePSP	Encoded polystyrene probes
EURECAT	Tecnological center of Catalonia
FdUMP	Fluorodeoxyuridine monophosphate
FT	Tegafur, Ftorafur
FUMP	Fluorouridine monophosphate
G	Guanine
GPTMS	(3-Glycidylxypropyl)trimethoxysilane
hACL	Acenocoumarol hapten

HCH	Horseshoe Crab Hemocyanin
HCV	Hepatitis C virus
HPLC	High Performance Liquid Chromatography
HRP	Horse Radish Peroxidase
IC ₅₀	Concentration in which the signal is 50 % inhibited
IC ₉₀	Concentration in which the signal is 10 % inhibited
IgG	Immunoglobulin G
IPCR	immuno polymerase chain reaction
IQAC	Institute of Advanced Chemistry of Catalonia
IVD	In Vitro Diagnostic
L	Liposome
LC	Loading capacity
iel	Insertion element gene
LOD	Limit of detection
LOL	Limit of linearity
LOQ	Limit of quantification
mAb	Monoclonal Antibody
MALDI-TOF-MS	Matrix Assisted Laser Desorption Ionization - Time of Flight Mass Spectrometry
MINECO	Ministry of Economy, Industry and Competitiveness
miRNA	micro ribonucleic acid
MP	Magnetic particle
milliQ	milli-Q deionized and purified water
mRNA	Messenger ribonucleic acid
MTT	3-(4,5-dimethylthiazol-2-yl)-2,5-diphenyltetrazolium bromide
MW	Molecular Weight
N2down	20-mer oligonucleotide, CGGAGGTACATTCGACTTGA
N2up	20-mer oligonucleotide, TCAAGTCGAATGTACCTCCG
N4down	20-mer oligonucleotide, TCCAGCGTTAGTGTACAGAG
N4up	20-mer oligonucleotide, CTCTGTACACTAACGCTGGA
Nb4D	Nanobiotechnology for Diagnostics Group
NHS	N-hydroxysuccinimide
NP	Nanoparticle
OVA	Albumin from chicken egg white
pAb	Polyclonal Antibody
PBS	Phosphate Buffered Saline solution
PBST	Phosphate Buffered Saline Tween-20 solution

PCR	Polymerase Chain Reaction
PEG	Polyethylene glycol
POC	Point-Of-Care
PSA	Prostate specific antigen
PSP	Polystyrene particles
QD	Quantum dots
RNA	Ribonucleic acid
SD	Standard Deviation
SDS	Sodium Dodecyl Sulphate
SPR	Surface Plasmon Resonance
T	Thymine
TAMRA	5-Carboxytetramethylrhodamine
TDM	Therapeutic drug monitoring
TEEA _c	Triethylammonium acetate
TEM	Transmission electron microscope
TFA	Trifluoroacetic acid
TMB	3,3',5,5'-TetraMethylBenzidine
Tris	tris(hydroxymethyl)aminomethane
TRM	Therapeutic response monitoring
Trp	Tryptophan
U1	3-(2,4-Dioxo-3,4-dihydropyrimidin-1(2H)-yl)propanoic acid
Urd	Uridine
WHO	World Health Organization

10.2 TABLE OF FIGURES

Figure 1.1 The structure of this thesis related to the different chapters and the parts included in each one. Dotted line corresponds to the work that could not be undertaken.	5
Figure 2.1 Performance parameters for a detection platform. The gold standard technique is actually a compromise between the multiplex level and platforms that are capable of high throughput analysis. ⁵	12
Figure 2.2 Diagram showing 'rule out' and 'rule in' approaches for pathogenic disease diagnostic. Multiplexed assays based on 'rule in' approach could boost pathogen identification ⁵	14
Figure 2.3 Scheme representing the path of a therapeutic drug in the human body. Analysis of the circulating drug concentration is performed in biofluids, which is referred to as therapeutic drug monitoring. The interaction of the therapeutic drug with the targeted cells can lead to morphological responses or to changes in the levels of biomarkers or metabolites, and TRM can be applied.....	16
Figure 3.1 Structure of chapter 3 related to the different sections	18
Figure 3.2 List of cytostatic drugs grouped by family. Colors indicate the cell-cycle stage in which each family acts (G0, resting; G1, growth or gap 1; S, DNA synthesis; G2, growth or gap 2; M, mitosis).....	20
Figure 3.3 Metabolic pathway of 5-fluorouracil. DHFU, dihydrofluorouracil; DPD, dihydropyrimidine dehydrogenase, 5FU, fluorouracil; FUMP, fluorouridine monophosphate; FdUMP, fluorodeoxyuridine monophosphate.....	22
Figure 3.4 Metabolic pathway of cyclophosphamide. CP, cyclophosphamide; 4OHCP, 4-hydroxycyclophosphamide; AldoCP, aldophosphamide; ALDH, aldehyde dehydrogenase 1; CXCP, carboxyphosphamide.	25
Figure 3.5 Scheme showing the procedure required for the production of antibodies against small molecules.	27
Figure 3.6 Structure of 5FU and design of 5FU haptens.....	28
Figure 3.7 Synthesis of 5FU6 proposal	29
Figure 3.8 Mechanism of solid phase synthesis of uridine rings	30
Figure 3.9 Antibody titer to evaluate the response of the antisera produced by non-competitive ELISA. Antigen had a concentration of 1 µg/mL, antisera had a concentration of 1/256000 for As337-342 and 1/64000 for As326-328.....	31
Figure 3.10 Indirect competitive assay. First, the competitor is adsorbed on the well; then, both competitor and analyte compete for the binding site of the antibody; after that a secondary labeled antibody is added and finally, a substrate allows the colorimetric reaction.....	32

Figure 3.11 Inhibition curve of the competitive ELISA and its fitted equation. IC_{50} : half maximal inhibitory concentration, A_{max} : maximum absorbance, A_{min} : minimum absorbance, Hillslope: slope of the linear part of the curve.	32
Figure 3.12 Affinity constants of the antibody for the analyte and for the competitor. There is no inhibition of the interaction with the competitor because the affinity constant with the analyte (K_{aff}) is smaller than with the competitor (K_{aff}).....	34
Figure 3.13 UV-Vis and IR spectra of 5FU and the three haptens	35
Figure 3.14 Cross-reactivity of the antibodies with 7 related compounds of 5FU: the drug and a control at 1 μ M (Antigen had a concentration of 0.03, 0.05 and 0.125 μ g/mL respectively for each conjugate, antisera (As337) had a concentration of 1/256000, 1/256000 and 1/4000 respectively for each conjugate). The data was normalized and the maximal absorbance, the blank control, was given a 100% of signal. The rest of absorbance inhibitions were calculated based upon the control's signal.	37
Figure 3.15 Structure of highly heterologous competitors	38
Figure 3.16 Calibration curve parameters of competitors with linker in position 1 versus antisera produced against HCH-5FU1.	39
Figure 3.17 Structure of CP hapten design.....	40
Figure 3.18 Synthesis design of CP2-Cl hapten.....	41
Figure 3.19 Synthesis of CP3 benzyl ester	42
Figure 3.20 Antibody titer to evaluate the response of the antisera produced. Antigen had a concentration of 1 μ g/mL, antisera had a concentration of 1/256000.	43
Figure 3.21 Calibration curve parameters of CXCP-BSA versus As343. Ag, CXCP-BSA, had a concentration of 0.0625 μ g/mL and As, As343, of 1/8000. Data has been extracted from the four-parameter equation used to fit the standard curves. Data shows the average and standard deviation of the parameters of the assay using three replicates for each concentration of CP measured.	44
Figure 4.1 Structure of chapter 4 related to the different sections	86
Figure 4.2 The most popular IPCR formats. (a) Sandwich format detection with a primary antibody adsorbed to the microwell and a secondary antibody linked to the DNA tag. (b) Direct detection format.	87
Figure 4.3 Scheme showing the biobarcode assay method.	88
Figure 4.4 Acenocoumarol chemical structure.....	91
Figure 4.5 CRP chemical structure.....	92
Figure 4.6 Schematic diagram of the sandwich biobarcode strategy.....	93
Figure 4.7 A) Glass slide functionalization with GPTMS. B) DNA microarray, coding oligonucleotide quantification strategy.	95

Figure 4.8. All material needed for the different steps involved in fluorescent microarray development: print, assemble, measure, analyze and data treatment.	96
Figure 4.9 Graph showing previous attempts for gold nanoparticle functionalization with both bioreceptor and coding oligonucleotide.	97
Figure 4.10 Scheme showing the design of the biobarcode assay for the detection of small molecules. Most reagents were already prepared or are commercially available.....	98
Figure 4.11 Acenocoumarol hapten, hACL, conjugation to oligonucleotide sequence.	99
Figure 4.12 A) TEM image of produced AuNPs (16 nm). B) UV-Vis spectra of the particle solution. Maximum absorbance corresponds to 520 nm, which can be correlated with particle size (16 nm) and particle concentration through the lambert-beer law.	99
Figure 4.13 Scheme showing conjugation and release procedure for AuNPs.....	100
Figure 4.14 Calibration curve of ELISA assay on eAuPs. The data has been extracted from the four-parameter equation used to fit the standard curves.	101
Figure 4.15 Preparation of prefunctionalized PEG-coated eAuPs.....	102
Figure 4.16 Scheme showing the design of the biobarcode assay for the detection of small molecules with PSP.	103
Figure 4.17 Scheme showing the design of the biobarcode assay for the detection of proteins with PSP.....	104
Figure 5.1 Structure of chapter 5 related to the different sections	172
Figure 5.2 Schematic representation of main multiplexed platforms.....	173
Figure 5.3 Schematic diagram of the multiplexed and multimodal biobarcode strategy.	176
Figure 5.4 Scheme of the step designs evaluated. Scheme is showing assays for sandwich format, in case of competitive format ePSPs are functionalized with an antigen instead of an antibody. The magnets represent a washing step.	177
Figure 5.5 Comparison of N2 quantification and N4 quantification in different step design. Red: ACL monoplexed assay, blue: CRP monoplexed assay, grey: multiplexed assay. Particles concentration were 0.5 mg/mL of pAb236-MP and 0.0125 % w/v of N2-ePSPs for ACL and 0.1 mg/mL of pAbCRP2-MP and 0.05 % w/v of N4-ePSPs for CRP. Each concentration point corresponds to the average of an assay; each calibration point was measured five times.	179
Figura 7.1 Estructura del capítol en relació amb les seves seccions.....	204
Figura 7.2 Esquema de l'assaig biobarcode.....	208
Figura 7.3 Estructura del 5FU i disseny dels seus haptens	209
Figura 7.4 Síntesi dels haptens del 5FU.....	210

Figura 7.5 Corba de calibració, condicions i paràmetres de l'immunoassaig per el tegafur. Les dades representades corresponen a la mitjana de sis assajos desenvolupats en 4 dies diferents, tres rèpliques per assaig. ^a IT correspon al interval de treball, calculat com la concentració donada entre el 20 i el 80 % de senyal.	211
Figura 7.6 Estructura de la CP i disseny dels haptens.....	212
Figura 7.7 Disseny i síntesi del haptè CP2-Cl	213
Figura 7.8 Corba de calibració, condicions i paràmetres de l'immunoassaig per la ciclofosfamida. Les dades representades corresponen a la mitjana de tres rèpliques.	213
Figura 7.9 Bioxip de ADN, quantificació de les seqüències codificants	215
Figura 7.10 Avantatges del Sistema biobarcode. A. Capacitat de amplificar la senyal. B. Capacitat de modular el interval de treball i la detectabilitat.....	216
Figura 7.11 Corba de calibració, condicions i paràmetres del biobarcode per al acenocoumarol. Les dades han sigut extretes de la regressió sigmoïdal de quatre parametres que s'ajusta a la corba. Les dades representades són la mitjana de tres assajos duts a terme en tres dies diferents, cinc rèpliques cada dia.	217
Figura 7.12 A. Corba de calibració, condicions i paràmetres del biobarcode per l'acenocoumarol. Les dades han sigut extretes de la regressió sigmoïdal de quatre parametres que s'ajusta a la corba. Les dades representades són la mitjana de tres assajos duts a terme en tres dies diferents, cinc rèpliques cada dia. B. Comparació de la quantificació del biobarcode amb l'ELISA i una assaig de referencia (Siemens dimensió analyzer). Les dades representades són la mitjana d'un assaig de cinc rèpliques pel biobarcode, tres repliques per l'ELISA.....	218
Figura 7.13 Grafica mostrant les concentracions trobades en 8 mostres dopades amb diferents concentracions de ACL i CRP. Els resultats són la mitja dels anàlisis de tres assajos, amb 5 repliques cada un.....	220
Figure 8.1 Structure of chapter 8 related to the different sections	224
Figure 8.2 Different types of nanocarriers	225
Figure 8.3 Structural and design considerations for liposomal drug delivery	226
Figure 8.4 Scheme showing the encapsulation mechanism by ammonium sulfate gradient.....	228
Figure 8.5 Diagram showing the 5-fluorouracil prodrug synthesized for encapsulation.....	230
Figure 8.6 Release of drug of both amino particles along time. Release was produced with PBS at different pH at 37°C.	232
Figure 8.7 Graphic scheme of the conjugation procedures of antibodies for both amino and carboxy functionalized particles	232
Figure 8.8 Inhibition curves of cell activity due to the presence of the drug and the liposomes for two different cell lines. A and B correspond to 4T1 and MDA-MB-231 cell lines respectively. Each concentration point corresponds to the average of three replicates.	234

Figure 8.9 Molecular structure of synthesized compounds: 5FURBocW (5) and 5FURW (6). Numbers correspond to NMR assignment..... 236

Figure 8.10 Equations used to calculate encapsulation efficiency and loading capacity. 238

10.3 TABLE OF TABLES

Table 3.1 Bioanalytical techniques for 5FU and FT detection	23
Table 3.2 Bioanalytical techniques for CP detection	26
Table 3.3 Hapten densities of produced immunogens for 5FU detection.....	30
Table 3.4 Hapten densities of produced competitors for 5FU detection	33
Table 3.5 Summary of hapten structure, antisera obtained from the immunized rabbits with hapten-HCH and the competitors prepared for 5-fluorouracil	33
Table 3.6 Comparison of the punctual charge and pKa of 5FU and the haptens	36
Table 3.7 Hapten densities of produced immunogens for CP detection.....	42
Table 3.8 Hapten densities of produced competitors for CP detection	43
Table 3.9 Summary of hapten structure, antisera obtained from the immunized rabbits with hapten-HCH and the competitors prepared for cyclophosphamide	43
Table 4.1 Developed biobarcode assays for a single analyte	90
Table 5.1 Developed biobarcode assays for multiple analytes	175
Taula 7.1 Paràmetres de l'assaig biobarcode multiplexat.....	220